



Yu, Fangxintian (2025) *Power flow analytics for power distribution networks*. PhD thesis.

<https://theses.gla.ac.uk/84924/>

Copyright and moral rights for this work are retained by the author

A copy can be downloaded for personal non-commercial research or study, without prior permission or charge

This work cannot be reproduced or quoted extensively from without first obtaining permission from the author

The content must not be changed in any way or sold commercially in any format or medium without the formal permission of the author

When referring to this work, full bibliographic details including the author, title, awarding institution and date of the thesis must be given

Enlighten: Theses

<https://theses.gla.ac.uk/>  
[research-enlighten@glasgow.ac.uk](mailto:research-enlighten@glasgow.ac.uk)

# **Power Flow Analytics for Power Distribution Networks**

FANGXINTIAN YU

Submitted in fulfilment of the requirements for the  
Degree of Doctor of Philosophy

James Watt School of Engineering  
College of Science and Engineering  
University of Glasgow



University  
of Glasgow

September 2024

# Abstract

Power flow analytics play a crucial role in the management and optimisation of power distribution networks, which are essential for ensuring the reliable and efficient delivery of electrical energy. This thesis explores the advanced methodologies and applications of power flow analytics within distribution networks, focusing on both the theoretical and practical aspects of analysing and improving network power transmitting performance.

The primary objective of this research is to enhance the understanding and applications of power flow analytics in the context of power networks at distribution levels. The research studies a range of analytical techniques to investigate power flow characteristics, including traditional methods and contemporary approaches. Key areas of focus include the development and application of advanced algorithms for power flow tracing, loss allocation, and the integration of new visualization techniques to aid in the interpretation of complex data. Simulation studies are conducted to evaluate the effectiveness of proposed power flow analytics methods. Significant findings include the loss allocation of complex power in distribution networks, and important applications. The benefits of integrating visualization tools are also highlighted, to enhance decision-making and operational management in power distribution networks. Finally, the application of power flow tracing to the wheeling charges calculation problem is investigated.

The conclusions drawn from this research underscore the importance of advanced power flow analytics in addressing the challenges faced by modern distribution networks. The study demonstrates that improved analytical methods can achieve accurate network performance and loss assessment and management, and effective planning and operation of power distribution systems.

# Contents

|   |           |
|---|-----------|
| <b>Abstract</b>   | <b>i</b>  |
| <b>Acknowledgements</b>   | <b>x</b>  |
| <b>Abbreviations and Nomenclature</b>                             | <b>xi</b> |
| <b>1 Introduction</b>   | <b>1</b>  |
| 1.1 Challenges Facing the Distribution Networks . . . . .         | 1         |
| 1.2 Objectives and Motivation of the Thesis . . . . .             | 9         |
| 1.3 Outline of Thesis . . . . .                                   | 12        |
| <b>2 Power Flow Tracing and Loss Allocation</b>                   | <b>15</b> |
| 2.1 Power Flow Analysis Method . . . . .                          | 15        |
| 2.1.1 The Newton-Raphson (NR) method . . . . .                    | 15        |
| 2.1.2 The Gauss-Seidel (GS) Method . . . . .                      | 17        |
| 2.2 Power Flow Tracing Method . . . . .                           | 18        |
| 2.2.1 Power Flow Tracing Principle . . . . .                      | 20        |
| 2.2.2 Treating Power Flow without Accounting for Losses . . . . . | 21        |
| 2.2.3 Power Tracing with Average Flows . . . . .                  | 23        |
| 2.2.4 Power Tracing with Gross Flows . . . . .                    | 27        |
| 2.2.5 Power Tracing with Net Flows . . . . .                      | 30        |
| 2.2.6 Loss Allocation Algorithms . . . . .                        | 33        |
| 2.3 Loss Allocation of Distribution Networks . . . . .            | 35        |

|          |  |           |
|----------|--|-----------|
| 2.3.1    | Pro-rata (PR) Method . . . . .   | 37        |
| 2.3.2    | Proportional Allocation (PA) Method . . . . .  | 39        |
| 2.3.3    | The Marginal Method . . . . .  | 41        |
| 2.3.4    | Z-bus Method . . . . .   | 43        |
| 2.3.5    | Y-bus method . . . . .   | 46        |
| 2.3.6    | The Flow-tracing Method . . . . .  | 48        |
| 2.3.7    | The Current-based Method . . . . .   | 50        |
| 2.4      | The Current-based Algorithm . . . . .  | 51        |
| 2.4.1    | The Method Based on a Cross-term Decomposition Method . . . . .  | 51        |
| 2.4.2    | Branch Current Decomposition Loss Allocation (BCDLA) Method . . . . .  | 54        |
| 2.4.3    | The method to extend the branch current decomposition loss allocation<br>(BCDLA) method to a three-phase power distribution system . . . . . | 57        |
| 2.4.4    | Loss Allocation Methods for Unbalanced Power Distribution Networks   | 58        |
| <b>3</b> | <b>Complex Loss Allocation Method</b>  | <b>62</b> |
| 3.1      | Introduction . . . . .   | 62        |
| 3.2      | Calculation of the Primitive Impedance Matrix . . . . .  | 64        |
| 3.2.1    | Carson's Equations . . . . .   | 69        |
| 3.2.2    | Modified Carson's Equations . . . . .  | 71        |
| 3.2.3    | Primitive Impedance Matrix for Overhead Lines . . . . .  | 75        |
| 3.2.4    | Phase Impedance Matrix for Overhead Lines . . . . .  | 75        |
| 3.2.5    | Series Impedance of Underground Lines . . . . .  | 79        |
| 3.3      | Complex Power Loss Allocation Method for Unbalanced Distribution Networks  | 83        |
| 3.4      | Methods of Allocating Current Cross Terms . . . . .  | 86        |
| 3.4.1    | Proportional allocation . . . . .  | 86        |
| 3.4.2    | Quadratic allocation . . . . .   | 87        |
| 3.4.3    | Geometric allocation . . . . .   | 87        |
| 3.5      | Case Study . . . . .   | 87        |
| 3.5.1    | Calculation of the Primitive Impedance Matrix . . . . .  | 88        |

|          |   |            |
|----------|---|------------|
| 3.5.2    | Simulation Results . . . . .                                  | 89         |
| 3.5.3    | Results Analysis . . . . .                                    | 104        |
| 3.5.4    | Discussion on Losses Allocation to Neutral . . . . .          | 106        |
| 3.6      | Conclusion . . . . .  | 108        |
| <b>4</b> | <b>Colouring Visualisation Application</b>                    | <b>109</b> |
| 4.1      | Introduction . . . . .  | 109        |
| 4.2      | Flow Colouring Method . . . . .                               | 112        |
| 4.3      | Case Study . . . . .  | 115        |
| 4.3.1    | Results Analysis . . . . .                                    | 116        |
| 4.4      | Discussion . . . . .  | 121        |
| 4.5      | Conclusion . . . . .  | 128        |
| <b>5</b> | <b>Wheeling Charge Design based on Power Flow Tracing</b>     | <b>129</b> |
| 5.1      | Introduction . . . . .  | 129        |
| 5.2      | Use of System Charges . . . . .                               | 130        |
| 5.3      | Elements of Use of System Charges . . . . .                   | 131        |
| 5.4      | Allocating a portion of the use of system charges . . . . .   | 131        |
| 5.5      | Wheeling and Wheeling Charges . . . . .                       | 132        |
| 5.5.1    | The Concept of Wheeling . . . . .                             | 133        |
| 5.5.2    | Types of Wheeling . . . . .                                   | 134        |
| 5.5.3    | Nature and Duration of Wheeling . . . . .                     | 135        |
| 5.5.4    | Costs related to wheels . . . . .                             | 137        |
| 5.6      | Wheeling charges derived from embedded cost methods . . . . . | 144        |
| 5.6.1    | Postage Stamp Method . . . . .                                | 145        |
| 5.6.2    | Contract Path Method . . . . .                                | 146        |
| 5.6.3    | Distance-Based MW-Mile Method . . . . .                       | 146        |
| 5.6.4    | Power Flow-Based MW-Mile Method . . . . .                     | 147        |
| 5.7      | Proposed Concept of Wheeling Charge Calculation . . . . .     | 151        |
| 5.7.1    | Power Flow Analysis . . . . .                                 | 151        |

|          |  |            |
|----------|--|------------|
| 5.7.2    | Cost Allocation . . . . .                            | 152        |
| 5.7.3    | Case Study . . . . .                                 | 153        |
| 5.7.4    | Results Analysis . . . . .                           | 155        |
| 5.8      | Conclusion . . . . .                                 | 158        |
| <b>6</b> | <b>Conclusions and Future Work</b>                   | <b>161</b> |
| 6.1      | Conclusions . . . . .                                | 161        |
| 6.2      | Limitations . . . . .                                | 166        |
| 6.3      | Future Work . . . . .                                | 166        |
| 6.4      | Publication List . . . . .                           | 169        |
| <b>A</b> | <b>Calculation of the Primitive Impedance Matrix</b> | <b>170</b> |
| <b>B</b> | <b>Branch Loss Allocation Results</b>                | <b>174</b> |
| <b>C</b> | <b>Wheeling Charges Results</b>                      | <b>177</b> |

# List of Tables

|     |   |     |
|-----|---|-----|
| 3.1 | Active loss (W) allocated to each node calculated using proportional allocation methods . . . . .     | 89  |
| 3.2 | Reactive loss (kVar) allocated to each node calculated using proportional allocation method . . . . . | 92  |
| 3.3 | Active loss (W) allocated to each node calculated using quadratic allocation methods . . . . .        | 95  |
| 3.4 | Reactive loss (kVar) allocated to each node calculated using quadratic allocation methods . . . . .   | 97  |
| 3.5 | Active loss (W) allocated to each node calculated using geometric allocation methods . . . . .        | 100 |
| 3.6 | Reactive loss (kVar) allocated to each node calculated using geometric allocation method . . . . .    | 102 |
| 3.7 | Loss of nodes connected to the DG . . . . .   | 105 |
| 5.1 | Adjustment factors for capacity and load . . . . .  | 155 |
| 5.2 | Results at node 33 . . . . .  | 155 |
| 5.3 | Impact of node 33 on downstream nodes (pence) . . . . .   | 156 |
| 5.4 | Results for node 75 and its downstream nodes . . . . .  | 156 |
| 5.5 | Results at node 47 . . . . .  | 157 |
| 5.6 | Impact of node 47 on downstream nodes (pence) at spring/autumn . . . . .                              | 158 |
| 5.7 | Impact of node 47 on downstream nodes (pence) in Summer . . . . .                                     | 159 |
| 5.8 | Impact of node 47 on downstream nodes (pence) in Winter . . . . .                                     | 160 |

|     |  |     |
|-----|--|-----|
| B.1 | The results of the loss allocation of modified IEEE 123-node system(unit - Watts)  | 174 |
| C.1 | The one-day wheeling charges for spring and autumn(pence) . . . . .  | 177 |
| C.2 | The one-day wheeling charges for summer(pence) . . . . .   | 180 |
| C.3 | The one-day wheeling charges for winter((pence) . . . . .  | 182 |
| C.4 | The spring and autumn wheeling charges for conventional and sustainable energy sources that do not differentiate between them(pence) . . . . . | 185 |

# List of Figures

|      |  |    |
|------|--|----|
| 1.1  | Global energy consumption . . . . .                                    | 3  |
| 1.2  | Competitive electricity market [1] . . . . .                           | 4  |
| 1.3  | Prosumers in the power system [2] . . . . .                            | 8  |
| 1.4  | Layout of the thesis . . . . .   | 14 |
| 2.1  | Four-line system illustrating power flow tracing principle. . . . .    | 21 |
| 2.2  | Proportional allocation method . . . . .                               | 40 |
| 2.3  | Schematic diagram of voltage and current of two-port network . . . . . | 47 |
| 2.4  | A four-node system . . . . .   | 52 |
| 2.5  | Two-node system for loss allocation. . . . .                           | 60 |
| 3.1  | Magnetic fields . . . . .  | 64 |
| 3.2  | Two-conductor system . . . . .   | 67 |
| 3.3  | The equivalent primitive circuit. . . . .                              | 68 |
| 3.4  | Conductor images . . . . .   | 70 |
| 3.5  | Four-wire grounded neutral line segment . . . . .                      | 76 |
| 3.6  | Three-phase line segment model . . . . .                               | 79 |
| 3.7  | Three-phase underground with additional neutral . . . . .              | 80 |
| 3.8  | Concentric neutral cable . . . . .                                     | 80 |
| 3.9  | Distances between concentric neutral cables . . . . .                  | 82 |
| 3.10 | Equivalent neutral cables . . . . .                                    | 83 |
| 3.11 | Modified IEEE 123-node system with renewable DG units . . . . .        | 88 |

|      |   |     |
|------|---|-----|
| 3.12 | Overhead line spacings . . . . .  | 89  |
| 3.13 | The process flow chart for the calculation stages . . . . .   | 92  |
| 3.14 | The cross-term allocation factor $\beta$ versus the ratio $i^e/i_f$ for different methods . . . . . | 105 |
| 4.1  | Parameters of RGB colour space. . . . .   | 114 |
| 4.2  | Comparison of initial values of different blue parameters . . . . .                                 | 115 |
| 4.3  | Power Flow Visualisation . . . . .  | 117 |
| 4.4  | Power flow at node 13 . . . . .   | 118 |
| 4.5  | Power flow at node 18 . . . . .   | 119 |
| 4.6  | Power flow at node 75 . . . . .   | 120 |
| 4.7  | Power flow at node 25 . . . . .   | 120 |
| 4.8  | Power flow at branches 44-47 . . . . .  | 121 |
| 4.9  | Power flow at branches 27-33 . . . . .  | 122 |
| 4.10 | Relationship between distribution network loss allocation and carbon tracing. . . . .               | 123 |
| 4.11 | The application of power flow tracing visualisation on distribution network stakeholders. . . . .   | 125 |
| 4.12 | Desired software interface . . . . .  | 127 |
| 5.1  | Basic Wheeling Topology . . . . .   | 134 |
| 5.2  | Power flow analysis along network lines. . . . .  | 152 |
| 5.3  | Modified IEEE 123-node system with renewable DG units . . . . .                                     | 154 |

# Acknowledgements

First and foremost, I would like to express my deepest gratitude to my supervisor, Dr Jin Yang, for his unwavering support, guidance, and encouragement throughout my PhD journey. His insightful feedback, invaluable expertise, and constant motivation have been instrumental in the completion of this thesis.

My heartfelt thanks go to my colleagues and friends in my group, whose warm concern and intellectual exchange have made this journey enjoyable and rewarding. Special thanks to Haiyang You, Yue Qi and Jiwei Li for their assistance with data analysis and to Yang Ding and Miaorui Ma for their encouragement and support during challenging times.

I would like to acknowledge the financial support provided by my parents, which has been crucial in facilitating the research and enabling access to essential resources.

To my family, I am deeply appreciative of their love, patience, and understanding. Their unwavering support and encouragement have been a source of strength and inspiration throughout this endeavor.

Finally, I would like to extend my gratitude to all those who have contributed to this research in various capacities. Your support and contributions have been invaluable and are deeply appreciated.

Thank you all for being a part of this journey.

# Abbreviations and Nomenclature

|       |  |
|-------|--|
| ADMS  | Advanced Distribution Management Systems     |
| AMI   | Advanced Metering Infrastructure             |
| BCDLA | Branch Current Decomposition Loss Allocation |
| CLP   | Classical Loss Partitioning                  |
| CTDM  | Cross-term Decomposition Method              |
| DERs  | Distributed Energy Resources                 |
| DG    | Distributed Generation                       |
| DLCs  | Direct Loss Coefficients                     |
| DNs   | Distribution Networks                        |
| DSM   | Demand-side Management                       |
| DSO   | Distribution System Operator                 |
| EPA   | Environmental Protection Agency              |
| KCL   | Kirchhoff's Current Law                      |
| KVL   | Kirchhoff's Voltage Law                      |
| LAF   | Loss Allocation Factor                       |
| MLC   | Marginal Loss Coefficient                    |
| MM    | Modulus Method                               |
| MPLAP | Multi-Phase Losses Allocation Method         |

|       |   |
|-------|---|
| MW    | Megawatts                                     |
| MWM   | MW-mile Method                                |
| NLAFs | Neutral Loss Allocation Factors               |
| PA    | Proportional Allocation                       |
| PD    | Power Demand                                  |
| PLAFs | Phase Loss Allocation Factors                 |
| PMUs  | Phasor Measurement Units                      |
| PR    | Pro-rata                                      |
| PV    | Photovoltaic                                  |
| R&D   | Research and Development                      |
| RCLP  | Resistive Component based Losses Partitioning |
| RES   | Renewable Energy Sources                      |
| RGB   | Red, Green, Blue                              |
| SCADA | Supervisory Control and Data Acquisition      |
| T&D   | Transmission and Distribution                 |
| ZCM   | Zero Counter Flow Method                      |

**Complex Loss Allocation Method**

|  |  |
|--|--|
| $D_{i-n}$  | Distance between conductor $i$ and conductor $n$ with the unit $ft$                |
| $GMR_i$  | Geometric mean radius of conductor $i$ with the unit $ft$                          |
| $GMR_d$  | Geometric mean radius of dirt  |
| $\hat{z}_{ii}$   | Self-impedance of conductor $i$ in $\Omega/mile$                                   |
| $\hat{z}_{ij}$   | Mutual impedance between conductors $i$ and $j$ in $\Omega/mile$                   |
| $r_i$  | Resistance of conductor $i$ in $\Omega/mile$                                       |
| $\omega = 2\pi f$                                      | System angular frequency in radians per second                                     |
| $RD_i$   | Radius of conductor $i$ in ft  |
| $D_{ij}$   | Distance between conductors $i$ and $j$ in ft                                      |
| $S_{ij}$   | Distance between conductor $i$ and image $j$ in ft                                 |
| $N_{(j)}$  | The set of contributing nodes downstream of branch $j$                             |
| $\mathbf{L}^{(j)}$                                     | Power loss on branch $j$   |
| $\mathbf{Z}^{(j)}, \mathbf{R}^{(j)}, \mathbf{X}^{(j)}$ | Matrices of the impedance, resistance and reactance of the branch $j$ respectively |
| $\beta^{kq}$   | Allocation factor matrix   |
| $\beta_e, \beta_f$                                     | Cross-term allocation factors  |

**Wheeling Charge Calculation**

$WC_i$       Wheeling charge at bus  $i$

$PLoss_{j,i}$       Line flow in line  $j$  induced by transaction on bus  $i$

$A, C_j$       Annualized cost of line  $j$

$M$       Set of branches which connect node  $k$  to the root node

$\beta^{kq}$       Allocation factor matrix

$C_k$       the cost of circuit  $k$

$f_k(u)$        $k$ -circuit flow caused by customer  $u$

$\bar{f}_k$       the capacity of  $k$ -circuit

# Chapter 1

## Introduction

### 1.1 Challenges Facing the Distribution Networks

Nowadays, the power industry continues to develop on a global scale, driven by technological advancements, environmental concerns, and changing economic paradigms. This evolution necessitates a more open market architecture, capable of accommodating diverse dispersed energy sources, dynamic pricing mechanisms, and increased consumer participation [3]. The traditional model of centralized, monopolistic power generation and distribution is giving way to a more decentralized, competitive landscape that demands new regulatory frameworks and market structures [4].

Energy consumers, ranging from individual households to large industrial users, are becoming increasingly engaged in their electricity usage. This engagement extends beyond passive consumption to active participation in energy production through distributed generation, demand response programs, and energy management practices [5]. Electricity has become a cornerstone of modern society and economy, powering everything from essential services and industrial processes to the vibrant digital economy. The reliability, affordability, and sustainability of electricity supply are now critical factors in economic development, social equity, and environmental management.

At present, the power industry is undergoing important and profound changes all around the world. These changes are multifaceted, involving technological innovations such as smart grids and renewable energy integration, market reforms aimed at increasing competition and efficiency, and policy shifts driven by climate change mitigation goals. The transition from fossil fuel-dominated energy systems to low-carbon alternatives is reshaping the entire energy landscape, as shown in Figure 1.1 [6], where changes all around the world are highlighted by the IEA (International Energy Agency), affecting everything from power generation technologies to grid management practices. The global energy crisis and the net zero target by 2050 have spurred a variety of new initiatives, particularly in advanced economies and China, aimed at accelerating the adoption of clean energy. While the specific measures differ across regions, they consistently focus on increasing the proportion of renewables in electricity generation, promoting the adoption of electric vehicles, and enhancing energy efficiency. Moreover, many countries have implemented policies to support the diversification of supply chains for clean energy technologies. These policies include initiatives to boost the manufacturing of clean energy technologies, such as the Inflation Reduction Act in the United States, the Net Zero Industry Act in the European Union, and the Production Linked Incentives scheme in India.

Most countries are promoting the commercialization of electricity and energy in their own ways, with different policies and governmental strategies tailored to their specific economic, geographic, and social contexts [7]. Some nations are focusing on unbundling vertically integrated utilities, while others are emphasizing the creation of wholesale electricity markets or incentivizing renewable energy deployment. These diverse approaches reflect the complex balance between ensuring energy security, promoting economic efficiency, and meeting environmental targets.

To build an effective electricity market and gradually eliminate monopolies, it is necessary to achieve fairness, equality, and transparency among electricity market participants. This involves creating level playing fields for different types of generators, including traditional large-scale plants and emerging distributed resources. It also requires transparent pricing mechanisms that accurately reflect the costs of generation, transmission, and distribution, as well as externalities

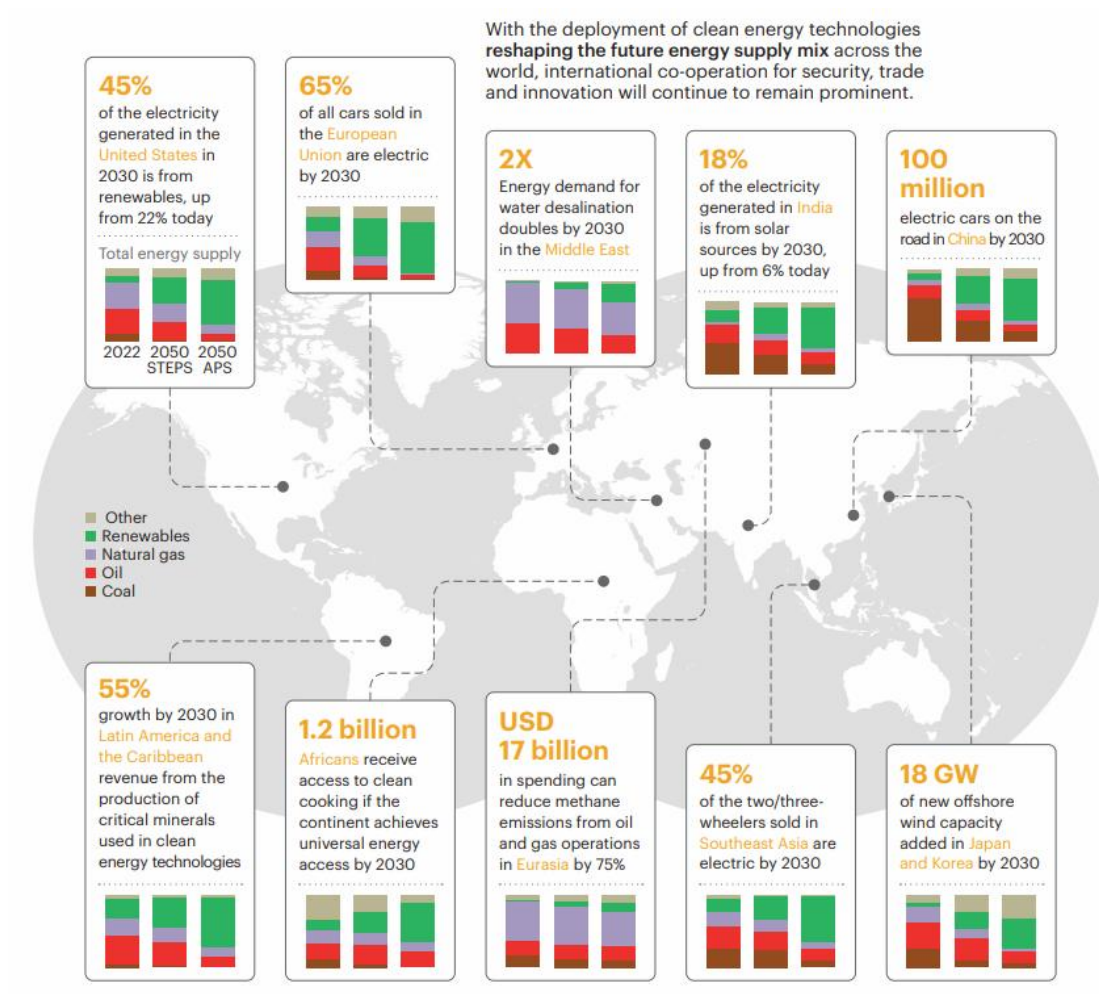


Figure 1.1: Global energy consumption

such as environmental impacts [8]. Ensuring non-discriminatory access to transmission and distribution networks is crucial for fostering competition and innovation.

Furthermore, the pursuit of fairness and transparency extends to the retail level, where consumers should have access to clear information about their energy options, pricing structures, and the environmental impacts of their consumption. Smart metering and advanced data analytics are enabling more sophisticated pricing models and customer engagement strategies, empowering consumers to make informed decisions about their energy usage [9, 10].

The transition to more open and competitive electricity markets also presents several challenges. As illustrated in Figure 1.2, generation companies compete in the wholesale market, where retailers purchase energy based on demand in the retail market. Consumers then acquire energy

from the competitive retail market, although large consumers often buy directly from the wholesale market. The distribution system operator (DSO) is responsible for maintaining the distribution systems. However, ensuring a balance between generation and consumption is critical for maintaining system operation near the nominal frequency and adhering to voltage limits [11]. These include ensuring system reliability in the face of increased variability from renewable sources, managing the social impacts of industry restructuring, and developing appropriate regulatory frameworks that can keep pace with technological and market innovations. Cybersecurity concerns and the need for significant infrastructure investments add further complexity to this transition.

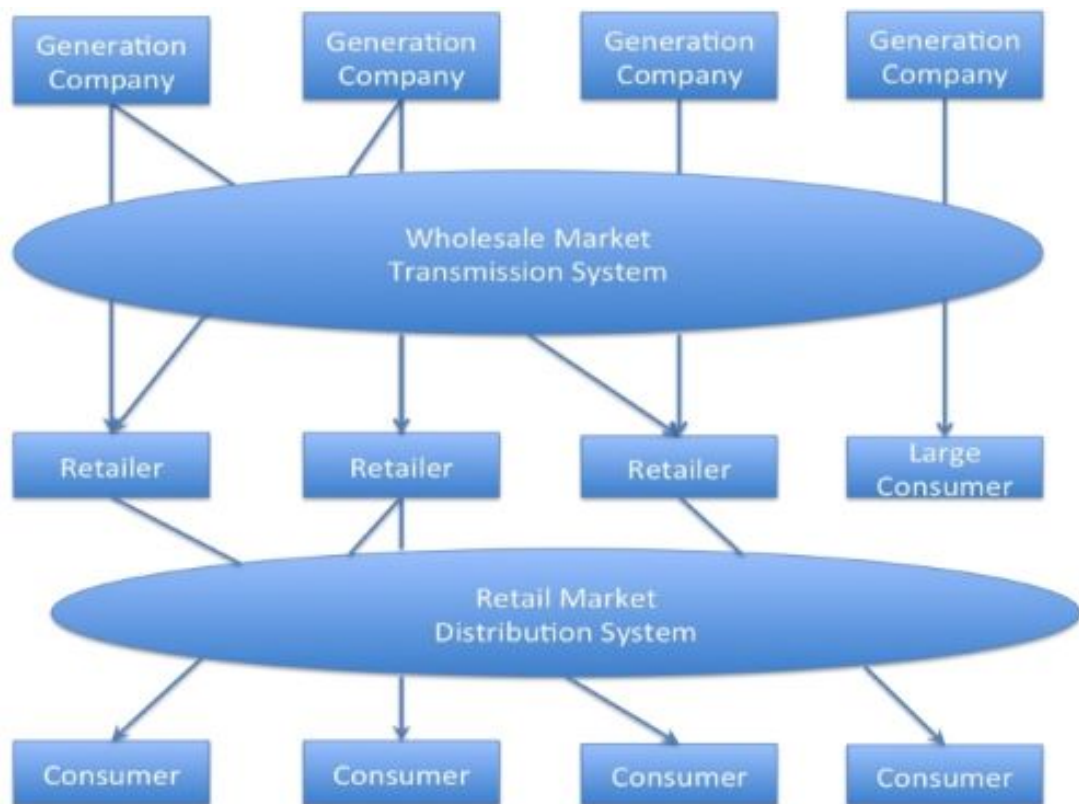


Figure 1.2: Competitive electricity market [1]

As the power industry evolves, international cooperation and knowledge sharing will be essential in addressing shared challenges and leveraging best practices [12]. The global nature of climate change and the interconnection of energy markets necessitate collaborative approaches to policy development, technology transfer, and market design. By working towards fair, transparent, and efficient electricity markets, countries can not only improve their domestic energy systems but

also contribute to global efforts for sustainable development and climate change mitigation.

Primary energy sources, including fossil fuels like coal, oil, and natural gas, as well as renewable resources such as wind, solar, and hydropower, form the foundation of the global energy supply. The dominance of fossil fuels in the global energy mix presents significant challenges, including environmental degradation, greenhouse gas emissions, and the depletion of finite resources [13, 14]. The transition to renewable energy sources is essential to mitigate these issues, but it also introduces new complexities for distribution networks, such as the need for grid integration of intermittent energy sources and the management of decentralized generation systems.

The global energy landscape is further complicated by the uneven geographical distribution of energy resources. Fossil fuels are concentrated in specific regions, such as oil in the Middle East, and natural gas and coal in Russia and North America. This uneven distribution creates geopolitical tensions and dependencies, as energy-importing countries must secure stable and affordable supplies from resource-rich areas [15–17]. Additionally, renewable energy potential varies significantly by location, with solar power being more viable in equatorial regions, while wind power is more effective in coastal and high-altitude areas. These geographical disparities necessitate the development of extensive and resilient distribution networks capable of transporting energy across vast distances, often through challenging and diverse terrains.

Furthermore, the global distribution of energy consumption is highly imbalanced, with developed countries consuming a disproportionate share of the world's energy. This disparity is intensified by the rapid industrialization and urbanization of developing nations, particularly in Asia and Africa, where energy demand is surging [18]. Meeting the energy needs of these growing economies while ensuring sustainability and minimizing environmental impacts poses a formidable challenge for distribution networks. The urgent need to expand and upgrade infrastructure in these regions is often hampered by financial, technical, and political constraints.

In conclusion, the challenges facing distribution networks are multifaceted and intricately linked to broader issues, including the new requirements of primary energy sources, rapidly changing global energy demands, and the vast geographical distribution of energy resources. As the world

transitions towards a more sustainable energy future, distribution networks must adapt to accommodate the shifting energy landscape, integrate new technologies, and address the inequalities in energy access and consumption. This adaptation requires not only significant investments in infrastructure and technology but also a concerted effort to develop policies and strategies that promote energy security, efficiency, and equity on a global scale.

In power systems, electric energy undergoes several processes, including power generation, conversion, transmission, and distribution, with the distribution network serving as the infrastructure that directly supplies power to end users. Distribution networks play a critical role in the efficient and reliable supply of electrical power to end-users. These networks consist of a complex web of interconnected components, including transformers, cables, and other equipment. Consequently, distribution networks encounter various challenges in the context of the rapidly evolving energy system.

In previous times, the transmission and distribution (T&D) systems were planned and constructed primarily to meet peak demand while ensuring reliability and service quality standards. It functioned as a passive delivery network, following a radial approach to deliver energy to consumers [19]. Consumers simply consumed the energy they required or desired, while the wholesale infrastructure supplied it without the necessity for real-time management by the T&D system. Distribution operations primarily focused on construction, maintenance, and outage management rather than actively managing energy delivery.

Today, customers are increasingly utilizing the grid to balance their own energy generation and consumption, relying on it as a backup source when their own generation is unavailable. As shown in Figure 1.3, the main components and energy/control flows in a typical smart consumer/prosumer model are outlined. In this setup, a home can acquire energy either directly from the grid or from its own resources, such as a photovoltaic (PV) array. This energy can be consumed by both controllable and non-controllable loads or stored in batteries. The operation of non-controllable loads is based on user preferences, while controllable loads can be scheduled at different times of the day to lower the electricity bill. This scheduling is managed by a home

energy management system, which uses electricity price signals and predicted PV generation to determine the optimal operation of controllable loads alongside the PV-battery system. If the home generates surplus energy from its own resources (PV and batteries), it can sell this excess to the utility grid to generate additional revenue [20]. They anticipate the ability to feed surplus generation back into the grid and receive compensation for it, without encountering restrictions on their production. Additionally, they still expect reliable grid access when needed [21]. Addressing these evolving consumer demands requires a fundamental shift in the architecture of the distribution grid, as well as adoption of new technologies, planning methods, and operational practices [22]. Consumers are requiring for change of business models, while regulators and policymakers are working to meet and even encourage these demands. The emergence of terms such as "smart grid", "grid of the future" and "grid modernisation" implies the importance of building a smart grid that can be monitored and controlled in real time [23]. This will enable the grid to provide reliable, safe and secure services, as well as enable customers to actively participate in and benefit from a wider and more diverse range of market opportunities and services. Building such a smart grid is critical but a challenging task.

To address the challenges facing distribution networks, power flow tracing serves as a valuable tool that enables utilities to optimize grid operations, enhance grid reliability, and integrate renewable energy sources and distributed energy resources (DERs). Firstly, power flow tracing provides utilities with detailed insights into how electricity flows through the distribution network. By tracking power flows in real time, utilities gain a comprehensive understanding of network behavior, allowing them to identify congestion, voltage violations, and other operational issues more effectively [24]. Secondly, power flow tracing enables utilities to implement demand-side management (DSM) programs more effectively. By understanding how electricity flows through the network and identifying areas of high demand or congestion, utilities can deploy DSM initiatives to reduce peak demand, balance load profiles, and enhance grid efficiency. Thirdly, power flow tracing facilitates the integration of renewable energy sources (RES) into distribution networks [25]. By accurately tracking the contributions of RES to power generation and grid injection, utilities can manage the variability and intermittency of renewable genera-

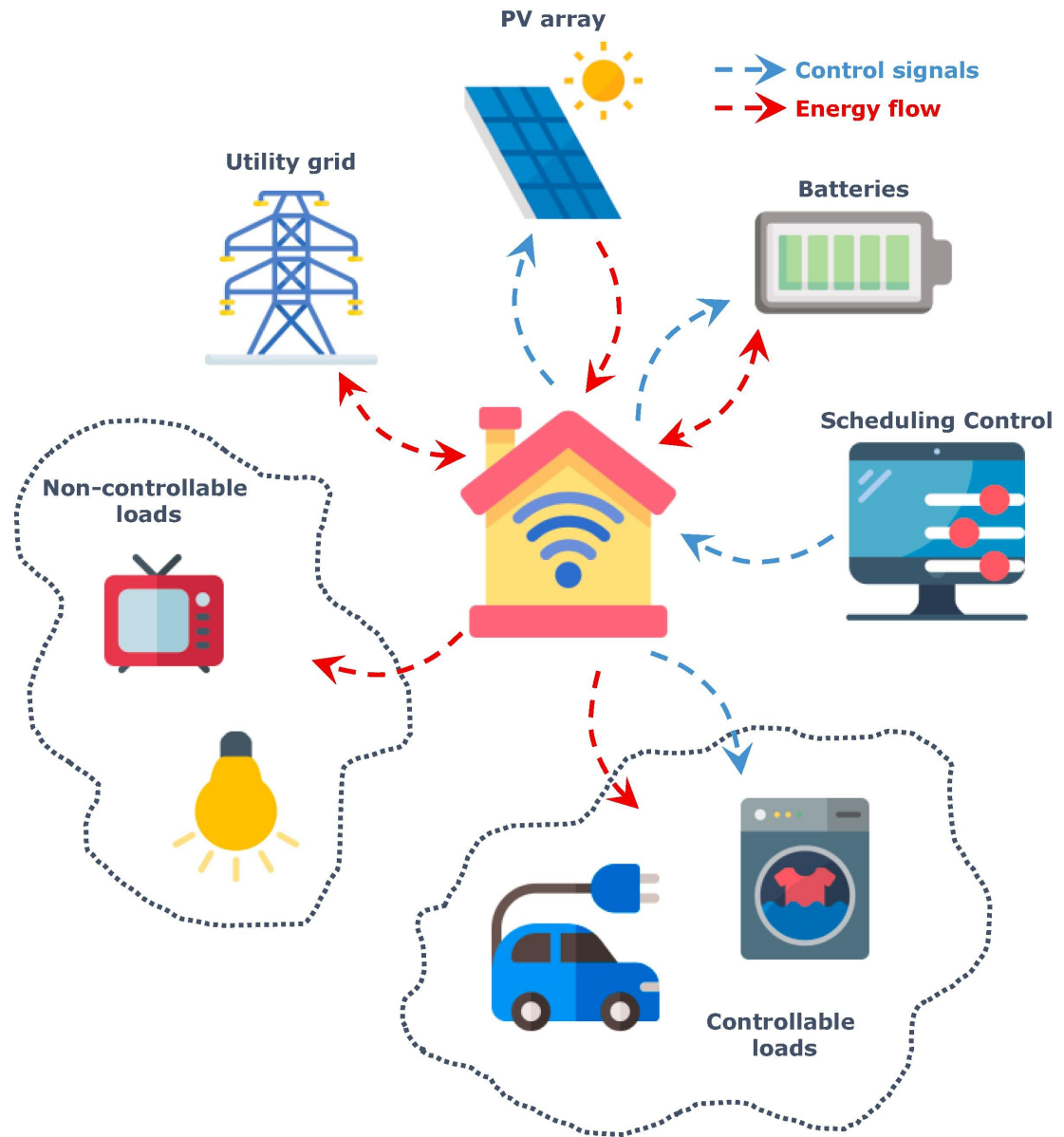


Figure 1.3: Prosumers in the power system [2]

tion, optimize its utilization, and ensure smooth grid integration without compromising reliability. Lastly, power flow tracing allows utilities to accurately allocate power flows to individual customers, generators, and grid elements. This enables utilities to implement fair and transparent billing practices, accurately bill customers for their energy usage, and allocate revenues appropriately, fostering trust and transparency in the energy market.

There has been an ongoing discussion regarding methods for power flow tracing in distribution networks. Loss allocation has been extensively studied as a solution for power flow tracing because it relies on actual electrical data from the grid. This thesis describes the current state of

development in loss allocation in distribution networks and provides a rationale for the research undertaken. On this basis, this research proposes a new method to solve the complex power loss allocation in unbalanced distribution networks. Based on the loss allocation method, the distribution network currents have been studied visually as a power colouring method. Finally, based on the proposed loss allocation method, a wheeling charges allocation method is proposed.

## 1.2 Objectives and Motivation of the Thesis

The increasing complexity and dynamic nature of modern power distribution networks present significant challenges that require advanced analytical tools and methodologies to ensure efficient and reliable operation. This PhD thesis, titled "Power Flow Analytics for Power Distribution Networks," is motivated by the need to address these challenges through the development and application of sophisticated power flow analytics. The primary objectives of this thesis are to enhance the understanding of power flow behavior in distribution networks, improve the accuracy and efficiency of power flow calculations, and propose innovative solutions to optimize network performance under various operating conditions.

The motivation for this research stems from the evolving landscape of power distribution, characterized by the integration of renewable energy sources, the proliferation of distributed generation, and the growing importance of smart grid technologies. These developments have fundamentally altered the traditional unidirectional flow of power from centralized generation to end-users, introducing bidirectional flows and increasing the complexity of power distribution networks. As a result, conventional power flow analysis techniques, which were designed for simpler, radial networks, are often inadequate for addressing the challenges posed by modern distribution systems.

This thesis aims to develop advanced power flow analytics that can accurately model and analyze the intricate behaviors of contemporary distribution networks. By improving the precision of power flow calculations, the research seeks to enable better decision-making for network planning, operation, and control. Moreover, the thesis explores the potential of innovative com-

putational methods and algorithms to enhance the scalability and efficiency of power flow analysis, making it feasible to handle large-scale networks with high penetration of renewable energy and distributed generation.

Another key motivation for this research is the need to address the challenges associated with the increasing variability and uncertainty in power generation and consumption. As renewable energy sources, such as solar and wind, become more prevalent, their inherent variability introduces significant fluctuations in power flows, which can impact network stability and reliability. The thesis investigates methods to incorporate these uncertainties into power flow analysis, enabling more robust and resilient network designs and operations.

In addition, power flow tracing visualization within electrical distribution networks is the second objective of this thesis. As the complexity of power distribution systems increases, particularly with the integration of renewable energy sources, electric vehicles, and distributed generation, traditional power flow analysis techniques are no longer sufficient to ensure the reliable and efficient operation of the grid. This thesis aims to address these challenges by advancing the tools available for tracing and visualizing power flows, providing deeper insights into how electricity moves through distribution networks in real-time.

The motivation behind this research stems from the growing need for network operators to understand the dynamic behavior of power flows in increasingly complex and distributed networks. With the proliferation of decentralized energy resources, the traditional unidirectional flow of electricity is being replaced by multidirectional flows that vary based on generation and consumption patterns.

Power flow tracing visualization offers a solution by allowing operators to see the real-time paths of electricity within the network, identify which sources are supplying specific loads, and understand how network reconfigurations impact these flows. Enhanced visualization tools not only improve operational decision-making but also support planning and investment strategies by revealing critical insights into network performance under various scenarios.

This thesis is driven by the necessity to equip modern distribution networks with advanced analytical capabilities that can keep pace with the evolving demands of the energy landscape. By focusing on power flow tracing and its visualization, the research aims to contribute to the development of smarter, more resilient, and more efficient distribution systems that can better accommodate the complexities of modern energy generation and consumption.

Finally, wheeling charges based on power flow tracing within the power system is another contribution of this thesis. As the energy market becomes more deregulated and competitive, accurate and fair allocation of transmission costs is crucial for ensuring an efficient and equitable power system. Wheeling charges need to be determined in a manner that reflects the actual usage of the network. This thesis will enhance the existing approaches to wheeling charge calculation by integrating power flow tracing techniques, thereby providing a more transparent and precise method for cost allocation.

The motivation for this research arises from the increasing complexity of power systems, characterized by the integration of renewable energy sources, decentralized generation, and the rise of bilateral power trading. Traditional methods for calculating wheeling charges, such as the postage stamp or contract path methods, often fail to accurately reflect the true usage of transmission networks, leading to potential inefficiencies and inequities in cost distribution. Power flow tracing, which tracks the actual flow of electricity through the network, offers a promising alternative by directly linking the charges to the physical paths taken by the power.

This research is driven by the need to create a more fair and efficient framework for cost allocation in transmission networks. By utilizing power flow tracing, the thesis aims to develop a methodology that not only improves the accuracy of wheeling charge calculations but also enhances the transparency of the process. This is particularly important in a deregulated market environment where stakeholders demand clarity and fairness in cost allocation.

Moreover, the integration of power flow tracing into wheeling charge determination could help mitigate disputes between market participants, foster more efficient use of transmission infrastructure, and support the ongoing transition towards more sustainable and distributed energy

systems. The ultimate goal is to contribute to the development of a pricing mechanism that reflects the true economic value of transmission services, thereby promoting more effective and balanced investment in the grid.

### **1.3 Outline of Thesis**

This thesis is presented in the following chapters with details and relationships of chapters as shown in the figure below:

#### **Chapter 2**

Literature review of power system power tracing is presented. Based on the principles of power flow tracing, several common power flow tracing algorithms are described in detail. Loss allocation algorithms have been studied in more detail as methods that provide more feedback on the true and real-time situation of the power system. Various methods for distribution network loss allocation are described in detail in this chapter. Eventually, the current-based loss allocation method was further investigated as it was considered to be relatively more efficient based on Kirchhoff's laws, which are the most fundamental in power systems.

#### **Chapter 3**

This chapter presents a complex power loss allocation method for unbalanced distribution networks. Starting from the impedance matrix, as the method is aimed at multi-phase distribution networks, a method for calculating the primitive impedance matrix is first identified. After determining the primitive impedance matrix, a loss allocation method for complex power is proposed based on Kirchhoff's law and the principle of current summation. The resulting current multiplication terms were then subjected to a study of current cross term allocation methods. Finally, the loss allocation algorithm for complex power is simulated in a modified IEEE123 node system (incorporating three distributed generation) and the results are discussed. The proposed method can effectively and equitably allocate losses to each phase and reflect the real situation in the power system.

**Chapter 4**

A methodology for visualising power system flow is proposed. Separate colouring of the currents of different energy sources according to the energy sources in the power system enables the visualisation of the power flow by means of the RGB principle. Based on the results of the trend tracing in Chapter 2, the method was used for power flow colouring in the same IEEE123 node system. The results of the power flow visualisation can reflect the real and effective current situation. And the visualisation results can provide effective information to the various participants in the power system.

**Chapter 5**

A detailed description of the power system wheeling fee methodology is provided. An wheeling fee allocation method based on loss allocation is proposed based on the loss allocation method in Chapter 2. The method effectively utilises the results of power flow tracing and fully considers the power flow paths of power transactions. The method was simulated in a modified IEEE123 node system. Simulation results show that the method is fair and effective. In addition, the pricing of wheeling charges is different for transactions involving fossil energy and those involving renewable energy. Not only does it provide a degree of security for renewable energy generation, but it also provides incentives for users to use renewable energy.

**Chapter 6**

A summary of the main research findings and contributions of the thesis is presented, along with conclusions drawn from the work and recommendations for future research.

Overall, the complex power loss allocation method proposed in Chapter 3 is a fair loss allocation method that meets expectations because it is based on circuit theoretical principles and has essentially no assumed premises. After implementing loss allocation based on this method, based on its results it is possible to visualise the power flow in the distribution network, which is the work of Chapter 4. In addition, the loss allocation method of Chapter 2 can be used to solve the problem of wheeling charges, i.e., the work of Chapter 5.

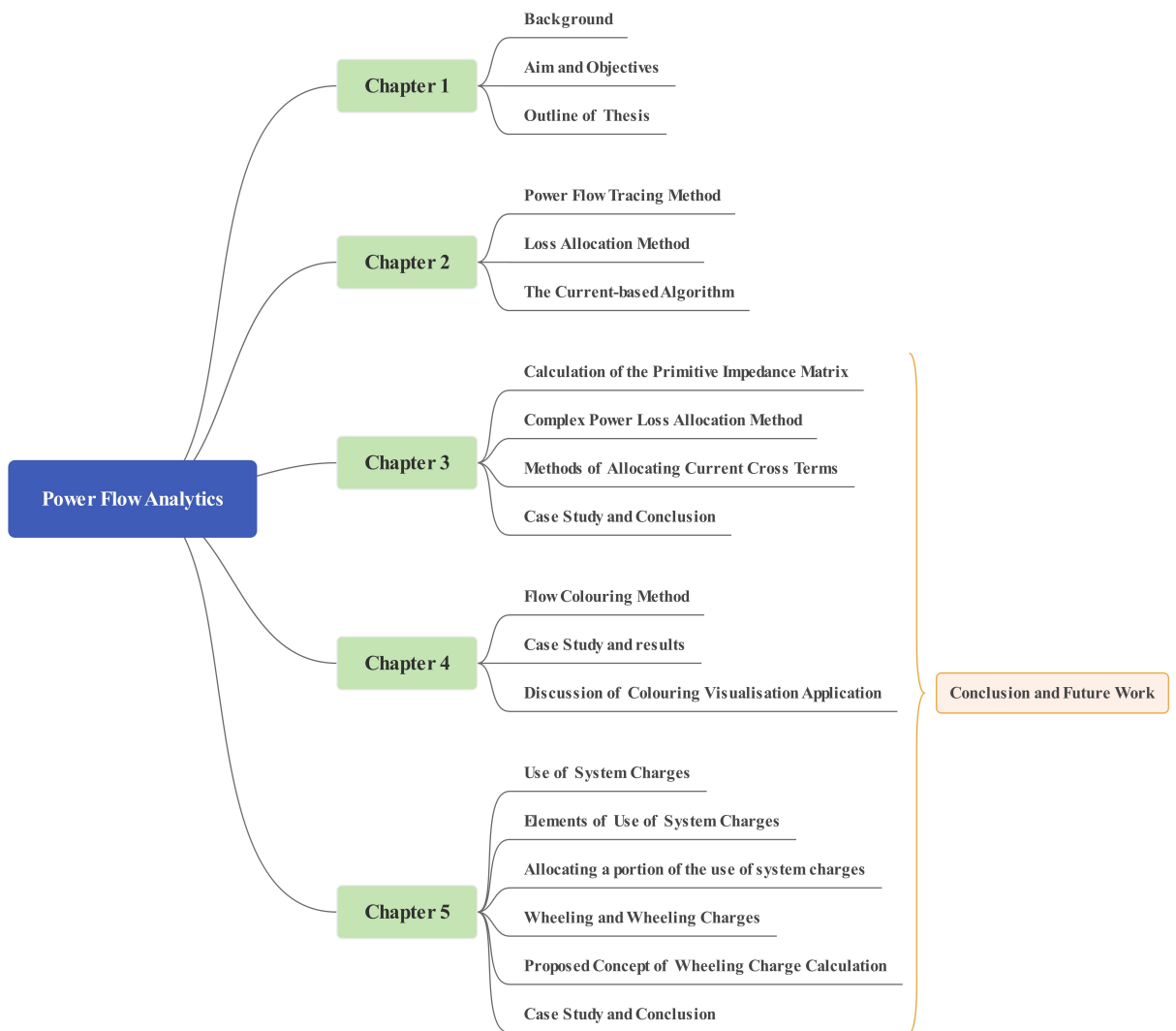


Figure 1.4: Layout of the thesis

# Chapter 2

## Power Flow Tracing and Loss Allocation

### 2.1 Power Flow Analysis Method

Before delving into the distribution network power flow tracing technique, it is important to highlight two foundational methods in power flow analysis: the Newton-Raphson (NR) method and the Gauss-Seidel (GS) method. These widely used approaches provide the basis for solving power flow equations and understanding system behavior, forming a critical starting point for advanced power flow techniques.

#### 2.1.1 The Newton-Raphson (NR) method

The Newton-Raphson (NR) Method The Newton-Raphson (NR) method is one of the most widely used techniques for solving nonlinear equations in power flow analysis. It is particularly valued for its high accuracy and fast convergence, especially in large-scale and complex power systems. The method is based on iterative numerical linearization, where nonlinear power flow equations are approximated using a first-order Taylor series expansion.

In the context of power systems, the NR method begins by expressing the power flow equations as nonlinear algebraic equations relating bus voltages, angles, and power injections. These equations can be represented compactly as:

$$F(x) = 0 \quad (2.1)$$

where  $F(x)$  is the vector of power flow mismatches, and  $x$  is the vector of state variables, typically bus voltage magnitudes and phase angles. The method then solves for corrections to the state variables,  $\Delta x$ , using the Jacobian matrix,  $J$ , which contains the partial derivatives of the power flow equations with respect to the state variables:

$$J(x_k) \cdot \Delta x_k = -F(x_k) \quad (2.2)$$

Here,  $x_k$  represents the state variables at the  $k$ -th iteration. The updated state variables are computed as:

$$x_{k+1} = x_k + \Delta x_k \quad (2.3)$$

The process is repeated until the power flow mismatches fall below a predefined tolerance, ensuring that the solution converges to a steady-state operating point.

One of the primary advantages of the NR method is its quadratic convergence property, meaning that the solution accuracy improves exponentially with each iteration when the initial guess is sufficiently close to the true solution. This makes it ideal for large-scale systems, where computational efficiency and precision are critical. However, the NR method requires the repeated computation and inversion of the Jacobian matrix, which can be computationally intensive, especially for systems with a high number of buses. To mitigate this, modern implementations often use sparse matrix techniques to improve efficiency.

Overall, the NR method remains a cornerstone of power flow analysis, offering a robust and reliable approach to solving the nonlinear equations that underpin power system operations.

### 2.1.2 The Gauss-Seidel (GS) Method

The Gauss-Seidel (GS) Method The Gauss-Seidel (GS) method is one of the earliest and simplest iterative techniques used for power flow analysis. Its computational simplicity and ease of implementation make it an attractive choice for smaller power systems or as a starting point for understanding iterative solution methods. The GS method is based on the successive approximation of state variables, updating each variable individually while using the most recently calculated values in subsequent iterations.

In power flow analysis, the GS method involves solving the nonlinear power flow equations iteratively for each bus. For a power system with  $n$  buses, the power flow equations for each bus can be expressed as:

$$P_i - jQ_i = V_i \sum_{j=1}^n Y_{ij} V_j^* \quad (2.4)$$

where  $P_i$  and  $Q_i$  are the real and reactive power injections at bus  $i$ ,  $V_i$  and  $V_j$  are the voltages at buses  $i$  and  $j$ ,  $Y_{ij}$  is the element of the admittance matrix, and  $V_j^*$  is the complex conjugate of  $V_j$ . The equation is rearranged to solve for the bus voltage  $V_i$ :

$$V_i = \frac{1}{Y_{ii}} \left( \frac{P_i - jQ_i}{V_i^*} - \sum_{j \neq i} Y_{ij} V_j \right) \quad (2.5)$$

In each iteration, the voltage at a particular bus is updated using the most recently computed values of the voltages at other buses. The process begins with an initial guess for the bus voltages and continues iteratively until the changes in voltage magnitudes and angles between successive iterations are below a predefined tolerance.

The main advantages of the GS method are its simplicity and minimal memory requirements, as it does not require the computation of a Jacobian matrix. This makes it computationally efficient for smaller systems or when high accuracy is not critical. However, the GS method has a slower convergence rate compared to more advanced techniques like the Newton-Raphson method. Its

convergence is linear, meaning the solution accuracy improves incrementally with each iteration. Moreover, its convergence depends on the ordering of buses and the system's condition; poorly conditioned systems or those with high R/X ratios may exhibit slower or even non-convergent behavior.

Despite its limitations, the GS method is still a useful tool for understanding basic power flow analysis and for solving simple or approximate power flow problems. It also provides a foundation for more sophisticated iterative techniques, such as the Newton-Raphson method.

## 2.2 Power Flow Tracing Method

The complexity of modern power systems has increased significantly due to the integration of renewable energy sources, distributed generation, and the growing demand for electricity [26]. In this evolving landscape, understanding and managing the flow of electrical power within a network has become critical for ensuring the stability, reliability, and efficiency of power distribution. Power flow tracing methods have emerged as essential tools in analyzing the movement of electricity across different components of a power grid. These methods enable utilities and grid operators to trace the path of electricity from generation sources through transmission lines to various load points, providing valuable insights into the network's operational characteristics.

Power flow tracing plays a pivotal role in a wide range of applications, including loss allocation, congestion management, and the determination of wheeling charges. By identifying the contributions of individual generators to specific loads, these methods offer a transparent and fair approach to cost allocation among users of the transmission network. Moreover, power flow tracing techniques are crucial in the context of deregulated electricity markets, where accurate allocation of costs and benefits is essential for market participants.

The power flow tracing method has many applications in the power market, playing an important role in various aspects of grid operation, planning, and market design. This thesis mainly studies the basic principles of the current commonly used power flow tracing technology and the problem of network loss allocation based on power flow tracing technology.

Power flow tracing involves resolving how the injected power from each node distributes across the outgoing branches, given that the power flow distribution is already determined. This entails identifying which loads are served by specific generators and the quantity of power from any generator, as well as discerning which power source provides energy to each load and the corresponding proportion utilized by any load. While power flow tracing technology enjoys widespread recognition, there remain divergent viewpoints regarding the specific resolution of certain issues. A solution suitable for large-scale systems was introduced by Kirschen et al. [27]. Kirschen and Strbac [28] devised a power flow tracing scheme based on current decomposition principles. Macqueen and Irving [29] provided the suggestion of allocating losses according to the square of the current. Wei and Chen [30] utilized graph theory to efficiently determine the sequence for tracing nodes in power systems. These studies have researched on specific facets of power flow tracing technology extensively. However, there remain areas requiring further investigation. These include refining the allocation principle and handling of network losses, addressing the coupling of active and reactive power, which involves considering the mutual influence of reactive power and active power flow on losses, and enhancing the speed, versatility, and simplicity of the methodologies employed.

Power flow tracing algorithm was first proposed in 1996 [31] and in recent years, it has been widely cited in power grid security and economic analysis [32–34]. Based on the research direction, power flow tracing in the grid can be categorized into two methods: downstream tracing, which traces from the power source to the load, and upstream tracing, which traces from the load to the power source [35, 36]. In terms of the solution approach, power flow tracing in the grid can be broadly categorized into two branches: one involves an iterative solution based on graph theory [37, 38], while the other relies on analytical solutions using linear equations [39, 40]. The former requires consideration of node tracing order, resulting in a relatively complex calculation process that is less suitable for programming applications and challenging to parallelize. Moreover, it often fails to address circularity issues. On the other hand, the latter employs simpler algorithms but involves matrix inversion, rendering the calculation process more intricate. This method is less suitable for large-scale power grids and cannot isolate individual sources or flow

paths.

Both the Newton-Raphson and Gauss-Seidel methods have their strengths and limitations, making them suitable for different types of power flow analysis. The Newton-Raphson method is preferred for large-scale systems due to its rapid convergence and robustness, while the Gauss-Seidel method offers simplicity and lower computational demands, making it useful for smaller systems or initial approximations. Together, these foundational methods provide the analytical groundwork for understanding power system behavior and solving nonlinear power flow equations. Building upon these classical approaches, more advanced techniques, such as the distribution network power flow tracing method discussed in the next section, have been developed to address the unique challenges of modern power systems.

### 2.2.1 Power Flow Tracing Principle

Power flow tracing relies on Kirchhoff's principle and the principle of proportional sharing. Kirchhoff's principle asserts that the total injected power at each node equals the total outflow power. It also specifies that the power injected and withdrawn at any node by a specific source or flow are equal.

The principle of proportional sharing forms the foundation and essence of the power flow tracing method, rooted in topology theory. It can be summarised as follows:

The total injected power (or outgoing power) at a node is termed the node power. For every node in the power grid, the ratio of power on each outgoing branch to the power of each incoming branch is identical to the ratio of the power of each incoming branch to the node power. As shown in Figure 2.1, four lines  $L_a$ ,  $L_b$ ,  $L_c$  and  $L_d$  are connected to node  $O$ . In this system,  $L_a$  and  $L_b$  are the inflow branches,  $L_c$  and  $L_d$  are the outflow branches.

According to the proportional sharing principle,

$$P_c = P_{ca} + P_{cb} = \frac{P_a}{P_a + P_b} P_c + \frac{P_b}{P_a + P_b} P_c \quad (2.6)$$

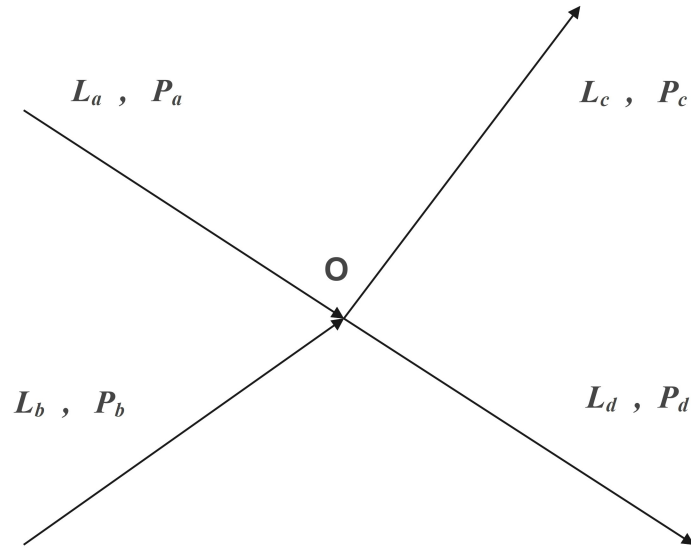


Figure 2.1: Four-line system illustrating power flow tracing principle.

$$P_d = P_{da} + P_{db} = \frac{P_a}{P_a + P_b} P_d + \frac{P_b}{P_a + P_b} P_d \quad (2.7)$$

$$P_{ca} = \frac{P_a}{P_a + P_b} P_c \quad (2.8)$$

$$P_{cb} = \frac{P_b}{P_a + P_b} P_c \quad (2.9)$$

$$P_{da} = \frac{P_a}{P_a + P_b} P_d \quad (2.10)$$

$$P_{db} = \frac{P_b}{P_a + P_b} P_d \quad (2.11)$$

where  $P_i$  is the power flowing on the line  $L_i$ , and  $P_{ij}$  is the contribution of the inflow line  $L_j$  to the power on the outflow line  $L_i$ .

### 2.2.2 Treating Power Flow without Accounting for Losses

According to a publication by Bialek [31], power flow tracing should be conducted in a network where losses are negligible. In this article, three methods for addressing network losses are presented:

- 1) Utilize the average flows from both the sending and receiving ends of the line for tracing.  
Distribute half of the loss occurring on each branch equally to the nodes at both ends of

the branch as equivalent loads to establish a network without losses.

- 2) Gross flows are employed for tracing, implying that no network losses are assumed, and the generator power without any adjustments is utilized for tracing purposes.
- 3) Net flows are utilized for tracing, under the assumption that network losses have been entirely eliminated. Hence, the load power unaffected by network losses is employed for tracing purposes.

Bialek [31] highlighted that the latter two approaches can assign network losses to both the load and the generator while achieving tracing outcomes. Essentially, these methods entail distributing the network loss of each line to the generator (or load) of the upstream (or downstream) node based on the primary proportional power relationship.

One of the primary advantages of using a lossless model in power flow analysis is the simplification it offers. By neglecting losses, the power flow equations become linear, making the mathematical treatment of the problem more straightforward. This linearization facilitates easier computation and allows for the application of analytical methods that might be otherwise complex or computationally intensive in a loss-included scenario. As a result, lossless power flow models are frequently employed in the initial design and optimization of power networks, where the primary concern is understanding the basic distribution of power flows under different operating conditions.

Furthermore, in certain applications, such as power flow tracing, treating power flow without accounting for losses can provide a clear and unambiguous understanding of how power generated by different sources is distributed across the network. By focusing solely on the "ideal" flow of power, this approach helps in attributing the contribution of each generator to specific loads, free from the confounding effects of losses. This can be particularly useful in scenarios where the primary interest lies in the proportional relationships between generation and consumption.

However, it is important to recognize the limitations of a lossless power flow approach. In reality, losses can constitute a significant portion of the power transmitted across the network,

and ignoring them can lead to inaccuracies in planning and operation. For instance, in highly loaded systems or in networks with long transmission lines, losses can affect voltage levels, system stability, and overall efficiency. Therefore, while a lossless model provides a useful approximation, it must eventually be supplemented with more detailed analyses that incorporate losses to ensure accurate and reliable system design and operation.

### 2.2.3 Power Tracing with Average Flows

Regarding the utilization of average flows to address network losses, Bialek [31] has introduced two power flow tracing algorithms: the downstream tracing method and the upstream tracing method.

#### 1) Downstream Tracing Algorithm

When representing the total flow ( $P_i$ ) through node  $i$  as outflow, the calculation formula is as follows:

$$P_i = \sum_{l \in \alpha_i^{(d)}} |P_{l-i}| + P_{Load_i} \quad for i = 1, 2, \dots, n \quad (2.12)$$

Here,  $\alpha_i^{(d)}$  represents the set of nodes directly supplying power to node  $i$  (i.e., where power on the corresponding branches must flow to node  $i$ ),  $P_{l-i}$  denotes the line flow into node  $i$  on line  $l$ , and  $P_{Load_i}$  stands for the load at node  $i$ . This is under the assumption of a lossless power network,  $|P_{i-l}| = |P_{l-i}|$ . The line flow, denoted by  $|P_{i-l}| = |P_{l-i}|$ , can be linked to the nodal flow at node  $l$  by substituting  $|P_{l-i}| = c_{li}P_l$ , resulting in

$$P_i = \sum_{l \in \alpha_i^{(d)}} c_{li}P_l + P_{Load_i} \quad (2.13)$$

can be rewritten as

$$P_i - \sum_{l \in \alpha_i^{(d)}} c_{li}P_l = P_{Load_i} \quad or \quad \mathbf{N}_d \mathbf{P} = \mathbf{P}_{Load} \quad (2.14)$$

Here,  $\mathbf{N}_d$  represents the  $n$ -order downstream matrix, while  $\mathbf{P}_{Load}$  stands for the vector of nodal demands. Additionally,  $\mathbf{P}$  signifies the vector of node through-flows. The equation concerning

the  $(i, l)$  element of  $\mathbf{N}_d$  is as follows:

$$[\mathbf{N}_d]_{il} = \begin{cases} 1 & \text{for } i = l \\ -c_{li} = -\frac{|P_{i-l}|}{P_i} & \text{for } l \in \alpha_i^{(d)} \\ 0 & \text{otherwise} \end{cases} \quad (2.15)$$

Moreover,  $\mathbf{N}_d$  in the equation is a sparse matrix that is nonsymmetric. Assuming the existence of  $\mathbf{N}_d^{-1}$ , the equation  $\mathbf{P} = \mathbf{N}_d^{-1} \mathbf{P}_{Load}$  is valid. The  $i$ -th element of  $\mathbf{P}$  is given by:

$$P_i = \sum_{k=1}^n [\mathbf{N}_d^{-1}]_{ik} P_{Lk} \quad i = 1, 2, \dots, n \quad (2.16)$$

Based on this equation, we can calculate the allocation of node power  $P_i$  among all loads in the system. In essence, the nodal through-flow  $P_i$  at node  $i$  equals the sum of the generation at that node and the power flowing into the node. Therefore, following the proportional sharing principle, the calculation equation for the inflow to node  $i$  from line  $i - j$ :

$$\begin{aligned} |P_{i-j}| &= \frac{|P_{i-j}|}{P_i} P_i = \frac{|P_{i-j}|}{P_i} \sum_{k=1}^n [\mathbf{N}_d^{-1}]_{ik} P_{Lk} \\ &= \sum_{k=1}^n D_{i-j,k}^L P_{Lk} \quad \text{for all } j \in \alpha_i^{(u)} \end{aligned} \quad (2.17)$$

In the equation above, the topological load distribution factor  $D_{(i-j,k)}^L = |P_{(i-j)}| [\mathbf{N}_d^{-1}]_{ik} / P_i$  indicates the portion of the  $k$ th load demand flowing through the line  $i - j$ . This expression resembles the definition of the generalized load distribution factor proposed by Rudnick et al. [41], which is based on DC load flow sensitivity analysis. However, the topological factor, representing the share of the load in the line flow, always appears as a positive value, whereas the generalized factor, determining the influence of the load on the line flow, may assume a negative value.

The power generation at node  $i$  also represents the incoming power. Following the proportional

sharing principle, its calculation formula can be expressed as:

$$P_{G_i} = \frac{P_{G_i}}{P_i} P_i = \frac{P_{G_i}}{P_i} \sum_{k=1}^n [\mathbf{N}_d^{-1}]_{ik} P_{L_k} \quad \text{for } i = 1, 2, \dots, n \quad (2.18)$$

From the equation above, it is evident that  $P_{G_i} [\mathbf{N}_d^{-1}]_{ik} P_{L_k} / P_i$  represents the allocation of output from the  $i$ th generator to satisfy the demand of the  $k$ th load, thereby enabling the tracing of power from a particular generator and identifying its destination.

## 2) Upstream Tracing Algorithm

When representing the total flow ( $P_i$ ) through node  $i$  as inflow, its calculation formula is as follows:

$$P_i = \sum_{j \in \alpha_i^{(u)}} |P_{i-j}| + P_{G_i} \quad \text{for } i = 1, 2, \dots, n \quad (2.19)$$

Here,  $\alpha_i^{(u)}$  represents the set of nodes that directly provide power to node  $i$  (i.e., where power on the corresponding lines must flow to node  $i$ ),  $P_{(i-j)}$  denotes the line flow into node  $i$  on line  $j-i$ , and  $P_{G_i}$  signifies the generation at node  $i$ . Due to the lossless nature of the power network,  $|P_{(i-j)}| = |P_{(j-i)}|$ .

The line flow  $|P_{(i-j)}| = |P_{(j-i)}|$  can be linked to the nodal flow at node  $i$  by substituting  $|P_{(i-j)}| = c_{ji} P_j$ , yielding

$$P_i = \sum_{j \in \alpha_i^{(u)}} c_{ji} P_j + P_{G_i} \quad (2.20)$$

can be written as

$$P_i - \sum_{j \in \alpha_i^{(u)}} c_{ji} P_j = P_{G_i} \quad \text{or} \quad \mathbf{N}_u \mathbf{P} = \mathbf{P}_G \quad (2.21)$$

Here,  $\mathbf{N}_u$  represents the  $n$ -order upstream matrix, and  $\mathbf{P}_G$  is the vector of nodal generations. The

equation concerning the  $(i, j)$  element of  $\mathbf{N}_u$  is given by:

$$[\mathbf{N}_u]_{ij} = \begin{cases} 1 & \text{for } i = j \\ -c_{ji} = -\frac{|P_{i-j}|}{P_j} & \text{for } j \in \alpha_i^{(d)} \\ 0 & \text{otherwise} \end{cases} \quad (2.22)$$

Furthermore,  $\mathbf{N}_u$  in the equation represents a nonsymmetric sparse matrix. Assuming  $\mathbf{N}_u^{-1}$  exists, the equation  $\mathbf{P} = \mathbf{N}_u^{-1} \mathbf{P}_G$  holds. Additionally, the sum of  $\mathbf{N}_d$  and  $\mathbf{N}_u$  yields a symmetric matrix with a structure identical to the nodal admittance matrix. The  $i$ -th element of  $\mathbf{P}$  is given by:

$$P_i = \sum_{k=1}^n [\mathbf{N}_u^{-1}]_{ik} P_{Gk} \quad \text{for } i = 1, 2, \dots, n \quad (2.23)$$

Based on the equation above,  $[\mathbf{N}_u^{-1}]_{ik} P_{Gk}$  indicates the contribution of the generator in the  $k$ th system to the nodal power at node  $i$ . Additionally, the nodal through-flow  $P_i$  at node  $i$  equals the sum of the load demand ( $P_{Loadi}$ ) at that node and the power flowing out of the node. Thus, according to the proportional sharing principle, the calculation equation for the outflow to node  $i$  from line  $i-l$  is:

$$|P_{i-l}| = \frac{|P_{i-l}|}{P_i} P_i = \frac{|P_{i-l}|}{P_i} \sum_{k=1}^n [\mathbf{N}_u^{-1}]_{ik} P_{Gk} = \sum_{k=1}^n D_{il,k}^G P_{Gk} \quad \text{for all } l \in \alpha_i^{(d)} \quad (2.24)$$

In the equation above, the topological generation distribution factor  $D_{(i-l,k)}^G = |P_{(i-l)}| [\mathbf{N}_u^{-1}]_{ik} / P_i$  represents the portion of the  $k$ th generation that flows through the line  $i-l$ . This definition bears similarity to the generalized generation distribution factor proposed by Ng [42]. However, this method was based on the superposition theorem applied to the DC linearization system model. Consequently, the distribution factor he proposed reflects the influence of a certain factor on the line flow, potentially resulting in negative values. In contrast, the topological distribution factor is grounded in the topological analysis of network flow, depicting the portion of a specific generation in the total line flow. Consequently, these factors consistently appear as positive values.

The load demand at node  $i$  also represents the outgoing power. Following the proportional sharing principle, its calculation formula can be expressed as:

$$P_{Load_i} = \frac{P_{Load_i}}{P_i} P_i = \frac{P_{Load_i}}{P_i} \sum_{k=1}^n [\mathbf{N}_u^{-1}]_{ik} P_{Gk} \quad \text{for } i = 1, 2, \dots, n \quad (2.25)$$

From the equation above, it is evident that  $P_{Load_i} [\mathbf{N}_u^{-1}]_{ik} P_{Gk} / P_i$  represents the portion contributed by the  $k$ th generator to the load demand at node  $i$ , thereby enabling the tracing of power from a specific load and identifying its source.

This method simplifies the complexity inherent in power flow analysis by focusing on average flows rather than instantaneous or peak values. This is particularly useful in scenarios where the objective is to determine the long-term usage patterns of the network rather than transient behaviors. By using average flows, the method smooths out short-term fluctuations and provides a stable and reliable basis for decision-making, whether it be for tariff setting, cost allocation, or network planning.

Despite its advantage, power tracing with average flows also presents challenges, particularly in ensuring accuracy when dealing with highly dynamic systems where power flows can change rapidly. The averaging process, while smoothing out variations, may overlook critical peak load conditions or fail to capture the nuances of real-time system behavior. Therefore, while it is a valuable tool for long-term planning and cost allocation, it may need to be complemented with more detailed, time-sensitive analyses in certain operational contexts.

## 2.2.4 Power Tracing with Gross Flows

In the preceding section, the system achieves losslessness by averaging line flows and adjusting injected power at both ends of the line. Assuming the system utilizes actual power generation as the feed source and there are no losses in the grid, a power tracing method that aligns with real-world conditions can be derived. This entails modifying node requirements while keeping node generation unchanged.

In certain simple systems, it's possible to determine all actual total gross flows through inspection. However, in more intricate networks, relying solely on inspection is insufficient for problem-solving, necessitating a more formal approach. To adhere to Kirchhoff's current law as a prerequisite, once the gross power flows are computed, the tracing method outlined in the preceding section can be directly employed.

According to Kirchhoff's current law, the gross power flows through node  $i$  are denoted by an unknown gross node power  $P_i^{(g)}$ . When the network utilizes actual power generation as the feed source and experiences no loss, the gross power will transit through node  $i$ . Similarly, the unknown gross flow of the line  $i - j$  is represented as  $P_{(i-j)}^{(g)}$ . In a lossless network, the gross flow will persist, establishing the relationship  $|P_{(i-j)}^{(g)}| = |P_{(j-i)}^{(g)}|$ .

When focusing on inflows, it is similar to the upstream tracing algorithm, the gross nodal power can be represented as:

$$P_i^{(g)} = \sum_{j \in \alpha_i^{(u)}} |P_{i-j}^{(g)}| + P_{G_i} \quad \text{for } i = 1, 2, \dots, n \quad (2.26)$$

Since  $|P_{(i-j)}^{(g)}| = |P_{(j-i)}^{(g)}|$  holds, the flow  $P_{(i-j)}^{(g)}$  can be reformulated as  $c_{ji}^{(g)} P_j^{(g)}$ , where  $c_{ji}^{(g)} = |P_{(j-i)}^{(g)}| / |P_j^{(g)}|$ . Typically, the transmission loss in the system is minimal, so  $|P_{(j-i)}^{(g)}| / |P_j^{(g)}| \approx |P_{(j-i)}| / P_j$  can be assumed, where  $P_j$  is the actual total power flow through node  $j$ , and  $P_{(j-i)}$  is the actual power flow from node  $j$  on line  $j - i$ . This assumption corresponds to the notion that the distribution of actual flows and gross flows at any node is identical. Generally, this is the sole approximate assumption for this tracing method. With this assumption in mind, Equation (2.26) can be rewritten as:

$$P_i^{(g)} - \sum_{j \in \alpha_i^{(u)}} \frac{|P_{j-i}|}{P_j} P_j^{(g)} = P_{G_i} \quad \text{or} \quad \mathbf{N}_u \mathbf{P}_g = \mathbf{P}_G \quad (2.27)$$

In the equation above,  $\mathbf{P}_g$  denotes the unknown vector of gross power flows at a specific node, while  $\mathbf{N}_u$  represents the upstream distribution matrix calculated from unaltered actual flows.

Given that  $\mathbf{P}_G$  and  $\mathbf{N}_u$  are known, solving Equation (2.27) allows for determining the unknown gross nodal flow. Once the gross nodal power flows are established, the gross demands and gross line power flows can also be derived using the proportional sharing principle. The gross flow of line  $i-l$  is:

$$\begin{aligned} |P_{i-l}^{(g)}| &= \frac{|P_{i-l}^{(g)}|}{P_i^{(g)}} P_i^{(g)} \\ &\cong \frac{|P_{i-l}|}{P_i} \sum_{k=1}^n [\mathbf{N}_u^{-1}]_{ik} P_{Gk} \quad \text{for all } l \in \alpha_i^{(d)} \end{aligned} \quad (2.28)$$

Moreover, the equation for calculating the gross demand at node  $i$  is:

$$\begin{aligned} P_{Loadi}^{(g)} &= \frac{P_{Loadi}^{(g)}}{P_i^{(g)}} P_i^{(g)} \\ &\cong \frac{P_{Loadi}}{P_i} P_i^{(g)} = \frac{P_{Loadi}}{P_i} \sum_{k=1}^n [\mathbf{N}_u^{-1}]_{ij} P_{Gk} \end{aligned} \quad (2.29)$$

This is a particularly important equation because it shows what the load demand is on a given node if a lossless network is supplied by actual power generation. Therefore, the difference between actual demand and gross demand is expressed as

$$\Delta P_{Loadi} = P_{Li}^{(g)} - P_{Loadi} \quad (2.30)$$

This equation demonstrates the loss incurred by the power transmitted from all generators to a specific load. In essence, the upstream tracing algorithm enables the examination of not only each generator's contribution to fulfilling a particular load demand but also the distribution of the total loss generated by the transmission system among various loads in the network [31]. This finding holds significant implications as it implies that loads can be individually billed based on actual power loss.

This method is especially valuable in the context of allocating network usage costs, as it allows for a more precise and comprehensive understanding of each participant's use of the network. In power systems, particularly those with multiple interconnected utilities, accurately allocating

costs based on gross power flows ensures that each user pays their fair share for the infrastructure they utilize. This is essential for maintaining fairness and transparency in the market, as well as for the efficient operation of the power system.

In addition to cost allocation, power tracing with gross flows plays a critical role in the determination of wheeling charges, where the costs associated with transmitting power across networks owned by third parties must be equitably distributed among users. The gross flow method ensures that wheeling charges reflect the total amount of power each user is responsible for transmitting, including any ancillary or secondary flows that occur due to network dynamics. This comprehensive approach helps to avoid underestimating the impact of certain users on the network, thereby ensuring that all participants contribute fairly to the maintenance and operation of the grid.

Furthermore, power tracing with gross flows can provide insights into network reliability and stability. By understanding the full extent of power flows, system operators can identify potential bottlenecks or areas where the network may be stressed under certain conditions. This information is crucial for planning upgrades, managing congestion, and ensuring the overall reliability of the power system.

However, while the gross flow method offers a detailed and accurate view of power distribution, it also presents challenges, particularly in terms of data collection and computational complexity. The need to capture the entire spectrum of power flows at any given moment requires extensive data and sophisticated analytical tools. Moreover, the dynamic nature of power systems means that these gross flows can change rapidly, necessitating continuous monitoring and analysis to maintain accuracy.

### **2.2.5 Power Tracing with Net Flows**

Power tracing with net flows is a method that examines the balance between the incoming and outgoing power at each node or bus in the network. Essentially, it accounts for the difference between the power generated or injected into the system and the power consumed or withdrawn

from it. This method is particularly valuable for identifying the net contribution of each participant in the power system, as it isolates the actual power delivered to loads after accounting for internal power exchanges within the network.

When eliminating transmission loss from the line flow of system, this technique becomes necessary for tracing network flow. This entails adjusting nodal generation while keeping nodal demands constant. The approach involves introducing  $P_i^{(n)}$  to denote an unknown net nodal power and  $P_{i-j}^{(n)}$  to represent an unknown net flow between nodes  $i$  and  $j$ , ensuring compliance with Kirchhoff's current law while directing flow where transmission loss is nullified. Additionally, it's established that  $|P_{i-j}^{(n)}| = |P_{j-i}^{(n)}|$ . When focusing on outflows akin to the downstream tracing algorithm, the net nodal power can be expressed as

$$P_i^{(n)} = \sum_{l \in \alpha_i^{(d)}} |P_{i-l}^{(n)}| + P_{Load_i} = \sum_{l \in \alpha_i^{(d)}} c_{li}^{(n)} P_l^{(n)} + P_{Load_i} \quad \text{for } i = 1, 2, \dots, n \quad (2.31)$$

In the given formula,  $c_{li}^{(n)}$  is calculated as  $|P_{i-l}^{(n)}|/P_l^{(n)}$ . Typically, system transmission loss is negligible, allowing  $|P_{l-i}^{(n)}|/P_l^{(n)}$  to be approximated as  $|P_{l-i}|/P_l$ . With this assumption, Equation (2.31) can be rewritten as

$$P_i^{(n)} - \sum_{i \in \alpha_i^{(d)}} \frac{|P_{l-i}|}{P_l} P_l^{(n)} = P_{Load_i} \quad \text{or} \quad \mathbf{N}_d \mathbf{P}_n = \mathbf{P}_{Load} \quad (2.32)$$

In the provided equation,  $\mathbf{P}_n$  denotes the unspecified vector of net power flows for a specific node, while  $\mathbf{N}_d$  stands for the downstream distribution matrix. With  $\mathbf{P}_{Load}$  and  $\mathbf{N}_d$  being known, the solution for Equation (2.32) yields the unknown net nodal flow.

Following the proportional sharing principle, the net flow of line  $i - j$  can be computed as

$$|P_{i-j}^{(n)}| = \frac{|P_{i-j}^{(n)}|}{P_i^{(n)}} P_i^{(n)} \cong \frac{|P_{i-j}|}{P_i} \sum_{k=1}^n [\mathbf{N}_d^{-1}]_{ik} P_{Lk} \quad \text{for all } j \in \alpha_i^{(u)} \quad (2.33)$$

Furthermore, to determine the net generation for node  $i$ , the equation is

$$P_{G_i}^{(n)} = \frac{P_{G_i}^{(n)}}{P_i^{(n)}} P_i^{(n)} \cong \frac{P_{G_i}}{P_i} P_i^{(n)} = \frac{P_{Load_i}}{P_i} \sum_{k=1}^n [N_d^{-1}]_{ij} P_{Lk} \quad (2.34)$$

This equation holds significant importance as it illustrates the required power at a specific node to satisfy the system demands within a lossless network framework. Hence, the variance between net generation and actual generation is represented as

$$\Delta P_{G_i} = P_{G_i} - P_{G_i}^{(n)} \quad (2.35)$$

This equation reveals the distribution of system losses resulting from the power flow of a specific generator among all loads. Typically, the downstream algorithm not only addresses how a particular generator's output can be allocated across all loads but also assigns all transmission losses incurred in the system to a single generator within the grid [31]. This finding holds immense significance as it enables the individual allocation of transmission loss attributed to the generator.

One of the key benefits of using net flows in power tracing is its ability to simplify the analysis of power distribution by focusing on the net effect of power transfers. This method effectively filters out the complexities associated with gross power flows, such as internal loop flows or circulating currents, which do not contribute directly to the end consumption. By concentrating on net flows, the analysis becomes more straightforward, providing clearer insights into the effective power delivery paths and helping to identify inefficiencies or imbalances in the network.

Additionally, power tracing with net flows can play a significant role in enhancing the reliability and stability of power systems. By focusing on the net power balance at each node, system operators can identify potential issues such as overloading or underutilization of network components. This information is critical for making informed decisions about system operations, maintenance, and upgrades. For example, areas of the network that consistently show high net

inflows or outflows may require reinforcement or expansion to prevent bottlenecks and ensure continuous, reliable power delivery.

Despite its advantages, power tracing with net flows also presents certain challenges. One of the primary challenges is accurately measuring and calculating net flows in real-time, particularly in complex, interconnected networks. The dynamic nature of power systems, with constantly fluctuating generation and consumption patterns, requires sophisticated monitoring and analytical tools to ensure that net flow calculations are accurate and up-to-date. Furthermore, the focus on net flows may sometimes overlook the importance of internal power exchanges, which, while not directly contributing to end consumption, can still impact the overall stability and efficiency of the network.

### **2.2.6 Loss Allocation Algorithms**

The increasing complexity of modern power systems, characterized by the integration of renewable energy sources, distributed generation, and ever-evolving consumption patterns, has heightened the need for precise methods of power flow analysis. Among these, power tracing with loss allocation algorithms stands out as a crucial approach for managing and optimizing the operation of electrical networks. This method not only traces the flow of electricity through the system but also accounts for the losses that occur during transmission and distribution. Such losses are inevitable due to the resistance of transmission lines and other components, but understanding and fairly allocating these losses among the various participants in the network is essential for efficient system operation and cost allocation. Loss allocation algorithms operate based on principles of network flow analysis and electrical engineering principles. They consider factors such as power flows, network topology, generator and load characteristics, and Kirchhoff's laws to distribute losses appropriately.

In recent years, the issue of loss allocation in distribution networks has been frequently discussed. Several methods have been developed for power loss allocation, each with its own advantages and challenges. For instance, proportional allocation methods distribute losses based on the proportion of power each generator contributes to the overall flow. This approach is

straightforward but may not always accurately reflect the actual contribution of each participant to the losses. On the other hand, more complex methods, such as those based on network sensitivities or marginal loss calculations, offer a more precise allocation by considering the specific impact of each participant on the system losses.

Moreover, loss allocation is not just for financial purposes but also a technical problem, closely linked to the efficiency and reliability of the power system. High losses in certain areas of the network can indicate inefficiencies or bottlenecks that need to be addressed. By accurately tracing and allocating losses, it becomes possible to identify areas where improvements can be made, whether through upgrading infrastructure, optimizing power flows, or adjusting operational practices.

In recent years, the advent of advanced metering infrastructure (AMI) and improved computational capabilities has significantly enhanced the feasibility and accuracy of power tracing with loss allocation algorithms. These technological advancements enable more detailed real-time monitoring and analysis of power flows, making it possible to apply loss allocation methods with greater precision and reliability. As a result, the integration of loss allocation algorithms into power tracing methods is becoming increasingly standard practice in the management of modern power systems.

Despite the progress made, there are still challenges associated with power tracing and loss allocation. These include the need for accurate data, the complexity of the algorithms involved, and the dynamic nature of power systems, where conditions can change rapidly. Moreover, the introduction of renewable energy sources, which can be intermittent and decentralized, adds another layer of complexity to the process. Therefore, ongoing research and development are necessary to refine these methods and ensure they can meet the evolving needs of power systems worldwide.

This thesis will explore the principles and applications of power tracing with loss allocation algorithms in power distribution networks. The research will focus on developing and testing new algorithm that can more accurately trace power flows and allocate losses in complex, intercon-

nected systems. By doing so, the thesis aims to contribute to the ongoing efforts to enhance the efficiency, fairness, and transparency of power system operations.

## 2.3 Loss Allocation of Distribution Networks

In modern power systems, distribution networks play a crucial role in delivering electricity from high-voltage transmission systems to end consumers. As power flows through these networks, energy losses inevitably occur due to the inherent resistance of electrical components such as transformers, cables, and conductors. These losses, though often small in percentage terms, represent a significant cost to the operation of the power system, especially in large-scale networks where even minor inefficiencies can translate into substantial financial impacts. Therefore, accurately allocating these losses among the various participants in the network is essential for both technical and economic reasons.

In power systems, electricity undergoes various stages of generation, conversion, transmission and distribution as delivery. Among these, the distribution network plays a crucial role by directly supplying power to consumers. However, it also constitutes a significant portion of power losses, accounting for over 70% of the total. Hence, there is a pressing need to explore advanced scientific methods to ensure equitable, fair, and efficient allocation of distribution network losses.

The distribution network typically denotes a power grid operating at voltages of 110kV and lower. In this context, low power factors and significant reactive power flow pose challenges in directly applying loss allocation methods from the transmission grid to the distribution network [43, 44]. In the traditional network loss allocation method, the loss cannot be naturally guaranteed to be allocated to all transactions in the power grid, i.e. to all power sources and loads. In addition, it is impossible to directly consider the cross-effects of active and reactive power. At the same time, different loss allocation methods will have an impact on the economic operation of the power system. As the research shows [45], observations from the operational dynamics of the UK electricity market indicate that various network loss allocation methods

could influence transaction prices by as much as 10%. An effective distribution network loss allocation method can optimise the distribution network structure, determine the best operational mode and economic dispatch of the distribution network, reduce the power loss of the distribution network, save resources and improve the power supply capacity [46]. Therefore, an effective, reasonable, and equitable method of allocating network losses can improve the overall economic benefits of the power system.

With the expanding scale of distributed power generation, ensuring equitable distribution network loss allocation has emerged as a critical challenge. The integration of renewable energy sources into distribution networks adds another layer of complexity to loss allocation. Renewables are often intermittent and decentralized, leading to fluctuating power flows that can change the loss profile of the network. As the share of renewables in the energy mix continues to grow, developing robust loss allocation methods that can adapt to these changing conditions is becoming increasingly important. Whether focusing on individual nodes, transactions, or both simultaneously, the primary objective in discussing loss allocation methods is to garner recognition from market participants, adhering to this fundamental principle [29]. To mitigate conflicts and enhance economic gains for market participants, the loss allocation method must adhere to the following criteria:

- 1) The computation process should be straightforward, comprehensible, and user-friendly.

The loss allocation method should maintain simplicity in calculations while accommodating real-time online analysis, ensuring easy comprehension for market participants. Transparency and fairness in displaying allocated shares to all participants are essential for feasibility.

- 2) Fair and reasonable.

Loss allocation outcomes must remain unaffected by human intervention. It is crucial to comprehensively consider the economic interests of all participants to mitigate risks and prevent unjustified profits or losses for users.

- 3) The financial equilibrium of the power system.

The loss allocation method should guarantee that the total cost of losses charged to market participants matches the total loss cost incurred by the grid.

- 4) Accurately represent network utilization.

The loss allocation method should rely on the genuine power flow within the grid, accurately reflecting usage of each participant of the network.

- 5) Offer accurate economic indicators to the power system.

The loss allocation method should furnish precise economic cues to transaction participants, thereby enhancing the economic advantages of the system and achieving optimal resource allocation.

Drawing from these principles, numerous articles have investigated distribution network loss allocation and put forth specific methodologies. Among these, common approaches include the Pro-rata (PR) method, the marginal method, the flow-tracing method, and the current-based method, which will be outlined subsequently.

### **2.3.1 Pro-rata (PR) Method**

According to Nikolaidis and Charalambous [47], the pro-rata method is to distribute the loss proportionally based on the integrated active power loss. This method is a straightforward and commonly used approach for allocating losses in distribution networks. This method distributes the total losses of the network among all users based on their proportional share of the total energy consumption. The fundamental principle behind the PR method is that each user contributes to the network losses in direct proportion to the amount of electricity they consume. This means that a user consuming more electricity will bear a larger share of the total losses compared to a user with lower consumption.

The calculation process for the PR method is relatively simple and involves determining the total

energy losses in the distribution network for a specific period. These total losses are then divided among the users based on their individual energy usage relative to the total energy consumed by all users in the network. Mathematically, if  $L$  represents the total losses and  $E_i$  represents the energy consumed by user  $i$ , the loss allocated to user  $i$  can be calculated using the formula:

$$L_i = L \times \frac{E_i}{\sum_j E_j} \quad (2.36)$$

where  $\sum_j E_j$  is the sum of the energy consumed by all users. This method ensures that the loss allocation is proportional to consumption, maintaining simplicity and transparency in the allocation process.

While the PR method is easy to implement and understand, it has some limitations. One of the primary drawbacks is that it does not account for the actual impact of each user on the network losses, which can vary depending on the location of the user within the network and the timing of their energy consumption [48]. Consequently, the PR method may not accurately reflect the true cost of losses caused by each user, potentially leading to inequities in cost allocation. Users located further from the source or consuming power during peak demand times may contribute more to the overall losses than users closer to the source or with off-peak consumption, but this is not reflected in the PR method.

Despite these limitations, the PR method remains widely used due to its simplicity and ease of application. It provides a clear and consistent framework for loss allocation, making it particularly useful in regulatory environments where transparency and ease of understanding are important. Moreover, the PR method can serve as a baseline or starting point for more sophisticated loss allocation techniques, providing a useful benchmark for comparing the outcomes of different allocation methods.

### 2.3.2 Proportional Allocation (PA) Method

Macqueen [29] suggests a proportional allocation method that primarily uses the grid's directed graph to distribute the losses from each line and transformer to the users they serve. To summarize the method, it involves several stages. Initially, the standard load flow of the power system is analyzed. Demand losses are allocated by performing the load flow study, and the system's energy losses are then calculated using its daily load curve, allowing for the determination of losses for each line and transformer at that time. Following this, a directed graph is constructed, where the arcs and vertices correspond to the branches and nodes of the load flow. The number of nodes is stored using an array model. In this graph, vertices labeled as source vertices do not have incoming arcs and correspond to the generators and inputs of the system. The vertices not connected to an output arc are the termination vertices, corresponding to consumer load and the system's exit point. The longest path from any source vertex to a termination vertex is logically regarded as the potential of each vertex. With these definitions, the distribution networks are correctly interconnected, and the longest path algorithm is used to allocate the potentials accurately. Finally, using a breadth-first traversal of the graph, the potentials of each vertex are processed in ascending order according to their potentials, which in turn performs the loss allocation. For each vertex, the losses on the input arcs are assigned to that vertex. Additionally, the losses assigned to each vertex are apportioned among the output arcs using a user-specified formula (Figure 2.2), considering the loads as outgoing arcs throughout the process.

Macqueen [29] provides a detailed and well-developed calculation and loss allocation formula. However, the proportional allocation method has inherent limitations that cannot be ignored. While simple to implement, this method only considers the proportion of the customer's load, neglecting the actual grid connections, line parameters, and specific operating conditions of the power system such as current and voltage. These factors significantly influence the loss distribution within the power system. Furthermore, in a real power system, factors such as grid topology, line parameters, and the system's operating state can cause a customer's load proportion to differ from its actual contribution to system losses. For instance, a customer located farther from the power source may contribute more to power system losses than its load

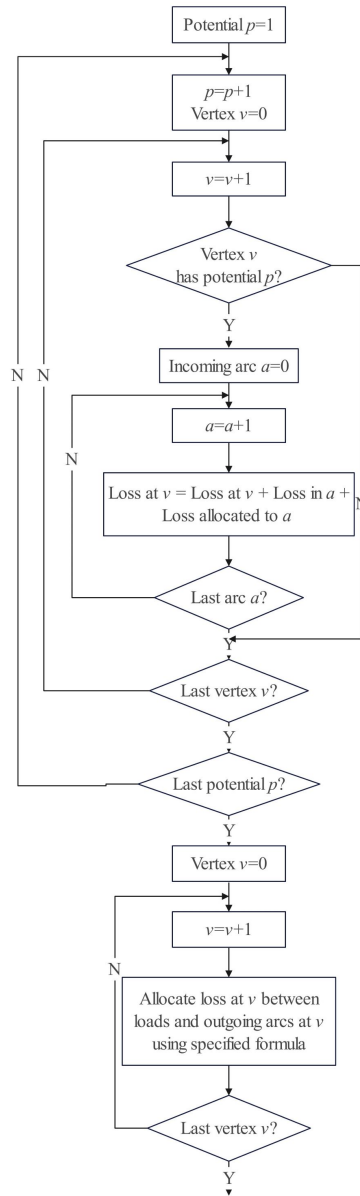


Figure 2.2: Proportional allocation method

ratio suggests due to higher line losses. The proportional allocation method overlooks these aspects, resulting in a lack of fairness in loss allocation outcomes.

The Proportional Allocation Method is appreciated for its simplicity and transparency. It is easy to understand and implement, making it a practical choice for utilities and regulatory bodies. By directly linking loss allocation to demand, it provides a straightforward mechanism for ensuring that users who draw more power from the system—and therefore are likely to cause more losses—are appropriately charged.

However, the method does have limitations. One significant drawback is that it does not consider the actual physical and temporal impact of each user's demand on network losses. For instance, users located farther from generation sources or those who consume power during peak periods can contribute disproportionately to network losses compared to users who are closer or consume power during off-peak times. The Proportional Allocation Method does not account for these variances, potentially leading to an allocation that is not fully reflective of each user's true impact on the network.

Despite these limitations, the Proportional Allocation Method remains widely used due to its balance of simplicity and fairness. It offers a clear and consistent approach to loss allocation, making it particularly valuable in settings where ease of understanding and implementation are critical. Moreover, this method can serve as a foundational approach, from which more complex and precise allocation techniques can be developed and compared.

### **2.3.3 The Marginal Method**

The marginal method allocates the loss based on the influence of the power incremental change on the total loss. Mutale [49] introduced two innovative loss allocation methodologies. The initial approach centered on marginal loss allocation. They characterized the marginal loss coefficient (MLC) as the alteration in total active power loss arising from marginal adjustments in active and reactive power generation and consumption at individual nodes within the network. The second method they presented involved direct loss coefficients (DLCs), establishing a direct correlation between losses and nodal injections. Given the temporal and spatial variability of Distributed Generation (DG) impacts on losses, the parameters of both methods could be positive or negative, enabling the identification of reverse power flow. However, challenges persisted with the calculators in both methodologies, stemming from intricate computations associated with the network Jacobian matrix and Hessian matrix. Application in extensive systems could diminish the computational efficiency of this approach. Moreover, it proved inefficient and unfeasible for deployment in electrical markets where real-time energy trades were settled at half-hourly or hourly intervals.

Building upon the research of Mutale, Costa [50] proposed a methodology to compute the marginal loss component of node prices during congestion periods. This method aims to provide a more precise reflection of each market participant's contribution to marginal losses. Additionally, it guarantees that each user allocates losses solely at the branch where it contributes current based on branch operation. This method also addresses cross-term allocation of loss and reactive power, aiming to minimize cross-subsidization. According to his perspective, since each user contributes to the losses in each network element, the allocation of losses should be conducted on a branch-by-branch basis. Additionally, losses could be attributed to both users and distributed generators. This approach enhances visibility, as every user becomes cognizant of the costs incurred in each network element. In Mutale's approach, the marginal loss coefficient-based methods are not suitable for real-time energy trades. However, Costa's proposed method introduces differentiation among network users based on the characteristics and state of network segments, where the distribution company responsible for public service is liable for all losses incurred by its customers. Additionally, the time structure of the marginal price could be integrated, and specific periods for applying the method can be defined.

This method can reflect short-term marginal costs, so it can provide a short-term price signal to the grid [51]. However, in order to prevent the loss caused by excessive recycling during the allocation process, this method generally requires a standardisation factor [52].

The Marginal Method offers a more accurate and equitable allocation of losses because it takes into account the actual impact of each user's consumption pattern on the network. Users who cause higher losses due to their location in the network or their consumption during peak periods are assigned a higher share of the losses. This creates economic signals that can incentivise users to adjust their consumption patterns, potentially leading to more efficient utilization of the network and reduced overall losses.

However, the Marginal Method also has its complexities and challenges. The calculation of marginal loss factors requires detailed and accurate data on the network's topology, load flows, and generation patterns. This can be computationally intensive and requires sophisticated mod-

eling and analysis tools. Additionally, the method's reliance on real-time or near-real-time data can complicate its implementation in practice, especially in large and dynamic power systems.

Despite these challenges, the Marginal Method is highly regarded for its theoretical robustness and its potential to promote economic efficiency. By aligning the allocation of losses with the marginal cost principles, it ensures that the costs reflect the true impact of each user's actions on the system. This not only enhances fairness but also provides strong incentives for users to contribute to the efficient operation of the network. As such, the Marginal Method is often advocated by economists and regulators aiming for an equitable and efficient approach to loss allocation in modern power systems.

### 2.3.4 Z-bus Method

The Z-bus method is an essential technique in power system analysis, offering enhanced accuracy and speed in solving power system issues. It facilitates the calculation of critical quantities like voltage, current, and power between nodes by transforming these problems into linear algebra problems using the impedance matrix. This approach leverages the computational efficiency and arithmetic properties of matrices, significantly improving analysis precision and efficiency. The Z-bus method relies on the node impedance matrix, also known as the Z-bus matrix, to analyze and solve power system issues. It is extensively used for stability analysis, short circuit calculations, load flow calculations, harmonic analysis, and various other power system problems [53].

The outcome of the Z-bus network loss sharing method depends on the node impedance matrix and the current injected into each node. The total system network loss,  $P_{loss}$ , is the aggregate of the network losses allocated to each node.

$$P_{loss} = \sum_{k=1}^n L_k \quad (2.37)$$

In equation (2.36),  $L_k$  represents the loss allocated to node  $k$ . Additionally, the system network

losses can be calculated using node voltages and injected currents with the following formula:

$$P_{loss} = Re \left\{ \sum_{k=1}^n V_k I_k^* \right\} \quad (2.38)$$

If the network has a tidal solution, the node impedance for the structurally defined network, based on the line data and system topology, is represented in equation (2.38):

$$Z = R + jX \quad (2.39)$$

Subsequently, by utilizing the array of nodal impedances, equation (2.37) can be expressed as follows:

$$P_{loss} = Re \left\{ \sum_{k=1}^n I_k^* \left( \sum_{j=1}^n Z_{kj} I_j \right) \right\} \quad (2.40)$$

From equation (2.39), it is evident that the current directly influences the allocation result. Since the current injected into each node is an independent variable, the loss allocation determined by the Z-bus method will naturally distribute to each node. By further combining equations (2.38) and (2.39), we get:

$$P_{loss} = Re \left\{ \sum_{k=1}^n I_k^* \left( \sum_{j=1}^n R_{kj} I_j \right) \right\} + Re \left\{ \sum_{k=1}^n I_k^* \left( \sum_{j=1}^n jX_{kj} I_j \right) \right\} \quad (2.41)$$

Given that the nodal impedance array  $Z$  is symmetric, the second term on the right side of equation (2.40) equals zero. Consequently, the network loss equation can be expressed as:

$$P_{loss} = Re \left\{ \sum_{k=1}^n I_k^* \left( \sum_{j=1}^n R_{kj} I_j \right) \right\} \quad (2.42)$$

Then, the expression for the network loss allocated to each node  $k$  is:

$$L_k = Re \left\{ I_k^* \left( \sum_{j=1}^n R_{kj} I_j \right) \right\} \quad (2.43)$$

The Z-bus method has several advantages: it requires no assumptions or simplifications, accu-

rately reflects the electrical structure of the system, and is easy to understand and implement. However, it also has notable shortcomings. Because the Z-bus method allocates network losses by using the conductance matrix multiplied by the net injected current of the nodes, the pure generator nodes typically have higher net injected currents compared to load nodes. Consequently, this method results in a disproportionately high network loss component for pure generator nodes, which is unfair to the generators.

Due to the unfair allocation of losses to generators by the Z-bus method, a secondary allocation is often necessary. Researchers attempted to address this by using a proportional method for secondary allocation of network losses, which somewhat reduces the burden on generators. However, this approach lacks a solid theoretical foundation and introduces a degree of arbitrariness, making it difficult to satisfy both merchants and users. To improve upon this, a secondary allocation method based on power is proposed, which effectively reduces the network losses borne by generators and provides a more theoretically sound basis for the secondary allocation of network losses.

First, it is assumed that the proportion of the network loss allocated to the generator relative to the total network loss of the system is denoted as  $\lambda$ :

$$\frac{L_g}{P_{loss}} = \lambda \quad (2.44)$$

where  $L_g$  represents the total network loss borne by the generator, and the value of  $\lambda$  can either be negotiated between the user and the merchant or determined from equation (2.43):

$$\lambda = \frac{P_G}{P_G + P_D} \quad (2.45)$$

Thus, the outcome of the Z-bus method can be represented as:

$$P_{loss} = \left( L_{g,z-bus} - \Delta L \right) + \left( L_{d,z-bus} + \Delta L \right) \quad (2.46)$$

$$\Delta L = \lambda P_{loss} - L_{g,z-bus} \quad (2.47)$$

where  $\Delta L$  represents the excess loss borne by the generator, and the reduction in loss for each generator  $k$  is based on its power:

$$\Delta L = \sum_{k=1}^n \frac{P_{gk}}{P_G} \Delta L \quad (2.48)$$

Similarly, the amount of  $\Delta L$  allocated to each load  $j$  is determined by the power of the load node:

$$\Delta L = \sum_{j=1}^m \frac{P_{dj}}{P_D} \Delta L \quad (2.49)$$

This approach effectively addresses the issue of generators bearing excessive network losses while retaining the benefits of the Z-bus method. It's seen as a potential solution for carbon emission accounting for both users and generators. However, upon closer examination, the optimized algorithm is found to have limited applicability and numerous constraints. For instance, the choice of the IEEE-14 node model is due to its approximate balance between power demand (PD) and power generation (PG), along with a fixed value of  $\lambda$  ( $\lambda = 0.5$ ). Furthermore, applying the Z-bus method based on power optimization becomes challenging for models with distributed energy sources due to the significant computational burden. This complexity escalates exponentially with the addition of distributed energy sources, making it difficult to achieve real-time visualization of current tracing based on this algorithm.

### 2.3.5 Y-bus method

The Y-bus method, also referred to as the admittance matrix method, holds significant prominence in power system analysis. Much like the Z-bus method, it relies on a fundamental data structure known as the admittance matrix. Primarily utilized for load flow analysis, fault analysis, and other stability-related calculations in power systems, the Y-bus method serves as a cornerstone in power system analysis.

To grasp the essence of the Y-bus method, it is crucial to delve into its fundamental element:

the admittance matrix. In various microwave networks, by defining the voltage and current (Figure 2.3) at each port on a chosen network reference plane, different linear combinations can be obtained through the selection of distinct independent and dependent variables. Since the voltage-current relationship is linear for such networks, akin to the theory of low-frequency two-port networks, these linear combinations of various variables can be characterized by diverse network parameters. The nodal admittance matrix serves as the covariance matrix of a microwave network, where the port voltage (considered as the independent variable) is used to represent the port current (considered as the dependent variable). In a power system, the relationship between electrical components can be expressed in terms of their conductance values, defined as the reciprocal of the ratio of current to voltage. Drawing from this concept, the admittance matrix is constructed, with each element representing the conductance or conductivity between two nodes in the power system [54].

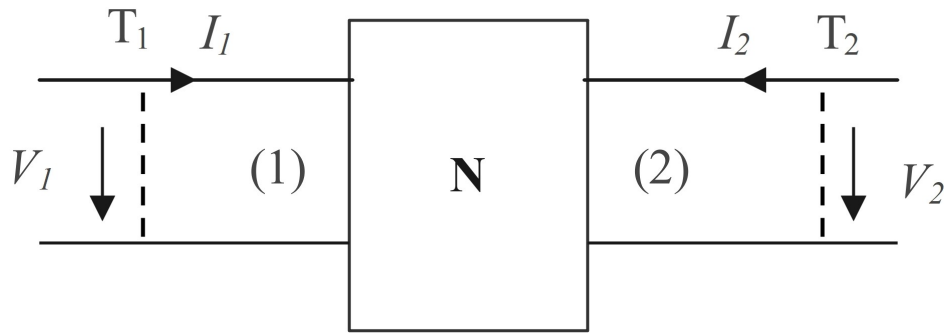


Figure 2.3: Schematic diagram of voltage and current of two-port network

The formula for the admittance matrix in such a two-port network is:

$$\begin{bmatrix} I_1 \\ I_2 \end{bmatrix} = \begin{bmatrix} Y_{11} & Y_{12} \\ Y_{21} & Y_{22} \end{bmatrix} \begin{bmatrix} V_1 \\ V_2 \end{bmatrix} \quad (2.50)$$

Similarly, in an  $N$ -port power system network, the admittance matrix  $Y$  is an  $N \times N$  matrix, where

$N$  represents the number of nodes:

$$\begin{bmatrix} I_1 \\ I_2 \\ \vdots \\ I_N \end{bmatrix} = \begin{bmatrix} Y_{11} & Y_{12} & \dots & Y_{1N} \\ Y_{21} & Y_{22} & & \vdots \\ \vdots & & \ddots & \vdots \\ Y_{N1} & \dots & \dots & Y_{NN} \end{bmatrix} \begin{bmatrix} V_1 \\ V_2 \\ \vdots \\ V_N \end{bmatrix} \quad (2.51)$$

In the admittance matrix, the element  $Y_{ii}$  along the diagonal signifies the self-conductance of node  $i$ , while the element  $Y_{ij}$  off the diagonal denotes the mutual conductance between nodes  $i$  and  $j$ . Once the conductance matrix as per equation (2.50) is derived, solving Kirchhoff's current law allows us to determine the voltage at each node in the power system.

However, despite its widespread use in traditional power system analysis, the Y-bus method exhibits certain limitations when addressing the current tracking challenge of distributed power circuits. Firstly, distributed power sources are typically situated on the low-voltage side, while the Y-bus method primarily deals with the high-voltage side. This discrepancy in system characteristics between the high and low-voltage sides means that the Y-bus method may not yield accurate results when handling distributed power sources [55]. Secondly, the integration of distributed power sources complicates the topology of the power system. Similar to the Z-bus method, the Y-bus method encounters efficiency and accuracy issues as the system complexity increases. Particularly in systems featuring multiple sources, loads, and paths, the computational load of the Y-bus method can become substantial. Lastly, the output of distributed power sources can be influenced by various factors such as weather conditions, equipment status, and energy prices. The variability of these factors leads to continuous changes in the power system's state, necessitating frequent updates to the admittance matrix. However, frequent updates to the conductance matrix escalate computational complexity and resource requirements [56].

### 2.3.6 The Flow-tracing Method

Power flow tracing is based on the system power flow distribution obtained by power flow calculation or state estimation, and traces the power flow according to the principle of node power

proportional distribution, so as to determine the share of each part of the power used [57]. The principle is to determine how the power injected by the power generation node is distributed among the various lines and load nodes of the power grid [58]. By tracing the specific flow of power, this method ensures that each participant in the power system pays for the exact portion of the losses that their power contributes to, thus promoting fairness and efficiency in cost allocation.

At the core of the Flow-tracing Method is the principle of tracing the power injected into the network from each generator and determining how this power is distributed among different consumers. This is achieved by analyzing the power flows on each line of the network, which involves detailed knowledge of the network's topology and the power injection patterns at each bus.

The process begins with constructing a power flow solution for the entire network, typically using techniques such as the Newton-Raphson method or the Fast Decoupled Load Flow method. Once the power flow solution is obtained, it provides the active power flows on each line and the power injections and withdrawals at each bus.

The next step involves decomposing these flows to determine the contribution of each generator to the power flowing through each line. This is achieved through a series of linear equations that represent the conservation of power at each bus and the proportional sharing of flows according to Kirchhoff's laws. By solving these equations, it is possible to trace back the flow of power from each generator to each consumer through the network's lines.

For instance, consider a simple network with two generators and several loads. The Flow-tracing Method will identify how much power from each generator is used to supply each load by examining the power flows along each path connecting the generators to the loads. The method accounts for the fact that power from a single generator can split and take multiple paths to reach different loads, and conversely, a single load may be supplied by multiple generators.

The key advantage of the Flow-tracing Method is its ability to accurately reflect the physical

reality of power flows in the network. This allows for a precise allocation of losses and costs, which is particularly important in deregulated power markets where transparent and fair cost allocation is crucial for market efficiency and participant satisfaction.

In addition to loss allocation, the Flow-tracing Method can also be used for other purposes such as congestion management and transmission pricing. By understanding the specific paths taken by power flows, system operators can identify congested lines and take measures to alleviate congestion, thus enhancing the reliability and efficiency of the power system.

However, the Flow-tracing Method also has some limitations. It requires detailed and accurate data on the network's topology and power flows, which can be complex and time-consuming to obtain. Additionally, the method involves solving large sets of linear equations, which can be computationally intensive for large networks.

Despite these challenges, the Flow-tracing Method remains a valuable tool for power system analysis and management. Its ability to provide a detailed and accurate allocation of losses and costs makes it a preferred choice in many applications, particularly in competitive electricity markets where precision and fairness are paramount.

### **2.3.7 The Current-based Method**

This method allocates the loss of the distribution network based on network characteristics and related circuit theory. Since the current-based method can truly and effectively reflect the status of the power grid and is widely concerned, it is regarded as a key research topic [59, 60]. This method is also the focus of my PhD research. For several specific algorithms, in-depth research work such as understanding of principles and derivation of formulae will be explained in the next session.

## 2.4 The Current-based Algorithm

The Current-based Method is a technique employed for allocating losses within distribution networks. This method hinges on analyzing the current flow through various network components to determine the proportion of losses attributed to each participant or node. By assessing the actual current utilization across the network, this approach aims to provide a more accurate and equitable distribution of loss costs among users. Through this method, stakeholders can gain insights into their specific contributions to network losses, facilitating a fairer and more transparent allocation process. Current-based loss allocation algorithms have evolved with a number of researchers, and these methods are described in detail below.

### 2.4.1 The Method Based on a Cross-term Decomposition Method

In power systems, the loss of a branch is composed of the square term and the cross term of the contributing node. The square term can be easily allocated to the relevant nodes, but how to allocate the cross term reasonably is the main concern. A method called cross-term decomposition method (CTDM) was proposed based on circuit theory [61].

Take the four-node system in Figure 2.4 as an example. The current flowing on branch 23 can be expressed as

$$I_{23} = I_3 + I_4 \quad (2.52)$$

The active power loss on branch 23 is

$$p_{loss}(23) = R_{23} \left[ \text{Re}(I(23))^2 + \text{Im}(I(23))^2 \right] \quad (2.53)$$

$$= R_{23} [(I_3 \cos \theta_3 + I_4 \cos \theta_4) + (I_3 \sin \theta_3 + I_4 \sin \theta_4)] \quad (2.54)$$

$$= 2R_{23} (I_3^2 + 2I_4^2) + 2R_{23} I_3 I_4 \cos(\theta_3 - \theta_4) \quad (2.55)$$

$$= ST(23) + CT(23) \quad (2.56)$$

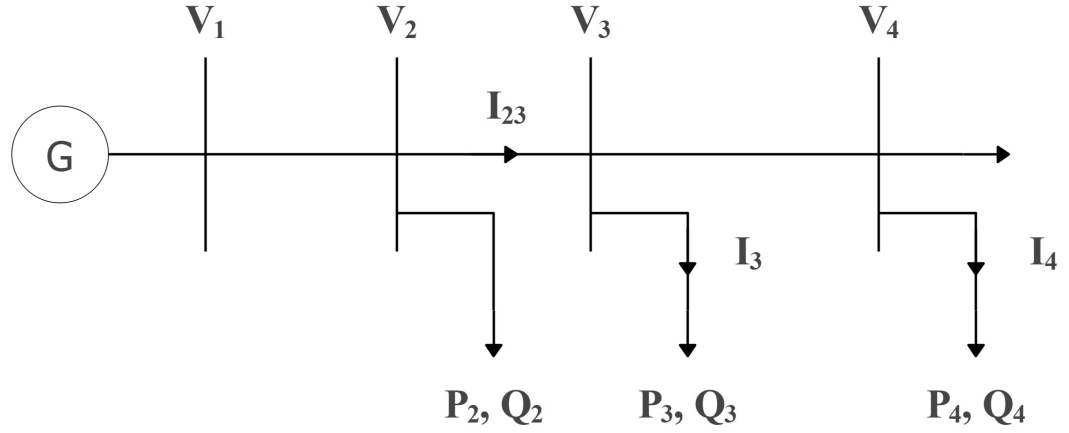


Figure 2.4: A four-node system

Among them,  $ST(23)$  represents the current square term of the loss on the branch 23, and  $CT(23)$  represents the current cross term of the loss on the branch 23. It can be seen that the first item of equation (2.55) can easily distinguish the partial contribution of each node to the active power loss of branch 23. However, the second item in equation (2.55) needs to be further allocated to clarify the contribution of each node. Considering the cross term,

$$\frac{\partial CT(23)}{\partial I_3} = 2R_{23}I_4 \cos(\theta_3 - \theta_4) \quad (2.57)$$

according to equation (2.54), (2.55), (2.56)

$$CT(23) = \frac{1}{2}[CT(23,3) + CT(23,4)] \quad (2.58)$$

where

$$CT(23,3) = 2R_{23}I_3I_4 \cos(\theta_3 - \theta_4) = I_3 \frac{\partial CT(23)}{\partial I_3} \quad (2.59)$$

$$CT(23,4) = 2R_{23}I_4I_3 \cos(\theta_4 - \theta_3) = I_4 \frac{\partial CT(23)}{\partial I_4} \quad (2.60)$$

$CT(23)$  contains the loss contributed by the current  $I_3$  in the cross term, but it can be clearly seen from equation (2.56) that its derivative term is independent of the current itself. Differentiating equation (2.58) with respect to  $I_3$  yields

$$\frac{\partial CT(23,3)}{\partial I_3} = \frac{\partial CT(23)}{\partial I_3} \quad (2.61)$$

From equations (1.58) and (1.60)

$$\frac{\partial CT(23,3)}{CT(23,3)} = \frac{\partial I_3}{I_3} \quad (2.62)$$

It can be obtained from equation (2.61) that there is a linear relationship between  $CT(23,3)$  and  $I_3$ . Therefore, in order to distribute the loss of each node in the cross term, a loss allocation factor (LAF) is defined as

$$K(23,3) = \frac{I_3}{I_{23}} \quad (2.63)$$

$$K(23,4) = \frac{I_4}{I_{23}} \quad (2.64)$$

Then, the contribution of current  $I_3$  to the power loss cross term on branch 23 is allocated as

$$CT(23,3) = K(23,3)CT(23) \quad (2.65)$$

For node 3, the power loss on branch 23 is allocated to it by

$$p_{loss}(23,3) = R_{23}I_3^2 + K(23,3)CT(23) \quad (2.66)$$

The Cross-term Decomposition Method provides several advantages. It allows for a detailed and accurate allocation of losses and costs based on the actual usage of the transmission network. By considering the interactions between different power injections, it ensures that each participant pays for the specific impact they have on the system, promoting fairness and efficiency in cost allocation.

Moreover, this method can be applied to various aspects of power system management, including loss allocation, congestion management, and transmission pricing. By understanding the detailed contributions of different participants to the power flows, system operators can make more informed decisions about resource allocation, investment planning, and pricing strategies.

However, the Cross-term Decomposition Method also presents some challenges. The need to linearize the power flow equations and calculate partial derivatives requires detailed and accurate data on the network's topology and operating conditions. Additionally, the method involves solving complex mathematical equations, which can be computationally intensive for large power systems.

In summary, this method is based on circuit theory and has its simplicity and originality. However, it takes the branches and nodes of the power system as the research object, and cannot solve the loss allocation under the three-phase unbalanced state of the system, therefore it requires further development.

## 2.4.2 Branch Current Decomposition Loss Allocation (BCDLA) Method

This method is based on branch currents and analyses how to allocate losses. For any branch  $l$ , the current flowing through it can be expressed as

$$\bar{I}_{(l)} = \alpha_{(l)} + j\beta_{(l)} \quad (2.67)$$

The output current from any node  $k$  is

$$\bar{I}_k = \alpha_k + j\beta_k \quad (2.68)$$

Then, the loss on branch  $l$  is calculated as

$$L_{(l)} = R_{(l)}(I_{(l)})^2 = R_{(l)} [(\alpha_{(l)})^2 + (\beta_{(l)})^2] = (R_{(l)}\alpha_{(l)}) \alpha_{(l)} + (R_{(l)}\beta_{(l)}) \beta_{(l)} \quad (2.69)$$

where  $R_{(l)}$  is the resistance of branch  $l$ .

In a radial power distribution system, define  $B_k$  as the set of branches connecting node  $k$  to the root node, and define  $N_{(l)}$  as the set of contributing nodes downstream of branch  $l$ . Furthermore, the components  $\alpha_{(l)}$  and  $\beta_{(l)}$  are respectively expressed as the sum of the real and imaginary parts of the current injected into the branch downstream of branch  $l$  in the distribution system, obtaining

$$L_{(l)} = R_{(l)} \alpha_{(l)} \sum_{k \in N_{(l)}} \alpha_k + R_{(l)} \beta_{(l)} \sum_{k \in N_{(l)}} \beta_k \quad (2.70)$$

The part of the loss of branch  $l$  that is allocated to node  $k$  is expressed as

$$L_{(l)k} = R_{(l)} \alpha_{(l)} \alpha_k + R_{(l)} \beta_{(l)} \beta_k \quad \text{for } k \in N_l \quad (2.71)$$

Then the total loss allocated to node  $k$  is

$$L_k = \sum_{l=1}^L L_{(l)k} = \alpha_k \sum_{l=B_k} (R_{(l)} \alpha_{(l)}) + \beta_k \sum_{l=B_k} (R_{(l)} \beta_{(l)}) = c_k \alpha_k + d_k \beta_k \quad (2.72)$$

where  $c_k$  and  $d_k$  are respectively regarded as the real and imaginary parts of a voltage at node  $k$ . Because this voltage is not the actual voltage in the power system, it is defined as a “virtual” voltage, expressed as

$$\bar{V}_{V,k} = c_k + jd_k \quad (2.73)$$

Then, the total loss of node  $k$  is allocated as

$$L_k = \text{Re}(\bar{V}_{V,k} \bar{I}_k^*) \quad (2.74)$$

The virtual voltage on each node can be easily and simultaneously calculated as the total voltage drop on the path. This voltage drop comes from a modified system whose structure is the same as the original network, but the series impedance of the branches is replaced by their resistance

term.

In addition, the current of node  $k$  is expressed by its net active and reactive output power

$$\bar{I}_k = \alpha_k + j\beta_k = \frac{\bar{S}_k^*}{\bar{V}_k^*} = \frac{P_k - jQ_k}{\bar{V}_k^*} \quad (2.75)$$

The voltage at node  $k$  can be expressed as

$$\bar{V}_k = e_k + jf_k \quad (2.76)$$

According to equation (2.74) and (2.75),

$$\alpha_k = \frac{P_k e_k + Q_k f_k}{e_k^2 + f_k^2} \quad (2.77)$$

$$\beta_k = \frac{P_k f_k - Q_k e_k}{e_k^2 + f_k^2} \quad (2.78)$$

From equation (2.71), the losses allocated to node  $k$  become

$$L_k = \frac{c_k P_k e_k + c_k Q_k f_k + d_k P_k f_k - d_k Q_k e_k}{e_k^2 + f_k^2} \quad (2.79)$$

Rewrite the above equation as

$$L_k = \phi_k P_k + \varepsilon_k Q_k \quad (2.80)$$

where

$$\phi_k = \frac{c_k e_k + d_k f_k}{e_k^2 + f_k^2} \quad (2.81)$$

$$\varepsilon_k = \frac{c_k f_k - d_k e_k}{e_k^2 + f_k^2} \quad (2.82)$$

so that  $\phi_k$  and  $\varepsilon_k$  are the loss allocation coefficients.

Compared with other loss allocation methods, this method has several obvious advantages [49,

50, 53, 56, 62]:

- i) This method is based on the circuit analysis, which can make full use of the power flow of the power system, and there are no additional assumptions and approximate values.
- ii) It is easy to implement.
- iii) Compared with other methods, there is no complicated process such as derivative calculation.
- iv) It has a loss allocation coefficient defined by the active and reactive power in the system.

However, implementing the BCDLA method requires detailed data on the network's topology, branch resistances, and real-time measurements of branch currents. Collecting and processing this data can be complex and resource-intensive, particularly for large and intricate distribution networks. Advances in smart grid technologies and real-time monitoring systems can facilitate the application of BCDLA by providing the necessary data and computational capabilities. Moreover, this method has not been extended to the application in unbalanced power distribution systems.

### 2.4.3 The method to extend the branch current decomposition loss allocation (BCDLA) method to a three-phase power distribution system

The two methods mentioned above both use branches and nodes as the research objects, but this method is based on phase analysis. For a radial distributed system, the net input current at node  $k$  is expressed as

$$\mathbf{i}_k = [\bar{I}_{k,1} \quad \bar{I}_{k,2} \quad \bar{I}_{k,3}]^T \quad (2.83)$$

Defining the three-phase loss allocated to node  $k$  as

$$\boldsymbol{\tau}_k = [L_{k,1} \quad L_{k,2} \quad L_{k,3}]^T \quad (2.84)$$

Defining  $N_{(l)}$  as the set of contributing nodes downstream of branch  $l$ , the branch current can be expressed as the sum of the injected node currents

$$\mathbf{i}_{(l)} = \sum_{k \in N_{(l)}} \mathbf{i}_k \quad (2.85)$$

Then, the power loss on branch  $l$  is

$$\Delta \mathbf{P}_{(l)} = \begin{bmatrix} \Delta P_{(l)1} \\ \Delta P_{(l)2} \\ \Delta P_{(l)3} \end{bmatrix} = Re \left\{ (\mathbf{R}_{(l)} (\mathbf{i}_{(l)})^*) \otimes \sum_{k \in N_{(l)}} \mathbf{i}_k \right\} \quad (2.86)$$

The part of the loss of branch  $l$  that is allocated to node  $k$  is expressed as

$$\tau_{(l)\mathbf{k}} = \begin{bmatrix} \tau_{(l)k,1} \\ \tau_{(l)k,2} \\ \tau_{(l)k,3} \end{bmatrix} = \begin{cases} \mathbf{i}_k \otimes (\mathbf{R}_{(l)} (\mathbf{i}_{(l)})^*), & k \in N_{(l)} \\ 0, & k \notin N_{(l)} \end{cases} \quad (2.87)$$

Defining  $B_k$  as the set of branches connecting node  $k$  to the root node, then the total loss allocated to node  $k$  is

$$\tau_k = \sum_{l=1}^L \tau_{(l)k} = Re \left[ \mathbf{i}_k \otimes \sum_{l \in B_k} (\mathbf{R}_{(l)} (\mathbf{i}_{(l)})^*) \right] \quad (2.88)$$

This method uses the impedance matrix and the current of each phase, so that the details of the neutral point and the ground connection no longer need to be shown in detail [63]. In addition, it also uses the actual power flow of the system for loss allocation, and the results obtained are physically valid.

#### 2.4.4 Loss Allocation Methods for Unbalanced Power Distribution Networks

With the advancement of the power system at distribution levels, the issue of three-phase load imbalance in distribution networks has gained prominence. Furthermore, as renewable energy

sources and Distributed Energy Resources (DERs) garner greater attention, the substantial connection of distributed power resources to distribution networks is becoming a prevalent trend. Consequently, achieving a rational and equitable distribution of losses within distribution networks poses a practical challenge. In this section, we will delve into a comprehensive review of three methods for allocating losses in unbalanced distribution systems.

a) Classical Loss Partitioning (CLP) Method

This approach focuses on analyzing a three-phase four-wire line and accounts for current flow in the neutral and ground due to unbalanced operations within distribution networks. Kersting [64] begins with the fundamental flux linkage equation and incorporates both self-impedance and mutual impedance of the line. By employing Kirchhoff's current law (KCL) and utilizing "modified Carson's Equations," a technique for computing the self-impedance and mutual impedance of conductors is derived.

$$\hat{z}_{ii} = r_i + 0.09530 + j0.12134 \left( \ln \frac{1}{GMR_i} + 7.93402 \right) \quad (2.89)$$

$$\hat{z}_{ij} = 0.09530 + j0.12134 \left( \ln \frac{1}{D_{ij}} + 7.93402 \right) \quad (2.90)$$

In these equations, the value of 0.0953 ohms/mile represents the equivalent resistance of earth, while the term 7.93402 denotes the equivalent mutual inductive reactance between soil and a conductor.

Once self and mutual impedances are determined, a 4x4 primitive impedance matrix ( $Z_{prime}$ ) is established. Kersting [64] then utilizes "Korn Reduction" to adjust the primitive impedance matrix, yielding a "phase impedance matrix" ( $Z_{abc}$ ). Following this, a methodology for calculating the real power loss of a line segment is introduced.

$$P_{lossa,b,c} = P_{ina,b,c} - P_{outa,b,c} \quad (2.91)$$

Nevertheless, it has been demonstrated that this approach harbors a conceptual contradic-

tion, rendering it unsuitable for direct application in distribution networks. Consequently, modifications are necessary to eliminate this paradox.

b) Resistive Component based Losses Partitioning (RCLP) Method

As a refinement to the previous method, RCLP was introduced to address the conceptual paradox. Carpaneto et al [63]. initially investigated this paradox within a two-node system (Figure 2.5).

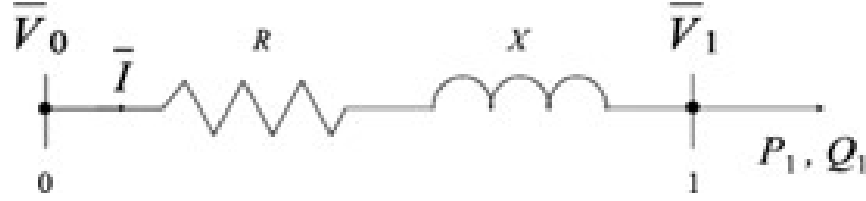


Figure 2.5: Two-node system for loss allocation.

In this system, the losses assigned to node 1 can be formulated as

$$\begin{aligned} L_1 &= Re(\bar{S}_0 - \bar{S}_1) = Re[(\bar{V}_0 - \bar{V}_1)\bar{I}^*] \\ &= \frac{RP_1 + XQ_1}{V_1^2}P_1 + \frac{RQ_1 - XP_1}{V_1^2}Q_1 \end{aligned} \quad (2.92)$$

In this expression, the terms  $\frac{RP_1 + XQ_1}{V_1^2}$  and  $\frac{RQ_1 - XP_1}{V_1^2}$  represent active and reactive loss coefficients, respectively. Notably, while the active coefficient typically remains positive, if the ratio  $\varphi_{line} = \frac{X}{R}$  exceeds  $\varphi_{load} = \frac{Q_1}{P_1}$ , the reactive coefficient can become negative. Hence, assuming the load comprises two components with identical active power but varying (inductive) reactive power, utilizing the loss coefficients derived from equation (2.91) would disadvantage the load exhibiting lower reactive power—a clear paradox. To address the paradox of loss allocation, it's crucial to acknowledge that the term  $\frac{XP_1Q_1}{V_1^2}$  and its counterpart in equation (2.76) can be simplified. Building on this recognition, equation (1.86) can be revised as

$$L_1 = \frac{RP_1}{V_1^2}P_1 + \frac{RQ_1}{V_1^2}Q_1 \quad (2.93)$$

Utilizing the real component of the impedance matrix for loss distribution enables the elimination of the paradox.

Like the CLP method, the RCLP technique employs "Korn Reduction" to adjust the primitive impedance matrix, yielding a "phase impedance matrix" ( $Z_{abc}$ ). However, unlike CLP, RCLP utilizes the real part of the phase impedance matrix ( $R_{abc}$ ) for loss allocation, with branch current serving as the intermediary parameter.

c) Multi-Phase losses allocation method

Usman [55] introduces a novel approach called Multi-Phase Losses Allocation Method (MPLAP) to address this limitation. In the RCLP method, the basis for applying Kron reduction is the assumption of equal voltage across the neutral conductor. In a completely balanced system, where there is no current flow at the neutral point, losses are consequently nonexistent. However, this scenario assumes a solidly grounded neutral configuration, which is often not the case in practice. In real-world unbalanced systems, assigning the loss of the neutral line to end users, especially single-phase end users, is impractical as their connection would exacerbate the inherent imbalance in the power grid. To address this issue within the framework of the RCLP method, this approach reallocates the losses associated with cross-terms and the neutral line among end users and different phases of the nodes.

Power flow tracing and loss allocation are critical areas of research in power system analysis, with significant implications for operational transparency, fairness, and efficiency in modern power grids. The literature highlights a range of methodologies, from classical approaches such as the Bialek tracing algorithm, which is based on proportional sharing principles, to more advanced techniques. These methods have evolved to address the increasing complexity of deregulated markets and the integration of renewable energy sources, enabling more precise allocation of transmission losses and identification of individual contributions to network usage. Despite significant progress, challenges remain in accurately modeling dynamic and distributed systems, particularly under conditions of high renewable penetration. This review forms the basis for the development of advanced power flow tracing and loss allocation techniques proposed in this thesis, aimed at meeting the demands of next-generation power systems.

# Chapter 3

## Complex Loss Allocation Method

### 3.1 Introduction

Electric power distribution networks play a critical role in delivering electricity from generation sources to end-users efficiently and reliably. As the demand for electricity continues to grow, distribution networks face increasing challenges in managing losses, particularly in unbalanced systems where asymmetrical loads and configurations are prevalent [65]. Losses in distribution networks not only lead to economic inefficiencies but also affect system reliability and voltage stability.

Traditionally, loss allocation methods in distribution networks have primarily focused on balanced systems, assuming symmetrical loads and configurations. However, with the proliferation of distributed generation, renewable energy sources, and electrification of loads, the assumption of balance is no longer valid in many distribution networks. As a result, there is a growing need for sophisticated loss allocation methods that can accurately account for the asymmetrical nature of modern distribution systems.

Complex loss allocation methods for unbalanced power distribution networks have emerged as a promising approach to address this challenge. These methods leverage advanced mathematical techniques to accurately allocate losses in unbalanced systems. By considering both active and

reactive power components, as well as network asymmetry, complex loss allocation methods provide a comprehensive and accurate assessment of losses in distribution networks.

One of the primary challenges of implementing complex loss allocation methods lies in the need for detailed data and sophisticated computational tools. These methods often require real-time or near-real-time data on power flows, network topology, and the operational state of various system components. Advanced technologies, such as smart meters, phasor measurement units (PMUs), and advanced distribution management systems (ADMS), are crucial enablers of these complex methods, as they provide the necessary data granularity and computational capacity.

Moreover, complex loss allocation methods are designed to reflect the actual impact of each network user on the system's losses, thereby incentivizing more efficient behavior. For example, users who operate in a way that minimizes their contribution to system losses—such as by shifting their consumption to off-peak times or by investing in energy-efficient equipment—can be rewarded with lower loss charges. This creates a more equitable and economically efficient allocation of costs, aligning individual incentives with overall system efficiency.

The integration of renewable energy sources further complicates the loss allocation process. Renewables, such as solar and wind, are typically intermittent and decentralized, leading to fluctuating power flows that can change the loss profile of the network. Complex loss allocation methods can account for these dynamics, ensuring that the costs associated with integrating renewables are fairly distributed among all system participants.

In addition to fairness and accuracy, the transparency of complex loss allocation methods is essential for gaining the trust and acceptance of stakeholders, including utilities, regulators, and consumers. Clear and understandable methodologies are more likely to be supported by the industry and can help avoid disputes over cost allocations.

The objective of this thesis is to develop and implement novel complex loss allocation algorithms that can accurately account for the asymmetrical nature of distribution systems. In this chapter, the proposed loss allocation method is described and derived in detail. Further, the simulation

will be implemented and results will be analysed based on the unbalanced system-IEEE123 node system.

### 3.2 Calculation of the Primitive Impedance Matrix

Before commencing the analysis of a distribution feeder, it is essential to establish the series impedance for overhead and underground lines. The series impedance of a single-phase, two-phase (V-phase), or three-phase distribution line encompasses conductor resistance and self and mutual inductive reactances generated by the magnetic fields surrounding the conductors.

The inductive reactance component (both self and mutual) of the impedance depends on the aggregate magnetic fields surrounding a conductor. Figure 3.1 illustrates conductors 1 to  $n$  alongside the magnetic flux lines produced by currents passing through each conductor.

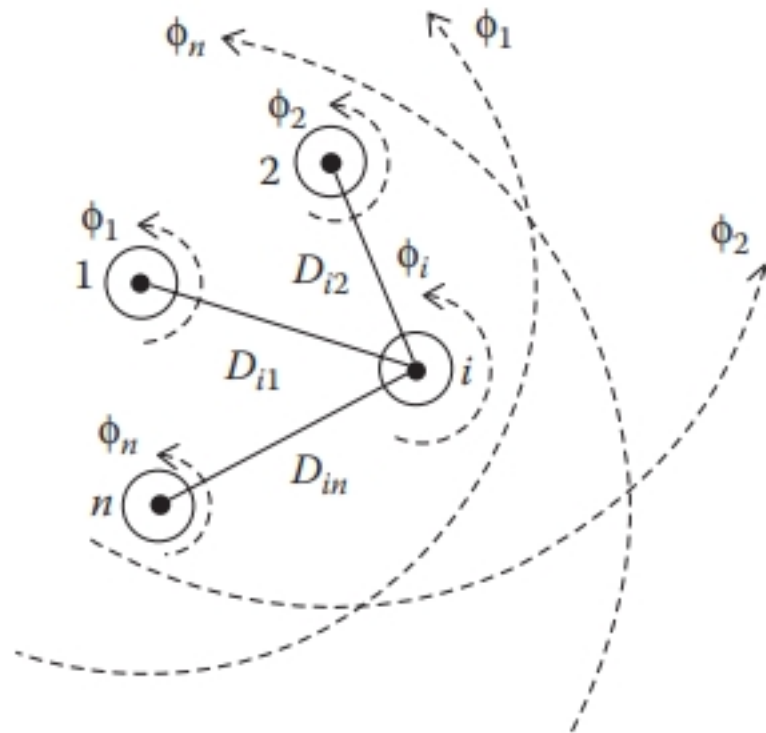


Figure 3.1: Magnetic fields

It is assumed that currents in all conductors flow outward from the page. Additionally, it is

presumed that the sum of these currents equals zero. The equation is:

$$I_1 + I_2 + \dots + I_i + \dots + I_n = 0 \quad (3.1)$$

The total flux associated with conductor  $i$  can be expressed as:

$$\lambda_i = 2 \cdot 10^{-7} \cdot \left( I_1 \cdot \ln \frac{1}{D_{i-1}} + I_2 \cdot \ln \frac{1}{D_{i-2}} + \dots + I_i \cdot \ln \frac{1}{GMR_i} + \dots + I_n \cdot \ln \frac{1}{D_{i-n}} \right) \text{W-T/m} \quad (3.2)$$

where  $D_{i-n}$  is the distance between conductor  $i$  and conductor  $n$  with the unit  $ft$  and  $GMR_i$  is the geometric mean radius of conductor  $i$  also with the unit  $ft$ .

The inductance of conductor  $i$  comprises both its "self-inductance" and the "mutual inductance" between conductor  $i$  and all remaining  $n - 1$  conductors. This relationship is defined as:

Self-inductance:

$$L_{ii} = \frac{\lambda_{ii}}{I_i} = 2 \cdot 10^{-7} \cdot \ln \frac{1}{GMR_i} \text{H/m} \quad (3.3)$$

Mutual inductance:

$$L_{in} = \frac{\lambda_{in}}{I_n} = 2 \cdot 10^{-7} \cdot \ln \frac{1}{D_{i-n}} \text{H/m} \quad (3.4)$$

Given the diversity of distribution systems, comprising single-phase, two-phase, and untransposed three-phase lines catering to unbalanced loads, it is necessary to maintain the distinctiveness of both self- and mutual impedance terms of the conductors. Furthermore, considering the ground return path for unbalanced currents is essential. Equations (3.3) and (3.4) are applied for calculating the self- and mutual inductive reactances of the conductors. The inductive reactance will be considered at a frequency of 60Hz, and the length of the conductor will be assumed to be 1 mile. Under these assumptions, the self- and mutual impedances are as follows:

The self-impedance:

$$\bar{z}_{ii} = r_i + j0.12134 \cdot \ln \frac{1}{GMR_i} \Omega/\text{mile} \quad (3.5)$$

The mutual impedance:

$$\bar{z}_{ij} = j0.12134 \cdot \ln \frac{1}{D_{ij}} \Omega/\text{mile} \quad (3.6)$$

John Carson published a paper in 1926 [66], presenting a set of equations for calculating the self- and mutual impedances of lines, which consider the return path of the current through the ground. His method involved modeling a line with conductors connected to a source at one end and grounded at the remote end. Figure 3.2 depicts a line with two conductors ( $i$  and  $j$ ) carrying currents ( $I - i$  and  $I - j$ ), where the remote ends are connected to the ground. A hypothetical "dirt" conductor with current  $I_d$  represents the return path for the currents.

In Figure 3.2, according to the Kirchhoff's voltage law (KVL), the equation for the voltage between conductor  $i$  and the ground can be calculated.

$$V_{iground} = \bar{z}_{ii} \cdot I_i + \bar{z}_{ij} \cdot I_j + \bar{z}_{id} \cdot I_d - (\bar{z}_{dd} \cdot I_d + \bar{z}_{di} \cdot I_i + \bar{z}_{dj} \cdot I_j) \quad (3.7)$$

Equation (3.7) can be rewritten as:

$$V_{iground} = (\bar{z}_{ii} - \bar{z}_{di}) \cdot I_i + (\bar{z}_{ij} - \bar{z}_{dj}) \cdot I_j + (\bar{z}_{id} - \bar{z}_{dd}) \quad (3.8)$$

According to the Kirchhoff's Current Law:

$$I_i + I_j + I_d = 0 \quad (3.9)$$

$$I_d = -I_i - I_j \quad (3.10)$$

Replace Equation (3.9) and (3.10) with Equation (3.8) and gather the terms.

$$V_{iground} = (\bar{z}_{ii} + \bar{z}_{dd} - \bar{z}_{di} - \bar{z}_{id}) \cdot I_i + (\bar{z}_{ij} + \bar{z}_{dd} - \bar{z}_{dj} - \bar{z}_{id}) \cdot I_j \quad (3.11)$$

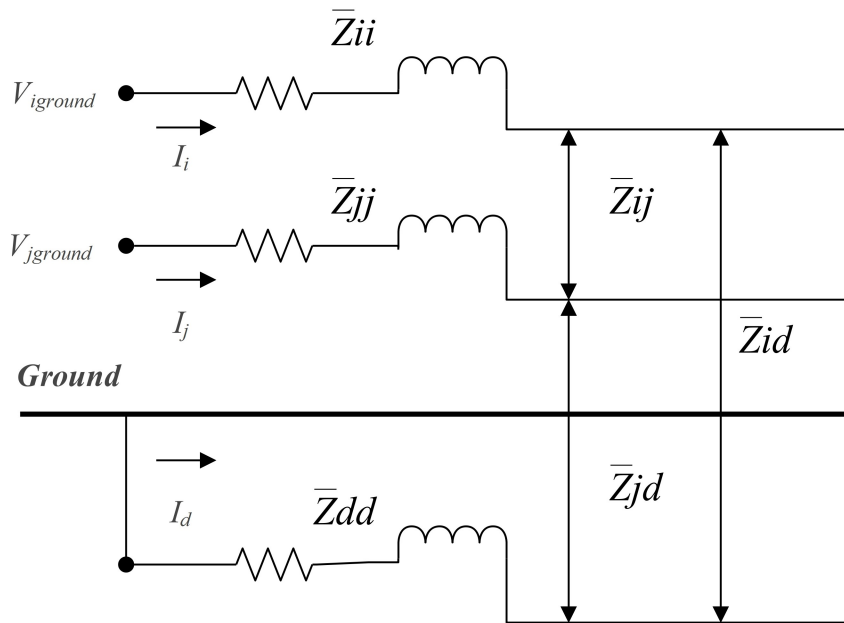


Figure 3.2: Two-conductor system

Above equation can be rewritten as:

$$V_{iground} = \hat{z}_{ii} \cdot I_i + \hat{z}_{ij} \cdot I_j \quad (3.12)$$

In Equation (3.12),

$$\hat{z}_{ii} = \bar{z}_{ii} + \bar{z}_{dd} - \bar{z}_{di} - \bar{z}_{id} \quad (3.13)$$

$$\hat{z}_{ij} = \bar{z}_{ij} + \bar{z}_{dd} - \bar{z}_{dj} - \bar{z}_{id} \quad (3.14)$$

In Equations (3.13) and (3.14), the "hat" impedances are defined by Equations (3.5) and (3.6). Note that these equations incorporate the effect of the ground return path into what are now termed the "primitive" self- and mutual impedances of the line. The "equivalent primitive circuit" is illustrated in Figure 3.3.

By substituting Equations (3.5) and (3.6) for the "hat" impedances into Equations (3.13) and

(3.14), the primitive self-impedance is determined as follows:

$$\hat{z}_{ii} = r_i + jx_{ii} + r_d + jx_{dd} - jx_{dn} - jx_{nd} \quad (3.15)$$

$$\hat{z}_{ii} = r_d + r_i + j0.12134 \cdot \left( \ln \frac{1}{GMR_i} + \ln \frac{1}{GMR_d} - \ln \frac{1}{D_{id}} - \ln \frac{1}{D_{di}} \right) \quad (3.16)$$

$$\hat{z}_{ii} = r_d + r_i + j0.12134 \cdot \left( \ln \frac{1}{GMR_i} + \ln \frac{D_{id} \cdot D_{dj}}{GMR_d} \right) \quad (3.17)$$

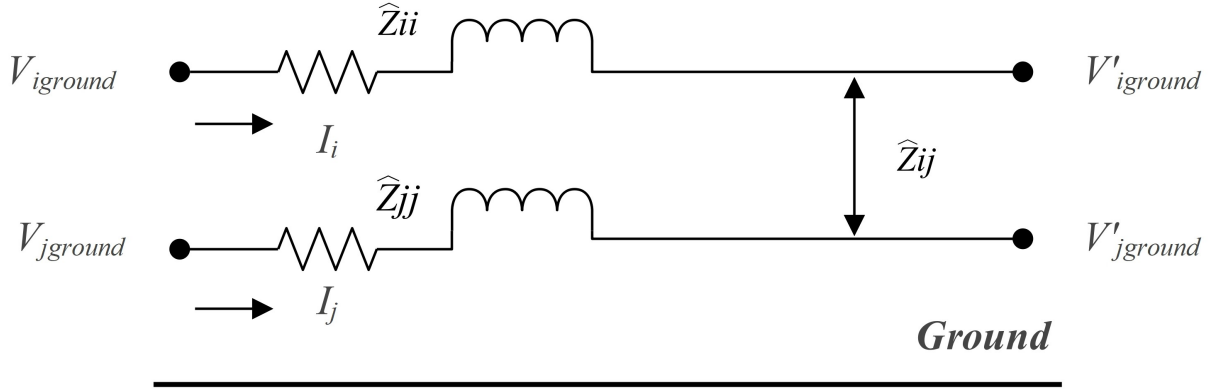


Figure 3.3: The equivalent primitive circuit.

Similarly, the primitive mutual impedance can be expanded as follows:

$$\hat{z}_{ij} = jx_{ij} + r_d + jx_{dd} - jx_{dj} - jx_{id} \quad (3.18)$$

$$\hat{z}_{ij} = r_d + j0.12134 \cdot \left( \ln \frac{1}{D_{ij}} + \ln \frac{1}{GMR_d} - \ln \frac{1}{D_{dj}} - \ln \frac{1}{D_{id}} \right) \quad (3.19)$$

$$\hat{z}_{ij} = r_d + j0.12134 \cdot \left( \ln \frac{1}{D_{ij}} + \ln \frac{D_{dj} \cdot D_{id}}{GMR_d} \right) \quad (3.20)$$

The clear issue with using Equations (3.15) to (3.20) is that we do not know the values for the

resistance of dirt ( $r_d$ ), the geometric mean radius of dirt ( $GMR_d$ ), and the distances from the conductors to dirt ( $D_{nd}, D_{dn}, D_{md}, D_{dm}$ ). This is where John Carson's work provides a solution.

### 3.2.1 Carson's Equations

Since a distribution feeder is inherently unbalanced, the most accurate analysis should avoid assumptions about conductor spacing, sizes, and transposition. In his 1926 paper [66], Carson developed a technique to determine the self- and mutual impedances for  $n_{cond}$  overhead conductors, which can also be applied to underground cables. Initially, this method did not gain much enthusiasm due to the tedious calculations required by slide rule and by hand. However, with the advent of digital computers, Carson's equations have become widely utilized.

In his research, Carson assumes the earth to be an infinite, uniform solid with a flat upper surface and constant resistivity. Any "end effects" introduced at the neutral grounding points are considered negligible at power frequencies and are therefore ignored.

Carson utilized conductor images, meaning that every conductor at a certain distance above ground has an image conductor at an equal distance below ground. This concept is illustrated in Figure 3.4.

As shown in Figure 3.4, the original Carson equations are presented as follow.

Self-impedance:

$$\hat{z}_{ii} = r_i + 4\omega P_{ii}G + j \left( X_i + 2\omega G \cdot \ln \frac{S_{ii}}{RD_i} + 4\omega Q_{ii}G \right) \Omega/\text{mile} \quad (3.21)$$

Mutual impedance:

$$\hat{z}_{ij} = 4\omega P_{ij}G + j \left( 2\omega G \cdot \ln \frac{S_{ij}}{D_{ij}} + 4\omega Q_{ij}G \right) \Omega/\text{mile} \quad (3.22)$$

In the Equations (3.21) and (3.22),

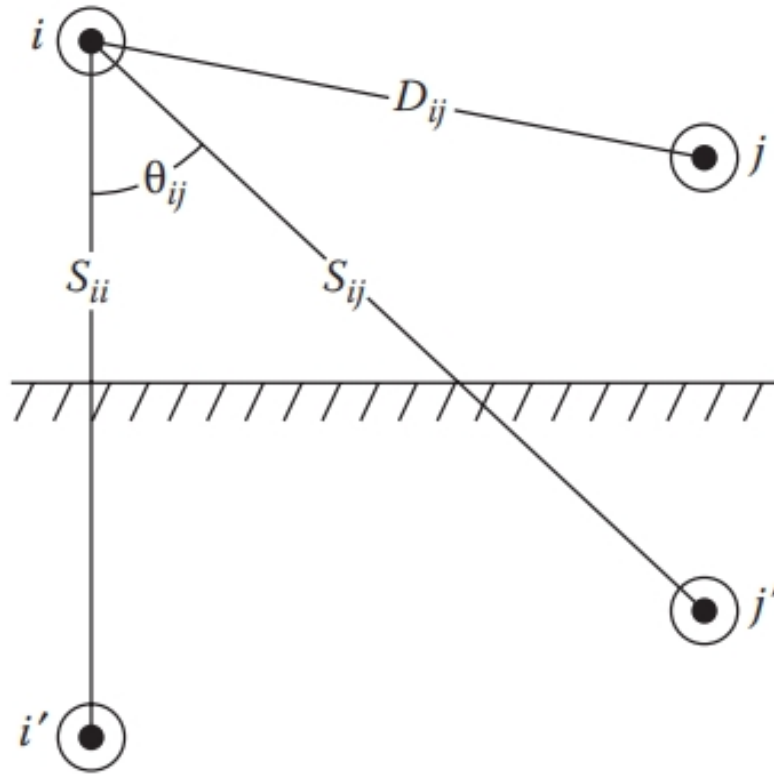


Figure 3.4: Conductor images

$\hat{z}_{ii}$  is the self-impedance of conductor  $i$  in  $\Omega/mile$ ;

$\hat{z}_{ij}$  is the mutual impedance between conductors  $i$  and  $j$  in  $\Omega/mile$ ;

$r_i$  is the resistance of conductor  $i$  in  $\Omega/mile$ ;

$\omega = 2\pi f$  is system angular frequency in radians per second;

$G = 0.1609347 \times 10^{-3} \Omega/mile$ ;

$RD_i$  is the radius of conductor  $i$  in ft;

$D_{ij}$  is the distance between conductors  $i$  and  $j$  in ft;

$S_{ij}$  is the distance between conductor  $i$  and image  $j$  in ft;

$$X_i = 2\omega G \cdot \ln \frac{RD_i}{GMR_i} \Omega/mile \quad (3.23)$$

where  $GMR_i$  the geometric mean radius of conductor  $i$  in ft

$$P_{ij} = \frac{\pi}{8} - \frac{1}{3\sqrt{2}}k_{ij} \cos(\theta_{ij}) + \frac{k_{ij}^2}{16} \cos(2\theta_{ij}) \cdot \left(0.6728 + \ln \frac{2}{k_{ij}}\right) \quad (3.24)$$

where  $\theta_{ij}$  is the angle between a pair of lines drawn from conductor  $i$  to its own image and to the image of conductor  $j$

$$Q_{ij} = -0.0386 + \frac{1}{2} \cdot \ln \frac{2}{k_{ij}} + \frac{1}{3\sqrt{2}}k_{ij} \cos(\theta_{ij}) \quad (3.25)$$

$$k_{ij} = 8.565 \cdot 10^{-4} \cdot S_{ij} \cdot \sqrt{\frac{f}{\rho}} \quad (3.26)$$

where

$f$  represents the system frequency in Hertz;

$\rho$  is the resistivity of earth in  $\Omega - meters$ .

### 3.2.2 Modified Carson's Equations

In deriving the "Modified Carson Equations," only two approximations are made. These involve the terms associated with  $P_{ij}$  and  $Q_{ij}$ . The approximations utilize only the first term of  $P_{ij}$  and the first two terms of  $Q_{ij}$ .

$$P_{ij} = \frac{\pi}{8} \quad (3.27)$$

$$Q_{ij} = -0.03860 + \frac{1}{2} \ln \frac{2}{k_{ij}} \quad (3.28)$$

Combine the Equation (3.21) and (3.23),

$$\hat{z}_{ii} = r_i + 4\omega P_{ii}G + j \left( 2\omega G \cdot \ln \frac{RD_i}{GMR_i} + 2\omega G \cdot \ln \frac{S_{ii}}{RD_i} + 4\omega Q_{ii}G \right) \quad (3.29)$$

Simplify the above equation,

$$\hat{z}_{ii} = r_i + 4\omega P_{ii}G + j2\omega G \left( \ln \frac{S_{ii}}{GMR_i} + \ln \frac{RD_i}{RD_i} + 2Q_{ii} \right) \quad (3.30)$$

Simplify Equation (3.22),

$$\hat{z}_{ij} = 4\omega P_{ij}G + j2\omega G \left( \ln \frac{S_{ij}}{D_{ij}} + 2Q_{ij} \right) \quad (3.31)$$

Replace the expressions for  $P$  (Equation (3.28)) and  $\omega$  ( $2\pi f$ ):

$$\hat{z}_{ii} = r_i + \pi^2 fG + j4\pi fG \left( \ln \frac{S_{ii}}{GMR_i} + 2Q_{ii} \right) \quad (3.32)$$

$$\hat{z}_{ij} = \pi^2 fG + j4\pi fG \left( \ln \frac{S_{ij}}{D_{ij}} + 2Q_{ij} \right) \quad (3.33)$$

Replace the expression for  $k_{ij}$  (Equation (3.26)) into the approximate expression for  $Q_{ij}$  (Equation (3.28)):

$$Q_{ij} = -0.03860 + \frac{1}{2} \ln \left( \frac{2}{8.565 \cdot 10^{-4} \cdot S_{ij} \cdot \sqrt{\frac{f}{\rho}}} \right) \quad (3.34)$$

This equation can be expanded as:

$$Q_{ij} = -0.03860 + \frac{1}{2} \ln \left( \frac{2}{8.565 \cdot 10^{-4}} \right) + \frac{1}{2} \ln \frac{1}{S_{ij}} + \frac{1}{2} \ln \sqrt{\frac{\rho}{f}} \quad (3.35)$$

Equation (3.35) can be reduced to:

$$Q_{ij} = 3.8393 - \frac{1}{2} \ln S_{ij} + \frac{1}{4} \ln \frac{\rho}{f} \quad (3.36)$$

It can also be expressed as:

$$2Q_{ij} = 2Q_{ij} = 7.6786 - \ln S_{ij} + \frac{1}{2} \ln \frac{\rho}{f} \quad (3.37)$$

Substitute Equation (3.37) into Equation (3.32) :

$$\hat{z}_{ii} = r_i + \pi^2 fG + j4\pi fG \left( \ln \frac{S_{ii}}{GMR_i} + 7.6786 - \ln S_{ii} + \frac{1}{2} \ln \frac{\rho}{f} \right) \quad (3.38)$$

Simplify the equation to:

$$\hat{z}_{ii} = r_i + \pi^2 fG + 4\pi fG \left( \ln \frac{1}{GMR_i} + 7.6786 + \frac{1}{2} \ln \frac{\rho}{f} \right) \quad (3.39)$$

Substitute Equation (3.37) into Equation (3.33):4

$$\hat{z}_{ij} = \pi^2 fG + j4\pi fG \left( \ln \frac{S_{ij}}{D_{ij}} + 7.6786 - \ln S_{ij} + \frac{1}{2} \ln \frac{\rho}{f} \right) \quad (3.40)$$

Simplify the equation to:

$$\hat{z}_{ij} = \pi^2 fG + j4\pi fG \left( \ln \frac{1}{D_{ij}} + 7.6786 + \frac{1}{2} \ln \frac{\rho}{f} \right) \quad (3.41)$$

Substitute the values of  $G$  and  $\pi$  :

$$\hat{z}_{ii} = r_i + 0.00158836 \cdot f + j0.00202237 \cdot f \left( \ln \frac{1}{GMR_i} + 7.6786 + \frac{1}{2} \ln \frac{\rho}{f} \right) \quad (3.42)$$

$$\hat{z}_{ij} = 0.00158836 \cdot f + j0.00202237 \cdot f \left( \ln \frac{1}{D_{ij}} + 7.6786 + \frac{1}{2} \ln \frac{\rho}{f} \right) \quad (3.43)$$

There are the assumptions as:

Frequency :  $f = 60\text{Hertz}$

Earth resistivity :  $\rho = 100\Omega - m$

Based on these assumptions and approximations, the “Modified Carson’s Equations” are:

$$\hat{z}_{ii} = r_i + 0.09530 + j0.12134 \left( \ln \frac{1}{GMR_i} + 7.93402 \right) \Omega/\text{mile} \quad (3.44)$$

$$\hat{z}_{ij} = 0.09530 + j0.12134 \left( \ln \frac{1}{D_{ij}} + 7.93402 \right) \Omega/\text{mile} \quad (3.45)$$

Recall that Equations (3.15) to (3.20) were unusable due to unknown variables such as the resistance of dirt, the  $GMR_d$ , and various distances from conductors to dirt. However, comparing Equations (3.17) and (3.20) to Equations (3.44) and (3.45) shows that the Modified Carson’s Equations have provided definitions for these previously missing parameters. A comparison of the two sets of equations reveals that:

$$r_d = 0.09530\Omega/\text{mile} \quad (3.46)$$

$$\ln \frac{D_{id} \cdot D_{di}}{GMR_d} = \ln \frac{D_{dj} \cdot D_{id}}{GMR_d} = 7.93402 \quad (3.47)$$

The "Modified Carson’s Equations" will be employed to calculate the primitive self- and mutual impedances of both overhead and underground lines.

### 3.2.3 Primitive Impedance Matrix for Overhead Lines

Equations (3.44) and (3.45) are used to compute the elements of an  $n_{cond} \times n_{cond}$  "primitive impedance matrix." For an overhead four-wire grounded wye distribution line segment, this results in a  $4 \times 4$  matrix. For an underground grounded wye line segment with three concentric neutral cables, the matrix will be  $6 \times 6$ . The primitive impedance matrix for a three-phase line with  $m$  neutrals will be of the form:

$$\left[ \hat{Z}_{primitive} \right] = \begin{bmatrix} \hat{Z}_{aa} & \hat{Z}_{ab} & \hat{Z}_{aa} & | & \hat{Z}_{an1} & \hat{Z}_{an2} & \hat{Z}_{anm} \\ \hat{Z}_{ba} & \hat{Z}_{bb} & \hat{Z}_{bc} & | & \hat{Z}_{bn1} & \hat{Z}_{bn2} & \hat{Z}_{bnm} \\ \hat{Z}_{ca} & \hat{Z}_{cb} & \hat{Z}_{cc} & | & \hat{Z}_{cn1} & \hat{Z}_{cn2} & \hat{Z}_{cnm} \\ \hline \hat{Z}_{n1a} & \hat{Z}_{n1b} & \hat{Z}_{n1c} & | & \hat{Z}_{n1n1} & \hat{Z}_{n1n2} & \hat{Z}_{n1nm} \\ \hat{Z}_{n2a} & \hat{Z}_{n2b} & \hat{Z}_{n2c} & | & \hat{Z}_{n2n1} & \hat{Z}_{n2n2} & \hat{Z}_{n2nm} \\ \hat{Z}_{nma} & \hat{Z}_{nmb} & \hat{Z}_{nmc} & | & \hat{Z}_{nmn1} & \hat{Z}_{nmn2} & \hat{Z}_{nmnm} \end{bmatrix} \quad (3.48)$$

Equation (3.48) can be rewritten as:

$$\left[ \hat{z}_{primitive} \right] = \begin{bmatrix} \left[ \hat{z}_{ij} \right] & \left[ \hat{z}_{in} \right] \\ \left[ \hat{z}_{nj} \right] & \left[ \hat{z}_{nn} \right] \end{bmatrix} \quad (3.49)$$

### 3.2.4 Phase Impedance Matrix for Overhead Lines

For most cases, the primitive impedance matrix needs to be reduced to a  $3 \times 3$  "phase frame" matrix, which includes the self- and mutual equivalent impedances for the three phases. Figure 3.5 illustrates a four-wire grounded neutral line segment.

A common method for reduction is the "Kron" reduction [67]. It is assumed that the line has a multi-grounded neutral, as shown in Figure 3.5. The Kron reduction method applies Kirchhoff's

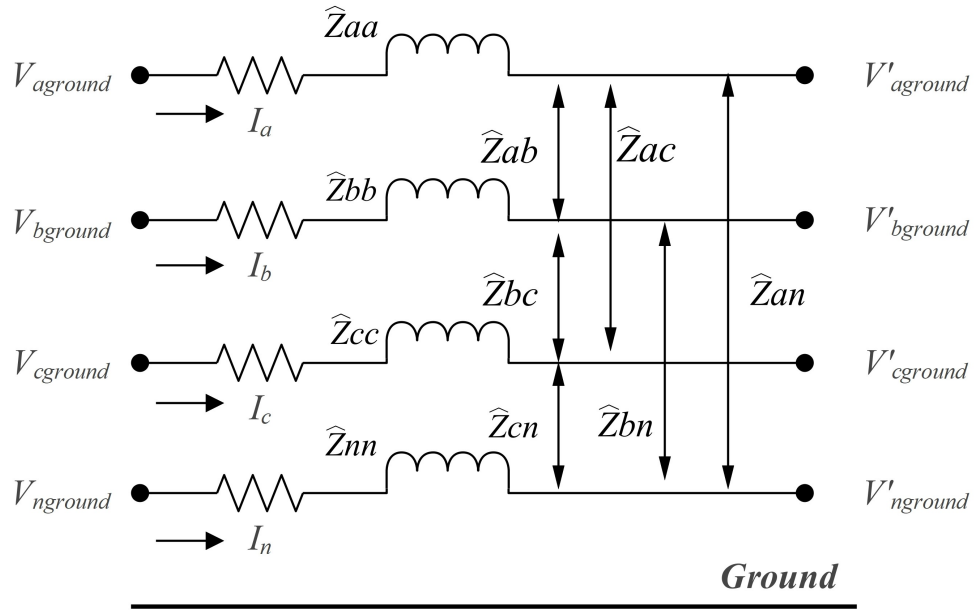


Figure 3.5: Four-wire grounded neutral line segment

Voltage Law (KVL) to the circuit.

$$\begin{bmatrix} V_{aground} \\ V_{bground} \\ V_{cground} \\ V_{nground} \end{bmatrix} = \begin{bmatrix} V'_{aground} \\ V'_{bground} \\ V'_{cground} \\ V'_{nground} \end{bmatrix} + \begin{bmatrix} \hat{Z}_{aa} & \hat{Z}_{ab} & \hat{Z}_{ac} & \hat{Z}_{an} \\ \hat{Z}_{ba} & \hat{Z}_{bb} & \hat{Z}_{bc} & \hat{Z}_{bn} \\ \hat{Z}_{ca} & \hat{Z}_{cb} & \hat{Z}_{cc} & \hat{Z}_{cn} \\ \hat{Z}_{na} & \hat{Z}_{nb} & \hat{Z}_{nc} & \hat{Z}_{nn} \end{bmatrix} \cdot \begin{bmatrix} I_a \\ I_b \\ I_c \\ I_n \end{bmatrix} \quad (3.50)$$

Equation (3.50) can be written in partitioned form,

$$\begin{bmatrix} [V_{abc}] \\ [V_{nground}] \end{bmatrix} = \begin{bmatrix} [V'_{abc}] \\ [V'_{nground}] \end{bmatrix} + \begin{bmatrix} [\hat{z}_{ij}] & [\hat{z}_{in}] \\ [\hat{z}_{nground}] & [\hat{z}_{nn}] \end{bmatrix} \cdot \begin{bmatrix} [I_{abc}] \\ [I_n] \end{bmatrix} \quad (3.51)$$

Since the neutral is grounded, the voltages  $V_{nground} = V'_{nground} = 0$ . Substituting these values into Equation (3.51) and expanding it results in:

$$[V_{abc}] = [V'_{abc}] + [\hat{z}_{ij}] \cdot [I_{abc}] + [\hat{z}_{in}] \cdot [I_n] \quad (3.52)$$

$$[0] = [0] + [\hat{z}_{nj}] \cdot [I_{abc}] + [\hat{z}_{nn}] \cdot [I_n] \quad (3.53)$$

According to equation (3.53), the  $[I_n]$  can be calculated as:

$$[I_n] = [\hat{z}_{nn}]^{-1} \cdot [\hat{z}_{nj}] \cdot [I_{abc}] \quad (3.54)$$

In Equation (3.54), once the line current has been calculated, the current flowing through the neutral conductor can be determined. In addition, the “neutral transformation matrix” is defined as:

$$[t_n] = -[\hat{z}_{nn}]^{-1} \cdot [\hat{z}_{nj}] \quad (3.55)$$

The equation (3.54) can be rewritten as:

$$[I_n] = [t_n] \cdot [I_{abc}] \quad (3.56)$$

Combine the equation (3.52) and (3.54),

$$[V_{abc}] = [V'_{abc}] + \left( [\hat{z}_{ij}] - [\hat{z}_{in}] \cdot [\hat{z}_{nn}]^{-1} \cdot [\hat{z}_{nj}] \right) \cdot [I_{abc}] \quad (3.57)$$

$$\begin{bmatrix} V_{abc} \end{bmatrix} = \begin{bmatrix} V'_{abc} \end{bmatrix} + \begin{bmatrix} Z_{abc} \end{bmatrix} \cdot \begin{bmatrix} I_{abc} \end{bmatrix} \quad (3.58)$$

In the equation (3.58),

$$[z_{abc}] = [\hat{z}_{ij}] - [\hat{z}_{in}] \cdot [\hat{z}_{nn}]^{-1} \cdot [\hat{z}_{nj}] \quad (3.59)$$

Equation (3.59) represents the final form of the "Kron" reduction technique. The resulting phase impedance matrix is:

$$\begin{bmatrix} z_{abc} \end{bmatrix} = \begin{bmatrix} Z_{aa} & Z_{ab} & Z_{ac} \\ Z_{ba} & Z_{bb} & Z_{bc} \\ Z_{ca} & Z_{cb} & Z_{cc} \end{bmatrix} \Omega/\text{mile} \quad (3.60)$$

For an untransposed distribution line, the diagonal terms of Equation (3.60) will not be equal

to each other, and the off-diagonal terms will also differ. However, the matrix will remain symmetrical.

In the case of two-phase (v-phase) and single-phase lines in earthed systems, the modified Carson's equations can be applied, resulting in initial  $3 \times 3$  and  $2 \times 2$  original impedance matrices. The application of the Kron reduction reduces the matrices to  $2 \times 2$  and one element. If a  $3 \times 3$  'phase frame' matrix is desired, this can be achieved by adding rows and columns consisting of zero elements. For example, for a v-phase line consisting of phases a and c, the phase impedance matrix is:

$$\begin{bmatrix} z_{abc} \end{bmatrix} = \begin{bmatrix} z_{aa} & 0 & z_{ac} \\ 0 & 0 & 0 \\ z_{ca} & 0 & z_{cc} \end{bmatrix} \Omega/\text{mile} \quad (3.61)$$

The phase impedance matrix for a phase b single-phase line can be expressed as:

$$\begin{bmatrix} z_{abc} \end{bmatrix} = \begin{bmatrix} 0 & 0 & 0 \\ 0 & z_{bb} & 0 \\ 0 & 0 & 0 \end{bmatrix} \Omega/\text{mile} \quad (3.62)$$

The phase impedance matrix of the three-wire delta line can be determined directly from the Carson equation without the need for a Kron reduction step.

In the case of current determination, the phase impedance matrix can be used to accurately determine the voltage drop across the feeder section. Since no approximation (e.g. transposition) is made for the spacing between conductors, the effects of mutual coupling between phases are accurately taken into account. The application of the phase frame matrix and the modified Carson's equation provides the most accurate line segment model. A Three-phase line segment model is shown in Figure 3.6. It is worth noting that some impedance values will be zero for v-phase and single-phase lines.

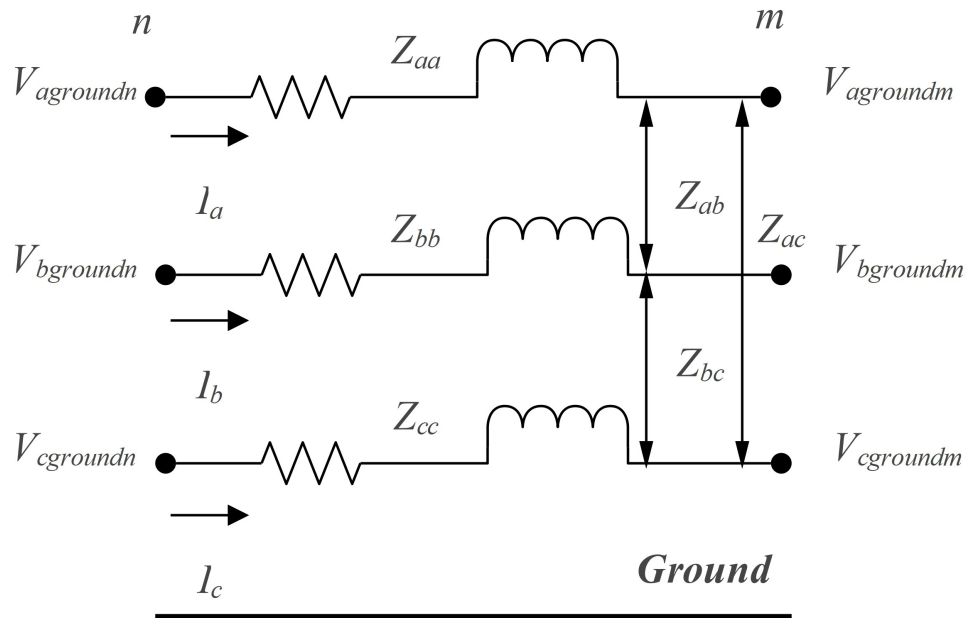


Figure 3.6: Three-phase line segment model

The voltage in matrix form for the line segment can be expressed as:

$$\begin{bmatrix} V_{aground} \\ V_{bground} \\ V_{cground} \end{bmatrix}_n = \begin{bmatrix} V_{aground} \\ V_{bground} \\ V_{cground} \end{bmatrix}_m + \begin{bmatrix} Z_{aa} & Z_{ab} & Z_{ac} \\ Z_{ba} & Z_{bb} & Z_{bc} \\ Z_{ca} & Z_{cb} & Z_{cc} \end{bmatrix} \cdot \begin{bmatrix} I_a \\ I_b \\ I_c \end{bmatrix} \quad (3.63)$$

Equation (3.63) can be written as:

$$\begin{bmatrix} VLG_{abc} \end{bmatrix}_n = \begin{bmatrix} VLG_{abc} \end{bmatrix}_m + \begin{bmatrix} Z_{abc} \end{bmatrix} \cdot \begin{bmatrix} I_{abc} \end{bmatrix} \quad (3.64)$$

### 3.2.5 Series Impedance of Underground Lines

The modified Carson equation can be applied not only to overhead lines but also to underground cables. The general configuration of the three underground cables is shown in Figure 3.7 (coaxial neutral or shielded), plus the neutral conductor. Based on the circuit in Figure 3.7, a primitive impedance matrix of  $7 \times 7$  will be obtained. In the case of an underground circuit with no additional neutral conductor, the raw impedance matrix would be  $6 \times 6$ .

Two common types of underground cables are 'tape-shielded cables' and 'concentric neutral

cables'. The application of the modified Carson equation assumes that the resistance and GMR of the phase conductors and the equivalent neutral are known.

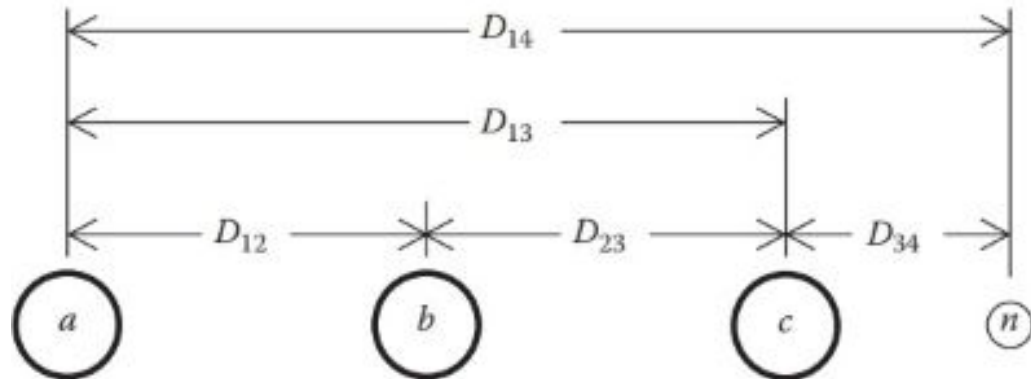


Figure 3.7: Three-phase underground with additional neutral

Figure 3.8 [68] illustrates the structure of a concentric neutral cable. It features a central "phase conductor" covered by a thin layer of nonmetallic semiconducting screen bonded to the insulating material. This insulation is then encased in a semiconducting insulation screen. Solid strands of concentric neutral are spiraled around the semiconducting screen with uniform spacing between strands. Some cables also include an insulating "jacket" surrounding the neutral strands.

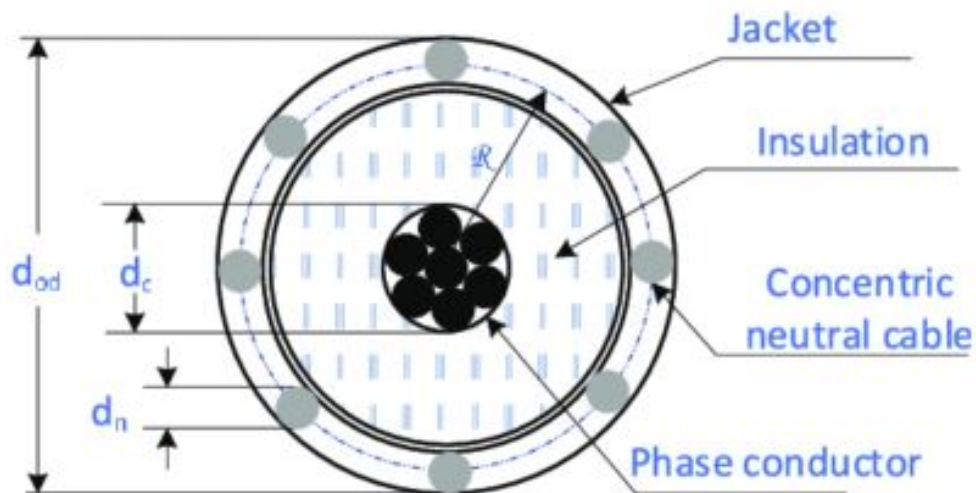


Figure 3.8: Concentric neutral cable

In the Figure 3.8,

$d_c$  is the phase conductor diameter in inch;

$d_{od}$  is the nominal diameter over the concentric neutrals of the cable in inch;

$d_s$  is the diameter of a concentric neutral strand in inch.

Using the equivalent geometric mean radius(GMR) formula for bundled conductors in high voltage transmission lines, the equivalent GMR for concentric neutrals can be calculated [66].

$$GMR_{cn} = \sqrt[k]{GMR_s \cdot k \cdot R^{k-1}} \text{ft} \quad (3.65)$$

where

$GMR_s$  is the geometric mean radius of a neutral strand in ft;

$R$  is the radius of a circle passing through the center of the concentric neutral strands;

$k$  is the number of concentric neutral strand;

$$R = \frac{d_{od} - d_s}{24} \text{ft} \quad (3.66)$$

The equivalent resistance of the concentric neutral can be calculated as:

$$r_{cn} = \frac{r_s}{k} \Omega/\text{mile} \quad (3.67)$$

where

$r_s$  is the resistance of a solid neutral strand in  $\Omega/\text{mile}$

The different spacings between a concentric neutral and the phase conductors, as well as other concentric neutrals, are as follows:

Concentric neutral to its associated phase conductor:

$$D_{ij} = R = \frac{d_{od} - d_s}{24} \text{ft} \quad (3.68)$$

Concentric neutral to an adjacent neutral conductor:

$D_{ij}$  = Centre-to-centre distance of phase conductors

Coaxial neutral to adjacent phase conductors:

Figure 3.9 illustrates the relationship between the distance between the centres of concentric circle neutrals and the radius of the circle passing through the centres of the neutrals [69].

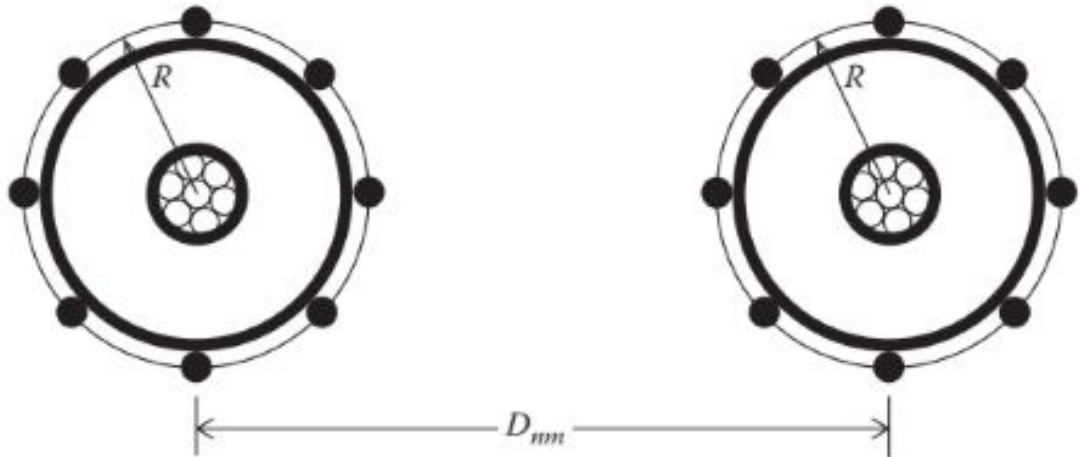


Figure 3.9: Distances between concentric neutral cables

The Geometric Mean Diameter (GMD) between a concentric neutral and an adjacent phase conductor can be calculated as:

$$D_{ij} = \sqrt[k]{D_{nm}^k - R^k} \text{ft} \quad (3.69)$$

In the equation (3.69),  $D_{nm}$  is the center-to-center distance between phase conductors.

The distance between the cables will be much greater than the radius  $R$ . Figure 3.10 shows an approximate diagram modelling a concentric neutral cable. Based on this figure it can be seen that the concentric neutral is modelled as an equivalent conductor directly above the phase

conductor (shown in black).

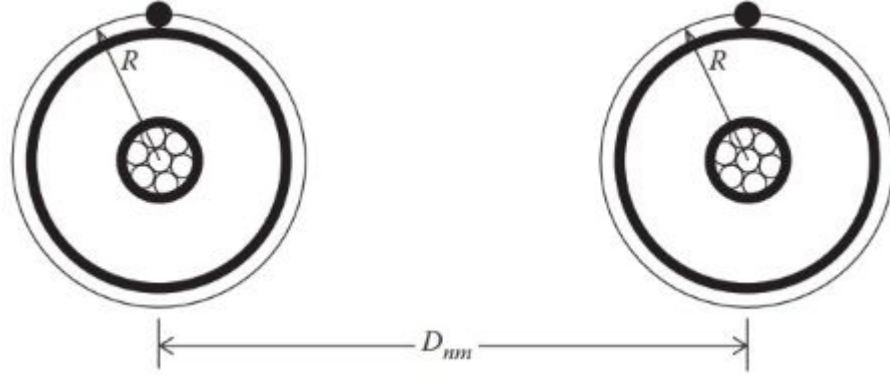


Figure 3.10: Equivalent neutral cables

Similar to overhead line, the primitive impedance matrix of underground line would be the form.

$$\left[ \hat{Z}_{primitive} \right] = \begin{bmatrix} \hat{Z}_{aa} & \hat{Z}_{ab} & \hat{Z}_{ac} & \hat{Z}_{an1} & \hat{Z}_{an2} & \hat{Z}_{anm} \\ \hat{Z}_{ba} & \hat{Z}_{bb} & \hat{Z}_{bc} & \hat{Z}_{bn1} & \hat{Z}_{bn2} & \hat{Z}_{bnm} \\ \hat{Z}_{ca} & \hat{Z}_{cb} & \hat{Z}_{cc} & \hat{Z}_{cn1} & \hat{Z}_{cn2} & \hat{Z}_{cnm3} \\ \hat{Z}_{n1a} & \hat{Z}_{n1b} & \hat{Z}_{n1c} & \hat{Z}_{n1n1} & \hat{Z}_{n1n2} & \hat{Z}_{n1nm} \\ \hat{Z}_{n2a} & \hat{Z}_{n2b} & \hat{Z}_{n2c} & \hat{Z}_{n2n2} & \hat{Z}_{n2n2} & \hat{Z}_{n2nm} \\ \hat{Z}_{nma} & \hat{Z}_{nmb} & \hat{Z}_{nmc} & \hat{Z}_{nmn1} & \hat{Z}_{nmn2} & \hat{Z}_{nmnm} \end{bmatrix} \quad (3.70)$$

### 3.3 Complex Power Loss Allocation Method for Unbalanced Distribution Networks

To allocate the complex power losses in an unbalanced distribution network, the current summation algorithm is integrated with the complex power loss calculation, considering each phase, including the neutral. For a radial distribution system, the net input current at node  $k$  is expressed as follows:

$$\mathbf{i}^k = \begin{bmatrix} \bar{I}_a^k & \bar{I}_b^k & \bar{I}_c^k \end{bmatrix}^T \quad (3.71)$$

$N_{(j)}$  is defined as the set of contributing nodes downstream of branch  $j$ , the branch current can

be represented as the sum of the injected currents.

$$\mathbf{i}^{(j)} = \sum_{k \in N(j)} \mathbf{i}^k \quad (3.72)$$

Based on these definitions, the power loss on branch  $j$  can be calculated as:

$$\mathbf{L}^{(j)} = \Delta \mathbf{P}^{(j)} + j\Delta \mathbf{Q}^{(j)} = \mathbf{i}^{\mathbf{T}(j)} \cdot \mathbf{Z}^{(j)} \cdot \mathbf{i}^{*(j)} = \mathbf{i}^{\mathbf{T}(j)} \cdot (\mathbf{R}^{(j)} + j\mathbf{X}^{(j)}) \cdot \mathbf{i}^{*(j)} \quad (3.73)$$

In the equation (3.73),  $\mathbf{Z}^{(j)}$ ,  $\mathbf{R}^{(j)}$  and  $\mathbf{X}^{(j)}$  are the matrices of the impedance, resistance and reactance of the branch  $j$  respectively.

According to the power summation method [70], the active and reactive losses of branch  $j$  can be expressed as follows:

$$\Delta \mathbf{P}^{(j)} + j\Delta \mathbf{Q}^{(j)} = Re\{\mathbf{i}^{*(j)} \otimes (\mathbf{R}^{(j)} \cdot \mathbf{i}^{(j)})\} + jIm\{\mathbf{i}^{*(j)} \otimes (\mathbf{X}^{(j)} \cdot \mathbf{i}^{(j)})\} \quad (3.74)$$

Substituting equation (3.72) into equation (3.74), complex power loss of branch  $j$  can be calculated as:

$$\Delta \mathbf{P}^{(j)} + j\Delta \mathbf{Q}^{(j)} = Re \left\{ \sum_{k \in N(j)} \mathbf{i}^{*k} \otimes (\mathbf{R}^{(j)} \cdot \sum_{k \in N(j)} \mathbf{i}^k) \right\} + jIm \left\{ \sum_{k \in N(j)} \mathbf{i}^{*k} \otimes (\mathbf{X}^{(j)} \cdot \sum_{k \in N(j)} \mathbf{i}^k) \right\} \quad (3.75)$$

The expansion of equation (3.75) includes the squared terms of the current per phase for each node, which should be allocated to their respective nodes. Besides these squared terms, there are several multiplicative cross terms for the currents at each node that need to be reasonably allocated. To rationalize the distribution of these current cross terms, allocation factors  $\beta$  are

introduced. Thus, equation (3.75) can be rewritten as:

$$\begin{aligned} \Delta P^{(j)} + j\Delta Q^{(j)} = & Re \left\{ \sum_{k \in N^{(j)}} \left( \mathbf{i}^{*k} \otimes \mathbf{R}^{(j)} \otimes \sum_{q \in N^{(j)}} (\beta^{kq} \otimes \mathbf{i}^{kq}) \right) \right\} \\ & + jIm \left\{ \sum_{k \in N^{(j)}} \left( \mathbf{i}^{*k} \otimes \mathbf{X}^{(j)} \otimes \sum_{q \in N^{(j)}} (\beta^{kq} \otimes \mathbf{i}^{kq}) \right) \right\} \end{aligned} \quad (3.76)$$

In the Equation (3.76),

$\beta^{kq}$  is the allocation factor matrix;

$\mathbf{R}^{(j)}$  contains the resistance of all conductors including neutral of branch  $j$ ;

$\mathbf{X}^{(j)}$  contains the reactance of all conductors including neutral of branch  $j$ ;

Equation (3.76) represents the complex power loss for each branch, which consists of the complex power loss from each contributing node. Consequently, the complex power loss for each node can be calculated as follows:

$$\begin{aligned} \Delta \mathbf{P}^k + j\Delta \mathbf{Q}^k = & Re \left\{ \sum_{k=1}^M \mathbf{i}^{*k} \otimes (\mathbf{R}^{(j)} * \sum_{q \in N^{(j)}} (\beta^{kq} \otimes \mathbf{i}^{kq})) \right\} \\ & + jIm \left\{ \sum_{k=1}^M \mathbf{i}^{*k} \otimes (\mathbf{X}^{(j)} * \sum_{q \in N^{(j)}} (\beta^{kq} \otimes \mathbf{i}^{kq})) \right\} \end{aligned} \quad (3.77)$$

In the Equation (3.77),  $M$  is the set of branches which connect node  $k$  to the root node.

The calculation of complex power loss allocation necessitates a detailed analysis of the cross-term allocation factor. The method for allocating current cross terms will be thoroughly described in the next section.

### 3.4 Methods of Allocating Current Cross Terms

Research was conducted on determining the cross-term allocation factors  $\beta_e$  and  $\beta_f$  (where subscripts  $e$  and  $f$  represent the nodes of the two currents involved in the cross multiplication). Exposito et al. [71] discussed three methods for allocating power cross-terms. However, when it comes to current cross-terms, typically only one or two methods are considered. This thesis will discuss three methods for allocating current cross-terms. Using the cross term of two nodal currents as an example, the relationship is as follows:

$$\beta_e(i^e i^f) + \beta_f(i^e i^f) = 2(i^e i^f) \quad (3.78)$$

The Equation (3.78) can be rewritten as:

$$\beta_e + \beta_f = 2 \quad (3.79)$$

One method allocates the cross terms equally, i.e.,  $\beta_e = \beta_f = 1$ . However, this approach is not fair to unbalanced networks. Consequently, for unbalanced distribution networks, three specific methods are generally employed to allocate the cross terms more equitably.

#### 3.4.1 Proportional allocation

The simplest and most straightforward method is to allocate the cross terms proportionally, i.e.

$$\frac{\beta_e}{i^e} = \frac{\beta_f}{i^f} \quad (3.80)$$

Combine the Equations (3.79) and (3.80), the following relationship is obtained as

$$\beta_e = \frac{2i^e}{i^e + i^f}; \quad \beta_f = \frac{2i^f}{i^e + i^f} \quad (3.81)$$

### 3.4.2 Quadratic allocation

Since current is quadratic with respect to power loss, it is presumed that the loss distribution factor is likewise quadratic with respect to current, i.e.

$$\frac{\beta_e}{i^e} = \frac{\beta_f}{i^f} \quad (3.82)$$

Combine the Equations (3.79) and (3.82), it yields

$$\beta_e = \frac{2i^e}{i^e + i^f}; \quad \beta_f = \frac{2i^f}{i^e + i^f} \quad (3.83)$$

### 3.4.3 Geometric allocation

The geometric mean is represented as the product of two numbers, hence it can also be utilized to manage the allocation of current multiplication cross terms. Their relationship can be expressed as:

$$\beta_e - \log i^e = \beta_f - \log i^f \quad (3.84)$$

Combining the Equations (3.79) and (3.84) it results in

$$\beta_e = 1 + \frac{1}{2} \log \frac{i^e}{i^f}; \quad \beta_f = 1 + \frac{1}{2} \log \frac{i^f}{i^e} \quad (3.85)$$

In the subsequent section, the three aforementioned methods will be employed for simulation calculations on the IEEE123 node system.

## 3.5 Case Study

In this research, the IEEE123-node system is chosen as the simulation model. On the one hand, it is because it is an unbalanced system, which corresponds to a really distribution network situation. On the other hand, the IEEE123-node system is relatively large and allows for richer results. In addition, the original IEEE123-node system was modified in order to analyse the

impact of distributed generations in the distribution network, as shown in Figure 3.11.

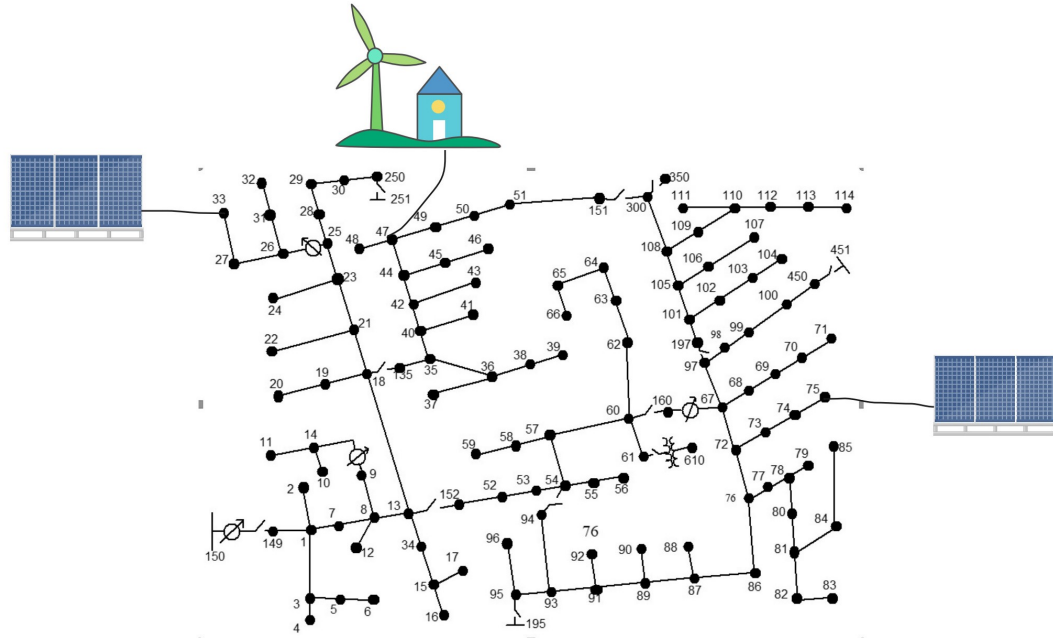


Figure 3.11: Modified IEEE 123-node system with renewable DG units

A 1MW/500kVar wind turbine unit is connected at node 47. Two 40kW/20kVar PV panels are connected at node 33 and node 75. It is worth noting that the same system is used in the case study of Chapter 5.

### 3.5.1 Calculation of the Primitive Impedance Matrix

In IEEE 123 node system there are 3 types of overhead lines models as shown in figure 3.12. Before applying the modified Carson equation, it is necessary to calculate the distance matrix  $D_{ij}$ . Kersting [69] provided an effective method to determine the distances between all conductors by using a complex representation to locate each point on the pole within a Cartesian coordinate system. The ordinate is chosen as a point on the ground directly beneath the position on the left.

The Overhead Line Configurations for the IEEE123 node system and the primitive impedance matrices calculated from them are shown in Appendix A.

In addition, the whole process of loss allocation is based on the real currents in the power system. So the information about the current in the power system needs to be obtained before the loss

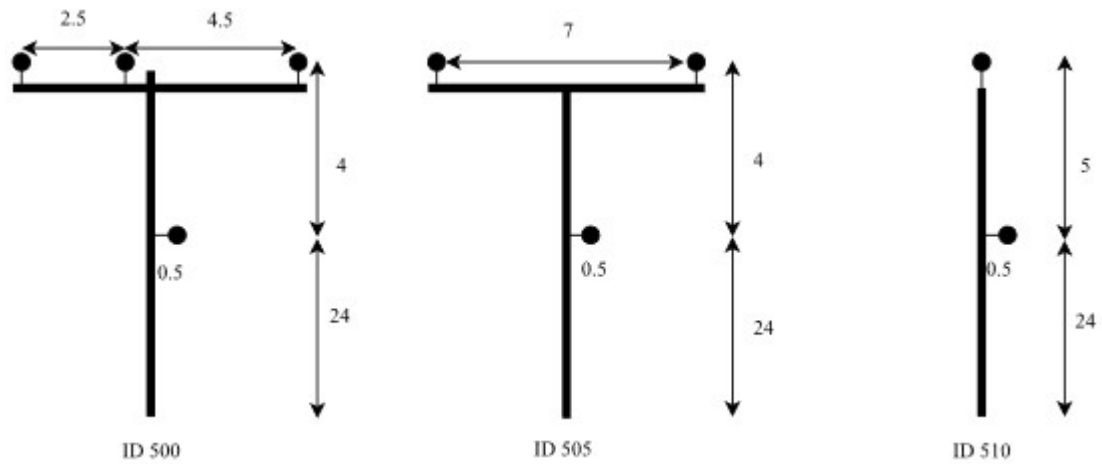


Figure 3.12: Overhead line spacings

allocation algorithm is carried out.

### 3.5.2 Simulation Results

Figure 3.13 illustrates the process flow chart for the calculation stages.

The data in Table 3.1 and Table 3.2 is the active loss and reactive loss allocated to each node calculated using proportional allocation methods, respectively.

Table 3.1: Active loss (W) allocated to each node calculated using proportional allocation methods

| node | a     | b    | c     | n      | node | a      | b      | c      | n       |
|------|-------|------|-------|--------|------|--------|--------|--------|---------|
| 1    | 533.6 | 0.0  | 294.5 | 6056.5 | 63   | 2193.4 | -0.1   | -0.1   | 904.8   |
| 2    | 0.0   | 85.6 | 0.0   | -42.5  | 64   | -0.2   | 3789.0 | -0.1   | -1047.8 |
| 3    | 0.0   | 0.0  | 0.0   | 0.0    | 65   | 4122.2 | 1918.2 | 3496.0 | 0.0     |
| 4    | 0.0   | 0.0  | 338.8 | 28.7   | 66   | -0.2   | -0.1   | 4090.8 | -681.7  |
| 5    | 0.0   | 0.0  | 134.7 | 20.6   | 67   | 0.0    | 0.0    | 0.0    | 0.0     |
| 6    | 0.0   | 0.0  | 430.8 | 86.7   | 68   | 745.3  | 0.0    | 0.0    | 347.8   |
| 7    | 228.9 | -0.1 | 0.0   | 109.7  | 69   | 2231.6 | 0.0    | 0.0    | 1045.0  |
| 8    | 0.0   | 0.0  | 0.0   | 0.0    | 70   | 783.8  | 0.0    | 0.0    | 384.4   |

|    |         |       |       |        |    |         |         |         |         |
|----|---------|-------|-------|--------|----|---------|---------|---------|---------|
| 9  | 883.5   | 0.0   | 0.0   | 448.8  | 71 | 2271.1  | 0.0     | 0.0     | 1081.3  |
| 10 | 349.4   | 0.0   | 0.0   | 189.7  | 72 | 0.0     | 0.0     | 0.0     | 0.0     |
| 11 | 1032.1  | 0.0   | 0.0   | 564.9  | 73 | 0.0     | 0.0     | 1499.0  | -446.7  |
| 12 | 0.0     | 186.0 | 0.0   | -83.5  | 74 | 0.0     | 0.0     | 1732.2  | -508.6  |
| 13 | 0.0     | 0.0   | 0.0   | 0.0    | 75 | 0.0     | 0.0     | -1475.5 | 473.1   |
| 14 | 0.0     | 0.0   | 0.0   | 0.0    | 76 | 9183.2  | 5836.2  | 4649.9  | -0.1    |
| 15 | 0.0     | 0.0   | 0.0   | 0.0    | 77 | 0.0     | 1589.4  | 0.0     | -441.7  |
| 16 | 0.0     | 0.0   | 827.8 | -95.9  | 78 | 0.0     | 0.0     | 0.0     | 0.0     |
| 17 | 0.0     | 0.0   | 280.7 | -39.3  | 79 | 2513.6  | 0.0     | 0.0     | 1050.1  |
| 18 | 0.0     | 0.0   | -0.1  | 0.3    | 80 | 0.0     | 1588.8  | 0.0     | -462.2  |
| 19 | 1348.5  | 0.0   | 0.0   | 619.9  | 81 | 0.0     | 0.0     | 0.0     | 0.0     |
| 20 | 1409.1  | 0.0   | 0.0   | 660.9  | 82 | 2199.3  | 0.0     | 0.0     | 901.6   |
| 21 | 0.0     | 0.0   | 0.0   | 0.0    | 83 | -4419.5 | -2419.8 | -451.0  | -179.0  |
| 22 | 0.0     | 971.5 | 0.0   | -404.0 | 84 | 0.0     | 0.0     | 553.5   | -112.5  |
| 23 | 0.0     | 0.0   | 0.0   | 0.0    | 85 | 0.0     | 0.0     | 1658.6  | -283.2  |
| 24 | 0.0     | 0.0   | 989.8 | -80.0  | 86 | 0.0     | 568.4   | 0.0     | -120.5  |
| 25 | 0.0     | 0.0   | -0.1  | 0.0    | 87 | 0.0     | 1693.7  | 0.0     | -315.0  |
| 26 | 0.0     | 0.0   | 0.0   | 0.0    | 88 | 1499.9  | 0.0     | 0.0     | 288.5   |
| 27 | 0.0     | 0.0   | 0.0   | 0.0    | 89 | 0.0     | 0.0     | 0.0     | 0.0     |
| 28 | 1382.6  | 0.0   | 0.0   | 580.6  | 90 | 0.0     | 1259.0  | 0.0     | 862.5   |
| 29 | 1432.9  | 0.0   | 0.0   | 605.6  | 91 | 0.0     | 0.0     | 0.0     | 0.0     |
| 30 | 0.0     | 0.0   | 998.3 | -70.6  | 92 | 0.0     | 0.0     | 1173.1  | -1053.9 |
| 31 | 0.0     | 0.0   | 354.8 | -12.8  | 93 | 0.0     | 0.0     | 0.0     | 0.0     |
| 32 | 0.0     | 0.0   | 360.3 | -7.5   | 94 | 2267.6  | 0.0     | 0.0     | 907.2   |
| 33 | -1312.5 | 0.0   | 0.0   | -484.4 | 95 | 0.0     | 600.4   | 0.0     | -80.6   |
| 34 | 0.0     | 0.0   | 862.9 | -147.4 | 96 | 0.0     | 604.0   | 0.0     | -77.2   |
| 35 | 521.8   | 333.3 | 0.0   | 0.0    | 97 | 0.0     | 0.0     | 0.0     | 0.0     |

|    |          |          |          |        |     |        |        |        |        |
|----|----------|----------|----------|--------|-----|--------|--------|--------|--------|
| 36 | 0.0      | 0.0      | 0.0      | 0.0    | 98  | 2160.9 | 0.0    | 0.0    | 951.0  |
| 37 | 1483.2   | 0.0      | 0.0      | 666.0  | 99  | 0.0    | 1537.9 | 0.0    | -485.5 |
| 38 | 0.0      | 340.9    | 0.0      | -113.9 | 100 | 0.0    | 0.0    | 1737.1 | -496.6 |
| 39 | 0.0      | 324.0    | 0.0      | -100.8 | 101 | 0.0    | 0.0    | 0.0    | 0.0    |
| 40 | 0.0      | 0.0      | 0.0      | 0.0    | 102 | 0.0    | 0.0    | 517.9  | -153.6 |
| 41 | 0.0      | 0.0      | 328.7    | -73.1  | 103 | 0.0    | 0.0    | 1581.5 | -370.6 |
| 42 | 495.3    | 0.0      | 0.0      | 217.4  | 104 | 0.0    | 0.0    | 1629.3 | -323.5 |
| 43 | 0.0      | 1042.3   | 0.0      | -375.2 | 105 | 0.0    | 0.0    | 0.0    | 0.0    |
| 44 | 0.0      | 0.0      | 0.0      | 0.0    | 106 | 0.0    | 1581.6 | 0.0    | -477.6 |
| 45 | 527.9    | 0.0      | 0.0      | 237.2  | 107 | 0.0    | 1624.3 | 0.0    | -439.4 |
| 46 | 515.3    | 0.0      | 0.0      | 234.5  | 108 | 0.0    | 0.0    | 0.0    | 0.0    |
| 47 | -20117.9 | -12366.1 | -12871.3 | 23.9   | 109 | 2424.5 | 0.0    | 0.0    | 1230.5 |
| 48 | 4280.8   | 2872.5   | 2977.0   | -19.8  | 110 | 0.0    | 0.0    | 0.0    | 0.0    |
| 49 | 1918.3   | 2716.1   | 1220.4   | -592.0 | 111 | 876.0  | 0.0    | 0.0    | 474.0  |
| 50 | 0.0      | 0.0      | 981.2    | -222.2 | 112 | 926.2  | 0.0    | 0.0    | 499.9  |
| 51 | 512.7    | 0.0      | 0.0      | 221.1  | 113 | 2875.4 | 0.0    | 0.0    | 1547.7 |
| 52 | 1344.2   | 0.0      | 0.0      | 620.2  | 114 | 908.5  | 0.0    | 0.0    | 505.1  |
| 53 | 1462.6   | 0.0      | 0.0      | 671.3  | 115 | 0.0    | 0.0    | 0.0    | 0.0    |
| 54 | 0.0      | 0.0      | 0.0      | 0.0    | 116 | 0.0    | 0.0    | 0.0    | 0.0    |
| 55 | 551.7    | 0.0      | 0.0      | 255.3  | 117 | 0.0    | 0.0    | -0.1   | 0.3    |
| 56 | 0.0      | 345.6    | 0.0      | -119.5 | 118 | 564.0  | 17.3   | 113.2  | 139.7  |
| 57 | 0.0      | 0.0      | 0.0      | 0.0    | 119 | 512.7  | 0.0    | 0.0    | 221.1  |
| 58 | 0.0      | 424.9    | 0.0      | -127.2 | 120 | 733.9  | 0.0    | -0.1   | 330.0  |
| 59 | 0.0      | 404.9    | 0.0      | -115.5 | 121 | 0.0    | 0.0    | 0.0    | 0.0    |
| 60 | 733.9    | 0.0      | -0.1     | 330.0  | 122 | 0.0    | 0.0    | 0.0    | 0.0    |
| 61 | 0.0      | 0.0      | 0.0      | 0.0    | 123 | 0.0    | 0.0    | 0.0    | 0.0    |
| 62 | -0.1     | -0.1     | 1575.4   | -428.5 |     |        |        |        |        |

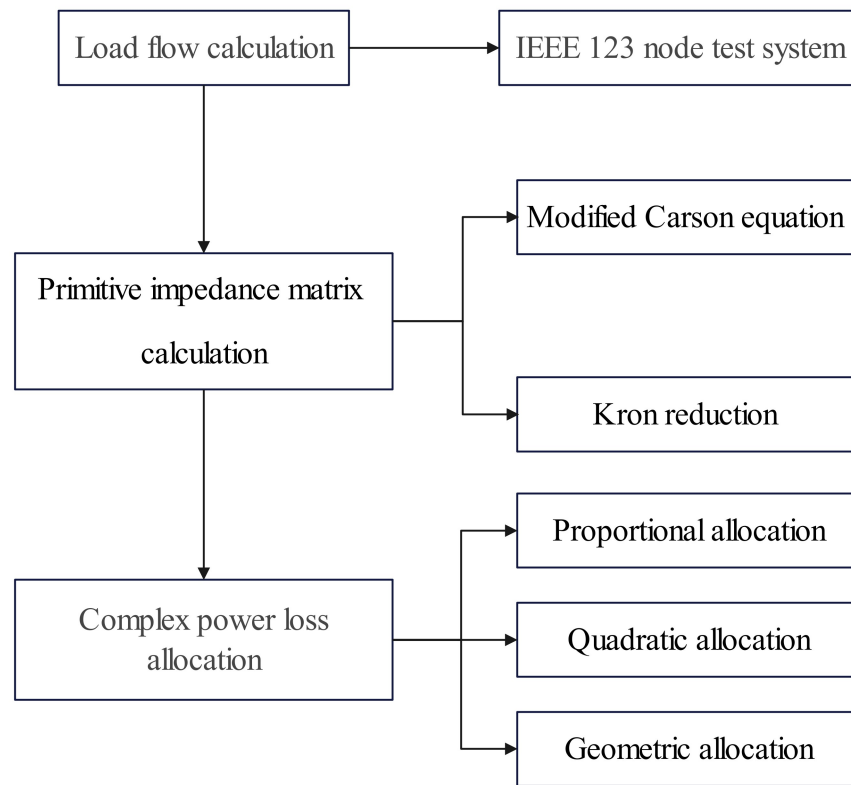


Figure 3.13: The process flow chart for the calculation stages

Table 3.2: Reactive loss (kVar) allocated to each node calculated using proportional allocation method

| node | a     | b    | c       | n      | node | a      | b      | c      | n       |
|------|-------|------|---------|--------|------|--------|--------|--------|---------|
| 1    | 249.1 | 0.2  | 24969.3 | -933.8 | 63   | 990.1  | -1.4   | -1.3   | 174.6   |
| 2    | 0.0   | 9.0  | 0.0     | 128.8  | 64   | -5.0   | 1532.9 | -3.6   | 5037.7  |
| 3    | 0.0   | 0.0  | 0.0     | 0.0    | 65   | 9354.2 | 2594.5 | 2157.1 | 0.1     |
| 4    | 0.0   | 0.0  | 11.7    | -548.2 | 66   | -4.2   | -3.3   | 2190.4 | -5136.9 |
| 5    | 0.0   | 0.0  | 7.8     | -193.6 | 67   | 0.0    | 0.0    | 0.0    | 0.0     |
| 6    | 0.0   | 0.0  | 12.2    | -612.2 | 68   | 335.3  | 0.0    | 0.0    | 19.7    |
| 7    | 42.3  | -0.3 | -0.1    | 63.0   | 69   | 1105.2 | 0.0    | 0.0    | 93.1    |
| 8    | 0.0   | 0.0  | 0.0     | 0.0    | 70   | 339.7  | 0.0    | 0.0    | 20.7    |
| 9    | 199.8 | 0.0  | 0.0     | 226.0  | 71   | 1114.8 | 0.0    | 0.0    | 95.4    |
| 10   | 63.7  | 0.0  | 0.0     | 74.1   | 72   | 0.0    | 0.0    | 0.0    | 0.0     |

|    |         |       |       |         |    |           |          |          |         |
|----|---------|-------|-------|---------|----|-----------|----------|----------|---------|
| 11 | 221.1   | 0.0   | 0.0   | 246.5   | 73 | 0.0       | 0.0      | 1142.6   | -2339.1 |
| 12 | 0.0     | 24.2  | 0.0   | 319.7   | 74 | 0.0       | 0.0      | 1341.0   | -2687.1 |
| 13 | 0.0     | 0.0   | 0.0   | 0.0     | 75 | 0.0       | 0.0      | -1142.9  | 2341.9  |
| 14 | 0.0     | 0.0   | 0.0   | 0.0     | 76 | 9889.5    | 15231.6  | 9335.2   | -0.1    |
| 15 | 0.0     | 0.0   | 0.0   | 0.0     | 77 | -0.9      | 1022.7   | -0.6     | 2394.7  |
| 16 | 0.0     | 0.0   | 255.5 | -1403.2 | 78 | 0.0       | 0.0      | 0.0      | 0.0     |
| 17 | 0.0     | 0.0   | 81.4  | -482.5  | 79 | 1610.9    | -0.2     | -0.2     | 9.4     |
| 18 | 0.0     | 0.0   | 2.3   | -0.3    | 80 | -0.7      | 1141.1   | -0.3     | 2309.6  |
| 19 | 306.1   | 0.0   | 0.0   | 370.8   | 81 | 0.0       | 0.0      | 0.0      | 0.0     |
| 20 | 317.5   | 0.0   | 0.0   | 382.0   | 82 | 1627.8    | -0.2     | -0.3     | 234.3   |
| 21 | 0.0     | 0.0   | 0.0   | 0.0     | 83 | -111863.6 | -81282.5 | -79948.2 | -2433.2 |
| 22 | 0.0     | 66.3  | 0.0   | 1345.6  | 84 | 0.0       | 0.0      | 464.2    | -831.2  |
| 23 | 0.0     | 0.0   | 0.0   | 0.0     | 85 | 0.0       | 0.0      | 1539.4   | -2377.3 |
| 24 | 0.0     | 0.0   | 225.6 | -1662.2 | 86 | -0.5      | 311.7    | -0.6     | 885.7   |
| 25 | 0.0     | 0.0   | 0.0   | 0.1     | 87 | -0.7      | 1120.2   | -0.3     | 2555.8  |
| 26 | 0.0     | 0.0   | 0.0   | 0.0     | 88 | -10705.6  | 0.0      | 0.0      | -3270.4 |
| 27 | 0.0     | 0.0   | 0.0   | 0.0     | 89 | 0.0       | 0.0      | 0.0      | 0.0     |
| 28 | 322.2   | -0.1  | -0.1  | 687.9   | 90 | 0.0       | -8000.4  | 0.0      | 2391.7  |
| 29 | 335.2   | -0.1  | -0.1  | 749.3   | 91 | 0.0       | 0.0      | 0.0      | 0.0     |
| 30 | -0.3    | -0.1  | 227.4 | -1785.9 | 92 | 0.0       | 0.0      | -7263.1  | 1225.0  |
| 31 | 0.0     | 0.0   | 74.4  | -578.3  | 93 | 0.0       | 0.0      | 0.0      | 0.0     |
| 32 | 0.0     | 0.0   | 74.6  | -578.7  | 94 | 1430.8    | 0.0      | 0.0      | -584.6  |
| 33 | -313.3  | 0.0   | 0.0   | -719.3  | 95 | -0.3      | 351.8    | -0.2     | 928.6   |
| 34 | 0.0     | 0.0   | 280.5 | -1536.4 | 96 | 0.0       | 352.0    | 0.0      | 928.8   |
| 35 | -1266.3 | 865.3 | -0.1  | 0.0     | 97 | 0.0       | 0.0      | 0.0      | 0.0     |
| 36 | 0.0     | 0.0   | 0.0   | 0.0     | 98 | 1101.7    | -0.1     | -0.2     | 111.2   |
| 37 | 323.8   | 0.0   | 0.0   | 200.0   | 99 | -0.6      | 788.3    | -0.5     | 2377.8  |

|    |         |         |         |         |     |        |       |        |         |
|----|---------|---------|---------|---------|-----|--------|-------|--------|---------|
| 38 | 0.0     | -5.9    | 0.0     | 538.2   | 100 | -0.3   | -0.2  | 1237.0 | -2748.6 |
| 39 | 0.0     | -5.9    | 0.0     | 502.8   | 101 | 0.0    | 0.0   | 0.0    | 0.0     |
| 40 | 0.0     | 0.0     | 0.0     | 0.0     | 102 | 0.0    | 0.0   | 324.1  | -885.2  |
| 41 | 0.0     | 0.0     | 60.3    | -575.7  | 103 | 0.0    | 0.0   | 1049.4 | -2512.9 |
| 42 | 82.5    | -0.1    | 0.0     | 89.9    | 104 | 0.0    | 0.0   | 1053.7 | -2515.1 |
| 43 | 0.0     | -14.7   | 0.0     | 1611.7  | 105 | 0.0    | 0.0   | 0.0    | 0.0     |
| 44 | 0.0     | 0.0     | 0.0     | 0.0     | 106 | 0.0    | 796.0 | 0.0    | 2630.1  |
| 45 | 82.0    | 0.0     | 0.0     | 95.3    | 107 | 0.0    | 801.1 | 0.0    | 2634.7  |
| 46 | 79.2    | 0.0     | 0.0     | 92.2    | 108 | 0.0    | 0.0   | 0.0    | 0.0     |
| 47 | -9198.1 | -2999.2 | -3732.9 | -431.1  | 109 | 1149.4 | 0.0   | 0.0    | 71.5    |
| 48 | 4521.6  | 2330.8  | 2985.3  | 79.3    | 110 | 0.0    | 0.0   | 0.0    | 0.0     |
| 49 | 2117.3  | 2130.4  | 621.7   | 2341.6  | 111 | 357.3  | 0.0   | 0.0    | 15.8    |
| 50 | -0.2    | -0.1    | 153.4   | -1675.7 | 112 | 380.9  | 0.0   | 0.0    | 17.4    |
| 51 | 71.9    | -0.1    | -0.1    | 105.2   | 113 | 1311.5 | 0.0   | 0.0    | 89.3    |
| 52 | 432.5   | 0.0     | 0.0     | 206.1   | 114 | 361.9  | 0.0   | 0.0    | 17.0    |
| 53 | 505.1   | 0.0     | 0.0     | 164.2   | 115 | 0.0    | 0.0   | 0.0    | 0.0     |
| 54 | 0.0     | 0.0     | 0.0     | 0.0     | 116 | 0.0    | 0.0   | 0.0    | 0.0     |
| 55 | 173.6   | -0.1    | -0.1    | 26.9    | 117 | 0.0    | 0.0   | 2.3    | -0.3    |
| 56 | -0.1    | 94.4    | -0.1    | 601.4   | 118 | -956.5 | -62.1 | -381.7 | -304.3  |
| 57 | 0.0     | 0.0     | 0.0     | 0.0     | 119 | 71.9   | -0.1  | -0.1   | 105.2   |
| 58 | 0.0     | 134.2   | 0.0     | 697.8   | 120 | 314.1  | -1.5  | -1.2   | 36.9    |
| 59 | 0.0     | 125.7   | 0.0     | 658.7   | 121 | 0.0    | 0.0   | 0.0    | 0.0     |
| 60 | 314.1   | -1.5    | -1.2    | 36.9    | 122 | 0.0    | 0.0   | 0.0    | 0.0     |
| 61 | 0.0     | 0.0     | 0.0     | 0.0     | 123 | 0.0    | 0.0   | 0.0    | 0.0     |
| 62 | -2.7    | -1.8    | 1038.9  | -2479.3 |     |        |       |        |         |

Table 3.3 and Table 3.4 show the active loss and reactive loss allocated to each node calculated using quadratic allocation methods, respectively.

Table 3.3: Active loss (W) allocated to each node calculated using quadratic allocation methods

| node | a      | b      | c      | n      | node | a       | b       | c       | n       |
|------|--------|--------|--------|--------|------|---------|---------|---------|---------|
| 1    | 570.4  | 0.0    | 95.1   | 6186.4 | 63   | 2321.3  | -0.1    | -0.1    | 1051.4  |
| 2    | 0.0    | 65.9   | 0.0    | -20.6  | 64   | -0.3    | 4568.5  | -0.2    | -1217.3 |
| 3    | 0.0    | 0.0    | 0.0    | 0.0    | 65   | 4853.8  | 2054.2  | 3905.9  | 0.0     |
| 4    | 0.0    | 0.0    | 366.5  | 33.7   | 66   | -0.3    | -0.2    | 4942.7  | -830.9  |
| 5    | 0.0    | 0.0    | 95.4   | 9.9    | 67   | 0.0     | 0.0     | 0.0     | 0.0     |
| 6    | 0.0    | 0.0    | 482.0  | 102.7  | 68   | 525.5   | 0.0     | 0.0     | 279.2   |
| 7    | 166.6  | 0.0    | 0.0    | 81.5   | 69   | 2334.7  | 0.0     | 0.0     | 1167.1  |
| 8    | 0.0    | 0.0    | 0.0    | 0.0    | 70   | 554.9   | 0.0     | 0.0     | 306.9   |
| 9    | 946.3  | 0.0    | 0.0    | 469.5  | 71   | 2426.3  | 0.0     | 0.0     | 1254.5  |
| 10   | 265.5  | 0.0    | 0.0    | 150.2  | 72   | 0.0     | 0.0     | 0.0     | 0.0     |
| 11   | 1143.3 | 0.0    | 0.0    | 618.1  | 73   | 0.0     | 0.0     | 1486.4  | -536.7  |
| 12   | 0.0    | 138.9  | 0.0    | -49.3  | 74   | 0.0     | 0.0     | 1794.9  | -623.9  |
| 13   | 0.0    | 0.0    | 0.0    | 0.0    | 75   | 0.0     | 0.0     | -1435.0 | 591.9   |
| 14   | 0.0    | 0.0    | 0.0    | 0.0    | 76   | 11407.3 | 7455.9  | 5856.3  | -0.1    |
| 15   | 0.0    | 0.0    | 0.0    | 0.0    | 77   | 0.0     | 1635.1  | 0.0     | -464.2  |
| 16   | 0.0    | 0.0    | 890.6  | -103.7 | 78   | 0.0     | 0.0     | 0.0     | 0.0     |
| 17   | 0.0    | 0.0    | 199.7  | -32.6  | 79   | 2724.3  | 0.0     | 0.0     | 1204.8  |
| 18   | 0.0    | 0.0    | 0.0    | 0.0    | 80   | 0.0     | 1643.1  | 0.0     | -488.3  |
| 19   | 1479.4 | 0.0    | 0.0    | 663.7  | 81   | 0.0     | 0.0     | 0.0     | 0.0     |
| 20   | 1578.7 | 0.0    | 0.0    | 733.3  | 82   | 2317.0  | 0.0     | 0.0     | 997.5   |
| 21   | 0.0    | 0.0    | 0.0    | 0.0    | 83   | -5872.8 | -3640.0 | -1075.5 | -165.8  |
| 22   | 0.0    | 1111.0 | 0.0    | -384.0 | 84   | 0.0     | 0.0     | 365.0   | -92.4   |
| 23   | 0.0    | 0.0    | 0.0    | 0.0    | 85   | 0.0     | 0.0     | 1712.2  | -312.8  |
| 24   | 0.0    | 0.0    | 1104.5 | -66.0  | 86   | 0.0     | 399.2   | 0.0     | -81.3   |

|    |          |          |          |        |     |        |        |        |         |
|----|----------|----------|----------|--------|-----|--------|--------|--------|---------|
| 25 | 0.0      | 0.0      | 0.0      | 0.0    | 87  | 0.0    | 1746.3 | 0.0    | -317.8  |
| 26 | 0.0      | 0.0      | 0.0      | 0.0    | 88  | 1503.6 | 0.0    | 0.0    | 310.1   |
| 27 | 0.0      | 0.0      | 0.0      | 0.0    | 89  | 0.0    | 0.0    | 0.0    | 0.0     |
| 28 | 1527.7   | 0.0      | 0.0      | 622.1  | 90  | 0.0    | 1244.5 | 0.0    | 1047.8  |
| 29 | 1594.1   | 0.0      | 0.0      | 651.6  | 91  | 0.0    | 0.0    | 0.0    | 0.0     |
| 30 | 0.0      | 0.0      | 1077.4   | -90.7  | 92  | 0.0    | 0.0    | 1138.3 | -1190.1 |
| 31 | 0.0      | 0.0      | 257.9    | -9.3   | 93  | 0.0    | 0.0    | 0.0    | 0.0     |
| 32 | 0.0      | 0.0      | 268.7    | 1.2    | 94  | 2376.8 | 0.0    | 0.0    | 1021.4  |
| 33 | -1420.8  | 0.0      | 0.0      | -486.9 | 95  | 0.0    | 427.9  | 0.0    | -44.3   |
| 34 | 0.0      | 0.0      | 927.3    | -186.5 | 96  | 0.0    | 435.1  | 0.0    | -37.4   |
| 35 | 428.2    | 273.7    | 0.0      | 0.0    | 97  | 0.0    | 0.0    | 0.0    | 0.0     |
| 36 | 0.0      | 0.0      | 0.0      | 0.0    | 98  | 2257.5 | 0.0    | 0.0    | 1069.3  |
| 37 | 1688.2   | 0.0      | 0.0      | 743.6  | 99  | 0.0    | 1574.3 | 0.0    | -513.6  |
| 38 | 0.0      | 260.2    | 0.0      | -78.7  | 100 | 0.0    | 0.0    | 1800.8 | -612.9  |
| 39 | 0.0      | 247.1    | 0.0      | -60.3  | 101 | 0.0    | 0.0    | 0.0    | 0.0     |
| 40 | 0.0      | 0.0      | 0.0      | 0.0    | 102 | 0.0    | 0.0    | 332.2  | -137.0  |
| 41 | 0.0      | 0.0      | 241.3    | -55.6  | 103 | 0.0    | 0.0    | 1571.8 | -458.6  |
| 42 | 378.2    | 0.0      | 0.0      | 178.9  | 104 | 0.0    | 0.0    | 1666.8 | -364.7  |
| 43 | 0.0      | 1205.5   | 0.0      | -365.2 | 105 | 0.0    | 0.0    | 0.0    | 0.0     |
| 44 | 0.0      | 0.0      | 0.0      | 0.0    | 106 | 0.0    | 1618.6 | 0.0    | -512.1  |
| 45 | 413.2    | 0.0      | 0.0      | 201.5  | 107 | 0.0    | 1701.8 | 0.0    | -434.8  |
| 46 | 403.7    | 0.0      | 0.0      | 202.7  | 108 | 0.0    | 0.0    | 0.0    | 0.0     |
| 47 | -22526.9 | -14560.8 | -14954.9 | 19.6   | 109 | 2551.4 | 0.0    | 0.0    | 1378.7  |
| 48 | 5695.6   | 3967.7   | 4161.8   | -17.7  | 110 | 0.0    | 0.0    | 0.0    | 0.0     |
| 49 | 2216.6   | 3434.3   | 1384.6   | -643.2 | 111 | 646.1  | 0.0    | 0.0    | 399.4   |
| 50 | 0.0      | 0.0      | 1094.4   | -264.7 | 112 | 687.9  | 0.0    | 0.0    | 418.5   |
| 51 | 395.1    | 0.0      | 0.0      | 188.5  | 113 | 3110.3 | 0.0    | 0.0    | 1757.9  |

|    |        |       |        |        |     |       |     |      |       |
|----|--------|-------|--------|--------|-----|-------|-----|------|-------|
| 52 | 1441.7 | 0.0   | 0.0    | 675.7  | 114 | 666.8 | 0.0 | 0.0  | 418.6 |
| 53 | 1566.1 | 0.0   | 0.0    | 736.9  | 115 | 0.0   | 0.0 | 0.0  | 0.0   |
| 54 | 0.0    | 0.0   | 0.0    | 0.0    | 116 | 0.0   | 0.0 | 0.0  | 0.0   |
| 55 | 409.1  | 0.0   | 0.0    | 206.2  | 117 | 0.0   | 0.0 | 0.0  | 0.0   |
| 56 | 0.0    | 247.9 | 0.0    | -76.8  | 118 | 424.7 | 9.4 | 58.6 | 91.1  |
| 57 | 0.0    | 0.0   | 0.0    | 0.0    | 119 | 395.1 | 0.0 | 0.0  | 188.5 |
| 58 | 0.0    | 311.8 | 0.0    | -86.2  | 120 | 533.7 | 0.0 | 0.0  | 275.1 |
| 59 | 0.0    | 295.2 | 0.0    | -70.4  | 121 | 0.0   | 0.0 | 0.0  | 0.0   |
| 60 | 533.7  | 0.0   | 0.0    | 275.1  | 122 | 0.0   | 0.0 | 0.0  | 0.0   |
| 61 | 0.0    | 0.0   | 0.0    | 0.0    | 123 | 0.0   | 0.0 | 0.0  | 0.0   |
| 62 | -0.1   | -0.1  | 1595.3 | -534.7 |     |       |     |      |       |

Table 3.4: Reactive loss (kVar) allocated to each node calculated using quadratic allocation methods

| node | a     | b    | c       | n       | node | a      | b      | c      | n       |
|------|-------|------|---------|---------|------|--------|--------|--------|---------|
| 1    | 259.0 | 0.3  | 26649.9 | -1005.1 | 63   | 597.3  | -1.4   | -1.3   | 74.8    |
| 2    | 0.0   | -4.7 | 0.0     | 97.9    | 64   | -5.9   | 637.8  | -4.3   | 6112.6  |
| 3    | 0.0   | 0.0  | 0.0     | 0.0     | 65   | 9654.9 | 2188.2 | 1442.3 | 0.1     |
| 4    | 0.0   | 0.0  | 44.5    | -499.8  | 66   | -5.0   | -3.9   | 1599.5 | -6085.3 |
| 5    | 0.0   | 0.0  | 12.1    | -128.8  | 67   | 0.0    | 0.0    | 0.0    | 0.0     |
| 6    | 0.0   | 0.0  | 51.9    | -568.5  | 68   | 140.7  | 0.0    | 0.0    | -24.0   |
| 7    | 13.8  | -0.2 | 0.0     | 22.4    | 69   | 673.2  | 0.0    | 0.0    | -9.3    |
| 8    | 0.0   | 0.0  | 0.0     | 0.0     | 70   | 143.6  | 0.0    | 0.0    | -23.5   |
| 9    | 92.6  | 0.0  | 0.0     | 163.5   | 71   | 682.3  | 0.0    | 0.0    | -6.8    |
| 10   | 23.7  | 0.0  | 0.0     | 27.0    | 72   | 0.0    | 0.0    | 0.0    | 0.0     |
| 11   | 105.6 | 0.0  | 0.0     | 185.5   | 73   | 0.0    | 0.0    | 694.0  | -2561.7 |
| 12   | 0.0   | -7.6 | 0.0     | 251.6   | 74   | 0.0    | 0.0    | 852.0  | -3019.1 |

|    |         |       |       |         |     |           |          |          |         |
|----|---------|-------|-------|---------|-----|-----------|----------|----------|---------|
| 13 | 0.0     | 0.0   | 0.0   | 0.0     | 75  | 0.0       | 0.0      | -693.9   | 2565.4  |
| 14 | 0.0     | 0.0   | 0.0   | 0.0     | 76  | 8966.0    | 16131.7  | 9531.1   | -0.1    |
| 15 | 0.0     | 0.0   | 0.0   | 0.0     | 77  | -0.9      | 466.6    | -0.6     | 2717.9  |
| 16 | 0.0     | 0.0   | 178.0 | -1457.6 | 78  | 0.0       | 0.0      | 0.0      | 0.0     |
| 17 | 0.0     | 0.0   | 41.3  | -353.0  | 79  | 970.7     | -0.2     | -0.2     | -92.3   |
| 18 | 0.0     | 0.0   | 0.0   | -0.1    | 80  | -0.7      | 500.6    | -0.3     | 2611.8  |
| 19 | 179.7   | 0.0   | 0.0   | 335.5   | 81  | 0.0       | 0.0      | 0.0      | 0.0     |
| 20 | 187.6   | 0.0   | 0.0   | 348.3   | 82  | 873.1     | -0.2     | -0.3     | 176.2   |
| 21 | 0.0     | 0.0   | 0.0   | 0.0     | 83  | -126474.9 | -93153.2 | -92402.5 | -2408.5 |
| 22 | 0.0     | -89.0 | 0.0   | 1498.2  | 84  | 0.0       | 0.0      | 172.0    | -636.3  |
| 23 | 0.0     | 0.0   | 0.0   | 0.0     | 85  | 0.0       | 0.0      | 835.9    | -2591.1 |
| 24 | 0.0     | 0.0   | 158.0 | -1748.3 | 86  | -0.4      | 97.9     | -0.4     | 719.4   |
| 25 | 0.0     | 0.0   | 0.0   | 0.0     | 87  | -0.7      | 609.2    | -0.3     | 2898.5  |
| 26 | 0.0     | 0.0   | 0.0   | 0.0     | 88  | -12132.3  | 0.0      | 0.0      | -3826.3 |
| 27 | 0.0     | 0.0   | 0.0   | 0.0     | 89  | 0.0       | 0.0      | 0.0      | 0.0     |
| 28 | 192.7   | -0.1  | -0.1  | 686.8   | 90  | 0.0       | -9073.3  | 0.0      | 2699.6  |
| 29 | 202.0   | -0.1  | -0.2  | 753.7   | 91  | 0.0       | 0.0      | 0.0      | 0.0     |
| 30 | -0.3    | -0.1  | 159.9 | -1869.5 | 92  | 0.0       | 0.0      | -8047.1  | 1532.5  |
| 31 | 0.0     | 0.0   | 39.4  | -436.0  | 93  | 0.0       | 0.0      | 0.0      | 0.0     |
| 32 | 0.0     | 0.0   | 39.6  | -436.4  | 94  | 912.2     | 0.0      | 0.0      | -760.0  |
| 33 | -183.0  | 0.0   | 0.0   | -729.7  | 95  | -0.2      | 119.8    | -0.1     | 747.6   |
| 34 | 0.0     | 0.0   | 200.4 | -1623.5 | 96  | 0.0       | 120.0    | 0.0      | 747.9   |
| 35 | -1077.5 | 660.0 | -0.1  | 0.0     | 97  | 0.0       | 0.0      | 0.0      | 0.0     |
| 36 | 0.0     | 0.0   | 0.0   | 0.0     | 98  | 670.3     | -0.1     | -0.2     | 10.1    |
| 37 | 197.8   | 0.0   | 0.0   | 140.7   | 99  | -0.6      | 353.6    | -0.5     | 2747.2  |
| 38 | 0.0     | -36.7 | 0.0   | 434.1   | 100 | -0.4      | -0.3     | 795.6    | -3105.0 |
| 39 | 0.0     | -33.3 | 0.0   | 393.7   | 101 | 0.0       | 0.0      | 0.0      | 0.0     |

|    |          |         |         |         |     |        |       |        |         |
|----|----------|---------|---------|---------|-----|--------|-------|--------|---------|
| 40 | 0.0      | 0.0     | 0.0     | 0.0     | 102 | 0.0    | 0.0   | 140.4  | -698.6  |
| 41 | 0.0      | 0.0     | 31.9    | -452.9  | 103 | 0.0    | 0.0   | 645.1  | -2767.0 |
| 42 | 42.9     | 0.0     | 0.0     | 62.5    | 104 | 0.0    | 0.0   | 649.2  | -2769.8 |
| 43 | 0.0      | -155.2  | 0.0     | 1828.2  | 105 | 0.0    | 0.0   | 0.0    | 0.0     |
| 44 | 0.0      | 0.0     | 0.0     | 0.0     | 106 | 0.0    | 361.5 | 0.0    | 3014.6  |
| 45 | 43.1     | 0.0     | 0.0     | 68.1    | 107 | 0.0    | 365.9 | 0.0    | 3020.9  |
| 46 | 41.4     | 0.0     | 0.0     | 65.4    | 108 | 0.0    | 0.0   | 0.0    | 0.0     |
| 47 | -10549.1 | -3868.3 | -6183.6 | -407.1  | 109 | 716.5  | 0.0   | 0.0    | -22.6   |
| 48 | 5097.8   | 2588.6  | 3789.4  | 87.3    | 110 | 0.0    | 0.0   | 0.0    | 0.0     |
| 49 | 2211.5   | 2120.0  | 609.3   | 2677.3  | 111 | 155.6  | 0.0   | 0.0    | -20.1   |
| 50 | -0.2     | -0.1    | 99.5    | -1835.6 | 112 | 170.2  | 0.0   | 0.0    | -21.4   |
| 51 | 37.3     | 0.0     | -0.1    | 75.3    | 113 | 846.6  | 0.0   | 0.0    | -7.9    |
| 52 | 232.9    | 0.0     | 0.0     | 124.1   | 114 | 158.8  | 0.0   | 0.0    | -19.3   |
| 53 | 277.4    | 0.0     | 0.0     | 72.8    | 115 | 0.0    | 0.0   | 0.0    | 0.0     |
| 54 | 0.0      | 0.0     | 0.0     | 0.0     | 116 | 0.0    | 0.0   | 0.0    | 0.0     |
| 55 | 71.3     | -0.1    | -0.1    | -28.2   | 117 | 0.0    | 0.0   | 0.0    | -0.1    |
| 56 | -0.1     | 11.4    | -0.1    | 491.7   | 118 | -711.0 | -42.1 | -223.3 | -229.7  |
| 57 | 0.0      | 0.0     | 0.0     | 0.0     | 119 | 37.3   | 0.0   | -0.1   | 75.3    |
| 58 | 0.0      | 24.7    | 0.0     | 590.8   | 120 | 136.5  | -1.1  | -0.8   | -16.2   |
| 59 | 0.0      | 22.6    | 0.0     | 544.2   | 121 | 0.0    | 0.0   | 0.0    | 0.0     |
| 60 | 136.5    | -1.1    | -0.8    | -16.2   | 122 | 0.0    | 0.0   | 0.0    | 0.0     |
| 61 | 0.0      | 0.0     | 0.0     | 0.0     | 123 | 0.0    | 0.0   | 0.0    | 0.0     |
| 62 | -2.9     | -1.8    | 665.6   | -2793.7 |     |        |       |        |         |

The data in Table 3.5 and Table 3.6 is the active loss and reactive loss allocated to each node calculated using geometric allocation methods, respectively.

Table 3.5: Active loss (W) allocated to each node calculated  
using geometric allocation methods

| node | a      | b     | c     | n      | node | a       | b      | c       | n      |
|------|--------|-------|-------|--------|------|---------|--------|---------|--------|
| 1    | 427.6  | 0.0   | 306.9 | 5113.5 | 63   | 1594.9  | -0.1   | 0.0     | 683.4  |
| 2    | 0.0    | 94.0  | 0.0   | -71.2  | 64   | -0.1    | 2690.9 | 0.0     | -802.9 |
| 3    | 0.0    | 0.0   | 0.0   | 0.0    | 65   | 3026.2  | 1494.9 | 2671.0  | 0.0    |
| 4    | 0.0    | 0.0   | 303.3 | 29.5   | 66   | -0.1    | -0.1   | 2952.7  | -440.3 |
| 5    | 0.0    | 0.0   | 152.1 | 26.7   | 67   | 0.1     | -0.4   | -0.3    | 0.1    |
| 6    | 0.0    | 0.0   | 382.2 | 84.0   | 68   | 870.9   | 0.0    | 0.0     | 400.0  |
| 7    | 194.0  | 0.0   | 0.0   | 85.4   | 69   | 2073.7  | 0.0    | 0.0     | 1004.8 |
| 8    | 0.0    | -0.1  | 0.0   | 0.5    | 70   | 915.2   | 0.0    | 0.0     | 442.8  |
| 9    | 787.2  | 0.0   | 0.0   | 479.0  | 71   | 2114.1  | 0.0    | 0.0     | 1043.1 |
| 10   | 388.3  | 0.0   | 0.0   | 235.6  | 72   | 0.0     | 0.0    | 0.1     | -0.1   |
| 11   | 914.1  | 0.0   | 0.0   | 588.8  | 73   | 0.0     | 0.0    | 1413.4  | -391.9 |
| 12   | 0.0    | 204.8 | 0.0   | -119.0 | 74   | 0.0     | 0.0    | 1590.0  | -437.8 |
| 13   | 0.0    | 0.2   | 0.0   | -0.3   | 75   | 0.0     | 0.0    | -1390.2 | 417.4  |
| 14   | 0.0    | 0.0   | 0.0   | 0.0    | 76   | 6566.6  | 4094.2 | 3325.2  | 0.1    |
| 15   | 0.0    | 0.0   | 0.0   | 0.0    | 77   | -0.1    | 1068.2 | 0.0     | -320.8 |
| 16   | 0.0    | 0.0   | 727.9 | -78.9  | 78   | 0.0     | 0.1    | 0.0     | 0.0    |
| 17   | 0.0    | 0.0   | 315.4 | -39.1  | 79   | 1443.6  | 0.0    | 0.0     | 698.3  |
| 18   | 0.0    | 0.0   | -0.6  | -3.0   | 80   | 0.0     | 1042.6 | 0.0     | -327.8 |
| 19   | 1143.1 | 0.0   | 0.0   | 635.5  | 81   | 0.0     | 0.0    | 0.0     | 0.1    |
| 20   | 1192.3 | 0.0   | 0.0   | 674.5  | 82   | 1343.2  | 0.0    | 0.0     | 616.9  |
| 21   | 0.0    | 0.0   | 0.0   | 0.0    | 83   | -2519.7 | -910.8 | 457.8   | -171.2 |
| 22   | 0.0    | 781.6 | 0.0   | -431.4 | 84   | 0.0     | 0.0    | 654.8   | -120.9 |
| 23   | 0.0    | 0.0   | 0.0   | 0.0    | 85   | 0.0     | 0.0    | 1538.2  | -247.5 |
| 24   | 0.0    | 0.0   | 819.5 | -69.7  | 86   | 0.0     | 461.5  | 0.0     | -95.6  |

|    |          |         |         |        |     |        |        |        |         |
|----|----------|---------|---------|--------|-----|--------|--------|--------|---------|
| 25 | 0.0      | 0.0     | -0.4    | -0.2   | 87  | 0.0    | 1095.9 | 0.0    | -221.4  |
| 26 | 0.0      | 0.0     | 0.0     | 0.0    | 88  | 1532.0 | 0.0    | 0.0    | 330.1   |
| 27 | 0.0      | 0.0     | 0.0     | 0.0    | 89  | -0.2   | 0.0    | 0.0    | 0.0     |
| 28 | 853.1    | 0.0     | 0.0     | 373.2  | 90  | 0.0    | 1294.8 | 0.0    | 762.9   |
| 29 | 927.8    | 0.0     | 0.0     | 412.9  | 91  | 0.0    | 0.0    | 0.0    | 0.0     |
| 30 | 0.0      | 0.0     | 682.1   | -46.1  | 92  | 0.0    | 0.0    | 1153.4 | -1020.1 |
| 31 | 0.0      | 0.0     | 376.2   | -15.2  | 93  | 0.1    | 0.0    | 0.0    | 0.0     |
| 32 | 0.0      | 0.0     | 381.6   | -9.9   | 94  | 2080.7 | 0.0    | 0.0    | 897.0   |
| 33 | -1095.9  | 0.0     | 0.0     | -504.2 | 95  | 0.0    | 419.2  | 0.0    | -60.2   |
| 34 | 0.0      | 0.0     | 741.2   | -127.0 | 96  | 0.0    | 680.1  | 0.0    | -122.5  |
| 35 | 399.2    | 294.7   | 0.0     | 0.0    | 97  | 0.0    | 0.1    | 0.0    | 0.0     |
| 36 | 0.0      | 0.0     | 0.0     | 0.0    | 98  | 1231.3 | 0.0    | 0.0    | 622.6   |
| 37 | 1219.5   | 0.0     | 0.0     | 676.5  | 99  | 0.0    | 1014.7 | 0.0    | -347.9  |
| 38 | 0.0      | 346.2   | 0.0     | -152.4 | 100 | 0.0    | 0.0    | 1046.9 | -333.0  |
| 39 | 0.0      | 335.2   | 0.0     | -138.5 | 101 | 0.0    | 0.0    | 0.0    | 0.0     |
| 40 | 0.0      | 0.0     | 0.0     | 0.0    | 102 | 0.0    | 0.0    | 626.4  | -159.6  |
| 41 | 0.0      | 0.0     | 334.3   | -81.5  | 103 | 0.0    | 0.0    | 1496.2 | -317.0  |
| 42 | 465.1    | 0.0     | 0.0     | 206.9  | 104 | 0.0    | 0.0    | 1543.6 | -269.9  |
| 43 | 0.0      | 785.5   | 0.0     | -396.5 | 105 | 0.0    | 0.0    | 0.0    | 0.1     |
| 44 | 0.0      | 0.0     | 0.0     | 0.0    | 106 | 0.0    | 1468.0 | 0.0    | -491.8  |
| 45 | 530.9    | 0.0     | 0.0     | 276.3  | 107 | 0.0    | 1509.8 | 0.0    | -453.5  |
| 46 | 523.1    | 0.0     | 0.0     | 274.0  | 108 | -0.1   | 0.0    | 0.0    | 0.0     |
| 47 | -15835.5 | -9108.8 | -9517.6 | 27.4   | 109 | 2249.7 | 0.0    | 0.0    | 1172.6  |
| 48 | 3121.9   | 1937.5  | 2004.9  | -24.2  | 110 | 0.1    | 0.0    | 0.0    | 0.0     |
| 49 | 1471.1   | 1813.9  | 883.9   | -609.3 | 111 | 1014.1 | 0.0    | 0.0    | 537.6   |
| 50 | 0.0      | 0.0     | 725.0   | -147.4 | 112 | 1059.1 | 0.0    | 0.0    | 561.9   |
| 51 | 444.5    | 0.0     | 0.0     | 153.8  | 113 | 2622.7 | 0.0    | 0.0    | 1451.9  |

|    |        |       |        |        |     |        |      |       |       |
|----|--------|-------|--------|--------|-----|--------|------|-------|-------|
| 52 | 1202.7 | 0.0   | 0.0    | 627.9  | 114 | 1051.8 | 0.0  | 0.0   | 574.0 |
| 53 | 1315.2 | 0.0   | 0.0    | 672.3  | 115 | 0.0    | 0.0  | 0.0   | 0.0   |
| 54 | 0.2    | -0.1  | 0.0    | -0.3   | 116 | 0.0    | 0.2  | 0.0   | -0.3  |
| 55 | 388.3  | 0.0   | 0.0    | 184.4  | 117 | 0.0    | 0.0  | -0.6  | -3.0  |
| 56 | 0.0    | 259.5 | 0.0    | -81.2  | 118 | 664.2  | 30.0 | 164.4 | 191.5 |
| 57 | 0.0    | 0.1   | 0.0    | 0.2    | 119 | 444.5  | 0.0  | 0.0   | 153.8 |
| 58 | 0.0    | 478.9 | 0.0    | -168.1 | 120 | 661.4  | -0.1 | 0.0   | 295.4 |
| 59 | 0.0    | 462.5 | 0.0    | -155.9 | 121 | 0.0    | 0.1  | 0.0   | 0.0   |
| 60 | 661.4  | -0.1  | 0.0    | 295.4  | 122 | 0.0    | 0.0  | 0.0   | 0.0   |
| 61 | 0.0    | 0.0   | 0.0    | 0.0    | 123 | 0.0    | 0.0  | 0.0   | 0.0   |
| 62 | -0.1   | -0.1  | 1196.2 | -318.7 |     |        |      |       |       |

Table 3.6: Reactive loss (kVar) allocated to each node calculated using geometric allocation method

| node | a     | b    | c       | n      | node | a      | b      | c      | n       |
|------|-------|------|---------|--------|------|--------|--------|--------|---------|
| 1    | 167.9 | 0.2  | 18696.2 | -827.7 | 63   | -0.6   | -0.2   | -0.1   | -88.0   |
| 2    | 0.0   | 38.3 | 0.0     | 180.6  | 64   | -1.7   | 193.8  | -1.3   | 2942.4  |
| 3    | 0.0   | 0.0  | 0.0     | -0.1   | 65   | 6351.1 | 1832.2 | 1619.8 | 0.0     |
| 4    | 0.0   | 0.0  | -105.1  | -723.8 | 66   | -1.1   | -1.0   | 949.5  | -2708.0 |
| 5    | 0.0   | 0.0  | -29.1   | -296.9 | 67   | 1.2    | 1.7    | 0.1    | -0.6    |
| 6    | 0.0   | 0.0  | -118.3  | -796.5 | 68   | 656.6  | 0.0    | 0.0    | 77.6    |
| 7    | -69.1 | 0.0  | 0.0     | -76.9  | 69   | 1661.9 | 0.0    | 0.0    | 218.4   |
| 8    | 0.0   | -2.4 | 0.3     | 0.7    | 70   | 662.4  | 0.0    | 0.0    | 79.0    |
| 9    | 347.1 | 0.0  | 0.0     | 326.4  | 71   | 1671.6 | 0.0    | 0.0    | 220.8   |
| 10   | 142.7 | 0.0  | 0.0     | 132.9  | 72   | 0.0    | 0.4    | 0.3    | -0.2    |
| 11   | 373.8 | 0.0  | 0.0     | 350.2  | 73   | 0.0    | 0.0    | 1593.3 | -2325.0 |
| 12   | 0.0   | 90.7 | 0.0     | 391.7  | 74   | 0.0    | 0.0    | 1802.4 | -2621.8 |

|    |        |       |       |         |     |          |          |          |         |
|----|--------|-------|-------|---------|-----|----------|----------|----------|---------|
| 13 | 0.0    | 1.3   | 0.3   | 0.6     | 75  | 0.0      | 0.0      | -1593.8  | 2327.4  |
| 14 | 0.1    | 0.0   | 0.0   | 0.1     | 76  | 7236.1   | 10749.4  | 6655.6   | 0.0     |
| 15 | 0.0    | 0.0   | 0.0   | 0.0     | 77  | 0.0      | -545.1   | 0.1      | 839.2   |
| 16 | 0.0    | 0.0   | 271.4 | -1509.2 | 78  | -0.6     | 0.2      | 0.3      | -0.1    |
| 17 | 0.0    | 0.0   | 122.1 | -619.1  | 79  | -970.8   | 0.1      | 0.1      | -272.0  |
| 18 | 0.2    | 0.0   | 13.4  | 2.2     | 80  | 0.2      | -738.6   | 0.1      | 715.1   |
| 19 | 488.7  | 0.0   | 0.0   | 452.6   | 81  | 0.7      | 0.0      | 0.6      | 0.0     |
| 20 | 502.4  | 0.0   | 0.0   | 464.3   | 82  | -1088.5  | 0.2      | 0.1      | -162.6  |
| 21 | 0.3    | 0.1   | 0.1   | 0.2     | 83  | -93744.3 | -67850.7 | -66154.7 | -2291.3 |
| 22 | 0.0    | 263.2 | 0.0   | 1338.2  | 84  | 0.0      | 0.0      | 921.3    | -993.1  |
| 23 | 0.3    | 0.1   | 0.1   | -0.1    | 85  | 0.0      | 0.0      | 2291.1   | -2369.0 |
| 24 | 0.0    | 0.0   | 233.6 | -1746.6 | 86  | 0.2      | -376.6   | 0.1      | 293.0   |
| 25 | 0.1    | 0.0   | -0.4  | -13.7   | 87  | 0.2      | -561.5   | 0.1      | 796.1   |
| 26 | 0.2    | 0.0   | 0.1   | 0.1     | 88  | -9223.7  | 0.0      | 0.0      | -3015.0 |
| 27 | 0.2    | 0.0   | 0.1   | 0.0     | 89  | 0.9      | 0.1      | 0.8      | 0.1     |
| 28 | -295.1 | 0.0   | 0.0   | -86.7   | 90  | 0.0      | -6726.4  | 0.0      | 2365.2  |
| 29 | -225.8 | 0.0   | 0.0   | 9.7     | 91  | 0.7      | 0.7      | 0.4      | 0.1     |
| 30 | 0.0    | 0.0   | 208.4 | -118.8  | 92  | 0.0      | 0.0      | -6260.5  | 965.2   |
| 31 | 0.0    | 0.0   | 108.8 | -724.1  | 93  | 0.8      | 0.7      | 0.6      | 0.0     |
| 32 | 0.0    | 0.0   | 109.1 | -724.4  | 94  | 2081.7   | 0.0      | 0.0      | -408.8  |
| 33 | -498.8 | 0.0   | 0.0   | -771.1  | 95  | 0.2      | -542.4   | 0.1      | 149.8   |
| 34 | 0.0    | 0.0   | 290.1 | -1632.0 | 96  | 0.0      | 712.6    | 0.0      | 1052.7  |
| 35 | -997.2 | 531.0 | -0.1  | 0.0     | 97  | 0.7      | 0.5      | 0.4      | 0.3     |
| 36 | 0.3    | 0.1   | 0.0   | 0.1     | 98  | -792.9   | 0.0      | 0.1      | -249.2  |
| 37 | 506.2  | 0.0   | 0.0   | 300.8   | 99  | 0.1      | -493.1   | 0.1      | 801.5   |
| 38 | 0.0    | 71.6  | 0.0   | 635.1   | 100 | 0.1      | 0.1      | -206.0   | -432.3  |
| 39 | 0.0    | 67.0  | 0.0   | 601.4   | 101 | 0.8      | 0.8      | 0.6      | -0.2    |

|    |         |         |         |         |     |         |        |        |         |
|----|---------|---------|---------|---------|-----|---------|--------|--------|---------|
| 40 | 0.0     | 0.0     | 0.0     | -0.1    | 102 | 0.0     | 0.0    | 591.8  | -1041.1 |
| 41 | 0.0     | 0.0     | 89.8    | -707.0  | 103 | 0.0     | 0.0    | 1449.4 | -2476.5 |
| 42 | -10.6   | 0.0     | 0.0     | 14.1    | 104 | 0.0     | 0.0    | 1453.5 | -2478.4 |
| 43 | 0.0     | 172.7   | 0.0     | 1560.9  | 105 | 0.9     | 0.1    | 0.6    | 0.0     |
| 44 | 0.0     | 0.0     | 0.0     | -0.2    | 106 | 0.0     | 1337.1 | 0.0    | 2454.4  |
| 45 | 172.5   | 0.0     | 0.0     | 138.0   | 107 | 0.0     | 1342.4 | 0.0    | 2457.9  |
| 46 | 167.6   | 0.0     | 0.0     | 134.0   | 108 | 0.9     | 0.6    | 0.7    | 0.1     |
| 47 | -8573.6 | -3099.1 | -2445.0 | -422.8  | 109 | 1705.3  | 0.0    | 0.0    | 191.9   |
| 48 | 4057.6  | 2092.4  | 2202.0  | 78.2    | 110 | 0.3     | 0.0    | 0.0    | 0.1     |
| 49 | 1985.0  | 1989.5  | 501.4   | 2218.4  | 111 | 684.3   | 0.0    | 0.0    | 68.8    |
| 50 | -0.1    | 0.0     | 189.7   | -10.6   | 112 | 719.1   | 0.0    | 0.0    | 73.1    |
| 51 | -173.8  | 0.0     | -0.1    | -104.0  | 113 | 1887.1  | 0.0    | 0.0    | 218.2   |
| 52 | 696.5   | 0.0     | 0.0     | 320.7   | 114 | 690.1   | 0.0    | 0.0    | 70.3    |
| 53 | 803.6   | 0.0     | 0.0     | 285.5   | 115 | 0.0     | 0.0    | 0.0    | 0.0     |
| 54 | -0.2    | 1.7     | -0.3    | -0.8    | 116 | 0.0     | 1.3    | 0.3    | 0.6     |
| 55 | -300.5  | 0.0     | 0.0     | -147.6  | 117 | 0.2     | 0.0    | 13.4   | 2.2     |
| 56 | 0.1     | -298.3  | 0.0     | 26.0    | 118 | -1083.1 | -80.8  | -508.2 | -379.4  |
| 57 | 0.4     | -1.3    | 0.0     | 0.8     | 119 | -173.8  | 0.0    | -0.1   | -104.0  |
| 58 | 0.0     | 329.3   | 0.0     | 782.0   | 120 | -89.8   | -0.6   | -0.1   | -70.6   |
| 59 | 0.0     | 312.9   | 0.0     | 746.6   | 121 | 0.7     | 0.5    | 0.4    | 0.3     |
| 60 | -89.8   | -0.6    | -0.1    | -70.6   | 122 | 2.2     | 1.6    | 1.8    | 0.1     |
| 61 | 1.4     | 0.9     | 0.8     | 0.0     | 123 | 0.3     | 0.1    | 0.1    | 0.0     |
| 62 | -0.5    | -0.4    | 389.3   | -1138.8 |     |         |        |        |         |

### 3.5.3 Results Analysis

The results show that the use of different allocation methods for the cross-term has a clear impact on the results of the loss allocation. Figure 3.14 shows the cross-term allocation factor  $\beta$  versus

the ratio  $i^e/i_f$  for different methods. It can be seen that at current ratios around 1 (i.e. when the two relevant current values of the cross term are close), the difference between the results obtained with these three methods are not significant.

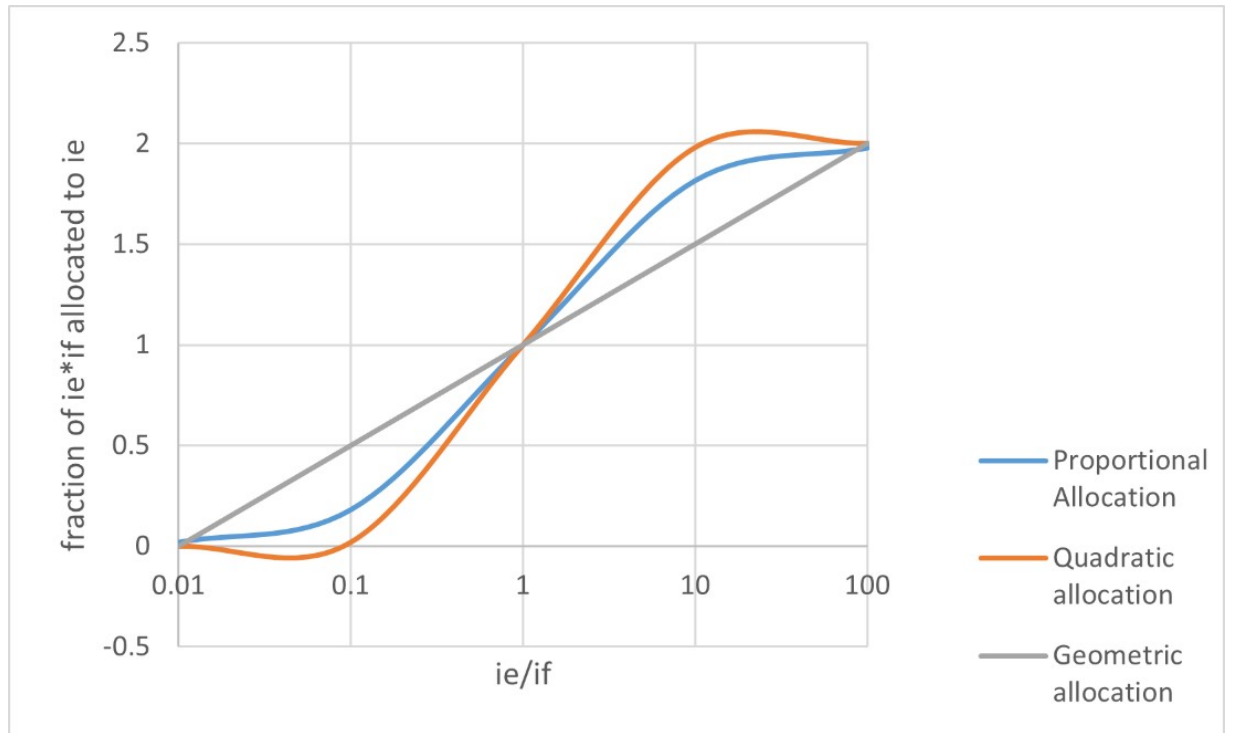


Figure 3.14: The cross-term allocation factor  $\beta$  versus the ratio  $i^e/i_f$  for different methods

As can be seen in Table 3.7, the negative active power loss occurs due to the fact that node 33, 47 and node 75 are connected to DGs, which indicates that the nodes are not penalised by the distribution network supplier regarding system losses. This is suitable in the modern electricity market encouraging installations of renewable energy DGs.

Table 3.7: Loss of nodes connected to the DG

| Node | Phase $a$ | Phase $b$ | Phase $c$ | Neutral $n$ |
|------|-----------|-----------|-----------|-------------|
| 33   | -1312.5   | 0         | 0         | -484.4      |
| 47   | -20117.9  | -12366.1  | -12871.3  | 23.9        |
| 75   | 0         | 0         | -1475.5   | 473.1       |

In addition, the results of the loss allocation method proposed in this paper reflect the role of each node in the distribution system through positive and negative power losses. For active power

losses, most of which are positive except for the nodes connected to the DG, the distribution network can consider incentives and penalties depending on the amount of losses allocated at each node. For reactive power losses, the impact of each node in the distribution system on regulating the service role of the system can be determined by positive and negative losses.

### 3.5.4 Discussion on Losses Allocation to Neutral

The losses allocated to the neutral raise several intriguing questions, such as the meaning of Neutral Loss Allocation Factors (NLAFs), whether they convey the same information as Phase Loss Allocation Factors (PLAFs), the significance of a negative sign in NLAFs, and whether NLAFs can be actively utilized in managing Distribution Networks (DNs). The answers to these questions are briefly discussed below.

PLAFs represent the losses allocated to each phase of a node due to the net power injection or absorption by its connected loads. These losses would not occur in a system without these users. In contrast, NLAFs indicate the degree of imbalance in a network, which depends on the non-uniform distribution of end-users and their varying energy consumption patterns. In a perfectly balanced system, no current would flow in the neutral, resulting in no losses assigned to it. However, in an unbalanced system, especially in low-voltage distribution networks, it is unreasonable to allocate neutral losses to end-users, particularly single-phase users, as their connection inherently causes the grid to be unbalanced.

Furthermore, both PLAFs and NLAFs can have positive and negative values, as seen in the results tables. However, factors with the same signs do not necessarily correlate. Passive end-users are assigned positive PLAFs because they consume energy, increasing system losses. In contrast, active end-users may receive positive PLAFs if they overproduce, causing reverse power flow, or negative PLAFs if they partially or fully meet local demand, thereby reducing branch currents and losses. Negative NLAFs are given to nodes that help reduce the net neutral current in their upstream branches, thereby decreasing the imbalance of networks.

Since NLAFs indicate the balancing condition of networks, DSOs can effectively use them to

identify critical nodes with positive NLAFs. This allows for the implementation of appropriate unbalance reduction management schemes at these specific nodes.

### **3.6 Conclusion**

The findings from the loss allocation method underscore its rationality and fairness in the context of the distribution network with distributed generation. By thoughtfully accounting for the positive impact of distributed power sources, the method empowers nodes to act as power providers while fulfilling their internal power demands. This approach significantly curtails overall power grid losses, enhances energy utilization efficiency, and accelerates the adoption of distributed power sources. Consequently, the method aligns with broader goals of promoting renewable and clean energy adoption, reducing dependence on conventional power plants, and expediting the transition towards achieving NET-ZETO objectives.

In order for the theory and results of loss allocation to be applied, a large amount of data is relatively abstract and therefore visualising the results deserves to be discussed. This will be further explored in the next chapter.

# Chapter 4

## Colouring Visualisation Application

### 4.1 Introduction

Currently, electricity and heat production account for 25% of global greenhouse gas emissions [72], with fossil fuels being the source of 80% of the electricity of world over the past few decades [49]. Moreover, as the electrification of vehicles progresses, electricity demand will continue to increase [53]. Given the complexity of carbon emissions and energy consumption, effectively using data to trace and visualize these factors has become crucial in the decarbonization process. In the global fight against climate change, having a transparent and accurate accounting system for electricity carbon emissions is of paramount importance.

The evolution of power systems has brought about significant challenges in managing and visualizing the complex flows of electricity across vast networks. As power grids become increasingly intricate with the integration of distributed generation, renewable energy sources, and advanced technologies, understanding the distribution and tracing of power flow has become crucial. One of the innovative approaches to tackling this complexity is through power flow tracing, a method that allows for the detailed analysis of how power is generated, transmitted, and consumed across a network. However, the sheer complexity and volume of data involved in power flow tracing necessitate effective visualization techniques to make the insights derived

from this analysis accessible and actionable [73].

Power flow tracing visualization involves collecting, analyzing, and displaying various types of data related to tidal currents in an intuitive and comprehensible manner to reveal changes, developments, and trends [74]. In the context of decarbonization, this method can help us understand the dynamics of carbon emissions, identify and forecast the development of low-carbon technologies, and assess the impact of low-carbon policies, thereby enhancing the promotion of the decarbonization process.

Firstly, flow tracing visualization enables real-time monitoring of carbon emissions. Statistics indicate that annual global carbon emissions total around 3,644 million tons, with electricity and heat production being the primary sources [75]. Real-time carbon emission data, along with related analysis and forecasts, can help us understand the specifics of carbon emissions, identify issues, and develop or adjust low-carbon strategies. For instance, the "Carbon Emission Inventory" released by the U.S. Environmental Protection Agency (EPA) details the carbon emissions of various regions and industries in the U.S. through data visualization, providing crucial data support for the development and implementation of carbon emission reduction policies [16].

Secondly, power flow tracing visualization can uncover the development trends of low-carbon technologies. The advancement and application of these technologies are crucial for achieving decarbonization. By gathering and analyzing various data related to low-carbon technologies, such as patent data, market data, and policy data, we can understand the current state of different low-carbon technologies, forecast their future development, and provide decision-making support for their research, promotion, and application [76]. Additionally, power flow tracing visualization can help assess the impact of low-carbon policies. By analyzing data from before and after the implementation of these policies, we can evaluate their actual effects, identify issues, and make ongoing optimizations. For instance, Tranberg et al. conducted a comprehensive analysis of carbon emissions and carbon intensity in European countries, providing a critical foundation for evaluating low-carbon policies in Europe [77].

The adoption of coloring visualization in power flow tracing also has educational and com-

municative value. It serves as an effective tool for training and informing both technical and non-technical audiences about the functioning of power systems. By presenting complex power flow data in a visually appealing and understandable format, it becomes easier to convey key concepts, trends, and issues to stakeholders, policymakers, and the public.

Despite the significant role power flow tracing visualization has played in the decarbonization process, several challenges remain. These include ensuring the accuracy, completeness, and timeliness of the data; refining data analysis methods and techniques; and addressing data security and privacy concerns. To effectively reduce carbon emissions from electricity production and consumption, investors, consumers, and regulators require real-time, accurate data [56]. "Scope 2 refers to the emissions generated from purchased electricity (or other forms of energy)," as defined by the Greenhouse Gas Protocol [78]. Tracking the storage from a specific generator to a specific consumer presents a significant challenge [62, 70].

To achieve this goal, Tranberg et al. proposed a novel real-time carbon accounting methodology using flow tracking techniques, applying it to hourly market data for 28 European regions [79]. The methodology introduces a new consumption-based accounting approach that more accurately reflects the fundamental physical characteristics of the power system compared to traditional input-output models for carbon accounting [50, 80–82]. The methodology takes a further step [80] by employing a similar flow-tracking approach to establish consumption-based carbon allocations among six regions in China. However, the study faced limitations as it relied on annual totals and aggregated data from various generation technologies. They implemented this methodology using real-time system data, enabling the differentiation between various power generation technologies. This allows for the provision of a real-time CO<sub>2</sub> signal to all stakeholders involved, enhancing the transparency and credibility of emissions accounting associated with electricity consumption, a crucial aspect [63]. To explore the effects of the novel consumption-based accounting method, they contrasted it with a direct production-based approach, which involves examining the real-time generation mix for each region.

## 4.2 Flow Colouring Method

In the modern era of power systems, the complexity of electricity generation, transmission, and distribution has increased significantly. With the integration of renewable energy sources, distributed generation, and the advent of smart grid technologies, power networks have become more dynamic and intricate [83]. Understanding the flow of power through these networks is critical for ensuring efficient operation, reliability, and stability. However, traditional methods of analyzing power flow often struggle to provide the clarity needed to make informed decisions in such complex environments. This is where the power flow coloring method comes into play a technique designed to enhance the visualization and interpretation of power flow data in electric grids.

The power flow coloring method is a visualization technique that assigns colors to different elements of the power system based on specific attributes of power flow, such as the magnitude, direction, or source of the power. By applying a color scheme to various parts of the network, this method allows for an intuitive and immediate understanding of how power is distributed, where it is coming from, and where it is being consumed. This approach is particularly valuable in large and complex networks where traditional data representation methods, such as tables or graphs, can become overwhelming and difficult to interpret.

The primary advantage of the power flow coloring method lies in its ability to simplify complex data into a visual format that is easy to understand at a glance. For instance, different colors can be used to represent power flows from different generators, highlighting the paths that electricity takes from its source to various load centers. Alternatively, colors might indicate the intensity of power flows, helping to identify areas of high load or potential congestion within the network. This immediate visual feedback is crucial for operators and engineers who need to monitor the system's performance and quickly identify any issues that may arise.

Moreover, the power flow coloring method is not only beneficial for real-time monitoring but also for planning and analysis. By visualizing historical power flow data, planners can better understand past system behavior, identify trends, and predict future scenarios. This can lead to

more informed decisions regarding infrastructure investments, such as where to reinforce the network or how to integrate new generation sources most effectively.

In this study, the RGB colour system, in combination with the results of the power flow tracing based on the results of the loss allocation, allows for an efficient visualisation of the tracing of power flow. The RGB (Red, Green, Blue) color model forms the foundation for color representation in various digital applications, including computer displays, televisions, and digital cameras. In the context of visualizing power flow data in electrical networks, the RGB color system offers a powerful tool for enhancing the clarity and interpretability of complex datasets.

The RGB color model is based on the additive color theory [84], where colors are created by combining different intensities of red, green, and blue light. Each color component in the RGB model is represented by a numerical value (Figure 4.1), typically ranging from 0 to 255 in digital systems, where 0 represents the absence of color (complete darkness), and 255 represents the full intensity of that color. By adjusting the intensity of each of these three primary colors, a wide spectrum of colors can be produced. For example, combining full intensity red (255, 0, 0) with full intensity green (0, 255, 0) results in yellow (255, 255, 0), while combining full intensity of all three primary colors (255, 255, 255) results in white [85].

In power flow visualization, the RGB color system is particularly useful for creating distinct and meaningful color maps that represent various aspects of power system behavior. For instance, the flow of electricity from different sources can be depicted using different colors, where each source is assigned a unique RGB value. By doing so, one can easily distinguish between the contributions of different generators to the overall power supply. Furthermore, color gradients can be employed to represent the magnitude of power flow, with darker or more intense colors indicating higher power levels, and lighter colors representing lower levels.

Moreover, the RGB color system's compatibility with digital technologies makes it an ideal choice for real-time monitoring and interactive visualizations. Operators can interact with power flow data on digital platforms, using color-coded maps to drill down into specific areas of the network, explore different scenarios, and make informed decisions based on visual cues. The

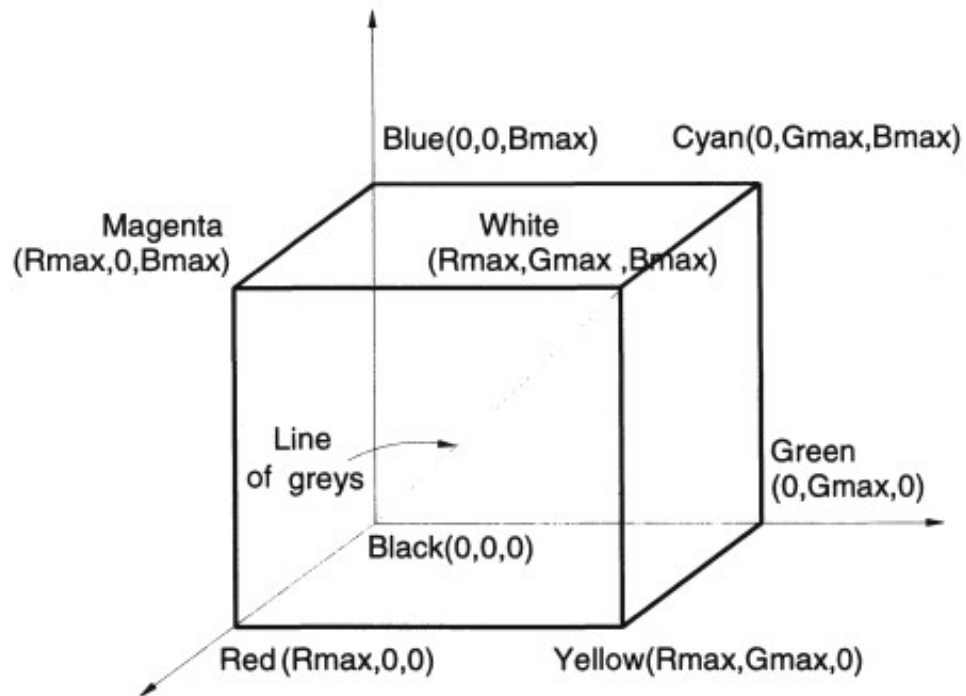


Figure 4.1: Parameters of RGB colour space.

RGB system's integration with various software tools and platforms ensures that the visualizations are consistent, accurate, and easily shareable among stakeholders.

When utilizing the RGB color system for visualizing the distribution network flows, it's recognized that most branches, particularly the terminal ones, contribute relatively small amounts of power. For instance, consider the color representation of a DG with a single blue energy source, where the no-energy state (with the initial value of the B parameter set at 0, 64, and 128) is illustrated in Figure 4.2. It is evident that the initial value of 128 appears distinctly blue rather than appearing close to black compared to the values of 0 and 64. Hence, to prevent a broad range of power flow being represented as black after applying color, the parameter range for the three primary colors is adjusted to 128-255 in this study.

The outcome of the distribution network loss allocation dictates the power flows attributed to each branch, thereby determining the RGB parameters associated with each branch. The distribution of losses from each energy source across the phases of each branch in the network influences the color parameter representing that energy source. Through aggregating the color

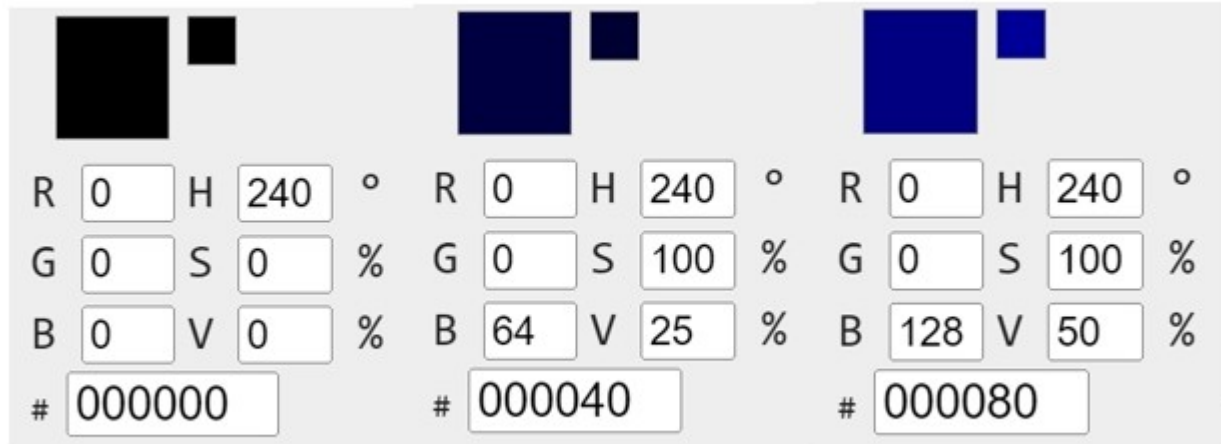


Figure 4.2: Comparison of initial values of different blue parameters

parameters in the RGB color system, it becomes feasible to visualize the energy distribution across each phase of every branch.

Moreover, to enhance the visualization's informativeness, power flow is depicted not only by coloring its energy composition but also by varying the width of the flow, indicating to some degree the magnitude of branch currents. By comparing the power flows of branches within the distribution network, the width in the visualization is proportionally determined.

In the subsequent section, the simulation model utilizes the IEEE123-node system. Initially, the current result serves as the foundation for system-wide loss allocation, thus determining the flow distribution across each branch. Subsequently, the described visualization method is employed to illustrate the power flow within each branch of the system. Lastly, the findings will be analyzed based on the visualization.

### 4.3 Case Study

This study selects the IEEE123-node system as its simulation model for several reasons. Firstly, it represents an unbalanced system, mirroring real-world distribution network scenarios. Secondly, its relatively large size allows for more comprehensive outcomes. Additionally, modifi-

cations were made to the original IEEE123-node system to assess the influence of distributed generations in the distribution network, as depicted in the figure 3.11.

A wind turbine unit with a capacity of 1MW/500kVar is linked to node 47. Additionally, two PV panels, each with a capacity of 40kW/20kVar, are connected to nodes 33 and 75. Losses are distributed across each branch of the system based on the adjusted IEEE123-node system power flow findings. The outcomes of this loss allocation process are detailed in Table B1 in the Appendix B.

### 4.3.1 Results Analysis

The loss allocation outcomes for the entire system, as depicted in the Table B1, reveal substantial figures. While these data offer precise electrical or economic indications for distribution network operators, they may be challenging for consumers to interpret. Consumers may find it difficult to discern the types and quantities of energy they consume from this data alone. The visualization approach proposed in this project effectively addresses this issue. In the modified IEEE123-node system, energy from the grid is defined as red, i.e., R. Define the energy source of the wind turbine connected at node 47 as green, i.e., G. Finally, the energy from the photovoltaic panels connected at nodes 33 and 75 is defined as blue B. The system power flow is coloured according to the results of the loss allocation. Figure 4.3 shows the results after visualising the IEEE123-node system.

Figure 4.3 provides a clear depiction of the energy composition, direction, and relative magnitude of power flows across the branches of the system. Overall, the majority of branches are dominated by energy from the grid and wind turbines. For instance, at node 13(Figure 4.4), three-phase grid energy flows towards node 34 and node 152. Subsequently, after passing through node 13, phases *b* and *c* carry energy towards nodes 34 and 152. Consequently, downstream branches of phases *b* and *c* exhibit combined red and green power flows, whereas phase *a* of the downstream branches remains solely red.

At node 18, depicted in Figure 4.5, all three phases of wind turbine energy flow towards nodes 19

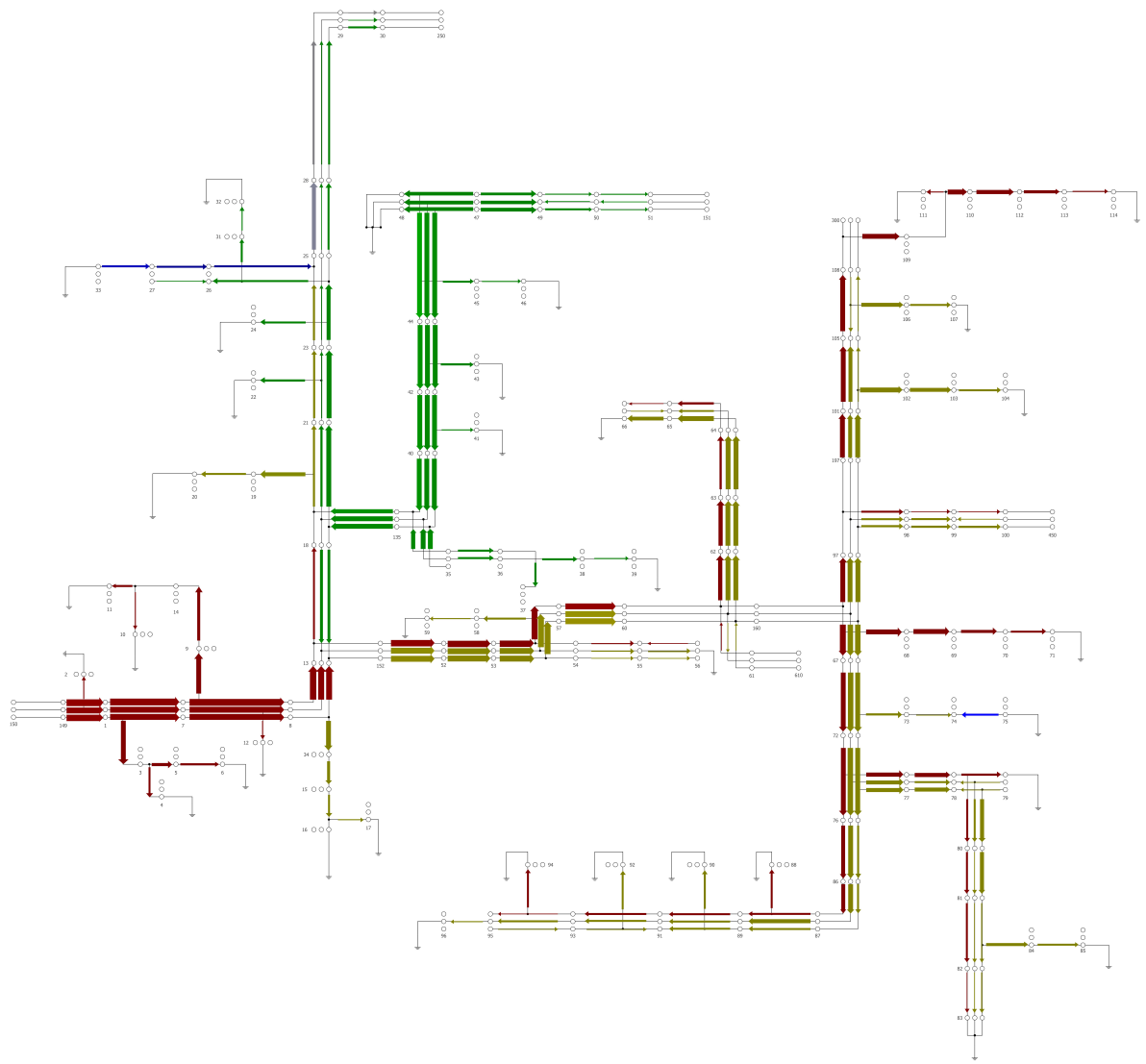


Figure 4.3: Power Flow Visualisation

and 21 from upstream. However, only phases *b* and *c* continue towards node 13. Additionally, energy from the grid, represented by phase *a*, also flows into the downstream branch of node 18. Consequently, phases *a* of branches 13-18 exhibit red power flow, while phases *b* and *c* show green power flow. Downstream branches of node 18 display both phases *b* and *c* as green power flows, while phase *a* represents a combination of red and green power flow.

Due to their substantial output, wind turbines exert a significant impact across the system. However, the influence of the two PV panels is limited to a few nearby branches due to their lower power output. Additionally, unlike wind turbines, many PV panels operate on a single phase, including the two panels integrated into the system examined in this study. As illustrated in Figure

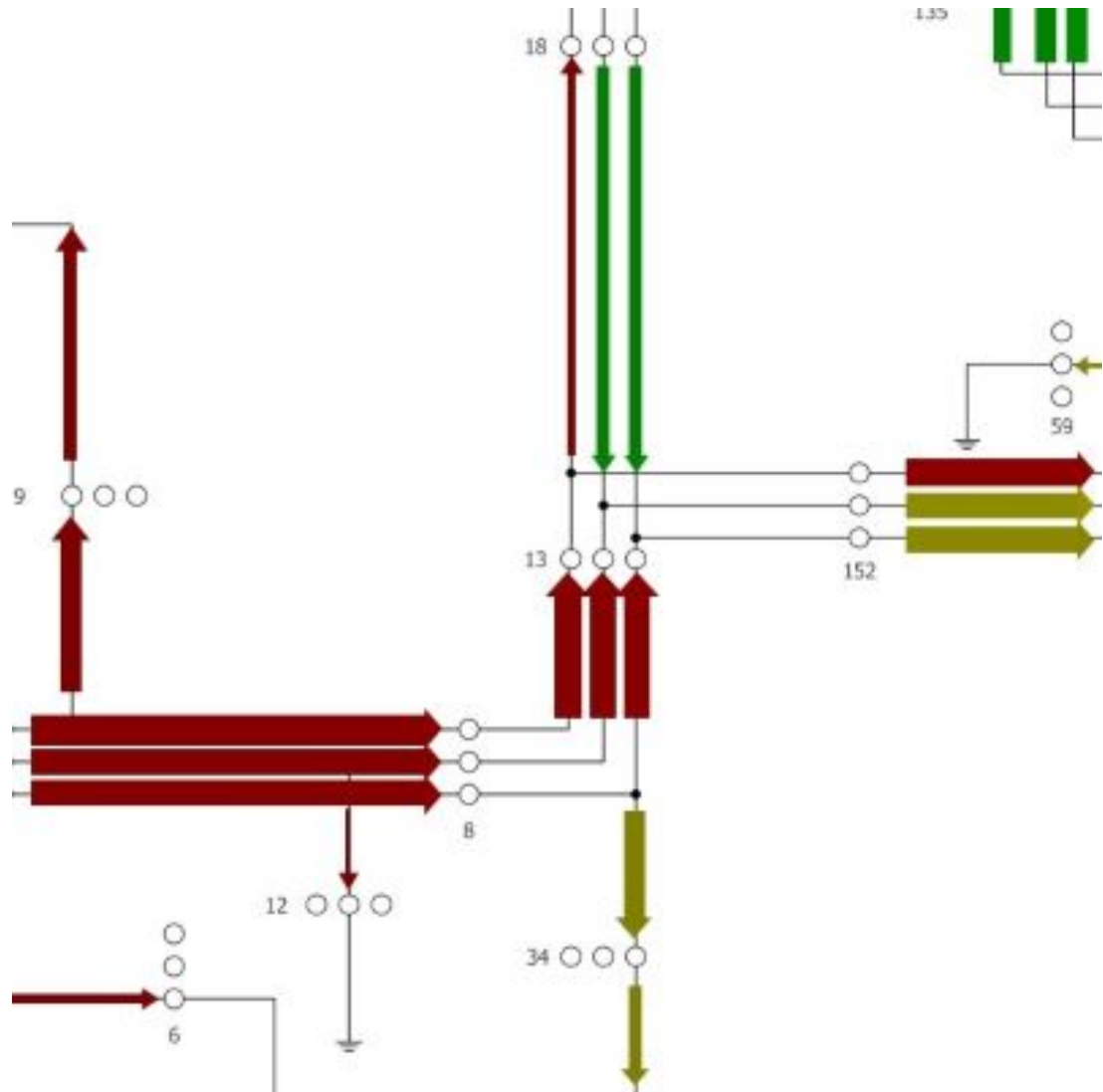


Figure 4.4: Power flow at node 13

4.6, the PV panel linked to node 75 influences only one branch, namely 74-75. Consequently, this branch displays blue power flow, representing 100 percent of the PV contribution, resulting in the parameter B reaching 255.

An *a*-phase PV panel is linked to node 33, manifesting solely in the *a*-phase of its succeeding node. As depicted in Figure 4.7, at node 25, energy from the PV panel travels towards node 28. Concurrently, the upstream *a*-phase power flow, comprising both red and green energy, also courses through node 25 en route to node 28. Consequently, the *a*-phase of the branch connecting node 25 and node 30 exhibits a combined power flow of red, green, and blue.

When comparing Figures 4.6 and 4.7, despite both nodes 33 and 75 being equipped with PV

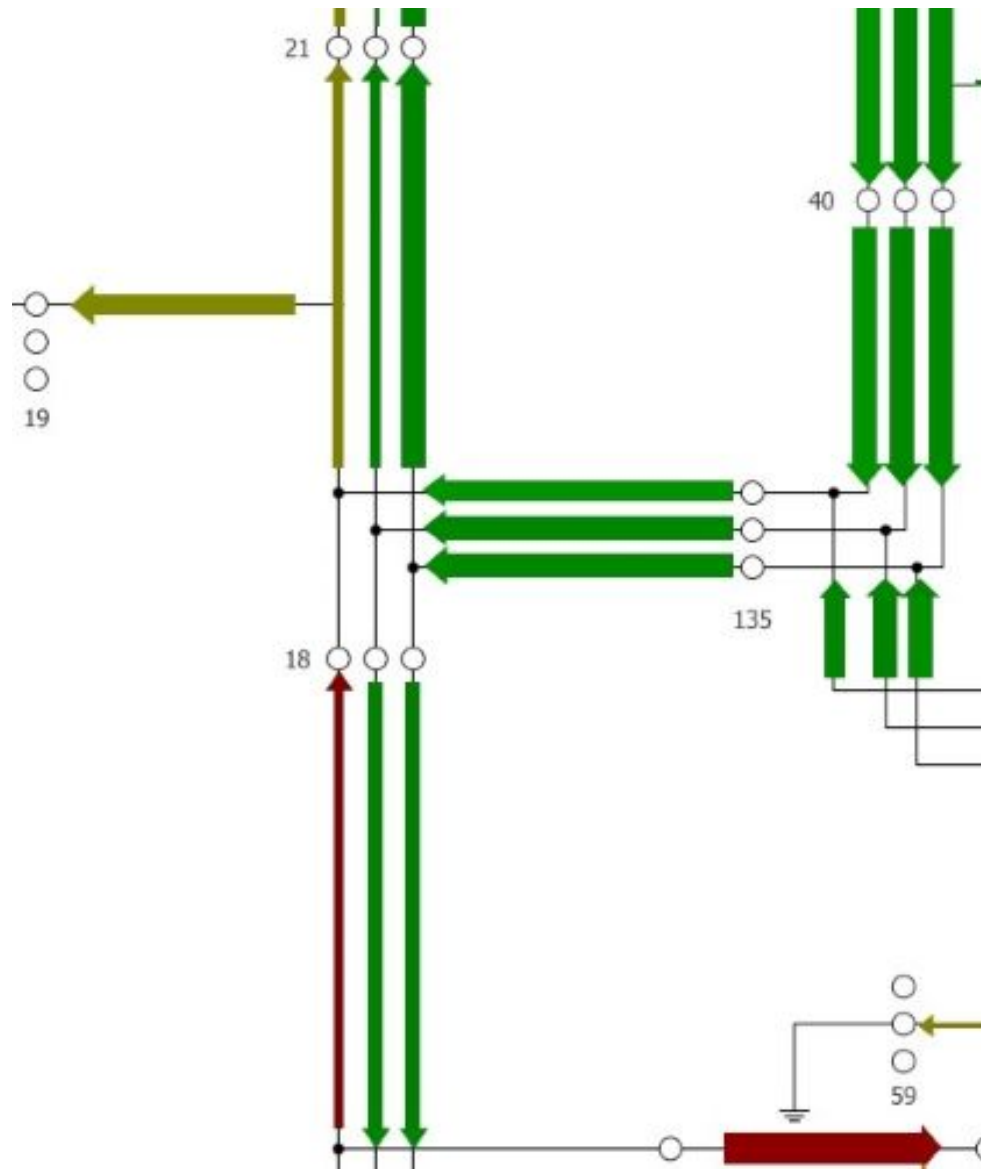


Figure 4.5: Power flow at node 18

panels of equal power, their impact outcomes vary. In the IEEE123 node system, identical line materials are employed for branches 27-33 and 74-75. However, there is a disparity in the materials utilized in their downstream branches. The downstream branches of branches 27-33 employ materials with lower impedance values in contrast to the downstream branches of branches 74-75. This disparity results in a broader scope of effects on the PVs at node 33 when the same PVs are connected. This suggests that the choice of transmission line materials significantly influences the energy flow through the power system.

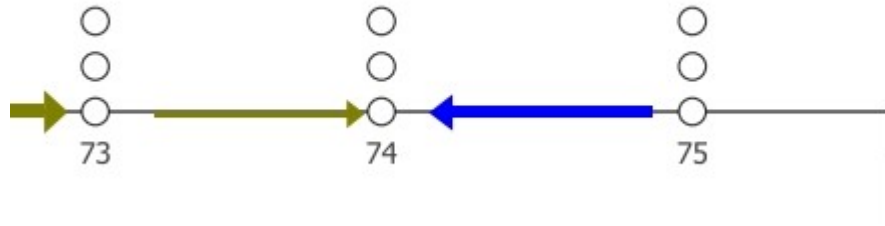


Figure 4.6: Power flow at node 75

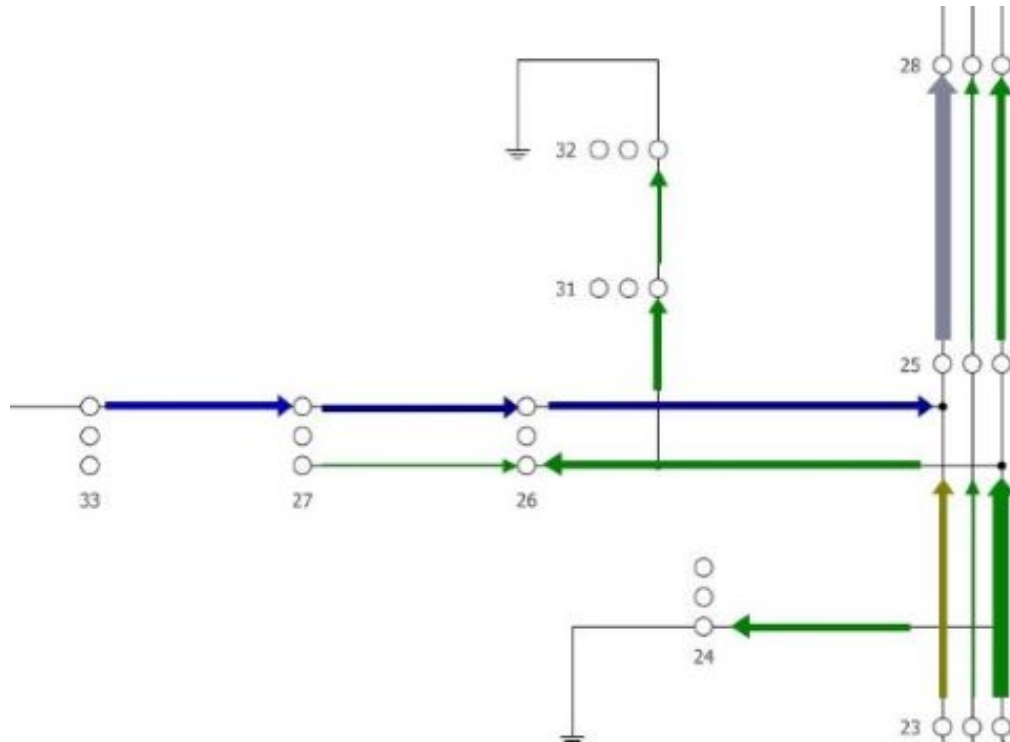


Figure 4.7: Power flow at node 25

Branches 44-47 and 27-33 appear brighter in color in Figures 4.8 and 4.9 compared to their downstream branches, indicating relatively higher G and B parameters. This aligns with the actual power system scenario, as these branches are circuits connecting to the distributed generation (DG).

In Figure 4.3, the magnitude of flows is depicted through power flow widths. It is noticeable that as the distance from the substation and DGs increases, the width of power flow on branches narrows. Unlike conventional systems without DG, the power flow in the radial distribution network gradually decreases along a uniform direction. However, with DGs, particularly the

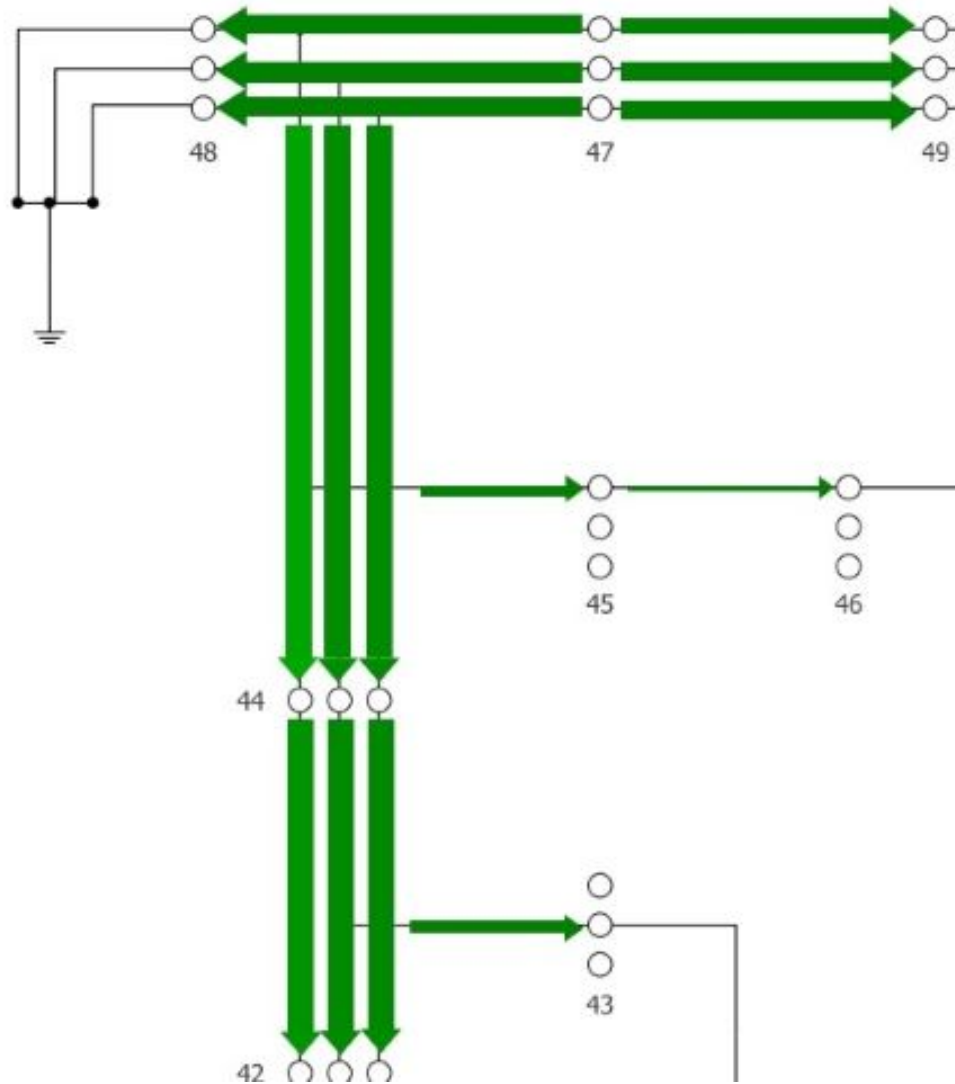


Figure 4.8: Power flow at branches 44-47

wind turbines at node 47, not only does the power direction change in the distribution network, but the power amount is also no longer uniform as the radial network diminishes.

## 4.4 Discussion

The examination of distribution network loss allocation extends beyond the equitable distribution of losses among participants. It serves as a valuable mechanism for facilitating power flow and energy flow tracing within distribution networks, as outlined previously. Furthermore, considering that carbon emissions in the power system stem from energy consumption [86], the

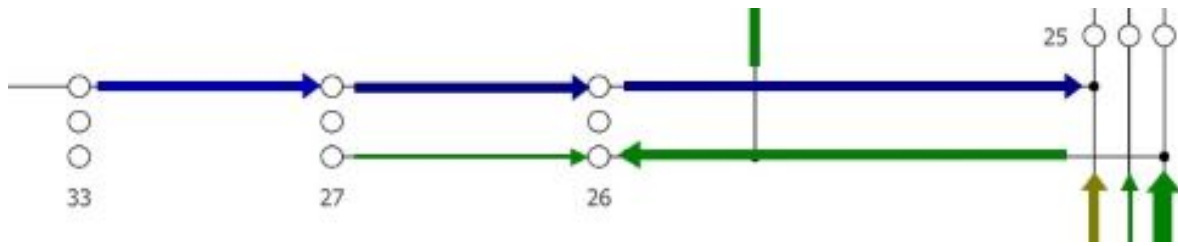


Figure 4.9: Power flow at branches 27-33

methodology outlined in this project also enables carbon tracing within the distribution network.

The surge in distributed energy resources (DERs) has transformed consumers into prosumers in the electricity market, fostering peer-to-peer energy trading [87, 88]. This shift raises pertinent questions for electricity markets regarding pricing and incentive tariff provision. The distribution network loss allocation method proposed in this paper offers a solution to the pricing dilemma, as it leverages circuit theory principles and considers the actual conditions of the power system. Figure 4.10 illustrates these interconnections. Power flow tracing involves tracking the path of electricity from generation to consumption, helping to identify how energy moves through the grid and where losses or bottlenecks may occur. This information is vital for determining appropriate pricing structures, as it allows grid operators to better understand the true costs associated with delivering electricity to different locations within the network. Energy flow tracing extends this concept by not only tracking the movement of electricity but also the contribution of various energy sources, particularly in a grid with a high penetration of renewables. By understanding which sources are feeding into the grid at any given time, and where that energy is consumed, energy flow tracing can inform the design of incentive tariffs that promote the use of clean energy. For instance, tariffs could be adjusted to provide higher incentives for consuming energy when renewable generation is high, thus supporting the integration of variable renewable sources like solar and wind. Carbon flow tracing adds another layer by tracking the carbon emissions associated with energy production and consumption. This tool is essential in a low-carbon transition, as it helps to ensure that energy is not only efficiently produced and consumed but also that it aligns with broader environmental goals. By accurately tracing carbon flows, policymakers can design tariffs and incentives that reflect the carbon intensity of energy consumed, encouraging the use of lower-carbon energy sources and helping to achieve emissions reduction targets.

The integration of these tracing methods with pricing and incentive tariff structures creates a more transparent and responsive electricity market. Prosumers can be better informed about the impact of their energy production and consumption decisions, allowing them to optimize their behavior not only to reduce costs but also to contribute to grid efficiency and sustainability.

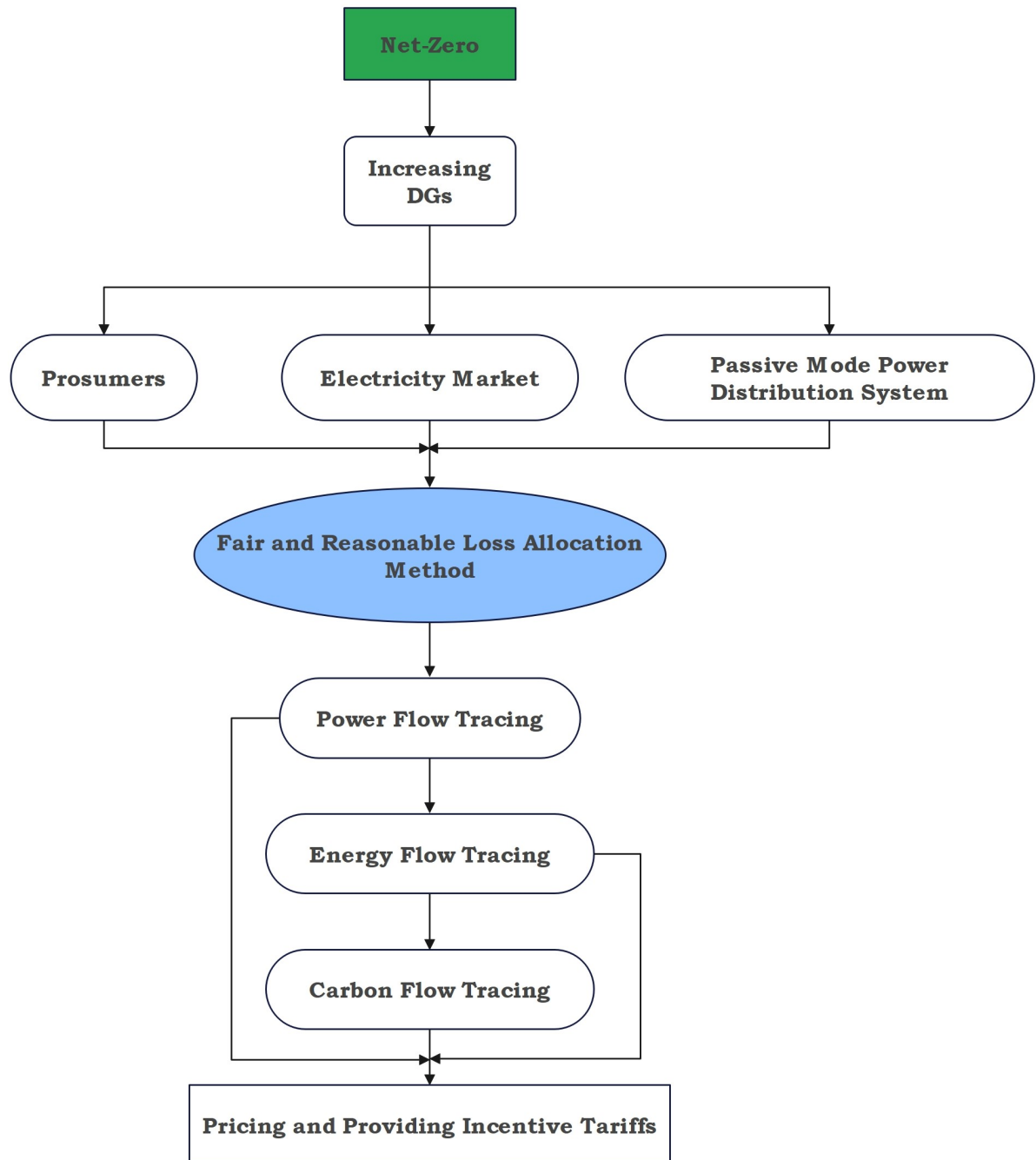


Figure 4.10: Relationship between distribution network loss allocation and carbon tracing.

Visual representations of power flow tracing offer clear energy insights to distribution network stakeholders. This is particularly valuable for users, encompassing consumers, distributed generators, and prosumers, aiding them in their planning for usage and generation. Figure 4.11 illustrates the practical application of power flow tracing visualization for these stakeholders in the distribution network. For network operators, such visualizations enable the quick identification of bottlenecks, congestion points, and areas of loss, thereby supporting more informed decision-making on load balancing, infrastructure upgrades, and efficiency improvements. For non-technical stakeholders, including policymakers and investors, these visual representations demystify the intricate workings of the power system, making it easier to comprehend and engage with energy management decisions. Additionally, visual tools enhance real-time monitoring and diagnostics, allowing for immediate responses to operational issues such as unexpected load fluctuations or generation shortfalls. For residential and commercial consumers, these visual tools make it easier to grasp the flow of electricity from generation sources, such as renewable energy installations, to their homes or businesses. This transparency allows consumers to see the impact of their energy usage patterns, helping them make informed decisions about energy efficiency and conservation. Additionally, visualizations can illustrate the benefits of participating in demand response programs, where consumers adjust their energy usage during peak times to reduce costs and support grid stability. For prosumers—those who both consume and produce energy, typically through solar panels—visual power flow tracing helps track the balance between their energy production, consumption, and any surplus sold back to the grid. By clearly depicting these energy flows, visual tools empower consumers to optimize their energy consumption, reduce costs, and contribute to a more sustainable energy future.

Power flow visualization provides operators with real-time insight into the current state of the electrical grid. By visually representing power flows, voltage levels, and system loads, operators can quickly identify areas of congestion, potential overloads, or voltage instability. This real-time feedback is crucial for making timely decisions to maintain grid reliability and prevent outages.

In addition, as renewable energy sources, such as wind and solar, become more prevalent, power

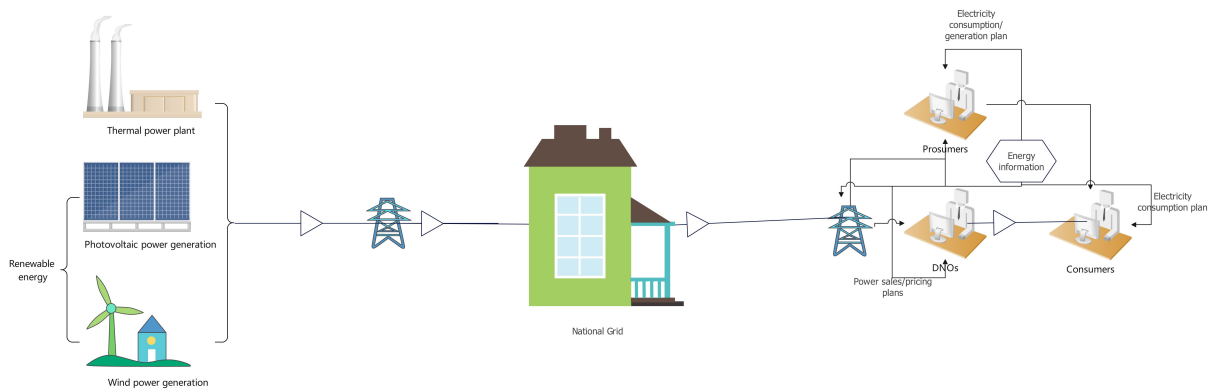


Figure 4.11: The application of power flow tracing visualisation on distribution network stakeholders.

flow visualization plays a critical role in managing their intermittent nature. Visualization tools can show the impact of renewable generation on grid stability, helping to optimize the integration of these sources while minimizing curtailment and ensuring that the grid remains balanced.

For consumers, particularly those who generate their own power (e.g., through solar panels), power flow visualization tools can provide insights into how their energy production interacts with the broader grid. This enables more informed decisions regarding energy usage, storage, and even participation in energy markets.

Moreover, consumers benefit from the increased transparency that power flow visualization provides. By making grid operations more understandable, consumers can gain insights into how their energy usage impacts the grid and how their costs are determined, particularly in systems with variable pricing or demand response programs. Additionally, consumers participating in demand response programs can better align their usage with grid conditions, potentially lowering their energy bills.

Finally, power flow visualization enhances decision-making processes by presenting data in a more accessible and interpretable format. Complex data sets related to grid conditions can be transformed into visual insights, making it easier for stakeholders at all levels to make informed decisions regarding grid operations, investments, and policy formulation.

Real-time monitoring of energy composition and transaction prices is increasingly critical in modern power systems due to its profound impact on energy management, consumer engagement, and overall grid efficiency. As energy systems become more complex and diverse, with a growing mix of renewable and traditional energy sources, the ability to track and respond to real-time data becomes essential. The goal of implementing power flow visualization in the distribution network is to present it in a straightforward manner for all participants. Figure 4.12 outlines a software interface designed for real-time monitoring of energy composition and transaction prices. This interface offers a platform for electricity market stakeholders to engage with information, promoting peer-to-peer energy trading. The real-time power flow displayed in the interface at different times of the day show the energy composition thereof by means of colour differences. Depending on the energy mix, the tariffs are adjusted for each time period. With this interface information, users can monitor their energy use and tariffs at any time to plan their own electricity consumption behaviour.

For consumers, this capability offers significant advantages. Enhanced decision-making is perhaps the most immediate benefit, as consumers can adjust their energy usage based on the current availability and cost of energy, leading to substantial cost savings. For instance, industrial consumers might shift operations to periods of lower energy prices or higher renewable energy availability, thereby optimizing their energy expenditure and reducing their carbon footprint. This also contributes to broader grid stability by flattening demand peaks and reducing stress on the system.

In addition to cost optimization, real-time monitoring introduces greater transparency into the energy market. Consumers gain insights into the environmental impact of their energy consumption, fostering a shift towards greener energy choices. This transparency also drives utilities to be more accountable, leading to more sustainable energy production and distribution practices.

From a grid management perspective, real-time monitoring enhances the ability to integrate renewable energy sources, which are inherently variable. By understanding the real-time composition of energy, grid operators can better manage supply and demand, reduce the need for costly

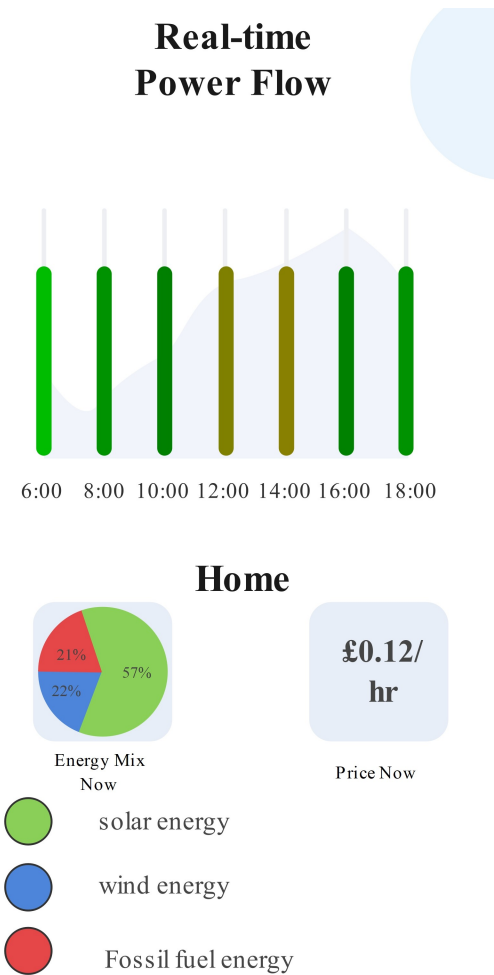


Figure 4.12: Desired software interface

reserves, and enhance grid reliability. This is especially important as the share of renewables in the energy mix continues to grow.

Moreover, the empowerment of consumers through access to real-time data cannot be understated. It enables them to engage more actively with the energy market, making informed choices about their energy provider and consumption patterns. This democratization of energy information aligns with broader trends towards decentralized and consumer-centric energy systems, ultimately supporting the transition to a more sustainable and resilient energy future.

## 4.5 Conclusion

This project introduces a method for allocating losses in unbalanced distribution networks, which serves as the foundation for visualizing flow tracing by colorizing power flows. The goal of power flow tracing can be achieved based on the results of the loss allocation in the distribution network, and the colouring method can be combined with the results of the power flow tracing to visualise the currents. This approach delivers dependable electrical and economic data to distribution network operators while providing consumers with easily comprehensible energy details through customizable colored and width-adjusted power streams. This contributes significantly to achieving the transparency and equity essential in the electricity market.

Through the simulation of the adjusted IEEE123 node system, it becomes evident that the visualization technique outlined in this study properly represents the energy makeup and magnitude of each branch. Furthermore, the integration of numerous Distributed Generators (DGs) not only alters the energy composition within the power system but also impacts the flow of power.

# Chapter 5

## Wheeling Charge Design based on Power Flow Tracing

### 5.1 Introduction

The restructuring of the electrical industry has transformed it from a vertically integrated sector into a segmented one characterized by competition among participants. This new framework has introduced open access to transmission lines and mandatory grid connections, enabling generators to deliver their energy to primary consumer centers. This shift has fostered a competitive environment among both generators and consumers, with the transmission network emerging as a crucial element in electricity markets.

A significant issue in this context is determining how to fairly charge users for utilizing transmission facilities while ensuring that transmission utilities can recover their costs. Numerous methodologies have been developed to cover the costs of transmission services. Additionally, methods have been devised to estimate the power contributed by individual generating units to lines and loads. Both approaches aim to allocate the charges for using the transmission system. This chapter will discuss the issues surrounding the use of system charges, particularly in relation to the pricing of transmission services. This chapter examines the phenomena of wheeling

and the associated costs, emphasizing the significance of wheeling charges as a component of use of system charges. Then, this chapter will propose a flow-tracing based allocation of the wheeling charges and apply it to the IEEE123 power saving system for simulation at the end of the chapter.

## 5.2 Use of System Charges

Use of system charges are fundamental to all current electricity transmission tariffs and are central to discussions on transmission open access arrangements. These charges cover the costs of constructing, maintaining, and operating the transmission system, which are incurred by the transmission utility in its business activities. The transmission utility imposes these charges on distributors, generators, and any transmission system users for their use of the shared transmission network facilities. The system charges design is generally following the rules below (the list is not comprehensive) [89]:

- 1) The charges should accurately recover the appropriate amount of revenue and maintain consistency.
- 2) The charges should offer efficient economic signals to users, reflecting the incremental costs of providing transmission capacity.
- 3) The charges should be non-discriminatory, treating all partners and classes of users equally.
- 4) The charges should be as simple, predictable, and transparent to users as possible.

While the concept of these charges varies among transmission utilities around the world, this chapter specifically discusses the use of system charges within the context of the transmission utilities of the UK.

### **5.3 Elements of Use of System Charges**

The determination of use of system charges is based on a point model that is independent of specific transactions. All users of the system contribute to its costs through annual use-of-system charges. The components included in the use-of-system charges are determined by the transmission utility. Typically, these charges for using the transmission system consist of the following elements:

- 1) A system service charge encompasses the assets necessary to establish and maintain a fundamental network with stable voltage and frequency, enabling the connection of generators and loads to all points of the main system.
- 2) An infrastructure charge encompasses the remaining assets of the main interconnected system needed to ensure firm transfer capacity and system security.
- 3) An exit charge pertains to the assets necessary for establishing connections between the transmission system and the distribution system, as well as between the transmission system and any customers connected directly to the transmission network.
- 4) An entry charge contributes to the assets needed for strengthening and connecting to the primary interconnected transmission system due to new generation connections.
- 5) A wheeling charge is the fee for utilizing the transmission network. This fee is applied when a vertically integrated utility provides wheeling services to particular entities, such as non-utility generators and large users.

### **5.4 Allocating a portion of the use of system charges**

Transmission utilities vary in their rationale for allocating use of system charges to users. In this context, users can be categorized as generators, demands, and wheelers. The wheelers refer to the utilities whose networks are utilized for wheeling purposes. Therefore, it is necessary to determine which entities are responsible for paying these charges and to what extent (design of the

pricing details). However, in essence, there are three possible fundamental ways of allocation:

- 1) All charges are allocated to the generator.
- 2) All charges are attributed to the electricity demand.
- 3) The charges are divided between the generator and the electricity demand.

However, to ensure fairness in transmission pricing, allocation schemes should possess the following characteristics: they must fully recover the costs of transmission services, and the allocation should accurately reflect the actual usage of the service. This means that generators or consumers should pay for transmission services based on their specific utilization of the transmission network. Within these frameworks, Latin American countries and certain European nations have adopted varied approaches to distribute charges for using transmission system services among users. For instance, in both Chile and Argentina, early adopters of deregulation, they opted to allocate the charges exclusively to the generators. This decision was justified on the basis that generators require transmission services to deliver electricity to consumers and compete in the market. On the contrary, in England and Wales, the charges for transmission services are allocated between generators and consumers in a ratio of approximately 27:73 [90]. This distribution helps maintain a balanced revenue structure for overall transmission services. Other countries expand the application of these charges to include consumers and entities involved in wheeling services.

## **5.5 Wheeling and Wheeling Charges**

Wheeling is one of the most significant electrical supply options available to transmitting utilities. Historically, wheeling was not a major concern as utilities were required to provide it only on a very limited basis. However, with deregulation, wheeling has garnered significant attention due to the increase in the number and variety of wheeling transactions, involving multiple parties. Electricity from the seller to the buyer travels through multiple intermediary utilities. Each utility operates as an individual control area, participating in a more intricate wheeling transac-

tion. The key issues to address in this context include determining the amount of power to be wheeled through each path, establishing the appropriate wheeling charges for each transaction, and finding optimal methods for making these decisions.

The following sections will cover the general concept of wheeling, including its various types and durations. It also examines the costs involved in wheeling transactions and the determination of wheeling charge rates.

### **5.5.1 The Concept of Wheeling**

Wheeling has various definitions depending on the preferences of different authors. Wheeling can be defined as the use of a system's transmission or distribution facilities to transmit power on behalf of another entity or entities. It can also be described as the utilization of one party's transmission system for the benefit of another party or parties. A straightforward definition would be "Wheeling involves transmitting power from a seller to a buyer using a network owned by a third party [91]". A wheeling transaction involves a utility transmitting electric power on behalf of another entity or entities, without generating or using the power to meet its own native load requirements. One condition that must be met is that the receipt and delivery of wheeled power are simultaneous [92].

A wheeling transaction involves at least three parties: a seller, a buyer, and one or more wheeling utilities that transmit the power from the seller to the buyer. The third party receives payment for the use of its network. Figure 5.1 illustrates a basic wheeling topology. In this example, Utility A aims to sell power to Utility C, but there is no direct connection between them. Utility B acts as the intermediary wheeling utility between A and C. Thus, the power sold by Utility A to Utility C must pass through Utility B, meaning the power is wheeled through B. These transactions are coordinated among the supplier, the recipient, and the intermediate wheeling systems. Whilst the topology and the direction of links seem straightforward, the combination of various utilities (various entities including energy suppliers and aggregators) can result in a complex network of transactions.

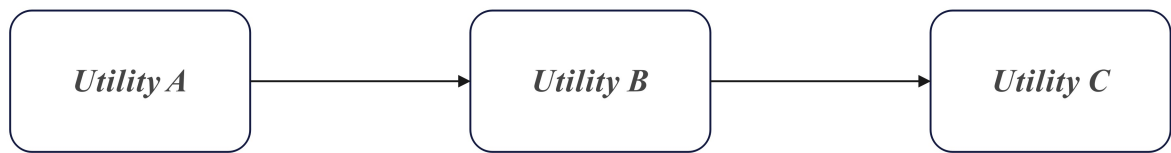


Figure 5.1: Basic Wheeling Topology

In this example, the power wheeling is achieved by increasing generation at the supplying utility, Utility A, and decreasing an equal amount of generation at the receiving utility, Utility C. This process alters the power flow pattern across the entire system, including the intermediate utility, Utility B. To compensate for the use of Utility B's transmission system assets, either Utility A, Utility C, or both should pay a wheeling charge for transmission access.

### 5.5.2 Types of Wheeling

There are various types of wheeling, determined by the relationship between the wheeling utility and the other two parties involved. There are four main categories of relationships involved in wheeling [93].

#### 1) Utility to Utility

This involves the transfer of bulk power from one regulated utility to another regulated utility through the transmission network of an intervening utility. For example, utility A in a region with surplus electricity supplies transmits power through Utility B's network to Utility C, which needs additional electricity.

#### 2) Utility to Private User or Requirements Customers

This scenario occurs when a private user or a requirements customer, such as an industrial customer, buys energy from a regulated utility outside their geographical service area. To facilitate this transaction, the intervention of an intermediate utility for transmission service is necessary. For example, a utility company delivers power to a large industrial factory that is not part of the utility's typical customer base, under a special wheeling agreement.

3) Private Generator to Utility

This situation involves a private generator selling power to a utility that does not cover the generator's geographic location within its service territory. For example, a wind farm owned by a private company transmits electricity to the local utility grid under a power purchase agreement.

4) Private Generator to Private User

This involves a private generator selling power to a private user, with both parties located within the service territory of the wheeling utility. For example, a solar power plant owned by a private company wheels electricity through the utility's transmission system to a private industrial complex under a bilateral contract.

Wheeling can occur between individual buses or areas.

- a) Type 1): illustrates area-to-area wheeling, where the selling and buying utilities cover geographical areas interconnected by a wheeling utility.
- b) Type 2): also represents area-to-area wheeling, unless the requirements customer is so small that it is fed at only one bus, in which case it becomes area wheeling.
- c) Type 3): represents bus-to-area wheeling.
- d) Type 4): represents bus-to-bus wheeling, where the seller and buyer are located at different buses.

### **5.5.3 Nature and Duration of Wheeling**

Wheeling services can vary in their firmness, ranging from firm to uninterruptible. The most stringent form of firmness is known as 'native' firm load, where the priority of the wheeling transaction equals that of the utility's own load. Interruptible wheeling services allow the utility to suspend transmission under certain conditions, such as when surplus capacity or transmission

availability is limited. Various categories exist to classify wheeling services based on their type, which will be elaborated upon below [94,95].

**A) Firm Wheeling Service**

This type of wheeling service guarantees transmission capacity to the wheeling customer without interruption. The utility providing the service ensures that the capacity will be available whenever needed by the customer. Typically, firm wheeling services are subject to higher fees due to the assured availability.

**B) Non-Firm (or Interruptible) Wheeling Service**

Non-firm wheeling services do not guarantee uninterrupted transmission. The utility providing the service reserves the right to interrupt or curtail transmission under certain conditions. These conditions may include periods of high system demand, maintenance needs, or unexpected system constraints. These conditions may include periods of high system demand, maintenance needs, or unexpected system constraints.

**C) Point-to-Point Wheeling**

Point-to-point wheeling involves the transmission of electricity between specific points, usually from one designated point of injection to a specific point of withdrawal. It requires a dedicated transmission capacity between the points identified in the agreement.

**D) Network (or Grid) Wheeling**

Network wheeling allows for the transmission of electricity over the utility's entire network or grid. It provides more flexibility than point-to-point wheeling as it allows access to various points within the grid. Network wheeling agreements are more complex and may involve multiple points of injection and withdrawal.

### **E) Dynamic (or Real-Time) Wheeling**

Dynamic wheeling refers to agreements where transmission capacity can be adjusted in real-time based on the changing needs of the grid and customers. It enables more flexible and responsive electricity transfers, optimizing the use of available transmission capacity.

### **F) Contract Wheeling**

Contract wheeling involves agreements between utilities and customers for the long-term or short-term transmission of electricity. These contracts specify the terms and conditions under which wheeling services are provided, including pricing, duration, and any special conditions.

### **G) Open Access Transmission**

Open access transmission policies allow multiple entities (generators, suppliers, consumers) to access and use the transmission system on a non-discriminatory basis. It promotes competition in electricity markets by ensuring fair and equal access to transmission services for all participants.

## **5.5.4 Costs related to wheels**

Wheeling costs are incurred by all utilities that experience changes in power flows over their transmission lines during a specific transaction, regardless of whether those lines are part of the contract path. The costs of providing wheeling services vary between different systems and types of wheeling transactions. While the existing capacity can cover most transactions, other transactions may have a need for additional lines. Depending on the circumstances, some of the cost components may appear differently, such as high, low, negative, or possibly not incurred at all. In this section, the cost components related to wheels transactions are discussed in detail [95].

### **A) Operating Cost**

Operating costs for electricity wheeling transactions involve expenses associated with the day-to-day functioning and maintenance of the transmission network, ensuring efficient, reliable, and safe operations. These costs include several key components. Maintenance costs cover routine inspection, repair, and upkeep of transmission lines, substations, transformers, and other infrastructure to prevent failures and ensure reliability. Corrective maintenance addresses repairs or replacements after faults or failures, while preventive maintenance aims at preventing breakdowns and extending the lifespan of equipment.

Labor costs encompass salaries and benefits for engineers, technicians, and other personnel involved in network operations and maintenance. Training and development expenses ensure staff are knowledgeable about the latest technologies, safety protocols, and regulatory requirements. Energy costs include station power for lighting, heating, cooling, and auxiliary equipment, as well as loss compensation to cover energy losses during transmission due to resistance and other factors.

Administrative costs involve billing and accounting for wheeling services, managing accounts, financial reporting, and customer service for handling inquiries, complaints, and service requests. Regulatory and compliance costs include expenses for meeting reporting requirements set by regulatory bodies, periodic audits for compliance with industry standards, safety regulations, environmental guidelines, and licensing fees for operating the transmission network.

Monitoring and control costs cover Supervisory Control and Data Acquisition (SCADA) systems for real-time network monitoring and control, along with communication systems necessary for coordinating operations and ensuring network security. Insurance costs consist of liability insurance for potential operational liabilities and property insurance for protecting physical assets against damage or loss.

Depreciation and amortization account for the reduction in value of transmission infrastructure over time due to wear and tear, and the gradual expensing of capital investments over their useful life. Miscellaneous costs include safety and security expenses for personnel and network pro-

tection, research and development (R&D) costs for technology advancements and operational improvements, and environmental management expenses for monitoring and mitigating the environmental impact of transmission operations.

These operating costs can vary based on the context, such as urban versus rural transmission, where urban areas may have higher labor and energy costs due to higher wages and denser infrastructure, whereas rural areas might incur more significant maintenance and line loss costs due to longer transmission distances. Similarly, high-voltage transmission networks generally have higher equipment and maintenance costs but lower line losses compared to low-voltage systems.

To manage these operating costs effectively, utilities can implement strategies such as efficiency improvements through advanced technologies and best practices, outsourcing specific operational tasks to third-party service providers to leverage specialized expertise and achieve cost savings, and optimizing energy use within the network to minimize station power consumption and loss compensation costs. Understanding and managing these operating costs is crucial for ensuring the financial viability and operational efficiency of electricity transmission networks, ultimately benefiting both utilities and their customers.

### **B) Opportunity Cost**

In the context of electricity wheeling transactions, opportunity cost is a crucial component that reflects the potential economic benefits forfeited when a utility allocates its transmission capacity to facilitate power transfers for third parties. This concept holds significant weight in assessing the overall cost implications of such arrangements. When a utility engages in wheeling, it essentially gives up the opportunity to utilize its transmission infrastructure for its own electricity distribution needs or for potentially more profitable commercial activities. Evaluating opportunity cost entails considering alternative revenue streams that could have been generated had the transmission capacity been used differently, such as for native load services during peak demand periods or for securing higher-paying wheeling contracts. Market conditions, including variations in electricity supply and demand dynamics and regulatory frameworks, further

influence the calculation of opportunity costs associated with wheeling transactions. By comprehensively analyzing these opportunity costs, utilities can make informed decisions regarding the optimal allocation of their transmission capacity to maximize revenue and operational efficiency in a competitive energy market landscape.

Some mechanisms through which benefits unrealised due to lost opportunities can rise:

- 1) Market price variations: When operational constraints prevent the optimal utilization of transmission capacity, it can lead to missed opportunities to sell electricity at higher market prices. This is particularly significant in volatile energy markets where prices fluctuate frequently [96].
- 2) Renewable energy integration: Constraints on transmission capacity can hinder the integration of renewable energy sources. For instance, when renewable energy generation exceeds local demand but transmission constraints prevent exporting surplus electricity to other regions, potential revenues from selling renewable energy can be lost [97].
- 3) Capacity utilization: Efficient use of transmission capacity allows for maximizing the utilization of existing infrastructure. Constraints that limit this capacity can lead to underutilization and missed opportunities to transport electricity from low-cost generation sources to demand centers.
- 4) Resource optimization: Optimal resource scheduling and dispatch depend on the availability of transmission capacity. Constraints can lead to suboptimal scheduling of resources, such as dispatching more expensive generation sources or relying on local generation despite cheaper alternatives being available elsewhere.
- 5) Investment decisions: Constraints in transmission capacity can influence investment decisions in new generation or transmission infrastructure. Higher costs or delays in realizing new projects due to capacity limitations can impact the overall economic benefits and long-term planning in the energy sector.

- 6) Risk Mitigation: Uncertainties and risks associated with transmission constraints may lead to higher costs for market participants, including increased hedging costs or risk premiums in energy trading and contracting.

Opportunity cost for a utility offering firm wheeling may arise depending on the terms of interruption outlined in the wheeling contract, whereas it may not arise with interruptible wheeling. This cost is closely tied to how effectively and intensively transmission facilities are utilized.

### **C) Reinforcement Cost**

Reinforcement costs in the context of electrical power systems refer to expenses incurred in upgrading or expanding transmission infrastructure to accommodate increased demand or integrate new generation sources. These costs are necessary when existing infrastructure lacks the capacity to efficiently transport electricity from generation centers to consumption centers due to factors like distance, voltage requirements, or network congestion. Typically, reinforcement costs involve investments in constructing new transmission lines, upgrading substations, installing transformers, or implementing advanced control and monitoring systems. The decision to incur reinforcement costs is driven by the need to ensure grid reliability, reduce transmission losses, and facilitate the integration of renewable energy sources. However, these investments can be substantial and require careful planning to optimize cost-effectiveness while meeting future demand growth and regulatory requirements.

### **D) Existing System Cost**

All the components of the wheeling transaction cost mentioned above stem directly from the transaction itself. These represent the immediate expenses associated with delivering transmission services and are collectively referred to as the incremental cost of transmission transactions. The existing system cost of a wheeling transaction refers to the portion of the existing transmission system's cost that needs to be allocated to that particular transaction. The cost of existing transmission encompasses the investment in constructing the transmission system and the ongoing expenses for maintaining it, including embedded costs and operation and maintenance

(O&M) costs of the transmission system hardware. Notably, the wheeling transaction would not actually be the cause of any new costs involving the use of existing transmission facilities. These facilities have been built and the costs concerning them have been paid. Therefore, the issue that needs to be addressed is not the costs incurred, but how to reasonably allocate the costs of the existing transmission system to those who use it.

In practice, the cost of the existing transmission system is generally greater, so in general, the largest component of the total cost of the transaction is the cost of the existing system for the transmission transaction. Due to this and other historical factors, regulatory agencies have focused significantly on this cost in their oversight of utilities' revenue collection.

Firstly, who should bear the cost of the existing transmission system? There is no communal approach to solving this problem. Some researchers have argued that new wheeling transactions should not be the bearer of these costs. Some researchers believe that all participants in the power system should bear the costs of the existing transmission system. However, most interested parties believe that the cost of the existing transmission system should be allocated by all customers of firm wheeling transactions. This consideration is based on the utility obligation to always reserve transmission capacity for firm wheeling transactions.

Secondly, on what basis should the costs of the existing transmission system be allocated? The more common approach is to first define and evaluate a measurement of the capacity of the transmission system used for wheeling transactions. This measurement is then used as the basis for allocating existing transmission system costs. Several measures for transmission system capacity usage are already in use or being proposed by the industry. The most straightforward and widely used capacity utilization measure is the power demand related to the transaction. This approach is commonly referred to as the "postage stamp" or "rolled-in method". Other proposed capacity use measures are based on power flow and reflect the actual operation of the power system. One such approach is the "MW-Mile methodology," which uses the MW-mile usage of the power system as the capacity use measure [92].

### **E) Wheeling Charges**

Wheeling charges are fees imposed by transmission service providers for the use of their transmission network to transport electricity from one location to another. These charges are crucial for covering the costs associated with maintaining, operating, and upgrading the transmission infrastructure. The primary components of wheeling charges include the cost of transmission losses, network usage, congestion management, and administrative expenses.

Transmission losses occur when some amount of electricity is lost as heat during the transmission process, reducing the overall efficiency of electricity delivery. Wheeling charges help compensate for these losses, ensuring that the transmission service provider recovers the cost of the lost energy. Network usage charges are based on the amount of electricity transmitted and the distance it travels through the network. This component ensures that users contribute fairly to the maintenance and operational expenses of the transmission infrastructure.

Congestion management costs are incurred when the transmission network reaches its capacity limits, necessitating measures to manage the flow of electricity and prevent overloads. These measures might include redispatching generation or investing in infrastructure enhancements. Administrative expenses cover the costs associated with managing the wheeling transactions, including billing, monitoring, and regulatory compliance.

Wheeling charges are essential for the efficient operation of the electricity market. They promote transparency and fairness by ensuring that users who benefit from the transmission network contribute to its upkeep. Additionally, these charges incentivize efficient use of the transmission infrastructure, encouraging users to optimize their electricity usage and consider the impact of their transmission needs on the overall network. Effective wheeling charge structures are vital for the sustainability and reliability of the power grid, supporting the seamless integration of various generation sources and facilitating the delivery of electricity to consumers across different regions.

The method for calculating wheeling costs is a high-priority issue in the power industry due to the expansion of transmission facilities. The central issue in the wheeling debate is determin-

ing the rates that a wheeling utility should charge [98]. Additional issues related to wheeling include identifying the beneficiaries of wheeling, determining the cost-risks the wheeling utility should recover, assessing which types of wheeling are socially desirable, and considering whether wheeling rates should be adjusted in near real-time to reflect changes in operating conditions. Several concepts for calculating wheeling charges have been proposed in the literature, including approaches based on marginal cost pricing and embedded cost pricing [99,100]. However, the predominant method used to price transmission services across the utility industry is typically based on embedded cost methods. These methods typically establish wheeling rates using approaches like the postage stamp, contract path (or red line), and megawatt mile methods. Each of these methods has its advantages and drawbacks in determining wheeling charges, which will be detailed in the following section.

## **5.6 Wheeling charges derived from embedded cost methods**

Wheeling charges based on embedded cost methods are a mechanism used to determine the fees for transmitting electricity through a transmission network. Unlike other pricing approaches such as marginal cost or postage stamp methods, embedded cost methods rely on historical or predetermined costs associated with building, operating, and maintaining the transmission infrastructure. These charges are typically calculated based on the past investments in the transmission network, including the costs of equipment, construction, maintenance, and depreciation over time.

Embedded cost methods aim to recover the original investment in transmission infrastructure fairly across all users who utilize the network. This approach considers the specific costs associated with each component of the transmission system, such as substations, transmission lines, and other equipment. It also accounts for ongoing operational and maintenance expenses incurred by the transmission service provider.

One of the key advantages of using embedded cost methods for wheeling charges is their simplicity and predictability [101]. Since these charges are based on historical costs that are known

in advance, they provide clarity for market participants regarding the cost implications of using the transmission network. This transparency can facilitate long-term planning and investment decisions in electricity generation and consumption.

However, a limitation of embedded cost methods is their potential lack of alignment with current market conditions and efficiency considerations. These methods do not necessarily reflect the dynamic changes in demand, supply patterns, or technological advancements that may influence the optimal use of transmission infrastructure. Moreover, critics argue that embedded cost methods may not provide the right incentives for efficient network utilization and could potentially lead to inefficient outcomes in electricity markets.

Overall, while embedded cost methods offer a straightforward approach to determining wheeling charges based on historical investments and operational costs, their effectiveness in promoting efficiency and fairness in electricity transmission depends on how well they adapt to evolving market conditions and regulatory frameworks.

Based on these calculations, some general calculation approaches are reviewed and listed as follows [94, 102–104].

### **5.6.1 Postage Stamp Method**

The postage stamp Method is a straightforward approach used in the electricity industry to allocate transmission costs uniformly across a grid network. Similar to how postage stamps are priced uniformly for mail delivery regardless of destination, this method charges all users the same rate per unit of electricity transmitted, irrespective of the distance traveled or specific path taken through the transmission network. This uniform pricing mechanism aims to simplify cost recovery and administrative processes, making it easier to implement and manage. However, critics argue that the Postage Stamp Method may not accurately reflect the actual costs incurred for transmitting electricity over different distances or through congested versus uncongested areas of the grid. As a result, it may lead to inefficiencies by not incentivizing optimal use of transmission resources or encouraging investments in infrastructure where they are most needed.

Despite these limitations, the Postage Stamp Method remains in use in certain jurisdictions due to its simplicity and ease of implementation, especially in regions with less complex grid structures or where regulatory oversight prioritizes cost stability over cost reflectiveness.

### **5.6.2 Contract Path Method**

The contract path method is a mechanism used for allocating transmission costs that differs from the postage stamp method by assigning costs based on specific contractual agreements for transmission paths. Under this approach, transmission costs are allocated to users based on the predetermined paths or corridors through which electricity is transmitted. Each user or entity holding a transmission contract pays for the costs associated with the specific path they utilize, regardless of whether they fully utilize the capacity or not. This method aims to provide more transparency and cost accountability compared to the Postage Stamp Method, as it directly ties costs to the actual use of transmission paths. By aligning costs with usage patterns, the Contract Path Method encourages efficient allocation of transmission resources and can incentivize users to optimize their utilization of contracted paths to minimize costs. However, like other allocation methods, the Contract Path Method also has drawbacks, such as administrative complexity in managing multiple contracts and potential disputes over cost allocations when transmission paths are congested or underutilized. Despite these challenges, the Contract Path Method is favored in regions where transparency and cost visibility are prioritized, and where the grid infrastructure supports such contractual arrangements efficiently.

### **5.6.3 Distance-Based MW-Mile Method**

The distance-based MW-Mile method is a cost allocation technique used in electricity transmission networks to assign transmission costs based on the product of the distance electricity is transmitted and the amount of power transmitted (MW-miles). Unlike the postage stamp and contract path methods, which allocate costs uniformly or based on specific contractual paths, the distance-based MW-Mile method calculates costs according to the actual physical distance electricity travels across the transmission grid and the volume of electricity transmitted.

In practice, this method involves determining the distance between the points of electricity injection (generation) and withdrawal (consumption) on the transmission grid. Costs are then allocated proportionally to the product of this distance and the amount of electricity transmitted, measured in megawatts (MW). This approach aims to reflect the actual use of transmission infrastructure more accurately compared to methods that do not account for distance.

The distance-based MW-Mile method is valued for its ability to incentivize efficient use of transmission resources by encouraging generators and consumers to locate closer to each other, thereby reducing transmission distances and associated costs. By linking costs directly to the physical distance electricity travels, this method promotes economic efficiency and can help mitigate congestion on the grid by reflecting the actual spatial utilization of transmission capacity.

However, implementing the distance-based MW-Mile method requires detailed knowledge of the grid topology, accurate measurement of transmission distances, and robust data on electricity flows. Challenges may arise in regions with complex grid layouts or where accurate distance measurements are difficult to ascertain. Despite these challenges, the distance-based MW-Mile method remains a significant approach in transmission cost allocation, particularly in jurisdictions aiming for greater cost reflectivity and efficiency in electricity transmission.

#### **5.6.4 Power Flow-Based MW-Mile Method**

The power flow-based MW-Mile method is a sophisticated approach to allocating transmission costs in electricity networks, designed to reflect the actual flow of electricity and the corresponding stress on the transmission infrastructure. Unlike simpler methods such as the postage stamp or distance-based MW-Mile methods, which allocate costs based on distance and volume of electricity transmitted, the power flow-based MW-Mile Method considers the specific power flows and their impact on the grid's operation.

This method relies on detailed modeling of power flows through the transmission network. It calculates transmission costs by analyzing the power flow patterns, including factors such as line loading, voltage levels, and congestion points. The costs are allocated based on the physi-

cal miles that electricity travels and the dynamic utilization of the transmission capacity under various operating conditions.

Implementing the power flow-based MW-Mile method requires advanced grid modeling tools and real-time data on power flows. It is particularly valued for its ability to incentivize efficient use of the transmission grid by assigning costs in proportion to the actual stress placed on the system. By reflecting the operational dynamics of the grid, this method encourages generators and consumers to optimize their locations and operational strategies to minimize transmission costs and alleviate grid congestion.

However, the power flow-based MW-Mile method can be complex to implement due to the need for sophisticated computational tools and accurate real-time data on grid conditions. It also requires continuous updates and adjustments to reflect changes in electricity demand, generation patterns, and grid infrastructure. Despite these challenges, this method is increasingly adopted in regions aiming for more accurate cost allocation and efficient utilization of transmission resources to support reliable and cost-effective electricity supply.

Based on the power flow-based MW-Mile method, there are some sub-concepts.

#### **A) MW-mile Method (MWM)**

The MW-mile Method (MWM) is a widely-used approach for allocating transmission costs in electricity networks, focusing on the physical distance and volume of electricity transmitted through the grid. This method assigns costs based on the product of the megawatts (MW) transmitted and the distance (miles) over which the electricity travels. Essentially, it calculates the transmission cost per unit of electricity per mile of transmission. Equation (5.1) shows the cost allocation principle of the method.

$$R(u) = \sum_{allk} C_k \frac{|f_k(u)|}{f_k} \quad (5.1)$$

In Equation (5.1),  $R(u)$  is the allocated cost to customer  $u$ ,

$C_k$  is the cost of circuit  $k$ ,

$f_k(u)$  is  $k$ -circuit flow caused by customer  $u$ , and

$\overline{f_k}$  the capacity of  $k$ -circuit. The unit of these two terms is *MW*

The MWM operates on the principle that transmission costs should be allocated in proportion to both the amount of electricity transmitted and the distance it travels, reflecting the wear and tear on the grid infrastructure and the opportunity cost associated with transmitting electricity over longer distances. This method is relatively straightforward compared to more complex methodologies like Power Flow-Based MW-Mile or Contract Path methods, making it easier to implement and understand.

To apply the MWM, utilities typically calculate the total amount of electricity transmitted (in megawatt-hours, MWh) over specific transmission paths and multiply this by the distance (in miles) each unit of electricity travels. The resulting product provides a basis for allocating transmission costs, ensuring that generators and consumers contributing to higher transmission distances incur higher costs. This approach incentivizes efficient use of the grid by encouraging placement of generation closer to demand centers and reducing transmission losses associated with longer distances.

While the MWM offers simplicity and transparency in cost allocation, it may oversimplify grid dynamics and fail to capture the full complexity of congestion and operational constraints. Nonetheless, it remains a valuable tool in many regulatory frameworks for its ability to provide a clear and equitable basis for distributing transmission costs among market participants, thereby supporting the overall reliability and efficiency of electricity transmission and distribution systems.

### **B) Modulus Method (MM)**

In the Modulus Method (MM), the traditional line capacities used in the MW-mile method are substituted with the total of absolute power flows generated by all customers. This adjustment

aims to achieve full recovery of embedded costs associated with transmission. Equation (5.2) outlines the fundamental charging principle applied in this method.

$$R(u) = \sum_{allk} C_k \frac{|f_k(u)|}{\sum_{alls} |f_k(s)|} \quad (5.2)$$

where  $f_k(s)$  is  $k$ -circuit flow caused by customer  $s$  with the unit  $MW$

This approach, often referred to as the utilization method, operates under the assumption that customers are charged based on the actual capacity they use, including any additional reserve capacity required for system reliability, stability, and security criteria, or to account for adjustments needed due to uncertainties in the planning process. However, this method lacks incentives for customers to reduce their circuit load, which could otherwise improve system performance and delay the need for transmission investments.

### C) Zero Counter Flow Method (ZCM)

The Zero Counter Flow Method is an approach used to allocate wheeling charges in power transmission. In this method, counter flows, which are flows in the opposite direction to the primary power transfer, are set to zero. This adjustment simplifies the calculation of transmission costs by considering only the net power flows along transmission lines. By ignoring counter flows, the method focuses on the direct usage of the transmission network by different customers. This technique aims to fairly distribute the embedded costs of the transmission network among users based on their actual impact on the system, enhancing the transparency and efficiency of cost allocation. Equation (5.3) presents the allocation charge concept for this method.

$$R(u) = \sum_{allk} C_k \frac{f_k(u)}{\sum_{alls \in \Omega_{k+}} f_k(s)} \quad \text{for } f_k(u) > 0$$

$$R(u) = 0, \quad \text{for } f_k(u) \leq 0 \quad (5.3)$$

In this equation,  $\Omega_{k+}$  is the set of customers with positive flows on circuit  $k$ .

## 5.7 Proposed Concept of Wheeling Charge Calculation

As discussed above, the more widely used methods currently is power flow-based MW-Mile method. It needs to be realised by comparing line currents in the presence and absence of power trading, and these calculation tasks, which are only for Wheeling Charge, are cumbersome. Using the loss allocation method proposed by the research in Chapter 2, not only can the method of allocating wheeling costs be effectively addressed, but also the results of the loss allocation can be fully utilised by eliminating the need for a dedicated wheeling charge calculation step.

### 5.7.1 Power Flow Analysis

All the power transmission in the power system is because of the demand from the user side. In other words, without the demand for electricity there would be no transmission of electricity. Therefore, the allocation of Wheeling charges in the power system should be closely linked to the electricity consumption behaviour of customers.

The power loss allocation method proposed in Chapter 2 completely considers the path of the power consumed by each node. As shown in Figure 5.2, the inflow power at node 4 passes through lines 1-2, 2-3 and 3-4. Similarly, the inflow power at node 5 consists of power originating from the grid that passes through lines 1-2 and 2-5 and power originating from the DG that passes through lines 7-6 and 6-5. Therefore, the loss allocation results obtained in this way are reasonable when used as a method for allocating wheeling charges. This is because the grid path (range) used for the injected power at each node is taken into account.

In addition, the power loss allocation is calculated based on realistic system currents, and each user (node) is assigned a loss based on their own needs. This is also very much in line with the principle of the allocation of wheeling charges.

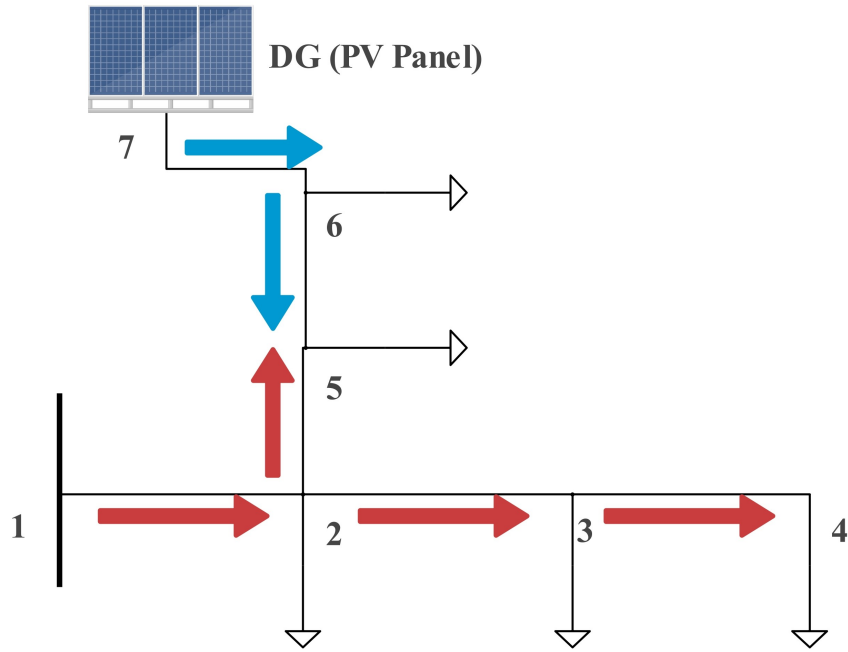


Figure 5.2: Power flow analysis along network lines.

### 5.7.2 Cost Allocation

As mentioned above, this research proposes the allocation of system cost based on “power flow tracing based power loss allocation method”, the Wheeling charge can then be calculated using

$$WC_i = \sum_{j=1}^n \frac{P_{Loss_{j,i}} \times A, C_j}{\sum_{k=1}^m P_{Loss_{j,k}}} \quad (5.4)$$

In Equation (5.4),  $WC_i$  is wheeling charge calculation based on power loss allocation method;  $P_{Loss_{j,i}}$  is the line flow in line  $j$  induced by transaction on bus  $i$ ;  $A, C_j$  is an annualized cost of line  $j$ ;  $n$  is a number of line in the system; and  $m$  is a number of load bus.

According to chapter 2, power loss can be calculated as:

$$P_{Loss_k} = Re \left\{ \sum_{k=1}^M i^{*k} \otimes (R^{(j)} * \sum_{q \in N(j)} (\beta^{kq} \otimes i^{kq})) \right\} \quad (5.5)$$

where  $M$  is the set of branches which connect node  $k$  to the root node,

$\beta^{kq}$  is the allocation factor matrix,

$R^{(j)}$  and  $X^{(j)}$  contain the resistance and reactance of all conductors including phases and neutral of branch  $j$ .

For the allocation factor matrix  $\beta^{kq}$ , the three allocation factors have been described in Chapter 2. Geometric allocation was chosen for wheeling charges allocation. Therefore, the allocation factor can be calculated with:

$$\beta_e = 1 + \frac{1}{2} \log \frac{i^e}{i^f}; \quad \beta_f = 1 + \frac{1}{2} \log \frac{i^f}{i^e} \quad (5.6)$$

### 5.7.3 Case Study

In this chapter, the IEEE123-node system is chosen as the system model for simulations. On one hand, it is because it is an unbalanced system, which corresponds to a real-world distribution network situation closely. On the other hand, the IEEE123-node system is relatively large and allows for comprehensive results for analysis. In addition, the original IEEE123-node system was modified in order to analyse the impact of distributed generations in the distribution network, as shown in the figure below (the same system in Chapter3).

In terms of distributed generation locations, to consider typical renewable power generation units; here a 1MW/500kVar wind turbine unit is connected at node 47, and two 40kW/20kVar PV panels are connected at node 33 and node 75 respectively.

For the current power system, the penetration of distributed generation is gradually increasing. Therefore, the pricing of wheeling charges should not be the same for different energy sources. In the case of sustainable energy generation, the wheeling charges arising from its use cannot be waived in order to incentivise users to use it. This does not guarantee the maintenance and protection costs of sustainable energy generation. In order to guarantee the cost to some extent and to have an incentive effect on the users, this study has priced the wheeling charges incurred by the use of sustainable energy sources and the use of conventional energy sources separately. In this case study, in addition to conventional energy sources, there is penetration of wind and solar energy respectively. In the United States, wheeling charges might range from 2 to 10 per

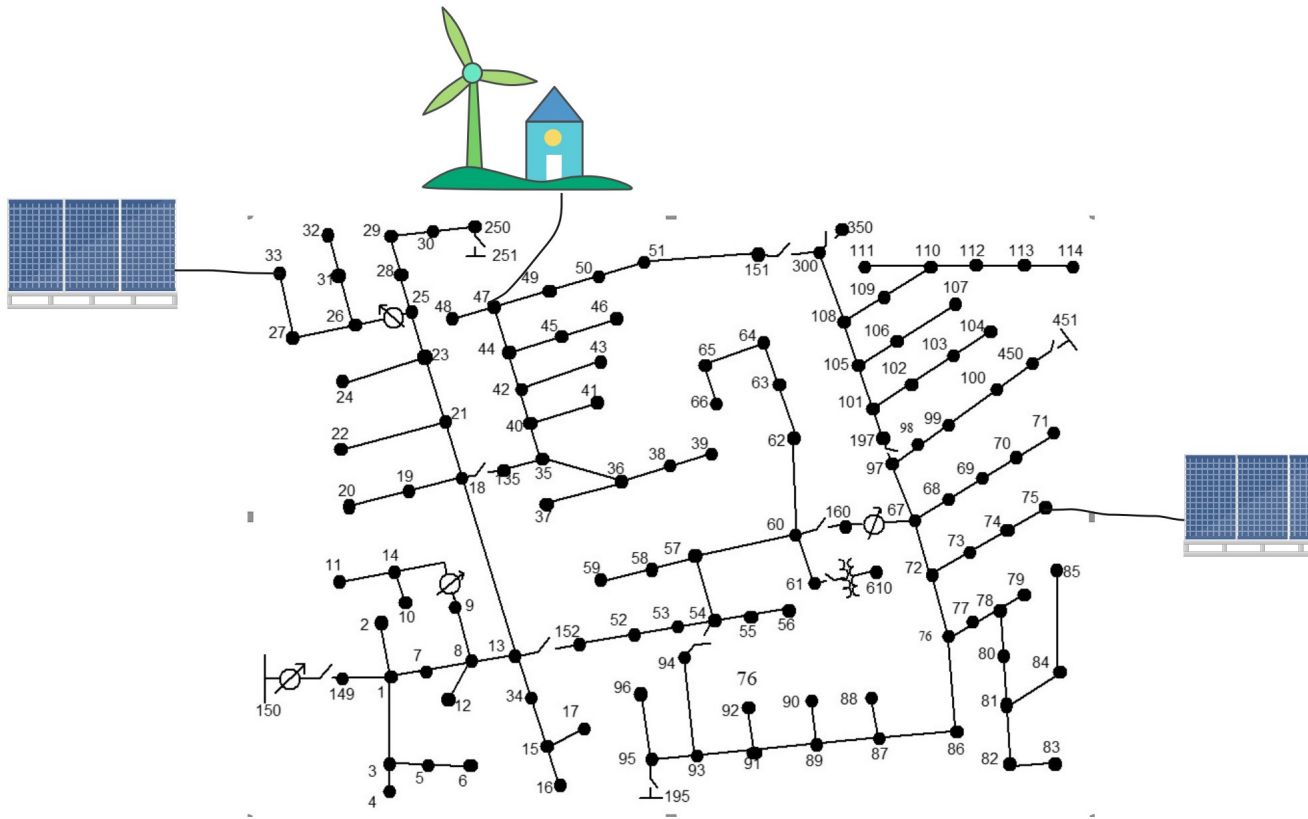


Figure 5.3: Modified IEEE 123-node system with renewable DG units

MWh, depending on the region and the specific transmission agreement. In this case study, the price is set at £3/MWh for wheeling charges generated from conventional energy sources and £1/MWh for wheeling charges generated from wind and solar energy.

In addition, wind and solar energy are seasonal. For solar, capacity is the highest in summer and the lowest in winter. Conversely, wind energy capacity is highest in winter but relatively low in summer. At the same time, there are also varying seasonal patterns in the electricity consumption behaviour of end users, with the general highest consumption in winter and the lowest in summer. Using the spring and autumn seasons as a baseline, Table 5.1 shows the adjustment factors for capacity and load for the simulations in this study based on season factors.

The one-day wheeling charges for spring and autumn, summer and winter are shown in separate tables in Appendix D. In addition, the spring and autumn wheeling charges for conventional and sustainable energy sources that do not differentiate between them are also shown in the tables in Appendix D.

Table 5.1: Adjustment factors for capacity and load

|              | Spring | Summer | Autumn | Winter |
|--------------|--------|--------|--------|--------|
| Wind Energy  | 1      | 0.75   | 1      | 1.5    |
| Solar Energy | 1      | 0.75   | 1      | 1.5    |
| Load         | 1      | 1.5    | 1      | 0.5    |

#### 5.7.4 Results Analysis

Comparing Tables D.1 and D.4, it is clear that separate pricing of fossil and sustainable energy wheeling charges can effectively reduce the wheeling charges borne by customers using sustainable energy. This is an incentive for users to use sustainable energy and for prosumers to become more involved. This fits the expectations of wheeling charges pricing and allocation.

For distributed generation at node 33, it is allocated a negative loss as shown in Table 5.2. However, just because it is in the role of generating electricity (it is assigned negative losses), it cannot be exempted from wheeling charges. At this point, the absolute value of the attrition reflects how much of the transaction it is involved in. It can be seen that because solar energy is more abundant in the summer, node 33 is involved in the most transactions. Node 33 is involved in fewer transactions in winter when solar capacity is lower, but it needs to replenish its own demand by consuming energy from the grid, so the wheeling charge borne by node 33 is not the lowest in winter.

Table 5.2: Results at node 33

| Node 33           | Spring/Autumn | Summer       | Winter       |
|-------------------|---------------|--------------|--------------|
| Allocated loss(w) | -1095.879966  | -1199.453933 | -743.2791438 |
| Cost(pence)       | 1028.810359   | 1091.311167  | 1044.099079  |

For nodes located downstream of the DG at node 33, they will pay different wheeling charges in different seasons. As shown in Table 5.3, the summer season has the least amount of wheeling charges to be paid by the users because of the availability of solar energy, and conversely the winter season has the most.

Table 5.3: Impact of node 33 on downstream nodes (pence)

| Node | Spring/Autumn | Summer      | Winter      |
|------|---------------|-------------|-------------|
| 25   | 0.029276526   | 0.003634522 | 0.069090338 |
| 26   | 0.006507644   | 0.004577409 | 0.030380723 |
| 27   | 0.005428319   | 0.004974046 | 0.010578977 |
| 28   | 800.9322452   | 442.7019025 | 2670.292458 |
| 29   | 871.0066429   | 483.0429265 | 2862.46515  |
| 30   | 0.004844673   | 0.010877447 | 0.011989469 |

Similarly, as solar distributed generation, the DG at node 75 has a smaller area of influence. With the exception of the summer months when solar capacity is sufficient to influence two of its downstream nodes (nodes 74 and 73), the other three seasons are only sufficient to supply their own demand. As a result, the wheeling costs borne by node 75 are highest in the summer months, as it is involved in more transactions. However, for nodes 74 and 73, which consume a portion of the sustainable energy, they have to pay the least amount of wheeling during the summer months.

Table 5.4: Results for node 75 and its downstream nodes

| Node | Spring/Autumn |             | Summer      |             | Winter       |             |
|------|---------------|-------------|-------------|-------------|--------------|-------------|
|      | Loss(w)       | Cost(pence) | Loss(w)     | Cost(pence) | Loss(w)      | Cost(pence) |
| 73   | 1413.362534   | 3502.732976 | 724.3971742 | 900.7569399 | 3614.785877  | 5790.019426 |
| 74   | 1590.035107   | 1637.283318 | 801.794868  | 833.6100884 | 3890.947471  | 5179.006722 |
| 75   | -1390.17232   | 1213.119974 | -1544.10571 | 1605.375825 | -940.5982364 | 530.4974053 |

As shown in Table 5.5, the wind distributed generation at Node 47 participates in more power transmission during the winter months due to the abundance of wind energy. On the other hand, the demand of users is highest during the winter season, which is why the wheeling charges are highest during the winter season.

As can be seen from Tables 5.6, 5.7 and 5.8, the majority of nodes downstream of node 47 bear higher wheeling charges in the spring and autumn under the influence of wind distributed

Table 5.5: Results at node 47

| Node 47       | Phase <i>a</i> |              |
|---------------|----------------|--------------|
|               | Loss (w)       | Cost (pence) |
| Spring/Autumn | -15835.50492   | 11348.35625  |
| Summer        | -8221.31225    | 7480.078738  |
| Winter        | -38670.50968   | 18107.07945  |
|               | Phase <i>b</i> |              |
|               | Loss (w)       | Cost (pence) |
| Spring/Autumn | -9108.785208   | 7907.154263  |
| Summer        | -4889.936227   | 5019.421739  |
| Winter        | -21613.12848   | 13196.11172  |
|               | Phase <i>c</i> |              |
|               | Loss (w)       | Cost (pence) |
| Spring/Autumn | -9517.557232   | 8305.401143  |
| Summer        | -4902.908555   | 5097.455966  |
| Winter        | -23687.18015   | 13359.56961  |

generation at node 47. Because wind energy is not the most abundant and user demand is not the lowest during these two seasons, the combination of these two factors results in relatively high wheeling charges.

Table 5.6: Impact of node 47 on downstream nodes (pence) at spring/autumn

| Node | Phase a     | Phase a     | Phase c     |
|------|-------------|-------------|-------------|
| 35   | 286.0897955 | 255.8505043 | 0.0008316   |
| 36   | 0.030957953 | 0.010543875 | 0           |
| 37   | 873.937669  | 0           | 0           |
| 38   | 0           | 300.5125271 | 0           |
| 39   | 0           | 290.9806319 | 0           |
| 40   | 0           | 0           | 0.004025479 |
| 41   | 0           | 0           | 291.7259714 |
| 42   | 333.2956384 | 0.010458996 | 0           |
| 43   | 0           | 681.8746177 | 0           |
| 44   | 0.023437593 | 0.011559278 | 0.000523176 |
| 45   | 380.463039  | 0           | 0           |
| 46   | 374.870751  | 0           | 0           |
| 48   | 2237.264712 | 1681.898629 | 1749.512796 |
| 49   | 1054.268312 | 1574.631882 | 771.3691066 |
| 50   | 0.004549642 | 0.011334791 | 632.6740475 |
| 51   | 318.5397603 | 0.01101389  | 0.002722497 |

## 5.8 Conclusion

This chapter proposes a method for allocating wheeling charges based on flow tracing (loss allocation). The method is also applied to the modified IEEE123 node system for simulation. The results show that this method is fully compatible with the principles and objectives of wheeling fee allocation in power systems. In addition, the wheeling charges arising from the transmission of fossil and sustainable energy are priced separately in the case studies. This not only provides a degree of cost assurance for promoting sustainable energy generation to reduce overall carbon emission of the whole system, but also acts as an incentive for consumers through lower prices. This is further corroborated by the simulation results with the allocating wheeling charges discussed for their fairness and effectiveness.

Table 5.7: Impact of node 47 on downstream nodes (pence) in Summer

| Node | Phase a     | Phase a     | Phase c     |
|------|-------------|-------------|-------------|
| 35   | 205.4875035 | 174.6397615 | 0.01323099  |
| 36   | 0.009087927 | 0.017936842 | 0           |
| 37   | 596.6145957 | 0           | 0           |
| 38   | 0           | 195.4311626 | 0           |
| 39   | 0           | 189.1723669 | 0           |
| 40   | 0.00748125  | 0.018984675 | 0.014700636 |
| 41   | 0           | 0           | 184.6666945 |
| 42   | 217.088888  | 0.013841942 | 0.008658268 |
| 43   | 0           | 441.0700591 | 0           |
| 44   | 0.006540739 | 0.010249515 | 0.010437208 |
| 45   | 258.8001353 | 0           | 0           |
| 46   | 252.6359865 | 0           | 0           |
| 48   | 1494.912373 | 1067.707957 | 1066.987344 |
| 49   | 698.5990704 | 1003.095408 | 478.8046591 |
| 50   | 0.008605172 | 0.014025725 | 422.9263383 |
| 51   | 231.0175562 | 0.013836124 | 0.014321646 |

Table 5.8: Impact of node 47 on downstream nodes (pence) in Winter

| Node | Phase a     | Phase a     | Phase c     |
|------|-------------|-------------|-------------|
| 35   | 103.0493758 | 71.71811533 | 0.009585504 |
| 36   | 0.022536469 | 0.002062043 | 0           |
| 37   | 1333.48185  | 0           | 0           |
| 38   | 0           | 489.1448914 | 0           |
| 39   | 0           | 474.5202759 | 0           |
| 40   | 0.01102898  | 0.007146287 | 0.054565736 |
| 41   | 0           | 0           | 457.1126804 |
| 42   | 445.7292001 | 0.004986678 | 0.003817136 |
| 43   | 0           | 1113.941831 | 0           |
| 44   | 0.058003774 | 0.003155274 | 0           |
| 45   | 591.2325486 | 0           | 0           |
| 46   | 594.5834089 | 0           | 0           |
| 48   | 3507.169455 | 2812.076693 | 2737.571777 |
| 49   | 1695.455736 | 2621.133987 | 1219.060766 |
| 50   | 0.0001304   | 0.006724103 | 929.46313   |
| 51   | 469.1828111 | 0.006268622 | 0.005032735 |

# Chapter 6

## Conclusions and Future Work

### 6.1 Conclusions

The analysis of power flow within distribution networks is a critical aspect of modern power systems management. As the complexity of electrical grids increases due to the integration of renewable energy sources, distributed generation, and the evolution of smart grids, effective power flow analytics becomes increasingly important. This thesis has explored various methods and techniques for analyzing and visualizing power flows in distribution networks, emphasizing the need for accurate, real-time power and energy flow data to support decision-making processes. The contributions of this thesis in the context of power flow analytics are summarised as follows.

- 1) The literature review on power flow analytics for power distribution networks highlights the extensive research and development that has been undertaken to address the challenges posed by modern electrical grids. The review has covered a wide range of methodologies, from traditional power flow analysis techniques to more contemporary approaches. These methodologies have evolved in response to the growing complexity of distribution networks and the need for real-time, accurate, and scalable solutions. Various studies have demonstrated the effectiveness of these advanced techniques in improving the reliability,

efficiency, and resilience of power distribution systems.

The literature review underscores the progress made in the field of power flow analytics for distribution networks, while also identifying areas where further research is needed. The continuous development of more sophisticated analytical tools and techniques will be crucial in addressing the ongoing challenges of modern power systems. This review serves as a foundation for understanding the current state of the art in power flow analytics and provides direction for future research aimed at enhancing the operational efficiency and reliability of power distribution networks.

- 2) The proposed complex loss allocation method represents a significant advancement in the field of power distribution network management. This method aims to address the limitations of traditional loss allocation approaches by using the most basic power system principles that better reflect the true costs and impacts of power flows within the network.

This thesis has detailed the development and implementation of the proposed method, which integrates advanced algorithms and models to achieve a more accurate and equitable distribution of losses. By leveraging concepts such as power flow tracing and loss allocation algorithms, the proposed method offers a delicate approach that accounts for the intricate interactions between different components of the power distribution network.

The key advantages of this method include its ability to provide a precise allocation of losses, improved fairness in cost distribution, and enhanced support for network planning and operational decision-making. Unlike traditional methods, which may oversimplify the complexities of power flows and network dynamics, the proposed approach offers a comprehensive framework that considers various factors such as network topology, load profiles, and generation sources.

Furthermore, the implementation of the proposed method demonstrates its practicality and effectiveness in real-world scenarios. Case studies and simulations have illustrated how the method can be applied to new types of power distribution networks, highlighting its

adaptability and potential for widespread use.

In conclusion, the proposed complex loss allocation method represents a significant step forward in the management of power distribution networks. Its ability to address the complexities of modern electrical grids and provide a fair and accurate distribution of losses makes it a valuable tool for utilities and grid operators.

- 3) The proposed coloring visualization method represents a novel and effective approach to enhancing the analysis and interpretation of power flow data in distribution networks. By integrating RGB colour system with power flow tracing, this method provides a more intuitive and informative way to visualize and understand the complexities of electrical systems.

Throughout this thesis, the proposed method has been demonstrated to offer several significant advantages over traditional visualization approaches. The use of colour coding to represent various attributes of power flow - such as magnitude, direction, and losses - allows for a clearer and more immediate understanding of network performance and behaviour. This is particularly valuable for identifying power and energy related usage/consumption patterns, diagnosing issues, and making informed decisions in both real-time operations and long-term planning.

The RGB colour system employed in the method provides a versatile and effective means of depicting a wide range of data variations. By mapping power flow characteristics to different color intensities and hues, the visualization effectively communicates critical information at a glance. This approach not only enhances the clarity of the visual representation but also improves the accessibility of complex data for operators, engineers, and decision-makers.

The implementation and evaluation of the proposed method have shown its practicality and effectiveness in various case studies and simulations. The results indicate that the method significantly improves the ability to track and manage power flows, visualize loss

distribution, and assess the impact of network modifications. Additionally, it offers valuable support for optimizing network performance and enhancing system reliability.

- 4) The proposed wheeling charge method based on power flow tracing represents a significant advancement in the approach to calculating and allocating transmission costs in power systems. This methodology integrates detailed power flow analysis with a refined cost allocation framework, offering a more accurate and equitable means of determining wheeling charges.

Throughout this thesis, the proposed method has demonstrated its effectiveness in addressing several key challenges associated with wheeling charge calculation. By leveraging power flow tracing, the method provides a granular view of how power flows through the transmission network, allowing for a precise assessment of the contributions of various entities to the overall system costs. This enhanced granularity ensures that charges are more accurately aligned with the actual usage and impact of each participant in the network.

One of the primary benefits of the proposed approach is its ability to better reflect the true costs of transmission services. Traditional methods often rely on simplified assumptions or average data, which can lead to inaccuracies and inequities in charge allocation. In contrast, the power flow tracing method accounts for the specific paths and magnitudes of power flows, capturing the complex interactions within the network. This results in a more nuanced and fair distribution of costs, addressing issues of cost recovery and fairness more effectively.

The implementation and validation of the proposed method have shown promising results. Case studies and simulations reveal that it improves the accuracy of wheeling charge calculations and enhances transparency in cost allocation. By providing a clear and detailed picture of power flows and their associated costs, the method supports better decision-making and helps to optimize network operation and investment.

In conclusion, power flow analytics is an indispensable tool for managing the challenges facing contemporary power distribution networks. By leveraging the latest advancements in computational techniques and visualization technologies, the power industry can better cope with the demands of modern energy systems. The research presented in this thesis contributes to the ongoing efforts to enhance the resilience, efficiency, and sustainability of power distribution networks, and it provides a foundation for future developments in this critical field. Further research is encouraged to continue refining these techniques and exploring new methods to meet the evolving needs of the power sector.

## 6.2 Limitations

There are also some degree of limitations for the power flow colouring method and the wheeling charges allocation method discussed in this project. For the power flow colouring method, the current project implements colouring by manual methods without the help of automated tools. This limits the scope of use of the method. Additionally, in the case of the wheeling charges allocation methodology, the methodology has been limited to practical use for the time being, pending engagement with stakeholders to gather quantitative information on the proposed wheeling fee methodology. These limitations provide direction for future work.

## 6.3 Future Work

As original fundamental research work presented in this PhD thesis, it can be extended with possible future work. This continuation can be from both theories and application aspects.

Here some originated potentials are listed as follows:

- 1) For the complex loss allocation method and theory - Future research should focus on further refining the method, exploring its applications in various network configurations, and integrating it with emerging technologies to enhance its capabilities and impact. This continued development will contribute to more efficient, reliable, and equitable power distribution systems, ultimately benefiting all stakeholders in the electricity market. Additionally, comprehensive validation of complex loss allocation methods through extensive benchmarking against real-world scenarios is necessary. This involves testing the methods across different network types, sizes, and operational conditions to ensure robustness and applicability.
- 2) For the colouring visualisation applications - Developing advanced visualisation techniques that go beyond traditional colour schemes could improve the interpretability of power flow data. This might include interactive visualisation tools that allow users to explore different aspects of the data dynamically and intuitively. Moreover, research should

focus on optimizing the user interface and experience for the colouring visualisation tools. Ensuring that these tools are user-friendly and accessible to various stakeholders, including operators and decision-makers, will be critical for their successful adoption and use. The envisaged future applications of this tool are also in the digital twin of energy systems, as an important component for the final product.

- 3) For market insights on the wheeling charge based on power flow tracing - Engaging with stakeholders, including utility companies, regulators, intermediates and consumers/prosumers (end users), to gather quantitative information on the proposed wheeling charge methods for further validation and improvement for implementation. As regulators (e.g. Ofgem in the UK) are constantly reviewing the market architecture of energy systems with their reviewing cycles, innovations in this aspect requires this engagement. The feedback can provide insights into potential challenges and areas for improvement when considering implementations in current and future market under reforming regulations.

## 6.4 Publication List

This thesis has resulted in the following publications:

### A. Refereed Conference Papers

- A1. Yu F. and Yang J., Loss allocation methods for unbalanced power distribution networks-a review, the 11th International Conference on Renewable Power Generation-Meeting net zero carbon (RPG 2022). IET, London, UK, 2022: 165-169.
- A2. Yu F. and Yang J., Complex Power Loss Allocation in Unbalanced Power Distribution Networks, the 15th International Green Energy Conference, Glasgow, UK, 2023.

### B. Non-refereed Conference Papers, Journal Papers

- B1. Yu F. and Yang J., Dynamic power and carbon flow tracing with visualization in three-phase power grids, *Energy Conversion and Management*, Elsevier, submitted for peer review.
- B2. Yu F., Lou C. and Yang J., Wheeling Charge Calculation Method Based on Power Flow Tracing, *Electric Power Energy Research*, Elsevier, to be submitted.

# Appendix A

## Calculation of the Primitive Impedance Matrix

The Overhead Line Configurations for the IEEE123 node system:

| Config. | Phasing | Phase Cond.  | Neutral Cond. | Spacing |
|---------|---------|--------------|---------------|---------|
|         |         | ACSR         | ACSR          | ID      |
| 1       | A B C N | 336,400 26/7 | 4/0 6/1       | 500     |
| 2       | C A B N | 336,400 26/7 | 4/0 6/1       | 500     |
| 3       | B C A N | 336,400 26/7 | 4/0 6/1       | 500     |
| 4       | C B A N | 336,400 26/7 | 4/0 6/1       | 500     |
| 5       | B A C N | 336,400 26/7 | 4/0 6/1       | 500     |
| 6       | A C B N | 336,400 26/7 | 4/0 6/1       | 500     |
| 7       | A C N   | 336,400 26/7 | 4/0 6/1       | 505     |
| 8       | A B N   | 336,400 26/7 | 4/0 6/1       | 505     |
| 9       | A N     | 1/0          | 1/0           | 510     |
| 10      | B N     | 1/0          | 1/0           | 510     |
| 11      | C N     | 1/0          | 1/0           | 510     |

The corresponding primitive unit impedance matrices are as follows:

Z1:

$$\begin{bmatrix} 0.4013 + 1.4133i & 0.0953 + 0.8515i & 0.0953 + 0.7266i & 0.0953 + 0.7524i \\ 0.0953 + 0.8515i & 0.4013 + 1.4133i & 0.0953 + 0.7802i & 0.0953 + 0.7865i \\ 0.0953 + 0.7266i & 0.0953 + 0.7802i & 0.4013 + 1.4133i & 0.0953 + 0.7674i \\ 0.0953 + 0.7524i & 0.0953 + 0.7865i & 0.0953 + 0.7674i & 0.6873 + 1.5465i \end{bmatrix} \quad (\text{A.1})$$

Z2:

$$\begin{bmatrix} 0.4013 + 1.4133i & 0.0953 + 0.7802i & 0.0953 + 0.8515i & 0.0953 + 0.7865i \\ 0.0953 + 0.7802i & 0.4013 + 1.4133i & 0.0953 + 0.7266i & 0.0953 + 0.7674i \\ 0.0953 + 0.8515i & 0.0953 + 0.7266i & 0.4013 + 1.4133i & 0.0953 + 0.7524i \\ 0.0953 + 0.7865i & 0.0953 + 0.7674i & 0.0953 + 0.7524i & 0.6873 + 1.5465i \end{bmatrix} \quad (\text{A.2})$$

Z3:

$$\begin{bmatrix} 0.4013 + 1.4133i & 0.0953 + 0.7266i & 0.0953 + 0.7802i & 0.0953 + 0.7674i \\ 0.0953 + 0.7266i & 0.4013 + 1.4133i & 0.0953 + 0.8515i & 0.0953 + 0.7524i \\ 0.0953 + 0.7802i & 0.0953 + 0.8515i & 0.4013 + 1.4133i & 0.0953 + 0.7865i \\ 0.0953 + 0.7674i & 0.0953 + 0.7524i & 0.0953 + 0.7865i & 0.6873 + 1.5465i \end{bmatrix} \quad (\text{A.3})$$

Z4:

$$\begin{bmatrix} 0.4013 + 1.4133i & 0.0953 + 0.7802i & 0.0953 + 0.7266i & 0.0953 + 0.7674i \\ 0.0953 + 0.7802i & 0.4013 + 1.4133i & 0.0953 + 0.8515i & 0.0953 + 0.7865i \\ 0.0953 + 0.7266i & 0.0953 + 0.8515i & 0.4013 + 1.4133i & 0.0953 + 0.7524i \\ 0.0953 + 0.7674i & 0.0953 + 0.7865i & 0.0953 + 0.7524i & 0.6873 + 1.5465i \end{bmatrix} \quad (\text{A.4})$$

Z5:

$$\begin{bmatrix} 0.4013 + 1.4133i & 0.0953 + 0.8515i & 0.0953 + 0.7802i & 0.0953 + 0.7865i \\ 0.0953 + 0.8515i & 0.4013 + 1.4133i & 0.0953 + 0.7266i & 0.0953 + 0.7524i \\ 0.0953 + 0.7802i & 0.0953 + 0.7266i & 0.4013 + 1.4133i & 0.0953 + 0.7674i \\ 0.0953 + 0.7865i & 0.0953 + 0.7524i & 0.0953 + 0.7674i & 0.6873 + 1.5465i \end{bmatrix} \quad (\text{A.5})$$

Z6:

$$\begin{bmatrix} 0.4013 + 1.4133i & 0.0953 + 0.7266i & 0.0953 + 0.8515i & 0.0953 + 0.7524i \\ 0.0953 + 0.7266i & 0.4013 + 1.4133i & 0.0953 + 0.7802i & 0.0953 + 0.7674i \\ 0.0953 + 0.8515i & 0.0953 + 0.7802i & 0.4013 + 1.4133i & 0.0953 + 0.7865i \\ 0.0953 + 0.7524i & 0.0953 + 0.7674i & 0.0953 + 0.7865i & 0.6873 + 1.5465i \end{bmatrix} \quad (\text{A.6})$$

Z7:

$$\begin{bmatrix} 0.4013 + 1.4133i & 0 + 0i & 0.0953 + 0.7266i & 0.0953 + 0.7524i \\ 0 + 0i & 0 + 0i & 0 + 0i & 0 + 0i \\ 0.0953 + 0.7266i & 0 + 0i & 0.4013 + 1.4133i & 0.0953 + 0.7674i \\ 0.0953 + 0.7524i & 0 + 0i & 0.0953 + 0.7674i & 0.6873 + 1.5465i \end{bmatrix} \quad (\text{A.7})$$

Z8:

$$\begin{bmatrix} 0.4013 + 1.4133i & 0.0953 + 0.7266i & 0 + 0i & 0.0953 + 0.7524i \\ 0.0953 + 0.7266i & 0.4013 + 1.4133i & 0 + 0i & 0.0953 + 0.7674i \\ 0 + 0i & 0 + 0i & 0 + 0i & 0 + 0i \\ 0.0953 + 0.7524i & 0.0953 + 0.7674i & 0 + 0i & 0.6873 + 1.5465i \end{bmatrix} \quad (\text{A.8})$$

Z9:

$$\begin{bmatrix} 1.2153 + 1.6795i & 0 + 0i & 0 + 0i & 0.0953 + 0.7668i \\ 0 + 0i & 0 + 0i & 0 + 0i & 0 + 0i \\ 0 + 0i & 0 + 0i & 0 + 0i & 0 + 0i \\ 0.0953 + 0.7668i & 0 + 0i & 0 + 0i & 1.2153 + 1.6195i \end{bmatrix} \quad (\text{A.9})$$

Z10:

$$\begin{bmatrix} 0+0i & 0+0i & 0+0i & 0+0i \\ 0+0i & 1.2153+1.6195i & 0+0i & 0.0953+0.7668i \\ 0+0i & 0+0i & 0+0i & 0+0i \\ 0+0i & 0.0953+0.7668i & 0+0i & 1.2153+1.6195i \end{bmatrix} \quad (\text{A.10})$$

Z11:

$$\begin{bmatrix} 0+0i & 0+0i & 0+0i & 0+0i \\ 0+0i & 0+0i & 0+0i & 0+0i \\ 0+0i & 0+0i & 1.2153+1.6195i & 0.0953+0.7668i \\ 0+0i & 0+0 & 0.0953+0.7668i & 1.2153+1.6195i \end{bmatrix} \quad (\text{A.11})$$

Z12:

$$\begin{bmatrix} 1.0653+1.5088i & 0.0953+1.0468i & 0.0953+0.9627i & 0.0953+1.3488i \\ 0.0953+1.0468i & 1.0653+1.5088i & 0.0953+1.0468i & 0.0953+1.3488i \\ 0.0953+0.9627i & 0.0953+1.0468i & 1.0653+1.5088i & 0.0953+1.3488i \\ 0.0953+1.3488i & 0.0953+1.3488i & 0.0953+1.3488i & 1.2391+1.3527i \end{bmatrix} \quad (\text{A.12})$$

# Appendix B

## Branch Loss Allocation Results

Table B.1: The results of the loss allocation of modified IEEE 123-node system(unit - Watts)

| branch | a       | b      | c      | branch | a      | b      | c       |
|--------|---------|--------|--------|--------|--------|--------|---------|
| 1      | 5029.17 | 1414.5 | 2147.1 | 63     | 74.444 | 97.234 | 134.849 |
| 2      | 0       | 2.9562 | 0      | 64     | 56.585 | 194.49 | 269.73  |
| 3      | 0       | 0      | 134.65 | 65     | 68.758 | 30.789 | 327.59  |
| 4      | 0       | 0      | 13.678 | 66     | 6E-06  | 7E-06  | 68.9824 |
| 5      | 0       | 0      | 66.111 | 67     | 1520.9 | 794.03 | 791.637 |
| 6      | 0       | 0      | 19.774 | 68     | 142.39 | 0      | 0       |
| 7      | 3355.14 | 970.65 | 1275.7 | 69     | 136.08 | 0      | 0       |
| 8      | 2140.2  | 647.16 | 850.46 | 70     | 57.972 | 0      | 0       |
| 9      | 119.492 | 0      | 0      | 71     | 18.639 | 0      | 0       |
| 10     | 4.60312 | 0      | 0      | 72     | 371.04 | 367.88 | 359.992 |
| 11     | 19.0189 | 0      | 0      | 73     | 0      | 0      | 26.3156 |
| 12     | 0       | 3.803  | 0      | 74     | 0      | 0      | 0.28436 |
| 13     | 2417.96 | 885.25 | 1275.7 | 75     | 0      | 0      | 27.0106 |
| 14     | 84.214  | 0      | 0      | 76     | 269.85 | 267.55 | 228.511 |

|    |         |        |        |     |        |        |         |
|----|---------|--------|--------|-----|--------|--------|---------|
| 15 | 0       | 0      | 18.236 | 77  | 300    | 295.94 | 299.696 |
| 16 | 0       | 0      | 25.983 | 78  | 74.995 | 80.832 | 74.9186 |
| 17 | 0       | 0      | 6.0564 | 79  | 4.9807 | 8E-09  | 1.2E-08 |
| 18 | -161.85 | -39.49 | -5.408 | 80  | 392.02 | 383.94 | 355.85  |
| 19 | 84.5847 | 0      | 0      | 81  | 392    | 434.01 | 355.836 |
| 20 | 23.9361 | 0      | 0      | 82  | 206.31 | 228.43 | 217.211 |
| 21 | 0.94074 | 10.648 | 71.998 | 83  | 109.61 | 110.13 | 104.602 |
| 22 | 0       | 42.038 | 0      | 84  | 0      | 0      | 119.871 |
| 23 | 0.78443 | 1E-06  | 59.998 | 85  | 0      | 0      | 32.0141 |
| 24 | 0       | 0      | 38.174 | 86  | 69.186 | 169.76 | 29.8169 |
| 25 | 0.86334 | 8E-07  | 27.226 | 87  | 44.476 | 81.703 | 19.1629 |
| 26 | 11.4319 | 0      | 10.918 | 88  | 16.486 | 0      | 0       |
| 27 | 8.98184 | 0      | 2E-08  | 89  | 8.2288 | 25.991 | 11.7099 |
| 28 | 14.4616 | 4E-07  | 3.5547 | 90  | 0      | 21.564 | 0       |
| 29 | 5.79252 | 4E-07  | 5.3319 | 91  | 6.7324 | 5.5948 | 9.58033 |
| 30 | 2.3E-07 | 2E-07  | 6.2222 | 92  | 0      | 0      | 28.8056 |
| 31 | 0       | 0      | 18.525 | 93  | 6.7326 | 5.5953 | 1.4E-07 |
| 32 | 0       | 0      | 5.2789 | 94  | 18.56  | 0      | 0       |
| 33 | 36.8299 | 0      | 0      | 95  | 6E-08  | 7.461  | 7.1E-08 |
| 34 | 0       | 0      | 79.958 | 96  | 0      | 3.4452 | 0       |
| 35 | 39.4012 | 48.168 | 259.64 | 97  | 143.6  | 59.666 | 83.6895 |
| 36 | 22.036  | 20.349 | 0      | 98  | 4.3079 | 5.1604 | 5.53232 |
| 37 | 22.9414 | 0      | 0      | 99  | 2E-06  | 10.32  | 11.0646 |
| 38 | 0       | 20.656 | 0      | 100 | 5E-07  | 6E-07  | 6.03662 |
| 39 | 0       | 5.495  | 0      | 101 | 97.899 | 30.402 | 46.3779 |
| 40 | 118.326 | 112.89 | 173.09 | 102 | 0      | 0      | 110.169 |
| 41 | 0       | 0      | 5.5834 | 103 | 0      | 0      | 101.791 |

|    |         |        |        |     |        |        |         |
|----|---------|--------|--------|-----|--------|--------|---------|
| 42 | 118.326 | 112.89 | 218.71 | 104 | 0      | 0      | 46.86   |
| 43 | 0       | 40.191 | 0      | 105 | 107.69 | 33.442 | 1.1E-06 |
| 44 | 122.614 | 158.43 | 174.96 | 106 | 0      | 72.219 | 0       |
| 45 | 16.871  | 0      | 0      | 107 | 0      | 39.486 | 0       |
| 46 | 5.29013 | 0      | 0      | 108 | 127.27 | 8E-07  | 8.9E-07 |
| 47 | 247.959 | 198.04 | 218.71 | 109 | 465.09 | 0      | 0       |
| 48 | 11.7401 | 12.108 | 12.018 | 110 | 161.65 | 0      | 0       |
| 49 | 18.8357 | 35.842 | 26.279 | 111 | 9.8599 | 0      | 0       |
| 50 | 1.18354 | 4E-07  | 4.0922 | 112 | 43.868 | 0      | 0       |
| 51 | 1.1836  | 2E-07  | 2E-07  | 113 | 104.25 | 0      | 0       |
| 52 | 3618.3  | 1807   | 1839.8 | 114 | 5.5997 | 0      | 0       |
| 53 | 1612.07 | 903.51 | 919.89 | 115 | 0      | 0      | 0       |
| 54 | 892.041 | 564.7  | 574.93 | 116 | 0      | 0      | 0       |
| 55 | 1.40489 | 1.2685 | 1E-07  | 117 | 0      | 0      | 0       |
| 56 | 1.8E-08 | 1.2772 | 2E-08  | 118 | 0      | 0      | 0       |
| 57 | 2374.93 | 1491.3 | 1609.8 | 119 | 0      | 0      | 0       |
| 58 | 0       | 20.777 | 0      | 120 | 0      | 0      | 0       |
| 59 | 0       | 4.278  | 0      | 121 | 0      | 0      | 0       |
| 60 | 5089.15 | 2709.6 | 3449.6 | 122 | 5E-07  | 6E-07  | 7.5E-07 |
| 61 | 2.3E-07 | 2E-07  | 2E-07  | 123 | 6E-09  | 4E-09  | 6.3E-09 |
| 62 | 106.322 | 138.88 | 326.85 |     |        |        |         |

# Appendix C

## Wheeling Charges Results

Table C.1: The one-day wheeling charges for spring and autumn(pence)

| node | cost of phase a | cost of phase b | cost of phase c | node | cost of phase a | cost of phase b | cost of phase c |
|------|-----------------|-----------------|-----------------|------|-----------------|-----------------|-----------------|
| 1    | 919.268         | 0.064           | 803.466         | 63   | 3429.014        | 0.128           | 0.021           |
| 2    | 0.000           | 244.707         | 0.000           | 64   | 0.255           | 6540.462        | 0.118           |
| 3    | 0.000           | 0.000           | 0.040           | 65   | 6506.133        | 3633.583        | 6619.618        |
| 4    | 0.000           | 0.000           | 794.050         | 66   | 0.189           | 0.241           | 7317.736        |
| 5    | 0.000           | 0.000           | 398.165         | 67   | 0.301           | 0.983           | 0.662           |
| 6    | 0.000           | 0.000           | 1000.483        | 68   | 1872.349        | 0.000           | 0.000           |
| 7    | 417.134         | 0.071           | 0.011           | 69   | 4458.319        | 0.000           | 0.000           |
| 8    | 0.000           | 0.137           | 0.003           | 70   | 1967.650        | 0.000           | 0.000           |
| 9    | 1692.490        | 0.000           | 0.000           | 71   | 4545.120        | 0.000           | 0.000           |
| 10   | 834.845         | 0.000           | 0.000           | 72   | 0.000           | 0.111           | 0.180           |
| 11   | 1965.169        | 0.000           | 0.000           | 73   | 0.000           | 0.000           | 3502.733        |
| 12   | 0.000           | 533.338         | 0.000           | 74   | 0.000           | 0.000           | 1637.283        |

|    |          |         |          |     |           |          |          |
|----|----------|---------|----------|-----|-----------|----------|----------|
| 13 | 0.000    | 0.432   | 0.014    | 75  | 0.000     | 0.000    | 1213.120 |
| 14 | 0.040    | 0.000   | 0.000    | 76  | 14117.586 | 9951.431 | 8240.863 |
| 15 | 0.000    | 0.000   | 0.015    | 77  | 0.155     | 2596.323 | 0.077    |
| 16 | 0.000    | 0.000   | 1803.908 | 78  | 0.015     | 0.150    | 0.006    |
| 17 | 0.000    | 0.000   | 781.766  | 79  | 3103.554  | 0.015    | 0.006    |
| 18 | 0.009    | 0.018   | 0.558    | 80  | 0.059     | 2534.146 | 0.006    |
| 19 | 1327.103 | 0.000   | 0.000    | 81  | 0.013     | 0.000    | 0.016    |
| 20 | 1384.217 | 0.000   | 0.000    | 82  | 2887.845  | 0.009    | 0.107    |
| 21 | 0.010    | 0.003   | 0.001    | 83  | 5417.103  | 2213.762 | 1134.606 |
| 22 | 0.000    | 678.496 | 0.000    | 84  | 0.000     | 0.000    | 1622.756 |
| 23 | 0.010    | 0.002   | 0.022    | 85  | 0.000     | 0.000    | 3812.218 |
| 24 | 0.000    | 0.000   | 715.105  | 86  | 0.026     | 1121.774 | 0.109    |
| 25 | 0.029    | 0.004   | 0.349    | 87  | 0.024     | 2663.797 | 0.009    |
| 26 | 0.007    | 0.000   | 0.011    | 88  | 3293.688  | 0.000    | 0.000    |
| 27 | 0.005    | 0.000   | 0.010    | 89  | 0.331     | 0.036    | 0.009    |
| 28 | 800.932  | 0.003   | 0.000    | 90  | 0.000     | 3147.150 | 0.000    |
| 29 | 871.007  | 0.006   | 0.002    | 91  | 0.030     | 0.075    | 0.045    |
| 30 | 0.005    | 0.007   | 595.212  | 92  | 0.000     | 0.000    | 2858.443 |
| 31 | 0.000    | 0.000   | 328.265  | 93  | 0.108     | 0.078    | 0.018    |
| 32 | 0.000    | 0.000   | 333.011  | 94  | 4473.442  | 0.000    | 0.000    |
| 33 | 1028.810 | 0.000   | 0.000    | 95  | 0.032     | 1018.947 | 0.005    |
| 34 | 0.000    | 0.000   | 1837.012 | 96  | 0.000     | 1653.092 | 0.000    |
| 35 | 286.090  | 255.851 | 0.001    | 97  | 0.042     | 0.155    | 0.090    |
| 36 | 0.031    | 0.011   | 0.000    | 98  | 2647.234  | 0.052    | 0.055    |
| 37 | 873.938  | 0.000   | 0.000    | 99  | 0.030     | 2466.280 | 0.014    |
| 38 | 0.000    | 300.513 | 0.000    | 100 | 0.013     | 0.003    | 2594.412 |
| 39 | 0.000    | 290.981 | 0.000    | 101 | 0.048     | 0.083    | 0.070    |

|    |           |          |          |     |          |          |          |
|----|-----------|----------|----------|-----|----------|----------|----------|
| 40 | 0.000     | 0.000    | 0.004    | 102 | 0.000    | 0.000    | 1552.383 |
| 41 | 0.000     | 0.000    | 291.726  | 103 | 0.000    | 0.000    | 3707.906 |
| 42 | 333.296   | 0.010    | 0.000    | 104 | 0.000    | 0.000    | 3825.535 |
| 43 | 0.000     | 681.875  | 0.000    | 105 | 0.054    | 0.060    | 0.000    |
| 44 | 0.023     | 0.012    | 0.001    | 106 | 0.000    | 3568.165 | 0.000    |
| 45 | 380.463   | 0.000    | 0.000    | 107 | 0.000    | 3669.853 | 0.000    |
| 46 | 374.871   | 0.000    | 0.000    | 108 | 0.161    | 0.039    | 0.002    |
| 47 | 11348.356 | 7907.154 | 8305.401 | 109 | 4836.672 | 0.000    | 0.000    |
| 48 | 2237.265  | 1681.899 | 1749.513 | 110 | 0.120    | 0.000    | 0.000    |
| 49 | 1054.268  | 1574.632 | 771.369  | 111 | 2180.335 | 0.000    | 0.000    |
| 50 | 0.005     | 0.011    | 632.674  | 112 | 2276.975 | 0.000    | 0.000    |
| 51 | 318.540   | 0.011    | 0.003    | 113 | 5638.694 | 0.000    | 0.000    |
| 52 | 2585.616  | 0.000    | 0.000    | 114 | 2261.269 | 0.000    | 0.000    |
| 53 | 2827.632  | 0.000    | 0.000    | 115 | 0.000    | 0.000    | 0.000    |
| 54 | 0.380     | 0.244    | 0.021    | 116 | 0.000    | 0.432    | 0.014    |
| 55 | 834.897   | 0.018    | 0.003    | 117 | 0.005    | 0.018    | 0.558    |
| 56 | 0.014     | 630.693  | 0.004    | 118 | 1427.998 | 72.875   | 407.326  |
| 57 | 0.024     | 0.275    | 0.000    | 119 | 955.619  | 0.031    | 0.008    |
| 58 | 0.000     | 1164.085 | 0.000    | 120 | 1421.863 | 0.360    | 0.086    |
| 59 | 0.000     | 1124.091 | 0.000    | 121 | 0.014    | 0.055    | 0.032    |
| 60 | 1421.863  | 0.360    | 0.086    | 122 | 0.001    | 0.071    | 0.022    |
| 61 | 0.092     | 0.058    | 0.054    | 123 | 0.008    | 0.001    | 0.015    |
| 62 | 0.186     | 0.192    | 2964.617 |     |          |          |          |

Table C.2: The one-day wheeling charges for summer(pence)

| node | cost of phase a | cost of phase b | cost of phase c | node | cost of phase a | cost of phase b | cost of phase c |
|------|-----------------|-----------------|-----------------|------|-----------------|-----------------|-----------------|
| 1    | 386.383         | 0.016           | 0.008           | 63   | 2409.206        | 0.205           | 0.292           |
| 2    | 0.000           | 158.553         | 0.000           | 64   | 0.474           | 4360.756        | 0.515           |
| 3    | 0.000           | 0.000           | 0.009           | 65   | 4570.400        | 2405.028        | 4268.031        |
| 4    | 0.000           | 0.000           | 510.280         | 66   | 0.412           | 0.430           | 4660.010        |
| 5    | 0.000           | 0.000           | 258.375         | 67   | 1.118           | 0.971           | 0.001           |
| 6    | 0.000           | 0.000           | 650.672         | 68   | 1306.677        | 0.000           | 0.000           |
| 7    | 323.357         | 0.006           | 0.000           | 69   | 3086.242        | 0.000           | 0.000           |
| 8    | 0.104           | 0.167           | 0.000           | 70   | 1367.169        | 0.000           | 0.000           |
| 9    | 1148.582        | 0.000           | 0.000           | 71   | 3136.528        | 0.000           | 0.000           |
| 10   | 575.971         | 0.000           | 0.000           | 72   | 0.037           | 0.045           | 0.216           |
| 11   | 1360.973        | 0.000           | 0.000           | 73   | 0.000           | 0.000           | 900.757         |
| 12   | 0.000           | 345.043         | 0.000           | 74   | 0.000           | 0.000           | 833.610         |
| 13   | 0.312           | 0.220           | 0.077           | 75   | 0.000           | 0.000           | 1605.376        |
| 14   | 0.037           | 0.000           | 0.000           | 76   | 9785.872        | 6262.606        | 4979.253        |
| 15   | 0.000           | 0.000           | 0.012           | 77   | 0.174           | 1719.982        | 0.204           |
| 16   | 0.000           | 0.000           | 1121.530        | 78   | 0.026           | 0.113           | 0.012           |
| 17   | 0.000           | 0.000           | 489.350         | 79   | 2339.808        | 0.044           | 0.066           |
| 18   | 0.026           | 0.028           | 0.031           | 80   | 0.078           | 1667.183        | 0.111           |
| 19   | 546.327         | 0.000           | 0.000           | 81   | 0.107           | 0.276           | 0.172           |
| 20   | 576.841         | 0.000           | 0.000           | 82   | 2219.602        | 0.046           | 0.136           |
| 21   | 0.008           | 0.008           | 0.004           | 83   | 1106.429        | 2114.561        | 6767.740        |
| 22   | 0.000           | 439.089         | 0.000           | 84   | 0.000           | 0.000           | 1004.989        |
| 23   | 0.006           | 0.008           | 0.015           | 85   | 0.000           | 0.000           | 2333.123        |

|    |          |          |          |     |          |          |          |
|----|----------|----------|----------|-----|----------|----------|----------|
| 24 | 0.000    | 0.000    | 450.181  | 86  | 0.120    | 757.821  | 0.190    |
| 25 | 0.004    | 0.009    | 0.512    | 87  | 0.192    | 1789.246 | 0.085    |
| 26 | 0.005    | 0.000    | 0.007    | 88  | 2454.571 | 0.000    | 0.000    |
| 27 | 0.005    | 0.000    | 0.005    | 89  | 0.042    | 0.040    | 0.135    |
| 28 | 442.702  | 0.006    | 0.007    | 90  | 0.000    | 2255.026 | 0.000    |
| 29 | 483.043  | 0.009    | 0.012    | 91  | 0.025    | 0.081    | 0.233    |
| 30 | 0.011    | 0.011    | 398.158  | 92  | 0.000    | 0.000    | 2333.170 |
| 31 | 0.000    | 0.000    | 208.273  | 93  | 0.035    | 0.004    | 0.080    |
| 32 | 0.000    | 0.000    | 211.364  | 94  | 3087.470 | 0.000    | 0.000    |
| 33 | 1091.311 | 0.000    | 0.000    | 95  | 0.074    | 707.627  | 0.083    |
| 34 | 0.000    | 0.000    | 1153.960 | 96  | 0.000    | 1045.716 | 0.000    |
| 35 | 205.488  | 174.640  | 0.013    | 97  | 0.029    | 0.038    | 0.145    |
| 36 | 0.009    | 0.018    | 0.000    | 98  | 2134.993 | 0.042    | 0.050    |
| 37 | 596.615  | 0.000    | 0.000    | 99  | 0.088    | 1659.028 | 0.170    |
| 38 | 0.000    | 195.431  | 0.000    | 100 | 0.048    | 0.041    | 1773.649 |
| 39 | 0.000    | 189.172  | 0.000    | 101 | 0.021    | 0.065    | 0.056    |
| 40 | 0.007    | 0.019    | 0.015    | 102 | 0.000    | 0.000    | 972.666  |
| 41 | 0.000    | 0.000    | 184.667  | 103 | 0.000    | 0.000    | 2307.589 |
| 42 | 217.089  | 0.014    | 0.009    | 104 | 0.000    | 0.000    | 2382.996 |
| 43 | 0.000    | 441.070  | 0.000    | 105 | 0.000    | 0.056    | 0.091    |
| 44 | 0.007    | 0.010    | 0.010    | 106 | 0.000    | 2261.246 | 0.000    |
| 45 | 258.800  | 0.000    | 0.000    | 107 | 0.000    | 2326.747 | 0.000    |
| 46 | 252.636  | 0.000    | 0.000    | 108 | 0.086    | 0.029    | 0.122    |
| 47 | 7480.079 | 5019.422 | 5097.456 | 109 | 3321.633 | 0.000    | 0.000    |
| 48 | 1494.912 | 1067.708 | 1066.987 | 110 | 0.136    | 0.000    | 0.000    |
| 49 | 698.599  | 1003.095 | 478.805  | 111 | 1498.050 | 0.000    | 0.000    |
| 50 | 0.009    | 0.014    | 422.926  | 112 | 1589.430 | 0.000    | 0.000    |

|    |          |         |          |     |          |        |         |
|----|----------|---------|----------|-----|----------|--------|---------|
| 51 | 231.018  | 0.014   | 0.014    | 113 | 3985.634 | 0.000  | 0.000   |
| 52 | 1514.682 | 0.011   | 0.000    | 114 | 1547.681 | 0.000  | 0.000   |
| 53 | 1903.778 | 0.000   | 0.000    | 115 | 0.000    | 0.000  | 0.000   |
| 54 | 0.456    | 0.198   | 0.627    | 116 | 0.312    | 0.220  | 0.077   |
| 55 | 632.038  | 0.032   | 0.038    | 117 | 0.026    | 0.028  | 0.031   |
| 56 | 0.011    | 440.447 | 0.038    | 118 | 948.506  | 44.143 | 224.623 |
| 57 | 0.013    | 0.185   | 0.000    | 119 | 691.205  | 0.039  | 0.040   |
| 58 | 0.000    | 750.682 | 0.000    | 120 | 992.214  | 0.284  | 0.305   |
| 59 | 0.000    | 721.617 | 0.000    | 121 | 0.010    | 0.014  | 0.052   |
| 60 | 992.214  | 0.284   | 0.305    | 122 | 0.165    | 0.113  | 0.346   |
| 61 | 0.021    | 0.140   | 0.108    | 123 | 0.004    | 0.006  | 0.005   |
| 62 | 0.344    | 0.403   | 1978.294 |     |          |        |         |

Table C.3: The one-day wheeling charges for winter((pence)

| node | cost of phase a | cost of phase b | cost of phase c | node | cost of phase a | cost of phase b | cost of phase c |
|------|-----------------|-----------------|-----------------|------|-----------------|-----------------|-----------------|
| 1    | 894.380         | 0.020           | 0.017           | 63   | 5190.673        | 0.019           | 0.082           |
| 2    | 0.000           | 400.198         | 0.000           | 64   | 0.030           | 10300.670       | 0.020           |
| 3    | 0.000           | 0.000           | 0.004           | 65   | 9676.892        | 5726.920        | 9839.871        |
| 4    | 0.000           | 0.000           | 1238.455        | 66   | 0.075           | 0.025           | 11306.433       |
| 5    | 0.000           | 0.000           | 610.214         | 67   | 0.756           | 0.588           | 0.956           |
| 6    | 0.000           | 0.000           | 1527.258        | 68   | 3036.907        | 0.000           | 0.000           |
| 7    | 692.976         | 0.000           | 0.008           | 69   | 7260.447        | 0.000           | 0.000           |
| 8    | 0.033           | 0.178           | 0.000           | 70   | 3195.247        | 0.000           | 0.000           |
| 9    | 2664.854        | 0.000           | 0.000           | 71   | 7408.924        | 0.000           | 0.000           |
| 10   | 1282.348        | 0.000           | 0.000           | 72   | 0.079           | 0.000           | 0.690           |
| 11   | 2973.673        | 0.000           | 0.000           | 73   | 0.000           | 0.000           | 5790.019        |

|    |          |          |          |     |           |           |           |
|----|----------|----------|----------|-----|-----------|-----------|-----------|
| 12 | 0.000    | 874.548  | 0.000    | 74  | 0.000     | 0.000     | 5179.007  |
| 13 | 0.392    | 0.061    | 0.345    | 75  | 0.000     | 0.000     | 530.497   |
| 14 | 0.018    | 0.000    | 0.000    | 76  | 21770.758 | 16875.159 | 13162.312 |
| 15 | 0.000    | 0.000    | 0.077    | 77  | 0.116     | 3871.349  | 0.069     |
| 16 | 0.000    | 0.000    | 2856.675 | 78  | 0.117     | 0.185     | 0.155     |
| 17 | 0.000    | 0.000    | 1231.154 | 79  | 4182.324  | 0.023     | 0.022     |
| 18 | 0.105    | 0.006    | 0.070    | 80  | 0.035     | 3904.873  | 0.007     |
| 19 | 3931.987 | 0.000    | 0.000    | 81  | 0.098     | 0.052     | 0.107     |
| 20 | 4004.171 | 0.000    | 0.000    | 82  | 5694.589  | 0.051     | 0.000     |
| 21 | 0.052    | 0.016    | 0.008    | 83  | 8979.061  | 6780.881  | 821.761   |
| 22 | 0.000    | 1107.380 | 0.000    | 84  | 0.000     | 0.000     | 2661.397  |
| 23 | 0.076    | 0.005    | 0.024    | 85  | 0.000     | 0.000     | 6315.140  |
| 24 | 0.000    | 0.000    | 1126.768 | 86  | 0.067     | 1732.696  | 0.036     |
| 25 | 0.069    | 0.003    | 0.222    | 87  | 0.056     | 4003.563  | 0.059     |
| 26 | 0.030    | 0.000    | 0.036    | 88  | 5583.497  | 0.000     | 0.000     |
| 27 | 0.011    | 0.000    | 0.010    | 89  | 0.121     | 0.072     | 0.194     |
| 28 | 2670.292 | 0.000    | 0.003    | 90  | 0.000     | 5168.569  | 0.000     |
| 29 | 2862.465 | 0.000    | 0.004    | 91  | 0.128     | 0.245     | 0.034     |
| 30 | 0.012    | 0.001    | 873.212  | 92  | 0.000     | 0.000     | 4551.049  |
| 31 | 0.000    | 0.000    | 513.704  | 93  | 0.131     | 0.000     | 0.050     |
| 32 | 0.000    | 0.000    | 520.878  | 94  | 7339.963  | 0.000     | 0.000     |
| 33 | 1044.099 | 0.000    | 0.000    | 95  | 0.014     | 1541.170  | 0.029     |
| 34 | 0.000    | 0.000    | 2841.236 | 96  | 0.000     | 2806.747  | 0.000     |
| 35 | 103.049  | 71.718   | 0.010    | 97  | 0.878     | 0.007     | 0.074     |
| 36 | 0.023    | 0.002    | 0.000    | 98  | 5590.319  | 0.000     | 0.034     |
| 37 | 1333.482 | 0.000    | 0.000    | 99  | 0.036     | 3841.716  | 0.037     |
| 38 | 0.000    | 489.145  | 0.000    | 100 | 0.026     | 0.044     | 3617.183  |

|    |           |           |           |     |          |          |          |
|----|-----------|-----------|-----------|-----|----------|----------|----------|
| 39 | 0.000     | 474.520   | 0.000     | 101 | 0.133    | 0.228    | 0.176    |
| 40 | 0.011     | 0.007     | 0.055     | 102 | 0.000    | 0.000    | 2524.583 |
| 41 | 0.000     | 0.000     | 457.113   | 103 | 0.000    | 0.000    | 6078.947 |
| 42 | 445.729   | 0.005     | 0.004     | 104 | 0.000    | 0.000    | 6276.151 |
| 43 | 0.000     | 1113.942  | 0.000     | 105 | 0.000    | 0.174    | 0.030    |
| 44 | 0.058     | 0.003     | 0.000     | 106 | 0.000    | 6025.052 | 0.000    |
| 45 | 591.233   | 0.000     | 0.000     | 107 | 0.000    | 6197.347 | 0.000    |
| 46 | 594.583   | 0.000     | 0.000     | 108 | 0.058    | 0.122    | 0.040    |
| 47 | 18107.079 | 13196.112 | 13359.570 | 109 | 7871.628 | 0.000    | 0.000    |
| 48 | 3507.169  | 2812.077  | 2737.572  | 110 | 0.236    | 0.000    | 0.000    |
| 49 | 1695.456  | 2621.134  | 1219.061  | 111 | 3540.080 | 0.000    | 0.000    |
| 50 | 0.000     | 0.007     | 929.463   | 112 | 3502.001 | 0.000    | 0.000    |
| 51 | 469.183   | 0.006     | 0.005     | 113 | 8239.147 | 0.000    | 0.000    |
| 52 | 2997.360  | 0.057     | 0.020     | 114 | 3670.531 | 0.000    | 0.000    |
| 53 | 3697.198  | 0.000     | 0.019     | 115 | 0.000    | 0.000    | 0.000    |
| 54 | 0.408     | 0.531     | 0.082     | 116 | 0.392    | 0.061    | 0.345    |
| 55 | 1081.527  | 0.037     | 0.007     | 117 | 0.035    | 0.006    | 0.070    |
| 56 | 0.041     | 941.703   | 0.006     | 118 | 2388.005 | 131.679  | 761.625  |
| 57 | 0.000     | 0.419     | 0.957     | 119 | 1407.548 | 0.018    | 0.014    |
| 58 | 0.000     | 1913.922  | 0.000     | 120 | 1990.453 | 0.045    | 0.155    |
| 59 | 0.000     | 1866.763  | 0.000     | 121 | 0.293    | 0.002    | 0.026    |
| 60 | 1990.453  | 0.045     | 0.155     | 122 | 0.181    | 0.299    | 0.091    |
| 61 | 0.211     | 0.050     | 0.108     | 123 | 0.017    | 0.005    | 0.010    |
| 62 | 0.038     | 0.009     | 4277.639  |     |          |          |          |

Table C.4: The spring and autumn wheeling charges for conventional and sustainable energy sources that do not differentiate between them(pence)

| node | cost of phase a | cost of phase b | cost of phase c | node | cost of phase a | cost of phase b | cost of phase c |
|------|-----------------|-----------------|-----------------|------|-----------------|-----------------|-----------------|
| 1    | 919.268         | 0.064           | 803.466         | 63   | 3429.014        | 0.137           | 0.023           |
| 2    | 0.000           | 244.707         | 0.000           | 64   | 0.255           | 7007.638        | 0.125           |
| 3    | 0.000           | 0.000           | 0.040           | 65   | 6506.133        | 3893.125        | 6992.554        |
| 4    | 0.000           | 0.000           | 794.050         | 66   | 0.189           | 0.258           | 7730.003        |
| 5    | 0.000           | 0.000           | 398.165         | 67   | 0.301           | 1.053           | 0.699           |
| 6    | 0.000           | 0.000           | 1000.483        | 68   | 1872.349        | 0.000           | 0.000           |
| 7    | 417.134         | 0.071           | 0.011           | 69   | 4458.319        | 0.000           | 0.000           |
| 8    | 0.000           | 0.137           | 0.003           | 70   | 1967.650        | 0.000           | 0.000           |
| 9    | 1692.490        | 0.000           | 0.000           | 71   | 4545.120        | 0.000           | 0.000           |
| 10   | 834.845         | 0.000           | 0.000           | 72   | 0.000           | 0.119           | 0.190           |
| 11   | 1965.169        | 0.000           | 0.000           | 73   | 0.000           | 0.000           | 3700.070        |
| 12   | 0.000           | 533.338         | 0.000           | 74   | 0.000           | 0.000           | 4162.585        |
| 13   | 0.000           | 0.462           | 0.015           | 75   | 0.000           | 0.000           | 3639.360        |
| 14   | 0.040           | 0.000           | 0.000           | 76   | 14117.586       | 10662.247       | 8705.137        |
| 15   | 0.000           | 0.000           | 0.016           | 77   | 0.155           | 2781.774        | 0.082           |
| 16   | 0.000           | 0.000           | 1905.537        | 78   | 0.015           | 0.160           | 0.007           |
| 17   | 0.000           | 0.000           | 825.809         | 79   | 3103.554        | 0.016           | 0.006           |
| 18   | 0.016           | 0.055           | 1.675           | 80   | 0.059           | 2715.157        | 0.006           |
| 19   | 2457.599        | 0.000           | 0.000           | 81   | 0.013           | 0.000           | 0.017           |
| 20   | 2563.366        | 0.000           | 0.000           | 82   | 2887.845        | 0.009           | 0.113           |
| 21   | 0.018           | 0.009           | 0.004           | 83   | 5417.103        | 2371.888        | 1198.527        |
| 22   | 0.000           | 2035.489        | 0.000           | 84   | 0.000           | 0.000           | 1714.179        |

|    |           |           |           |     |          |          |          |
|----|-----------|-----------|-----------|-----|----------|----------|----------|
| 23 | 0.018     | 0.006     | 0.066     | 85  | 0.000    | 0.000    | 4026.991 |
| 24 | 0.000     | 0.000     | 2145.314  | 86  | 0.026    | 1201.901 | 0.115    |
| 25 | 0.067     | 0.011     | 1.047     | 87  | 0.024    | 2854.069 | 0.009    |
| 26 | 0.015     | 0.000     | 0.032     | 88  | 3293.688 | 0.000    | 0.000    |
| 27 | 0.012     | 0.000     | 0.029     | 89  | 0.331    | 0.039    | 0.009    |
| 28 | 1834.196  | 0.010     | 0.000     | 90  | 0.000    | 3371.946 | 0.000    |
| 29 | 1994.672  | 0.017     | 0.007     | 91  | 0.030    | 0.080    | 0.048    |
| 30 | 0.011     | 0.020     | 1785.637  | 92  | 0.000    | 0.000    | 3019.482 |
| 31 | 0.000     | 0.000     | 984.796   | 93  | 0.108    | 0.084    | 0.019    |
| 32 | 0.000     | 0.000     | 999.032   | 94  | 4473.442 | 0.000    | 0.000    |
| 33 | 2356.054  | 0.000     | 0.000     | 95  | 0.032    | 1091.729 | 0.005    |
| 34 | 0.000     | 0.000     | 1940.506  | 96  | 0.000    | 1771.170 | 0.000    |
| 35 | 858.269   | 767.552   | 0.002     | 97  | 0.042    | 0.166    | 0.095    |
| 36 | 0.093     | 0.032     | 0.000     | 98  | 2647.234 | 0.055    | 0.058    |
| 37 | 2621.813  | 0.000     | 0.000     | 99  | 0.030    | 2642.443 | 0.015    |
| 38 | 0.000     | 901.538   | 0.000     | 100 | 0.013    | 0.004    | 2740.576 |
| 39 | 0.000     | 872.942   | 0.000     | 101 | 0.048    | 0.089    | 0.074    |
| 40 | 0.000     | 0.000     | 0.012     | 102 | 0.000    | 0.000    | 1639.841 |
| 41 | 0.000     | 0.000     | 875.178   | 103 | 0.000    | 0.000    | 3916.802 |
| 42 | 999.887   | 0.031     | 0.000     | 104 | 0.000    | 0.000    | 4041.058 |
| 43 | 0.000     | 2045.624  | 0.000     | 105 | 0.054    | 0.064    | 0.000    |
| 44 | 0.070     | 0.035     | 0.002     | 106 | 0.000    | 3823.034 | 0.000    |
| 45 | 1141.389  | 0.000     | 0.000     | 107 | 0.000    | 3931.985 | 0.000    |
| 46 | 1124.612  | 0.000     | 0.000     | 108 | 0.161    | 0.042    | 0.002    |
| 47 | 34045.069 | 23721.463 | 24916.203 | 109 | 4836.672 | 0.000    | 0.000    |
| 48 | 6711.794  | 5045.696  | 5248.538  | 110 | 0.120    | 0.000    | 0.000    |
| 49 | 3162.805  | 4723.896  | 2314.107  | 111 | 2180.335 | 0.000    | 0.000    |

|    |          |          |          |     |          |        |         |
|----|----------|----------|----------|-----|----------|--------|---------|
| 50 | 0.014    | 0.034    | 1898.022 | 112 | 2276.975 | 0.000  | 0.000   |
| 51 | 955.619  | 0.033    | 0.008    | 113 | 5638.694 | 0.000  | 0.000   |
| 52 | 2585.616 | 0.000    | 0.000    | 114 | 2261.269 | 0.000  | 0.000   |
| 53 | 2827.632 | 0.000    | 0.000    | 115 | 0.000    | 0.000  | 0.000   |
| 54 | 0.380    | 0.261    | 0.022    | 116 | 0.000    | 0.462  | 0.015   |
| 55 | 834.897  | 0.019    | 0.004    | 117 | 0.016    | 0.055  | 1.675   |
| 56 | 0.014    | 675.743  | 0.004    | 118 | 1427.998 | 78.081 | 430.274 |
| 57 | 0.024    | 0.295    | 0.000    | 119 | 955.619  | 0.033  | 0.008   |
| 58 | 0.000    | 1247.234 | 0.000    | 120 | 1421.863 | 0.385  | 0.090   |
| 59 | 0.000    | 1204.384 | 0.000    | 121 | 0.042    | 0.166  | 0.095   |
| 60 | 1421.863 | 0.385    | 0.090    | 122 | 0.001    | 0.076  | 0.024   |
| 61 | 0.092    | 0.062    | 0.057    | 123 | 0.008    | 0.002  | 0.045   |
| 62 | 0.186    | 0.206    | 3131.638 |     |          |        |         |

# Bibliography

- [1] M. A. Shoeb, *Integration of Wind Power into Electricity Markets*. PhD thesis, Master thesis, Eindhoven University of Technology, EES. 13, 2013.
- [2] M. Tostado-Véliz, S. Mouassa, and F. Jurado, “A milp framework for electricity tariff-choosing decision process in smart homes considering ‘happy hours’ tariffs,” *International Journal of Electrical Power & Energy Systems*, vol. 131, p. 107139, 2021.
- [3] J. Yang, J. Zhao, F. Luo, F. Wen, and Z. Y. Dong, “Decision-making for electricity retailers: A brief survey,” *IEEE Transactions on Smart Grid*, vol. 9, no. 5, pp. 4140–4153, 2017.
- [4] K. Kok and S. Widergren, “A society of devices: Integrating intelligent distributed resources with transactive energy,” *IEEE Power and Energy Magazine*, vol. 14, no. 3, pp. 34–45, 2016.
- [5] S. P. Burger and M. Luke, “Business models for distributed energy resources: A review and empirical analysis,” *Energy Policy*, vol. 109, pp. 230–248, 2017.
- [6] International Energy Agency, “World energy outlook 2023,” 2023. Accessed: 2024-08-13.
- [7] P. Cramton, “Electricity market design,” *Oxford Review of Economic Policy*, vol. 33, no. 4, pp. 589–612, 2017.

- [8] S. P. Burger, J. D. Jenkins, C. Batlle, and I. J. Perez-Arriaga, "Restructuring revisited part 2: Coordination in electricity distribution systems," *The Energy Journal*, vol. 40, no. 3, pp. 55–76, 2019.
- [9] P. Zhang, F. Li, and N. Bhatt, "Next-generation monitoring, analysis, and control for the future smart control center," *IEEE Transactions on Smart Grid*, vol. 1, no. 2, pp. 186–192, 2010.
- [10] P. Borazjani, N. I. A. Wahab, H. B. Hizam, and A. B. C. Soh, "A review on microgrid control techniques," *2014 IEEE Innovative Smart Grid Technologies-Asia (ISGT ASIA)*, pp. 749–753, 2014.
- [11] P. M. Anderson and A. A. Fouad, *Power system control and stability*. John Wiley & Sons, 2008.
- [12] P. Gaudel, "Cross-border electricity trade: Opportunities and challenges for nepal," *Bidhyut Bi-Yearly Publication*, 2018.
- [13] W. E. Council, "World energy resources 2013 survey," *World Energy Council*, pp. 1–468, 2013.
- [14] International Energy Agency, "Weo-2016 special report energy and air pollution," 2016.
- [15] Y. Yang, S. Xia, and X. Qian, "Geopolitics of the energy transition," *Journal of Geographical Sciences*, vol. 33, no. 4, pp. 683–704, 2023.
- [16] S. AlKheder and A. Almusalam, "Forecasting of carbon dioxide emissions from power plants in kuwait using united states environmental protection agency, intergovernmental panel on climate change, and machine learning methods," *Renewable Energy*, vol. 191, pp. 819–827, 2022.
- [17] J. B. Eisen, "New energy geopolitics: China, renewable energy, and the greentech race," *Chi.-Kent L. Rev.*, vol. 86, p. 9, 2011.

- [18] J. Maryam, A. Mittal, and V. Sharma, "Co2 emissions, energy consumption and economic growth in brics: an empirical analysis," *IOSR Journal Of Humanities And Social Science*, 2017. Published by IOSR Journal Of Humanities And Social Science.
- [19] J. R. Agüero, E. Takayesu, D. Novosel, and R. Masiello, "Modernizing the grid: Challenges and opportunities for a sustainable future," *IEEE Power and Energy Magazine*, vol. 15, no. 3, pp. 74–83, 2017.
- [20] B. Zhou, Y. Meng, W. Huang, H. Wang, L. Deng, S. Huang, and J. Wei, "Multi-energy net load forecasting for integrated local energy systems with heterogeneous prosumers," *International Journal of Electrical Power & Energy Systems*, vol. 126, p. 106542, 2021.
- [21] S. Razzaq, R. Zafar, N. A. Khan, A. R. Butt, and A. Mahmood, "A novel prosumer-based energy sharing and management (pesm) approach for cooperative demand side management (dsm) in smart grid," *Applied Sciences*, vol. 6, no. 10, p. 275, 2016.
- [22] J. R. Agüero, A. Khodaei, and R. Masiello, "The utility and grid of the future: Challenges, needs, and trends," *IEEE Power and Energy Magazine*, vol. 14, no. 5, pp. 29–37, 2016.
- [23] J. R. Agüero and A. Khodaei, "Roadmaps for the utility of the future," *The Electricity Journal*, vol. 28, no. 10, pp. 7–17, 2015.
- [24] K. Balamurugan and D. Srinivasan, "Review of power flow studies on distribution network with distributed generation," in *2011 IEEE Ninth International Conference on Power Electronics and Drive Systems*, pp. 411–417, IEEE, 2011.
- [25] E. Vega-Fuentes, J. Yang, C. Lou, and N. K. Meena, "Transaction-oriented dynamic power flow tracing for distribution networks—definition and implementation in gis environment," *IEEE Transactions on Smart Grid*, vol. 12, no. 2, pp. 1303–1313, 2020.
- [26] A. Mohd, E. Ortjohann, A. Schmelter, N. Hamsic, and D. Morton, "Challenges in integrating distributed energy storage systems into future smart grid," in *2008 IEEE international symposium on industrial electronics*, pp. 1627–1632, IEEE, 2008.

- [27] D. Kirschen, R. Allan, and G. Strbac, "Contributions of individual generators to loads and flows," *IEEE Transactions on Power Systems*, vol. 12, no. 1, pp. 52–60, 1997.
- [28] D. Kirschen and G. Strbac, "Tracing active and reactive power between generators and loads using real and imaginary currents," *IEEE Transactions on Power Systems*, vol. 14, no. 4, pp. 1312–1319, 1999.
- [29] C. Macqueen and M. Irving, "An algorithm for the allocation of distribution system demand and energy losses," in *Proceedings of Power Industry Computer Applications Conference*, pp. 234–239, IEEE, 1995.
- [30] H. Wei, P. Chen, "Power composition of transmission lines and power transmission relationship between generators and loads based on graph theory," *Canadian Society for Electrical Engineering*, vol. 20, no. 6, pp. 21–25, 2000.
- [31] J. Bialek, "Tracing the flow of electricity," *IEE Proceedings-Generation, Transmission and Distribution*, vol. 143, no. 4, pp. 313–320, 1996.
- [32] Y. Dai, Y. Ni, F. Wen, and Z. Han, "Reactive power pricing based on cost allocation through power flow tracing," *Automation of Electric Power Systems*, vol. 24, no. 18, pp. 13–17, 2000.
- [33] W. Wei, Z. Zhang, and H. Jia, "A voltage stability control method based on power flow tracing," *Proceedings-Chinese Society of Electrical Engineering*, vol. 28, no. 1, p. 1, 2008.
- [34] J. Zhao, H. Jia, and X. Yu, "Interface power control method based on power flow tracing and generator re-dispatch," *Automation of Electric Power Systems*, vol. 33, no. 6, pp. 16–20, 2009.
- [35] Z. Jing, Y. Liu, and L. Zeng, "Comparison between four commonly used power flow composition analytic methods," *Dianli Xitong Zidonghua(Automation of Electric Power Systems)*, vol. 34, no. 23, pp. 42–51, 2010.

- [36] W.-d. Li, L.-m. Wei, and H. Sun, "Research on comparison of power flow tracing methods," *Journal-Dalian University of Technology*, vol. 42, no. 4, pp. 491–497, 2002.
- [37] F. F. Wu, Y. Ni, and P. Wei, "Power transfer allocation for open access using graph theory-fundamentals and applications in systems without loopflow," *IEEE Transactions on Power Systems*, vol. 15, no. 3, pp. 923–929, 2000.
- [38] K. Xie and J. Zhou, "Power flow tracing algorithm for electric networks with loopflow," *Science in China Series E: Technological Sciences*, vol. 46, pp. 93–103, 2003.
- [39] K.-G. Xie, C.-Y. Li, Y. Zhao, Y. Liu, and J.-Q. Zhou, "Efficient analytical model and algorithm for distributing power using the downstream distribution matrix.," in *Zhongguo Dianji Gongcheng Xuebao(Proceedings of the Chinese Society of Electrical Engineering)*, vol. 25, pp. 27–31, 2005.
- [40] M. Pantos, G. Verbic, and F. Gubina, "Modified topological generation and load distribution factors," *IEEE Transactions on Power Systems*, vol. 20, no. 4, pp. 1998–2005, 2005.
- [41] H. Rudnick, R. Palma, and J. E. Fernández, "Marginal pricing and supplement cost allocation in transmission open access," *IEEE Transactions on Power Systems*, vol. 10, no. 2, pp. 1125–1132, 1995.
- [42] W. Y. Ng, "Generalized generation distribution factors for power system security evaluations," *IEEE Transactions on Power Apparatus and Systems*, no. 3, pp. 1001–1005, 1981.
- [43] A. Conejo, J. Arroyo, N. Alguacil, and A. Guijarro, "Transmission loss allocation: a comparison of different practical algorithms," *IEEE transactions on Power Systems*, vol. 17, no. 3, pp. 571–576, 2002.
- [44] J. Savier and D. Das, "Energy loss allocation in radial distribution systems: A comparison of practical algorithms," *IEEE Transactions on Power Delivery*, vol. 24, no. 1, pp. 260–

267, 2008.

- [45] G. Shuttleworth and I. Williams, "Allocation transmission losses: Methods and criteria," *A Submission to the DICG Prepared by NERA. London*, 1999.
- [46] S. M. Abdelkader, "Transmission loss allocation through complex power flow tracing," *IEEE transactions on Power Systems*, vol. 22, no. 4, pp. 2240–2248, 2007.
- [47] A. I. Nikolaidis and C. A. Charalambous, "Hidden cross-subsidies of net energy metering practice: energy distribution losses reallocation due to prosumers' and storsumers' integration," *IET Generation, Transmission & Distribution*, vol. 11, no. 9, pp. 2204–2211, 2017.
- [48] V. S. Lim, J. D. McDonald, and T. K. Saha, "Development of a new loss allocation method for a hybrid electricity market using graph theory," *Electric Power Systems Research*, vol. 79, no. 2, pp. 301–310, 2009.
- [49] J. Mutale, G. Strbac, S. Curcic, and N. Jenkins, "Allocation of losses in distribution systems with embedded generation," *IEE Proceedings-Generation, Transmission and Distribution*, vol. 147, no. 1, pp. 7–14, 2000.
- [50] P. M. Costa and M. A. Matos, "Loss allocation in distribution networks with embedded generation," *IEEE Transactions on Power Systems*, vol. 19, no. 1, pp. 384–389, 2004.
- [51] P. M. Sotkiewicz and J. M. Vignolo, "Towards a cost causation-based tariff for distribution networks with dg," *IEEE Transactions on Power Systems*, vol. 22, no. 3, pp. 1051–1060, 2007.
- [52] I. Bhand and S. Debbarma, "Transaction-tracing based loss allocation in distribution networks under te system," *IEEE Systems Journal*, vol. 15, no. 4, pp. 5664–5673, 2020.
- [53] A. J. Conejo, F. D. Galiana, and I. Kockar, "Z-bus loss allocation," *IEEE Transactions on Power Systems*, vol. 16, no. 1, pp. 105–110, 2001.

- [54] W.-C. Chu, B.-K. Chen, and C.-H. Liao, "Allocating the costs of reactive power purchased in an ancillary service market by modified y-bus matrix method," *IEEE Transactions on Power Systems*, vol. 19, no. 1, pp. 174–179, 2004.
- [55] M. Usman, M. Coppo, F. Bignucolo, R. Turri, and A. Cerretti, "Multi-phase losses allocation method for active distribution networks based on branch current decomposition," *IEEE Transactions on Power Systems*, vol. 34, no. 5, pp. 3605–3615, 2019.
- [56] J. Daniel, R. Salgado, and M. Irving, "Transmission loss allocation through a modified ybus," *IEE Proceedings-Generation, Transmission and Distribution*, vol. 152, no. 2, pp. 208–214, 2005.
- [57] J. Bialek, "Allocation of transmission supplementary charge to real and reactive loads," *IEEE transactions on Power Systems*, vol. 13, no. 3, pp. 749–754, 1998.
- [58] S. Tong and K. N. Miu, "A network-based distributed slack bus model for dgs in unbalanced power flow studies," *IEEE Transactions on Power Systems*, vol. 20, no. 2, pp. 835–842, 2005.
- [59] C. Unsuhay and O. R. Saavedra, "Transmission loss unbundling and allocation under pool electricity markets," *IEEE Transactions on Power Systems*, vol. 21, no. 1, pp. 77–84, 2006.
- [60] K. M. Jagtap and D. K. Khatod, "Current summation based approach for loss allocation with distributed generation," in *2018 International Conference on Power, Instrumentation, Control and Computing (PICCC)*, pp. 1–5, IEEE, 2018.
- [61] P. Kumar, N. Gupta, K. R. Niazi, and A. Swarnkar, "A circuit theory-based loss allocation method for active distribution systems," *IEEE Transactions on Smart Grid*, vol. 10, no. 1, pp. 1005–1012, 2017.
- [62] E. Carpaneto, G. Chicco, and J. S. Akilimali, "Branch current decomposition method for loss allocation in radial distribution systems with distributed generation," *IEEE Transac-*

- tions on Power Systems*, vol. 21, no. 3, pp. 1170–1179, 2006.
- [63] E. Carpaneto, G. Chicco, and J. S. Akilimali, “Loss partitioning and loss allocation in three-phase radial distribution systems with distributed generation,” *IEEE Transactions on Power Systems*, vol. 23, no. 3, pp. 1039–1049, 2008.
- [64] W. Kersting, “The computation of neutral and dirt currents and power losses,” in *IEEE PES Power Systems Conference and Exposition, 2004.*, pp. 213–218, IEEE, 2004.
- [65] O. Edohen, S. Ike, and M. Okhumeode, “Revenue loss analysis due to unbalanced loading in power distribution network,” *NIPES-Journal of Science and Technology Research*, vol. 2, no. 1, 2020.
- [66] J. R. Carson, “Wave propagation in overhead wires with ground return,” *The Bell System Technical Journal*, vol. 5, no. 4, pp. 539–554, 1926.
- [67] G. Kron, “Tensorial analysis of integrated transmission systems part i. the six basic reference frames,” *Transactions of the American Institute of Electrical Engineers*, vol. 70, no. 2, pp. 1239–1248, 1951.
- [68] S. Poudel, G. D. Black, E. G. Stephan, and A. P. Reiman, “Admittance matrix validation for power distribution system models using a networked equipment model framework,” *IEEE Access*, vol. 10, pp. 9108–9123, 2022.
- [69] W. H. Kersting, “Distribution system modeling and analysis,” in *Electric power generation, transmission, and distribution*, pp. 26–1, CRC press, 2018.
- [70] M. Atanasovski and R. Taleski, “Power summation method for loss allocation in radial distribution networks with dg,” *IEEE transactions on Power Systems*, vol. 26, no. 4, pp. 2491–2499, 2011.
- [71] A. G. Exposito, J. R. Santos, T. G. Garcia, and E. R. Velasco, “Fair allocation of transmission power losses,” *IEEE transactions on power systems*, vol. 15, no. 1, pp. 184–188,

2000.

- [72] N. Zhao, Y. Song, Z. Bie, S. Takahashi, and Y. Sekine, "Improved z-bus loss allocation method through redistribution," in *39th International Universities Power Engineering Conference, 2004. UPEC 2004.*, vol. 3, pp. 1101–1105, IEEE, 2004.
- [73] M. D. A. B. Rozmi, G. S. Thirunavukkarasu, E. Jamei, M. Seyedmahmoudian, S. Mekhilef, A. Stojcevski, and B. Horan, "Role of immersive visualization tools in renewable energy system development," *Renewable and Sustainable Energy Reviews*, vol. 115, p. 109363, 2019.
- [74] N. R. Shrestha, P. T. Sherpa, S. Gurung, K. Chapagain, B. Mallik, and B. R. Pokhrel, "A custom developed flexible tool for real-time distribution grid visualization," in *2024 IEEE 33rd International Symposium on Industrial Electronics (ISIE)*, pp. 1–5, IEEE, 2024.
- [75] I. C. Change *et al.*, "Mitigation of climate change," *Contribution of working group III to the fifth assessment report of the intergovernmental panel on climate change*, vol. 1454, p. 147, 2014.
- [76] S. Jiusto, "The differences that methods make: Cross-border power flows and accounting for carbon emissions from electricity use," *Energy Policy*, vol. 34, no. 17, pp. 2915–2928, 2006.
- [77] B. Tranberg, A. B. Thomsen, R. A. Rodriguez, G. B. Andresen, M. Schäfer, and M. Greiner, "Power flow tracing in a simplified highly renewable european electricity network," *New Journal of Physics*, vol. 17, no. 10, p. 105002, 2015.
- [78] W. Fang and H. Ngan, "Succinct method for allocation of network losses," *IEE Proceedings-Generation, Transmission and Distribution*, vol. 149, no. 2, pp. 171–174, 2002.
- [79] B. Tranberg, O. Corradi, B. Lajoie, T. Gibon, I. Staffell, and G. B. Andresen, "Real-time carbon accounting method for the european electricity markets," *Energy Strategy*

*Reviews*, vol. 26, p. 100367, 2019.

- [80] M. Atanasovski and R. Taleski, "Energy summation method for loss allocation in radial distribution networks with DG," *IEEE transactions on Power Systems*, vol. 27, no. 3, pp. 1433–1440, 2012.
- [81] S. Sharma and A. Abhyankar, "Loss allocation of radial distribution system using shapley value: A sequential approach," *International Journal of Electrical Power & Energy Systems*, vol. 88, pp. 33–41, 2017.
- [82] Z. Ghofrani-Jahromi, Z. Mahmoodzadeh, and M. Ehsan, "Distribution loss allocation for radial systems including DGs," *IEEE Transactions on Power Delivery*, vol. 29, no. 1, pp. 72–80, 2013.
- [83] N. M. Kumar, A. A. Chand, M. Malvoni, K. A. Prasad, K. A. Mamun, F. Islam, and S. S. Chopra, "Distributed energy resources and the application of AI, IoT, and blockchain in smart grids," *Energies*, vol. 13, no. 21, p. 5739, 2020.
- [84] S. Westland and T. L. V. Cheung, "RGB systems.," 2012. RGB Systems.
- [85] A. Ford and A. Roberts, "Colour space conversions," *Westminster University, London*, vol. 1998, no. 1-31, p. 657, 1998.
- [86] Y. Cheng, N. Zhang, and C. Kang, "Carbon emission flow: from electricity network to multiple energy systems," *Global Energy Interconnection*, vol. 1, no. 4, pp. 500–506, 2018.
- [87] Y. Luo, S. Itaya, S. Nakamura, and P. Davis, "Autonomous cooperative energy trading between prosumers for microgrid systems," in *39th annual IEEE conference on local computer networks workshops*, pp. 693–696, IEEE, 2014.
- [88] C. Zhang, J. Wu, Y. Zhou, M. Cheng, and C. Long, "Peer-to-peer energy trading in a microgrid," *Applied energy*, vol. 220, pp. 1–12, 2018.

- [89] M. Y. Hassan, "MW-mile charging methodology for wheeling transaction," 2004.
- [90] H. Rudnick, M. Soto, and R. Palma, "Use of system approaches for transmission open access pricing," *International Journal of Electrical Power & Energy Systems*, vol. 21, no. 2, pp. 125–135, 1999.
- [91] Y. R. Sood, N. P. Padhy, and H. O. Gupta, "Wheeling of power under deregulated environment of power system-a bibliographical survey," *IEEE Transactions on Power systems*, vol. 17, no. 3, pp. 870–878, 2002.
- [92] D. Shirmohammadi, P. R. Gribik, E. T. Law, J. H. Malinowski, and R. E. O'Donnell, "Evaluation of transmission network capacity use for wheeling transactions," *IEEE transactions on Power Systems*, vol. 4, no. 4, pp. 1405–1413, 1989.
- [93] K. Lo and S. Zhu, "A theory for pricing wheeled power," *Electric Power Systems Research*, vol. 28, no. 3, pp. 191–200, 1994.
- [94] W.-J. Lee, C. Lin, and K. Swift, "Wheeling charge under a deregulated environment," *IEEE Transactions on Industry Applications*, vol. 37, no. 1, pp. 178–183, 2001.
- [95] D. Shirmohammadi, C. Rajagopalan, E. R. Alward, and C. L. Thomas, "Cost of transmission transactions: an introduction," *IEEE Transactions on Power systems*, vol. 6, no. 4, pp. 1546–1560, 1991.
- [96] M. Bao, Y. Ding, X. Zhou, C. Guo, and C. Shao, "Risk assessment and management of electricity markets: A review with suggestions," *CSEE Journal of Power and Energy Systems*, vol. 7, no. 6, pp. 1322–1333, 2021.
- [97] L. E. Jones, *Renewable energy integration: practical management of variability, uncertainty, and flexibility in power grids*. Academic press, 2017.
- [98] M. Caramanis, N. Roukos, and F. Schweppe, "Wrates: A tool for evaluating the marginal cost of wheeling," *IEEE Transactions on Power Systems*, vol. 4, no. 2, pp. 594–605, 1989.

- [99] K. Lo and S. Zhu, "Wheeling and marginal wheeling rates: theory and case study results," *Electric Power Systems Research*, vol. 27, no. 1, pp. 11–26, 1993.
- [100] H. M. Merrill and B. W. Erickson, "Wheeling rates based on marginal-cost theory," *IEEE Transactions on Power Systems*, vol. 4, no. 4, pp. 1445–1451, 1989.
- [101] H. Hamada, H. Tanaka, and R. Yokoyama, "Wheeling charge based on identification of transaction paths in deregulated power markets," in *2009 44th International Universities Power Engineering Conference (UPEC)*, pp. 1–5, IEEE, 2009.
- [102] D. Shirmohammadi, B. Gorenstin, M. V. Pereira, *et al.*, "Some fundamental, technical concepts about cost based transmission pricing," *IEEE Transactions on Power Systems*, vol. 11, no. 2, pp. 1002–1008, 1996.
- [103] Y.-M. Park, J.-B. Park, J.-U. Lim, and J.-R. Won, "An analytical approach for transaction costs allocation in transmission system," *IEEE Transactions on Power Systems*, vol. 13, no. 4, pp. 1407–1412, 1998.
- [104] S. Chaitusaney and B. Eua-Arporn, "Ac power flow sensitivities for transmission cost allocation," in *IEEE/PES Transmission and Distribution Conference and Exhibition*, vol. 2, pp. 858–863, IEEE, 2002.